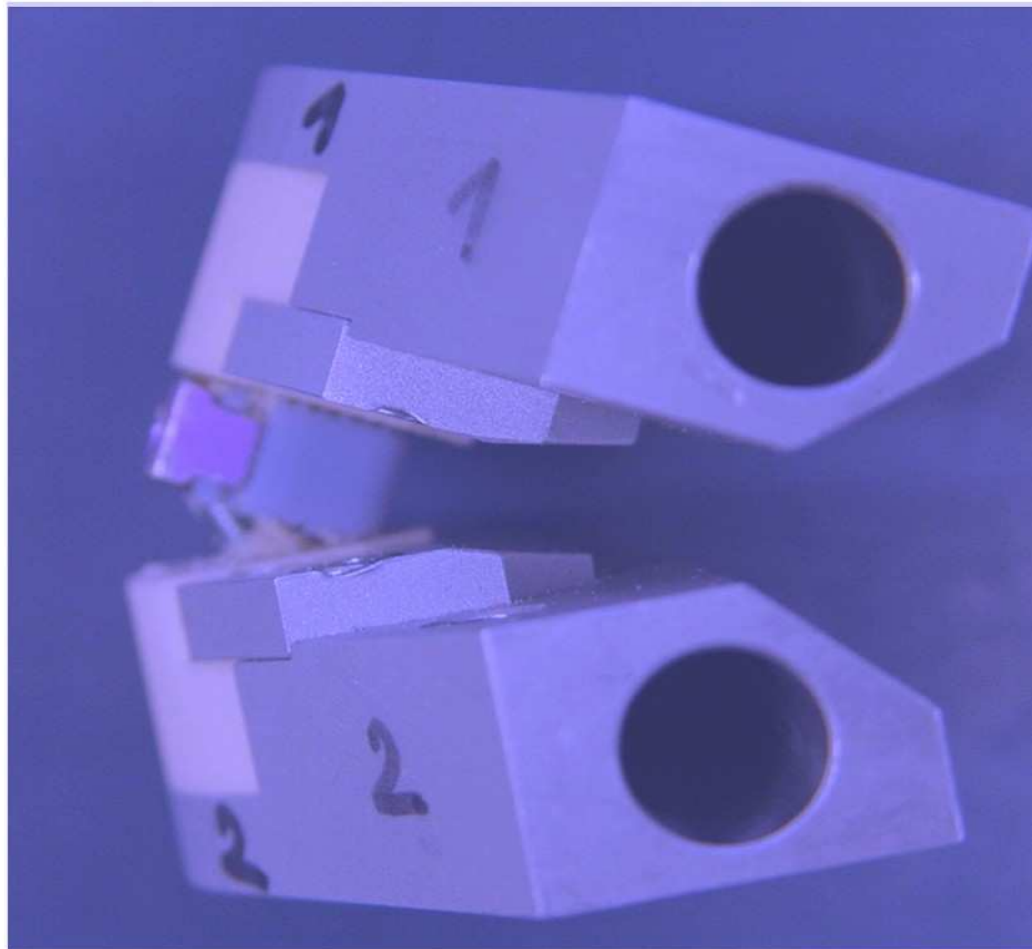


**MASTER PROJECT**

**École Polytechnique Fédérale de Lausanne  
Mechanical Engineering Section  
Laboraty of Biomechanical Orthopedics**

# **Biomechanical Investigation of a New Implant for Cervical Spine Fusion**

**Michael Davatz**



**Supervision:  
Prof. Dominique Pioletti (EPFL)  
Thomas Küenzi (Synthes)  
Arne Vogel (EPFL)**



**December 2006**

## ABSTRACT

This document treats the mechanical evaluation of a new kind of implant for cervical spine fusion. The idea of the new device is a combination of anterior plating systems (rigid fixation) and standard cages (unobtrusiveness). This so-called zero-profile design exists already in lumbar spine devices. The goals of the project were to define mechanical tests, measure the performance of different prototypes and make the comparison to existing systems destined for the same use and interpret test results.

In the first section, cervical spine anatomy and kinematics are analysed. The typical cervical vertebrae are C3 – C7. Spine kinematics is very complex and depends on many factors. Main motion has in general coupled motions. Range of motion, instantaneous axis of rotation and stiffness in flexion-extension, axial rotation and lateral bending in healthy subjects are presented.

Mechanical tests were performed in order to compare prototypes of the new device to existing anterior plating systems. Compression and tension tests were performed according to a modified ASTM F-1717 setup. Plating systems showed in general significantly higher maximum forces, but also larger displacements, particularly in tension. Initial stiffness of the new device was at a comparable level as plating systems when using three long screws or four standard screws. Rotation tests revealed a clear advantage for a device with four screws upon a device with three screws. The push-out and the subsidence tests showed the expected results: subsidence behaviour of the new device and a standard cage are at the same level. Push-out behaviour of the new device is clearly superior to a standard cage.

The compression test with the new device was simulated in a FEA. The model is reasonable for small deformations, before the foam material fails locally. A bone model (cancellous + cortical bone) was then integrated. Three different cancellous bone properties were used in three distinct simulations. The results showed a 5 to 20 times higher stiffness compared to the foam model.

### Conclusions

Screw length appeared to be more important than screw thickness for the stability. In contrast the thickness is a factor of construct strength. Push-out and subsidence tests are clinically relevant but couldn't give a lot of information for a design improvement. Compression test according to ASTM F-1717 is comparable to flexion-extension motion in the lower cervical spine. The tension test in contrast can not be related to motion present in daily situations. The FEA and comparison of material characteristics between foam and vertebral bone showed that foam is an acceptable bone model for mechanical testing.

Oberdorf 12 September 2006

Student: Michael Davatz

**Master Project (August – December 2006):** Biomechanical investigation of a new implant for cervical spine fusion

A prototype of an implant for cervical spine fusion (SynFix-C) is compared to three systems using an anterior plate. The compared systems are Vectra and CSLP (Cervical Spine Locking Plate) from Synthes and Zephir from Medtronic Sofamor Danek; these systems are tested using always the same type of spacer (Synthes Cervios). The mechanical tests are static compression, tension and axial rotation and take up the set up from the ASTM 1717-04 norm. Contrary to ASTM 1717 the devices are fixed in a PUR-foam block and geometry has to be modified. The mechanical properties of the foam are comparable to spongy bone and it is commonly in use for biomechanical tests. The results of interest are the stiffness and the mechanical resistance (maximum load). A push-out (static) and a subsidence test are also performed to compare the SynFix-C and a standard spacer (Cervios).

Of particular interest is the difference between the one-screw and the two-screw interface of the zero-profile device. To evaluate this difference the interfaces will be tested individually.

For the new implant, different length and diameters of screws are also compared.

Further tests will investigate mechanical performance of two and three level fixations.

A review of literature will relate the tests to the in vivo situation and should finally permit to qualify the product or propose modifications.

The mechanical tests should validate a finite element model that will be developed. The model will focus on the differences between the one- and two-screw interface. Only the tension model will be simulated. If time permits, a more sophisticated model of a bone with non-homogeneous properties will be developed.

The project consists of:

- Mechanical tests of the prototype of the new implant and comparison to existing anterior fixation systems in a bone model material; the test are static compression, tension, rotation and push-out and the set up follows the ASTM 1717 norm; tests for one, two and three level fusions are performed
- A literature research and review in order to classify the test results
- Development of a finite element model for the tension case, which will be validated by the mechanical tests.

The results should qualify the product or suggest possible modifications.

Senior Group Manager Cervical, Synthes  
Thomas Küenzi, Dipl. Ing. ETH

Responsible professor, EPFL  
Dominique P. Pioletti, PhD

Assistant, EPFL  
Arne Vogel, Ing. Dipl. EPF

## PREFACE

Implants have to work under various conditions which are not always entirely known. Their development is thus not straight forward, because standard benchmark can rarely be defined. The most important thing is to learn from experience, analyse clinical results and compare to successful products. This is why testing is paramount and starts quite early in the development. The underlying master project report is the documentation of a series of mechanical tests accompanying the development of a new type of implant, designed for interbody fusion of the human cervical spine. The project is completed by a literature research and a FEA of one of the mechanical tests. The project was performed at Synthes and also supervised by Prof. Dominique P. Pioletti and Arne Vogel from the Laboratory of Biomechanical Orthopedics LBO at the Swiss Federal Institute of Technology EPFL.

Oberdorf, January 2007

Michael Davatz

# CONTENT

1	Introduction	8
1.1	Goal of the Project	8
1.2	Structure of the Report	8
2	The Cervical Spine	9
2.1	The Spine	9
2.2	The Cervical Spine	9
2.2.1	Anatomy of the Cervical Spine	9
2.2.2	Typical Cervical Vertebrae Shape	10
2.2.3	Ligaments	11
2.2.4	Muscles	12
2.2.5	Intervertebral Disc	12
2.2.6	Typical Dimensions of Cervical Vertebrae	12
2.2.7	Bone Structure and Properties	15
2.3	Spine Kinematics	19
2.3.1	Definitions	19
2.3.2	Position of the Instantaneous Axe of Rotation	21
2.3.3	Range of Motion	23
2.3.4	Load-Displacement Properties of the Spine	26
2.4	Expected Axial Forces in the Cervical Spine in Static Postures	32
2.5	Pathology	34
2.5.1	Degenerative Diseases	34
2.5.2	Deformities	35
2.5.3	Tumours	36
2.5.4	Pathology after Surgical Intervention	36
2.6	Surgical Treatments	36
2.6.1	Discectomy	36
2.6.2	Corpectomy	36
2.6.3	Interbody Fusion	37
2.6.4	Arthroplasty	37
2.7	Anterior Plating Systems	37
2.7.1	Principle	37
2.7.2	Access	38
2.7.3	Types	38
2.7.4	Intervertebral Spacer	39
2.7.5	Indications	39
2.7.6	Main Drawbacks	39
2.7.7	Clinical Experience	40
2.8	Posterior Fixation Systems	40
2.9	Zero Profile Device	41
2.10	Quantitative Aspect of Anterior Interbody fusions	41
2.11	Summary and Conclusions	42
3	Biomechanical Tests	43
3.1	Introduction	43
3.2	Acceptance Criteria for the Tests	43
3.3	Testing Standards	44
3.4	Test Planning	45
3.4.1	Tested Specimens	45

---

3.4.2	Statistical Considerations	46
3.5	Data Analysis	47
3.5.1	Data Collection and Treatment	47
3.5.2	Statistical analysis	48
3.6	Compression Tests	49
3.6.1	Set-up for the Compression Test	49
3.6.2	Forces in the Specimen under Compressive Loads	50
3.6.3	Test Results Compression Tests	50
3.6.4	Discussion	57
3.7	Tension Tests	62
3.7.1	Set-up for the Tension Test	62
3.7.2	Forces in the Specimen under Tensile Loads	62
3.7.3	Test Results Tension Tests	63
3.7.4	Discussion	69
3.8	Isolated Interface Tests	70
3.8.1	Set-up for the Isolated Interface Test	70
3.8.2	Test Results Isolated Interface Tests	70
3.9	Rotation Tests	73
3.9.1	Set-up for Rotation Tests	73
3.9.2	Test Results Rotation Tests	74
3.9.3	Discussion	76
3.10	Push-out Tests	77
3.10.1	Set-up for Push-out Tests	77
3.10.2	Test Results Push-out Tests	78
3.10.3	Discussion	81
3.11	Subsidence Tests	82
3.11.1	Set-up for Subsidence Tests	82
3.11.2	Forces in the Specimen	82
3.11.3	Test Results Subsidence Tests	83
3.11.4	Discussion	85
3.12	Summary of the Test Results	87
3.12.1	Acceptance of Test Criteria	87
3.12.2	Method	87
3.12.3	Results	87
4	Vertebral Bone Model	88
4.1	Material Model	88
4.2	Basic Model	89
4.2.1	Assumptions	89
4.2.2	Geometry	89
4.2.3	Material Properties	91
4.2.4	Boundary Conditions and Contacts	91
4.2.5	Simulation	92
4.2.6	Results	92
4.3	Vertebral Bone Model	94
4.3.1	Material Properties and Dimensions	94
4.3.2	Results	94
4.4	Conclusions	96
5	Discussion	97
5.1	Comparing PUR Foam to Vertebral Bone	97
5.2	Lateral Bending	97
5.3	Preload	98

---

5.4	Limit of Elasticity	98
5.5	Further Analyses	98
5.5.1	Planned Tests	98
5.5.2	FE Model	99
5.5.3	Proposition of a New Test Setup for Adequate Flexion and Extension Simulation	99
5.5.4	Improved Vertebra Model	100
6	Conclusions	101
6.1	Design Improvement Proposals	102
6.2	Reasonable Tests	102
7	Close	103
8	Literature Index	104
8.1	Electronic Resources	106
9	Current Abbreviations	107
9.1	General Abbreviations	107
9.2	Abbreviations for Mechanical Tests	107
10	Annexe	108

# 1 INTRODUCTION

SynFix-C, a new kind of implant for cervical spine fusion is currently being developed by Synthes GmbH, Switzerland. The idea of the new device is a combination of anterior plating and standard fusion cages. The geometry of this implant offers surgeons the advantage of having an implant that does not protrude above the vertebral bodies and avoids adjacent level disc space contact. This new geometry also results in a different loading characteristic compared with current implants on the market. It was therefore necessary for Synthes to perform mechanical testing to understand optimise the implant and to understand how it compares to standard plating implants.

## 1.1 Goal of the Project

The project should give answers to the following questions:

- What is the mechanic performance related to existing, clinical known products?
- In particular:
  - o Provides a concept with three screws sufficient stability?
  - o What is the difference between a one screw and a two screw interface?
  - o What is the influence of screw dimension?
- Where can the weakness be located? What is the expected failure mechanism?
- How can polyurethane foam be interpreted as a vertebral bone model?
- Are currently used testing norms acceptable for a clinical relevant evaluation?

## 1.2 Structure of the Report

The report is subdivided into four main parts. The first part presents the relevant basics of the anatomy of the cervical spine. The focus is on the kinematics and its relevant elements. A review of different range of motion and stiffness analyses is given. The second part presents the mechanical tests performed during the project. In this section useful testing norms and the test setups are shown. In the third part, results of the finite element analyse is presented. One of the mechanical tests was simulated in this analyse to extrapolate the behaviour with vertebral bone. Finally, the results of these chapters are discussed in the fourth part; it is completed by a proposal of further analyses and the most important conclusions.



## 2 THE CERVICAL SPINE

This following chapter is a review of the basic anatomy of the cervical spine. The main focus is on cervical spine geometry and kinematics. A brief overview of spinal diseases and spinal instrumentation is also given.

### 2.1 The Spine

The functions of the spine are to protect the spinal cord, support the load of the trunk, the head and additional forces from the upper extremities and to give sufficient mobility.

The spine consists of the vertebrae, the intervertebral discs and the surrounding ligaments. It can be divided in three regions, where the vertebrae in each part have a characteristic geometry and size. The smallest vertebrae are in the cervical spine, where the load is the smallest; these seven vertebrae are denoted C1 to C7. The occiput, often denoted as C0, is located cranial to the cervical spine, caudal it's followed by the 12 thoracic vertebrae (T1 – T12). Caudal to the thoracic, there are 5 lumbar vertebrae (L1 – L5). The five sacral vertebrae are adhered together and don't have the same function as the cranial parts of the spine. Often they are considered as a part of the lumbar spine.

The spine is more or less a vertical rod, but there are three typical bendings: Lordosis in the lumbar and cervical spine, kyphosis in the thoracic spine. These characteristic bends help to make an efficient damper for the head.

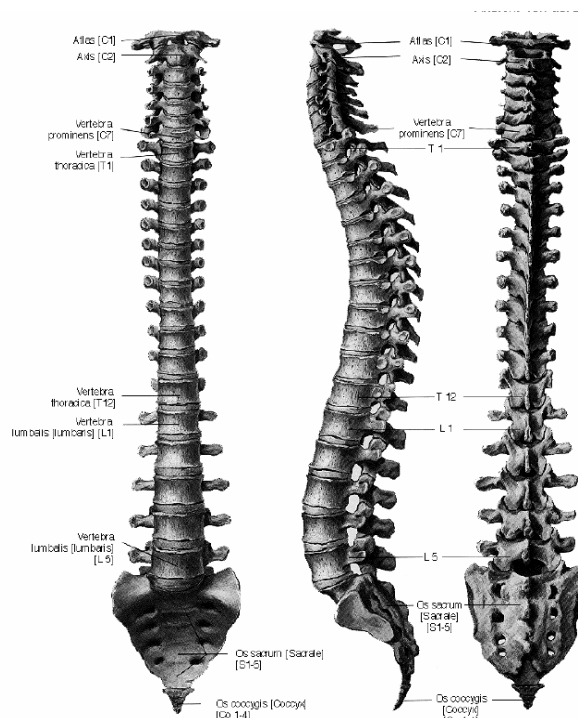


Figure 2.1: The human spine from ventral, lateral and dorsal [34]

### 2.2 The Cervical Spine

#### 2.2.1 Anatomy of the Cervical Spine

The cervical spine itself can also be divided in three regions: the upper, middle and lower cervical spine. C1 and C2, called the atlas and the axis are the upper cervical spine. These two vertebrae can be clearly distinguished from all others: the atlas, caudal to the occiput, doesn't

have a vertebral body. The axis has a cranial process - the dens - which acts as centre of rotation for C1. The upper cervical spine is, together with C0, responsible for 50 to 60 % of the axial rotation and flexion-extension motion of the cervical spine.

In the middle cervical spine (C3 – C5), the vertebrae have the more typical shape and are not basically different from those of the lower cervical spine (C5 – T1). As the stresses increase caudally, also the vertebral body, which supports 30 to 50 % of the load [13, 14], are getting bigger.



Fig 2.2: Cervical spine (C1-C7)

## 2.2.2 Typical Cervical Vertebrae Shape

### Atlas - C1

The atlas is the only vertebrae without a vertebral body. The spinous process is also missing. It consists mainly of two bows, an *arcus anterior* and an *arcus posterior*. Laterally the structure is thickened in the *massae laterales*, where the caudal and cranial contact faces are located, the *facies articularis superior* and *inferior*. Another joint face is inside the anterior bow, where the dens axis comes in contact. Lateral distal to the massae laterales are the *processus transverses* with the *foramen transverses* where the arteries pass.

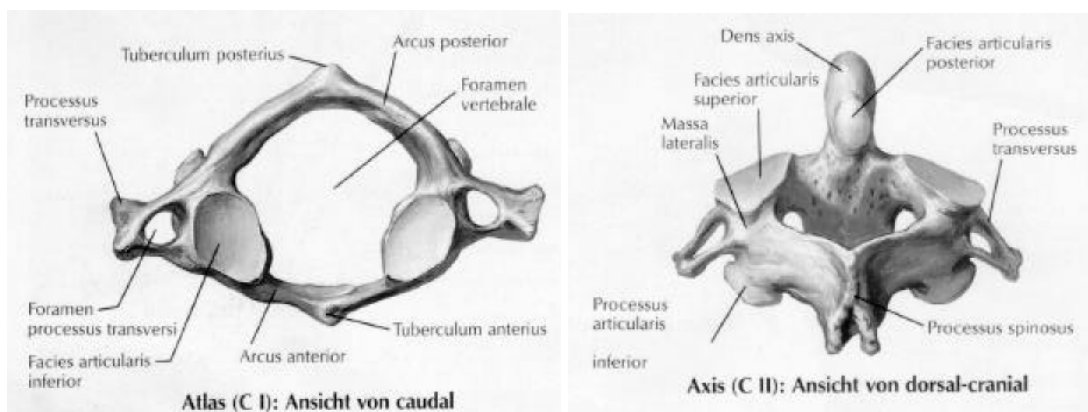


Figure 2.3 and 2.4: Caudal view of the atlas (left) and dorsal-cranial view of the axis (right) with the principal elements [45]

### Axis – C2

The vertebra caudal to the atlas has a particular shape too. In contrast to C1 this vertebrae has a vertebral body, but it features a cranial process, the *dens axis*, which acts as the axis of rotation for the atlas.

A part from the dens axis, the shape resembles strongly to the other vertebrae of the cervical spine; the posterior arcus vertebrae has a much more compact look, compared to C1 and also the *processus spinosus*, a bony extent at the posterior side, is present. The foramen transverses are narrower and inclined downwards. On the upper side the facies articularis are mostly in the transversal plane to admit a generous range of motion in axial rotation. The joints on the caudal side have already the characteristic inclination of the lower cervical spine vertebrae.

### Vertebrae of the Middle and Lower Cervical Spine

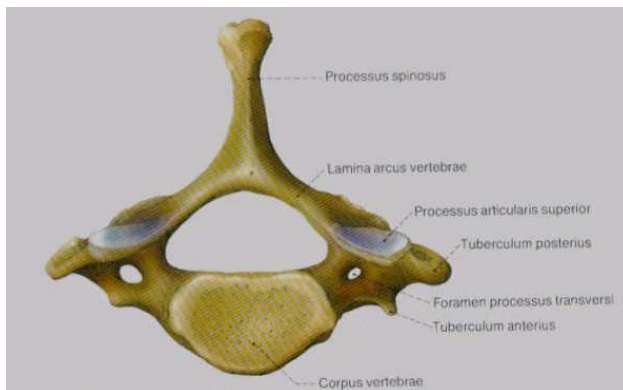


Fig. 2.5: Typical cervical vertebra (C7)

From C3 down to C7 the shape of the vertebrae is more or less the same. Moving downwards, the vertebrae are becoming bigger to come along with the increasing load and the *processus spinosus* becomes clearly longer. In C7, this process makes about the half of the length of the complete vertebra and can be groped on the neck.

The vertebral body is proceeded posteriorly in the *arcus vertebrae* and they form together a triangular *foramen vertebrae*, where the spinal cord passes. On the cranial side the vertebral body has laterally two bumps, the *processus uncinati*. They

play an important role in spine kinematics. The lateral processes are similar to C2; they accommodate the foramen transversarium (canal for the arteries) and cranial and caudal joint faces, inclined by an angle of about 45°, which is typical for the cervical spine. In contrast to the angle of 90° in the lumbar spine, the inclination in the cervical spine permits still a good range of motion in rotation and lateral bending.

### 2.2.3 Ligaments

The bony structure of the complete spine is surrounded by a series of different ligaments, which are crucial for the stability of the spine. An anterior ligament is attached to each of the vertebral bodies, the *ligamentum longitudinale anterius*; it starts at the atlas and is proceeded to the sacrum. The width increases in the caudal direction; a rigid bond to the intervertebral disc doesn't exist. The *ligamentum longitudinale posterius* is its pendant on the backside of the vertebral body. This ligament has two layers and bonds to the intervertebral discs are stronger than to the vertebral body. These ligaments have a high part of collageneous filaments, a part from their stabilising function they protect the intervertebral disc.

The *ligamentus flavum* is attached on the vertebral bows between the segments; these ligaments are much more elastic and are under tension even in the neutral position of the spine. Two other ligament types are intersegmental: the *ligamenta intertransversaria* between the lateral processes and the *ligamenta interspinalia* between the *processus spinosus*.

The ligaments are responsible for the limitation of the range of motion without damaging any structures. They consist of mostly in the longitudinal direction aligned collagen fibres. The limitation of extent is due to a with deformation increasing rigidity.

## 2.2.4 Muscles

The muscles are the only active motion element; they envelop in several layers the complete cervical spine. Basically anterior muscles are responsible for flexion, posterior muscles for extension and lateral muscles for lateral bending. Some of the muscles run obliquely around the head, which permits to rotate axially.

## 2.2.5 Intervertebral Disc

The intervertebral disc is a soft element between the vertebral bodies of two adjacent vertebrae. Its function is to keep the mobility of the spine and to act as a shock absorber. Furthermore stresses are evenly distributed due to the soft structure, whereby the demand for the vertebral body is reduced.

The disc consists of mainly two parts: an outer ring of a fibrous structure, the *annulus fibrosus* and an inner jelly-like substance, the *nucleus pulposus*. The nucleus has originally a high water content; it is a normal process of ageing, that the water content diminishes. Thereby, a part of the flexibility is lost, but this does not necessary create pain. The disc adheres completely to the adjacent vertebral bodies.

The disc has a slightly wedged shape, the posterior height is in the range of 40 to 60 % of the anterior height [36].

Disc height is mostly constant over the complete cervical spine and the range is from 2 to 6 [mm] with a mean height of 4 to 4.5 [mm] as mentioned in *Klinische Anatomie der Halswirbelsäule* by Lang [9]. Yogandan [36] published different values; as an average disc height he indicates 4 to 6 [mm] at C2-C3 level and this increases slightly moving downwards to a range from 5 to 7.5 [mm] at C6-C7.

Failure load is similar under compressive and tensile forces; in contrast, stiffness is ten times higher in compression.

## 2.2.6 Typical Dimensions of Cervical Vertebrae

Cervical vertebrae are rather complex, but efforts were made to quantify and compare geometry of vertebrae in this spine region. Dimensions of the vertebral body are of course of particular interest in this project.

Elaborated recent studies were done by Panjabi et al. [18] and Tan et al. [29]. The studies are not directly comparable, because the latter one is done on Chinese Singaporeans subjects. The study done by Panjabi does not refer to a specific group, but was probably done on Caucasian subjects.

Dimensions of interest are designated on the figure below as: width of the caudal and cranial endplate (EPWI, EPWu), depth of the caudal and cranial endplate (EPDI, EPDu) and vertebral body height (VBHp). In the following graphics, measured values of the cited studies are shown. Panjabi's study is represented with the thick line, Tan's study with a thin one.

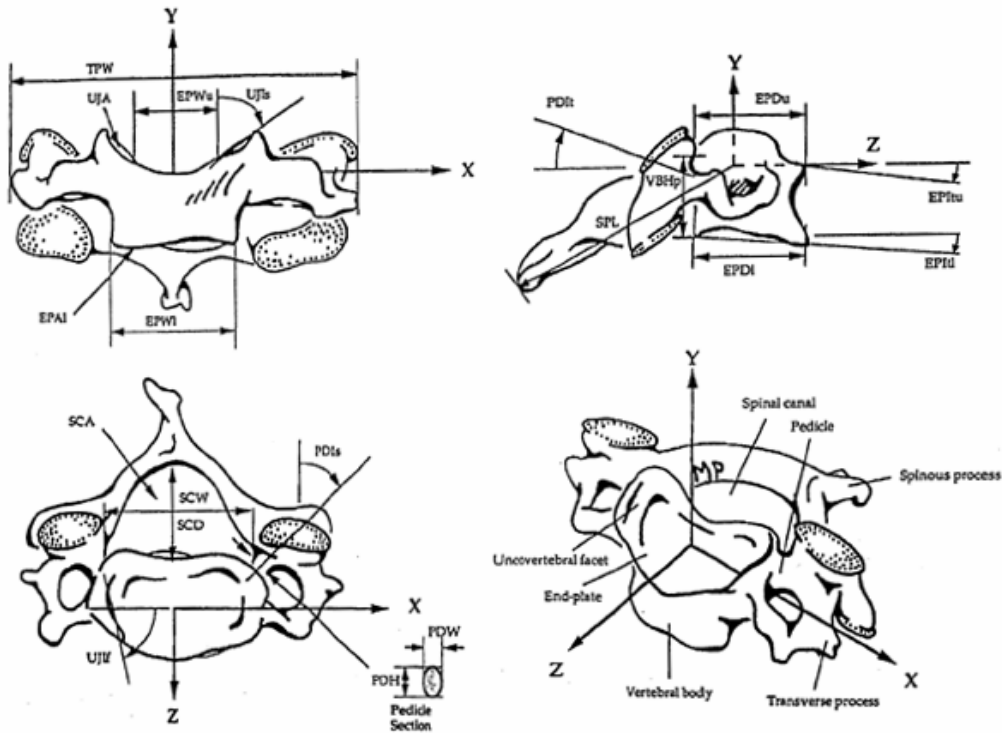


Fig. 2.6: Principal dimensions of a typical cervical vertebra (C3 – C7) [18]

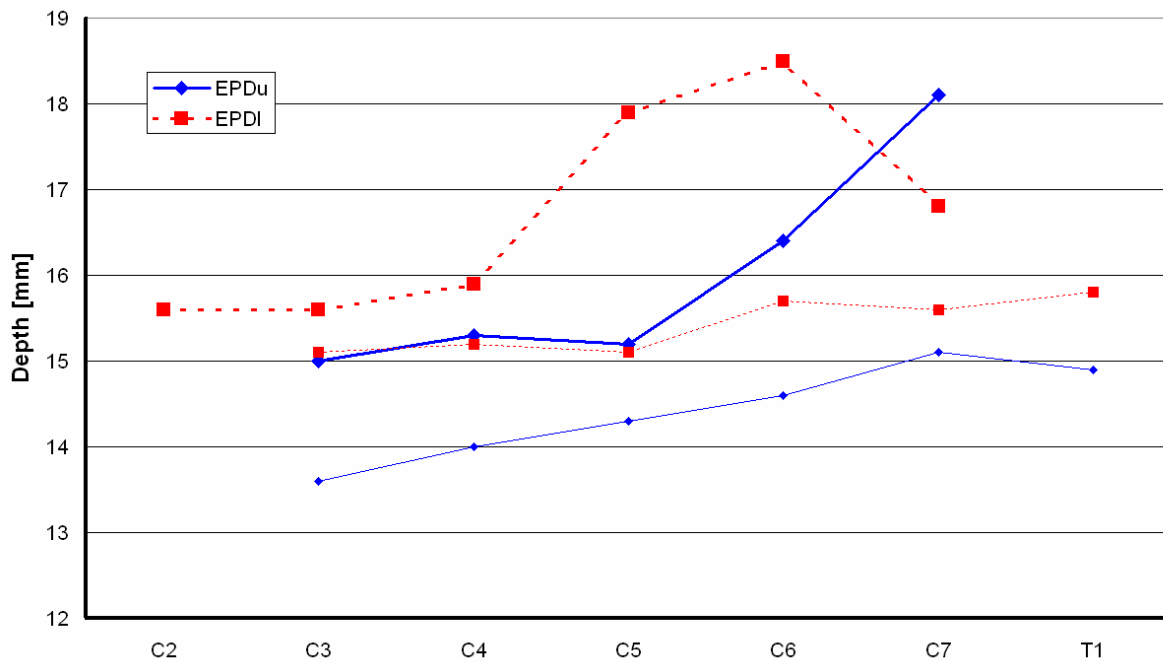


Figure 2.7: Inferior (EPDI) and superior (EPDu) endplate depth; thick line: Panjabi's study [18], thin line: Tan's study [29]

Vertebral body depth is shown in the figure above. Dimensions collected from the Chinese Singaporeans are steadily increasing moving caudally; measurements done by Panjabi are increasing as well, but a step from C4 to C5 on the inferior and on C5 to C6 on the upper endplate appears. The lower C7 endplate is even clearly less deep than on the cranial adjacent

vertebrae. The absolute values are going from 15 to 18.5 [mm] in the Panjabi study and from 13.5 to 16 [mm] in Tan's study.

The endplate width is increasing steadily in both studies (16 to 23 [mm]), those from Tan's study being smaller (13 – 20 [mm]). Increase has not a linear but rather quadratic appearance, which is especially visible in Tan's study. To be noted is the step from C7 to T1; T1 is not part of Panjabi's study.

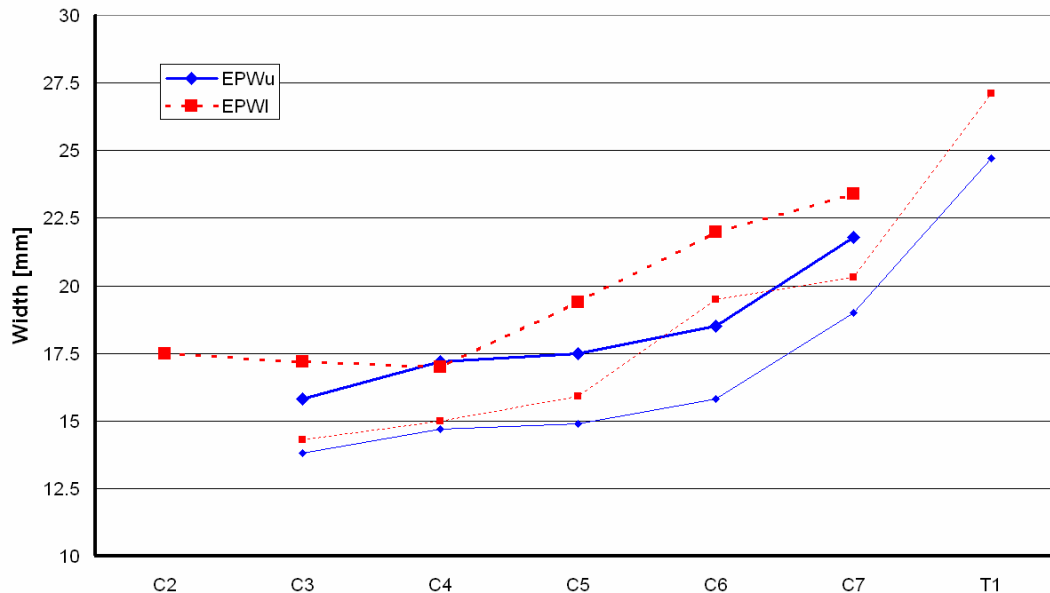


Figure 2.8: Inferior (EPWI) and superior (EPWu) endplate width; thick line: Panjabi's study [18], thin line: Tan's study [29]

Vertebral body height is changing similarly to endplate width; dimensions from C3 to C5 are close to each other and moving further downwards, height starts to increase. Anterior height is slightly lower than the posterior. Height varies from 10 to 13 [mm], T1 is 14 posteriorly.

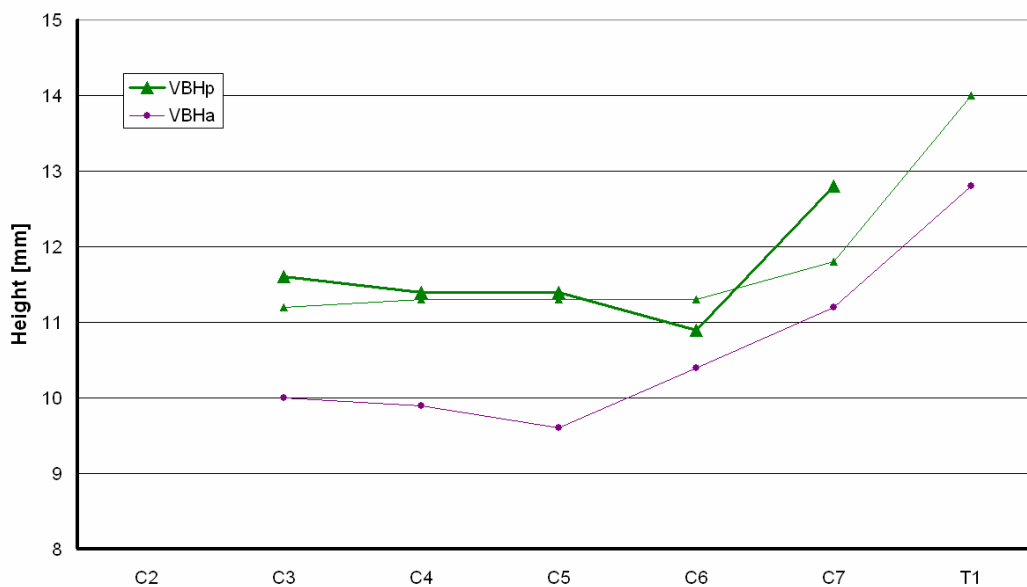


Figure 2.9: Posterior (VBHp) and anterior (VBHa) vertebral body height; thick line: Panjabi's study [18] (posterior height only), thin line: Tan's study [29]

### 2.2.7 Bone Structure and Properties

Bone consists basically of an organic matrix and mineral components. It is an ideal material for the skeleton due to the specific properties of the bone, its hardness, moderate elasticity and limited plasticity. Bone can thus give a typical shape to the body, protect organs and form levers with the attached muscles. Thanks to a cavity including structure, bone is an efficient composite material with good mass-to-strength ratio.

A part from its mechanical function, bone represents a reservoir for Calcium (99 % of Ca is in the bone), which is primordial for muscle activity and bone tissues are also site of formation of the blood cells [11].

#### Basic Components of Bone Matrix

The organic part of the bone consists principally of type I collagen fibrils. A part from the collagen there are other proteins: proteoglycans and phospholipids. The collagen fibres are responsible for the elastic properties of the bone. Bone obtains its hardness by deposited mineral substance, a calcium phosphate hydroxyapatite which appears in different forms of crystallisation.

All bones in the skeleton have a typical sandwich structure: The outer shape of the bone is a hard and dense material with a high degree of mineralisation, the cortical shell, at the inside the spongy or cancellous bone acts as a filling material. Density and mechanical resistance is much lower because of its sponge-like structure. This structure is formed of rod- or sheetlike elements called *trabeculae*. There is a clear orientation in direction of the main stresses.

In general, the degree of mineralisation increases with age, making the bone more brittle. Also the structure itself, in particular of the cancellous bone, becomes weaker with age.

#### Typical Bone properties

A large variance of data from bone properties can be found in the literature, because of the many factors influencing the properties.

Orientation of the trabeculae is leading to an anisotropic structure. Furthermore, the cancellous bone in the vertebrae is inhomogeneous. Recent studies showed that mechanical

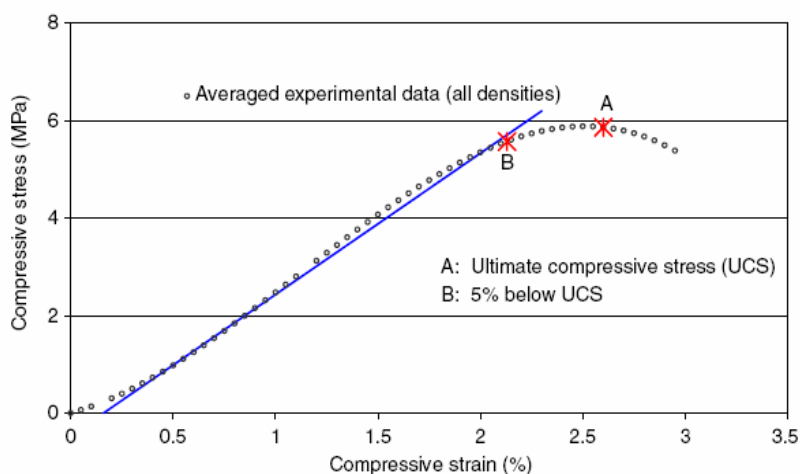


Fig 2.10: Stress-strain curve for cancellous bone [25]

properties are improving from anterior to posterior and also cranial to caudal. Mechanical properties are rather poor under tension load, which is not a physiological stress for bone structures. Under compressive loads, bone has an almost Hookeian behaviour over a wide range (cf. 2.10). Youngs modulus can be expressed as a function

of bone mineral density (BMD). Most researchers proposed a power-law when they studied influence of density on mechanical properties, so does Shim et al. [25]. In this study the compressive E modulus was measured in a range from 100 to 600 [MPa] in the longitudinal direction of the spine, the subjects were in the age of 40 – 79 years.

Wolff established that cortical bone is at the base the same as cancellous bone, only that its density is higher. In this case it would be possible to extrapolate cortical bone properties from these of cancellous bone, because they depend on the density. Tensile test and ultrasonic measures of specimens of each bone type showed that this assumption can not be verified. Individually tested trabeculae had a module of 10 to 15 [GPa], cortical bone specimens had 19 to 21 [GPa] [23].

Plastic deformation is limited in the cancellous bone; failure load is only 5 % lower than the ultimate stress. The compressive strength is in the order of 6 [MPa].

Anisotropy is shown in screw pull-out tests in [1] on lumbar vertebrae. The direction perpendicular to the trabeculae appeared to be about 40 % stronger than the parallel pull-out direction.

Measuring of the bone density seems to be another point of confusion, because publications differ about the definition of this term. “Fresh” bone, containing blood and fat have densities from 0.6 to 1.4 [g/cm<sup>3</sup>]; the range for defatted bone goes from approximately 0.2 to 1 [g/cm<sup>3</sup>]. Interestingly, the BMD decreases significantly from C1 down to C7, whereas the density in the lumbar spine is mostly constant [37]. The measured values, all from young subjects (mean = 25), were 0.27 [g/cm<sup>3</sup>] in the upper spine and 0.22 [g/cm<sup>3</sup>] at C7. First level of the thoracic spine had an even lower value 0.20 [g/cm<sup>3</sup>].

Properties of cortical bone are clearly superior; this bone type is quite compact, density is thus a factor 2 to 3 higher (1.7 [g/cm<sup>3</sup>]).

The values are summarised in the following table.

	Cancellous Bone	Cortical Bone [*]
Compressive Modulus [MPa]	300 <sup>1)</sup> (100...600)	12000
Compressive strength [MPa]	5.9 <sup>1)</sup>	
Tensile Modulus [MPa]	Lower	
Tensile strength [MPa]	Lower	
Shear Modulus [MPa]	41.7	4615
Poisson [-]	0.2...0.3	0.3
Density [g/m <sup>3</sup> ]	0.2...1	1.7

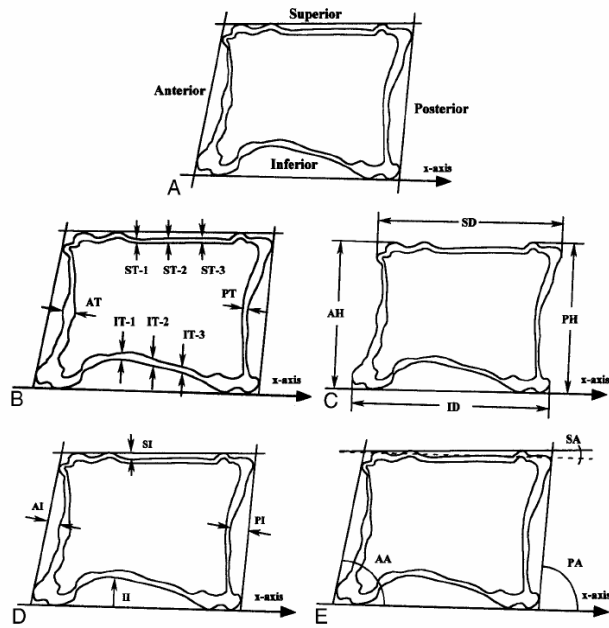
\*) Values for lumbar vertebrae [8]

- 1) Longitudinal direction (main stress)
- 2) Parallel to rise
- 3) Perpendicular to rise

### Typical Cortical Shell Thicknesses

As the cancellous bone has low mechanical properties compared to cortical bone, global resistance of the vertebrae is strongly influenced by the cortical shell. A further criteria is the architecture of this thin layer, which depends on vertebrae location. Panjabi et al. [15] analysed shell architecture of cervical vertebrae of human cadavers; abnormal vertebrae were





excluded from the analyse. Cortical shell thickness was measured on photographs of thin slices. The slices were cut in the sagittal plane.

Shell thickness was measured at three locations each on the caudal and cranial endplate and at one posteriorly and anteriorly.

Fig. 2.11: Measuring points for the cortical shell thickness [15]

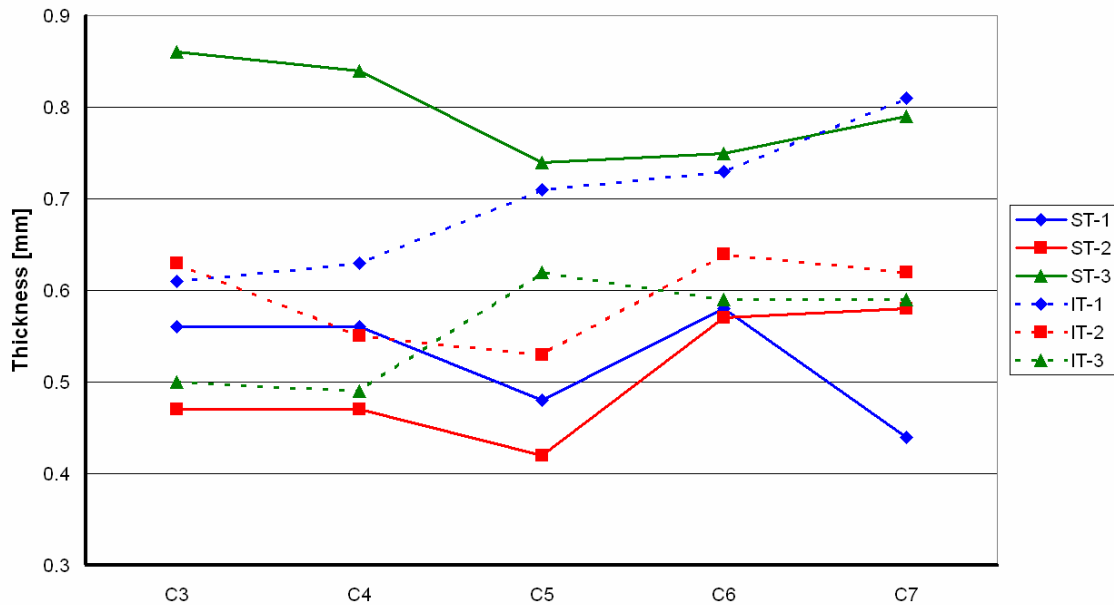


Fig. 2.12: Thickness of the superior (ST) and inferior (IT) endplate; exact locations of the measures indicated in figure 2.11.

In the diagram above, endplate thicknesses for the cervical vertebrae are represented; the dashed line are the values of the inferior (caudal) endplate, the continuous line those of the superior (cranial) endplate. Relative standard deviation is between 10 and 40 %, but is not indicated in the graphic above.

The superior endplate is weakest in the middle, except in C7 where the lowest measure is found anteriorly. Posteriorly the endplate is clearly thicker on all vertebrae. On the inferior endplate the layer is thickest anteriorly; posteriorly and in the middle thicknesses are similar, but lower than anteriorly. This is expected, because of the increased loading, that the shell

sees caudally. However, only the thickness anteriorly caudally increases. The thickness cranially in the middle and caudally posteriorly also increase, but not steadily.

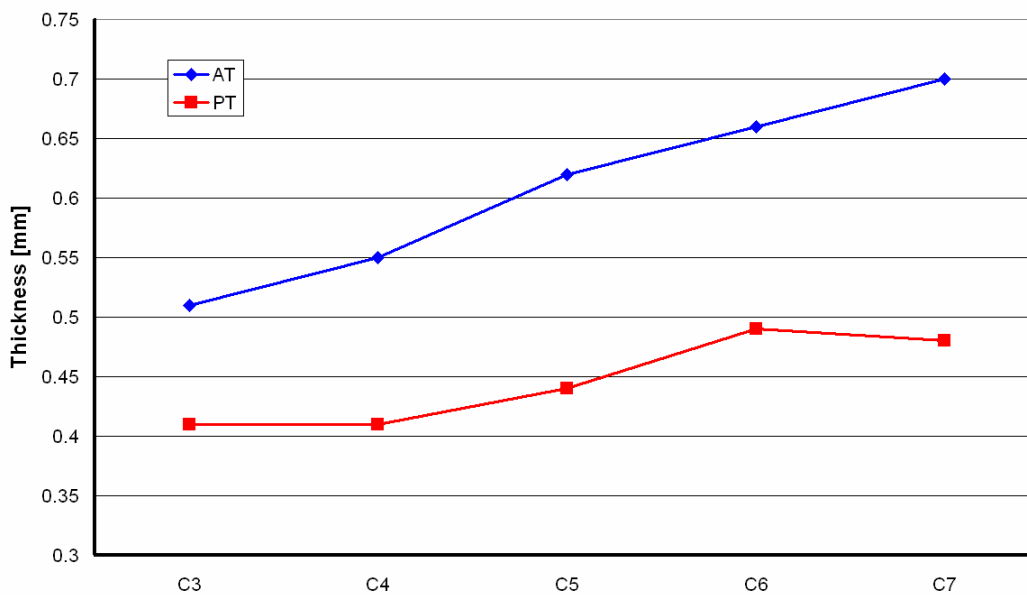


Fig. 2.13: Thickness of the anterior (AT) and posterior (PT) cortical shell

Including vertebral body dimensions in this analyse (cf. chapter 2.2.6), C7 seems to be relatively weaker than the cervical vertebrae. This is in coincidence with a clinical case study about anterior cervical interbody fusion with a titanium cage [30], where subsidence related complications were stressed on C7; Caughen et al. [4] found also highest subsidence on C6-C7 level.

In contrast cortical shell thickness on the posterior and anterior side of the vertebrae is clearly increasing moving caudally (cf. fig. 2.13). Posteriorly, the layer is thinner and also the increase is moderate. Thickness is in the same range as for the endplates (0.4...0.8 mm).

### Significance of the Cortical Shell for Device Fixation

Rigidity and pull-out strength of screws is dependent upon the cortical shell properties. The influence of screw length is marginal as relates to axial pull-out once a sufficient bone purchase has been reached. Zhang et al. [38] investigated this problem in a FE analyse. They compared screw pull-out strength in a homogeneous bone model of pure cancellous bone to a model with cortical shell. Forces transmitted by each thread are equal in cancellous bone, the cortical shell takes up manifestly higher forces, which are strongly increasing when deformation increases. With a doubled screw length the pull-out strength increased by 106% in the model without cortical shell and only by 34 % with cortical shell. To compensate for this disadvantage, unicortical screws are usually angled to form a wedge.

## 2.3 Spine Kinematics

The cervical spine is one of the most complex parts of the musculo-skeletal system. Motion is influenced by the geometry of the vertebrae, the intervertebral discs and the surrounding soft tissues. The conditions (degeneration, trauma...) of all these components also play an important role. Due to the geometry, motions appear in general as coupled movements and affect several motion segments or even the complete cervical spine.

The main elements of the spine as a movable organ are the vertebrae, the intervertebral disc, the ligaments and the muscles. The vertebrae are the rigid element of the structure, giving stability and shape. Their geometry is not favourable for relative movement, which is the role of the intervertebral discs. They introduce flexibility in the rigid structure and are also supporting about 35 - 50 % of the load [ref]. The range of motion is limited by the bony rigid geometry, particularly the pedicles, which limit rotation and lateral bending. Other important stabilising elements are the surrounding ligaments. They maintain the relative positions of the vertebrae and act as a movement limiter. The muscles are the only active element. They induce rotation, lateral bending, flexion and extension. Flexion and extension is achieved by simply activating the muscles anteriorly or posteriorly to the spine. Rotation is more complex because several different groups are active; because they are diagonal around the spine, when rotating the head, flexion or extension of vertebrae is induced at the same time; this is called *coupled motion*.

An important thing for understanding kinematics is that muscles and ligaments have a notable rigidity under tension only, but not under compression. Bone has rigidity in both directions and can sustain compressive loads particularly well.

### 2.3.1 Definitions

The following definitions are mainly taken from reference [32].

#### **Flexion**

From a neutral position, the head is moved forward, the look pivots downwards and the spine is bended.

#### **Extension**

Extension is the inverse movement to flexion; the head is moved backwards and the look pivots to the ceiling. Flexion and extension extent are not symmetric to the neutral position.

#### **Lateral Bending**

The spine is bended to the side. This movement is not feasible isolated; lateral bending is always accompanied by axial rotation. Lateroflexion is a commonly used synonym.

#### **Axial Rotation**

Axial rotation is a rotation about the vertical axis of the spine. Rotation happens mostly in the atlanto-axial joint; a part from these joint, a flexion or extension movement is coupled with axial rotation. In contrast a translation is present in the atlanto-axial joint when rotating.

**Functional Spinal Unit (FSU)**

The functional spinal unit is the assembly of two adjacent vertebrae and their intervening intervertebral disc. It is the base of kinetic studies and is sometimes also called *motion segment*.

**Range of motion (ROM)**

Range of motion is the difference between the two points of physiologic extent of movement without damage. It consists of a *neutral zone* and an *elastic zone*. In several studies, ROM in flexion/extension, rotation and lateral bending has been measured. Active (in vivo) and passive (cadaver) measurements differ; a summary of these values of important studies is given by Watier [31].

**Neutral zone (NZ)**

The neutral zone is a middle position, where resistance for movement is minimal. Keeping the same position is possible without muscular action. A summary of measured values can be found in Watiers publication [31].

**Elastic Zone (EZ)**

The elastic zone is the displacement between the maximum extent in the neutral zone and the maximum extent of the range of motion. Soft tissues are reversibly stretched, rigidity increases in general with increasing deformation.

**Plastic Zone (PZ)**

The plastic zone is reached after passing the elastic zone; in this zone tissues are damaged.

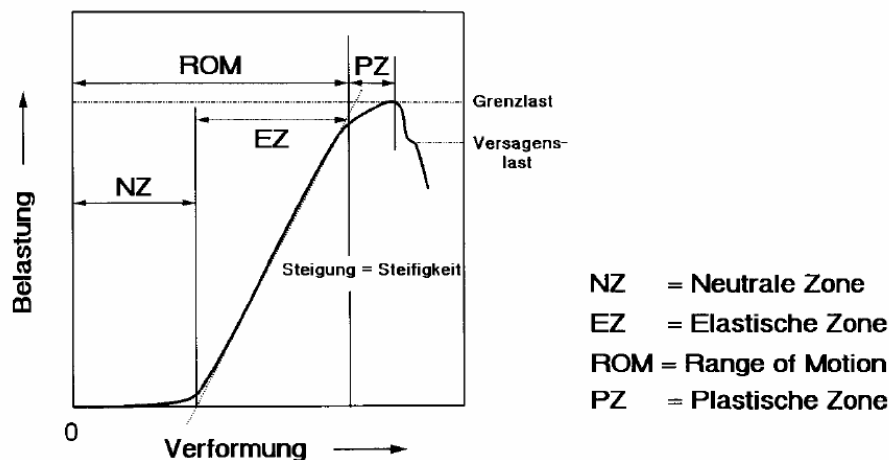


Fig. 2.14: Typical load-displacement curve with NZ, EZ, PZ and ROM [34]

**Instantaneous Axe of Rotation (IAR)**

The instantaneous axe of rotation (IAR), in some publications the term *instantaneous centre of rotation* (ICR) is used, is a fictive point in planar rotation that doesn't move. Experiments have been run to determine the IAR particularly for flexion/extension. It is not possible to determine one precise point, because it depends on direction of movement, velocity, other coupled movements etc.

**Coupling / Coupled Motion**

Coupling refers to motion in which rotation or translation of a body about or along one axis is consistently associated with simultaneous rotation or translation about or along another axis.

**Coordinate System**

In anatomy there is mainly one usual coordinate system. The x-axis is directed to the front, the y-axis to the top and the z-axis to the left. Rotations about these axes are described as lateral bending, axial rotation and flexion/extension (cf. Figure 2.15).

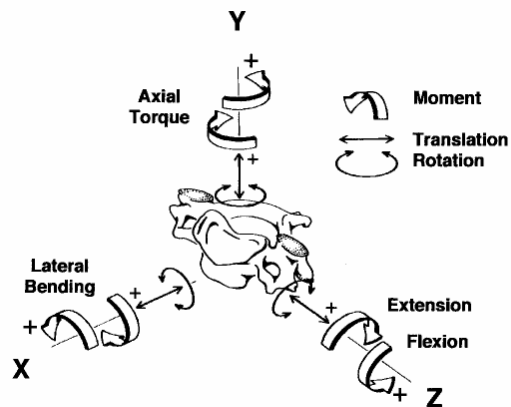


Fig. 2.15: Usual sign and coordinate system convention

**2.3.2 Position of the Instantaneous Axe of Rotation**

**Flexion/Extension**

Several studies have investigated the IAR of the cervical spine. The primary purpose of these studies was to detect spinal disorders by a visibly changed movement. Different studies proposed a large variety for positions of the IAR, which is partially the result of a lack of consistency in applied methods, as White and Panjabi [32] have observed. A plausible method is described in reference [5]: The patients are standing upright, the sternum and the mid-thoracic are fixed to prevent this region from flexion/extension. To measure a passive movement an examiner holds the head and the chin of the patient and induces the movement. In neutral position and at maximum extent a lateral x-ray is taken. Afterwards motion is analysed by superposing neutral and extreme position. IAR is determined manually by graphic methods or by a computer-assisted method.

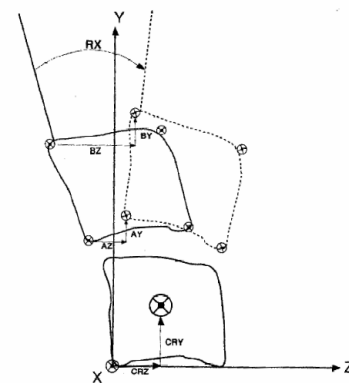


Fig. 2.16 : Graphical determination of IAR and motion [5]

The results of this study are shown in figure 2.17. The IAR is clearly in the caudal vertebrae for the FSU in the upper cervical spine and comes gradually closer to the intervertebral disc moving caudally. Therefore the upper FSU are including a relative translation, whereas the lower vertebrae have more a tilting movement. The more tilting movement is similar to lower spine regions (lumbar), where the loads are significantly higher. The horizontal position of the IAR is about the middle of the vertebral body.

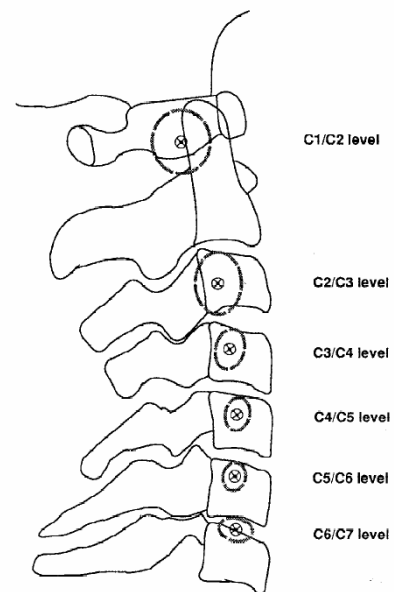


Fig. 2.17 : IAR position for flexion-extension [5]

Similar results have been already published in a study done by Penning in 1960. Both investigated a group of younger subjects.

Early studies done by White and Panjabi [31] showed different results for the IAR of the lower cervical spine. They located the IAR at the anterior side of the vertebral body and clearly on the caudal vertebrae in the vertical direction. This would lead to a more gliding motion, which is contradictory to the previously described study (cf. fig. 2.18).

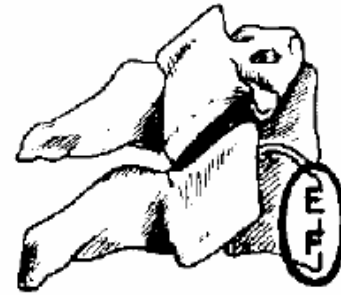


Fig. 2.18: IAR in flexion-extension proposed by White et al.[32]

**Rotation**

In most studies, to determine IAR for flexion and extension a lateral radiograph of the subject is taken in the extreme position. A simple superposition of the two images is sufficient to deduce the centre of rotation. For axial rotation this technique is useless, because images should be taken in the transversale plane. Visualising the vertebral motion is only possible with CT; transversal slices of the spine can be mapped and then a similar graphical superposition technique is

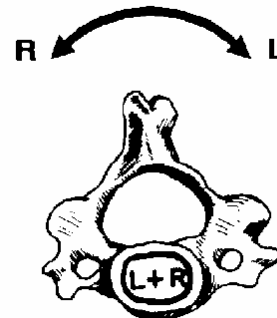


Fig. 2.19: Early estimation of the IAR in axial rotation [32]

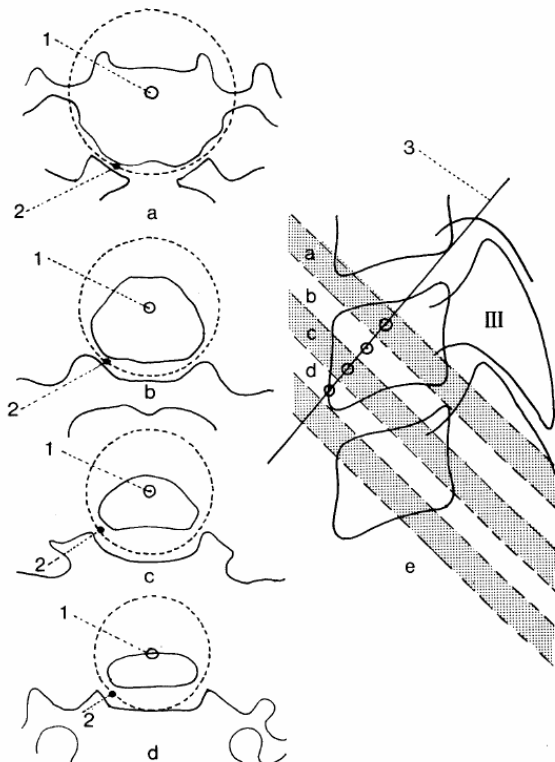


Fig. 2.20 : IAR proposed by Penning [21]

employed to determine the movement. CT has become popular only in the recent past and thus there are few studies. Nevertheless White and Panjabi [32] suggested already in the 1970ies an IAR for the axial rotation. They located it in the area of the intervertebral disc (cf. fig. 2.19).

Later studies using CT analyse showed a much more complex movement, where the axis of rotation is not strictly in the vertical axis. Penning [21] proposed, in accordance with different other studies, an axis of rotation clearly inclined backwards. An explanation could be found analysing the vertebrae shape: The axis of rotation is nearly perpendicular to the plane of the uncovertebral joints,

which inhibits simple axial rotation (cf. fig. 2.20).

Axial rotation is coupled with a lateroflexion in the same direction. This movement is also assisted by the musculature; to induce rotation, dorsal, diagonally arranged muscles are contracted.

### Lateral Bending

Lateral bending does not exist as an isolated movement; lateral translation and axial rotation is always coupled. Lysell proposed an axis of rotation close to the one for axial rotation. In his experiments he placed metall balls in the vertebrae and detected that the one in anterior part of the vertebral body didn't moved in axial rotation or lateroflexion. Therefore both axes have to pass through this point. The axis can't be horizontal because of the uncinate processes. The proposed axis of rotation in lateroflexion is slightly flatter than those of the axial rotation.

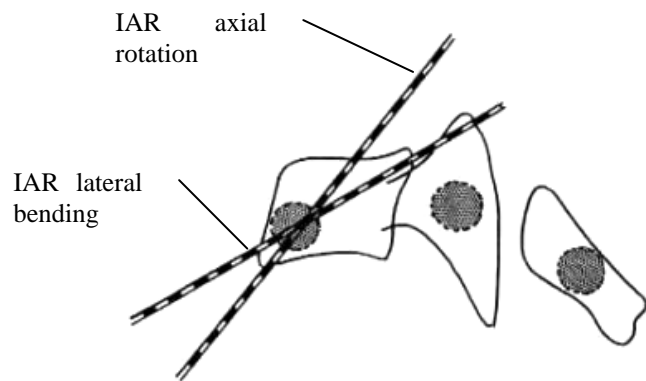


Fig. 2.21 : IAR in axial rotation and lateral bending [21]

## 2.3.3 Range of Motion

### Flexion/Extension

Range of motion can be found in a large number of publications. An overview of studies from the last 100 years is given in a publication of Watier [31].

In a study done by Panjabi et al. [17] data from different ROM measurements are listed and classified to in vitro and in vivo experiments.

The results of three in vivo and an in vitro study are showed in the diagram below; the indicated values are the complete extent between maximum flexion and maximum extension. Comparing the three in vivo studies done by White, Dvorak and Penning we find a good correlation between these experiments. The highest ROM is in the first two levels between occiput and C1 and C1/C2. The lowest value is measured on level C2/C3 and increases again moving caudally. C4/C5 and C5/C6 have the highest ROM of the middle and lower cervical spine. The showed in vitro experiment has significantly lower values from C2 downwards. In this study, the spine was loaded with a maximum torque of 1 [Nm] to avoid damaging any structures.

Except from level C0/C1, the motion in flexion is higher than in extension. In contrast, Panjabi [17] found on C0/C1 a rotation angle in extension two times of that in flexion.

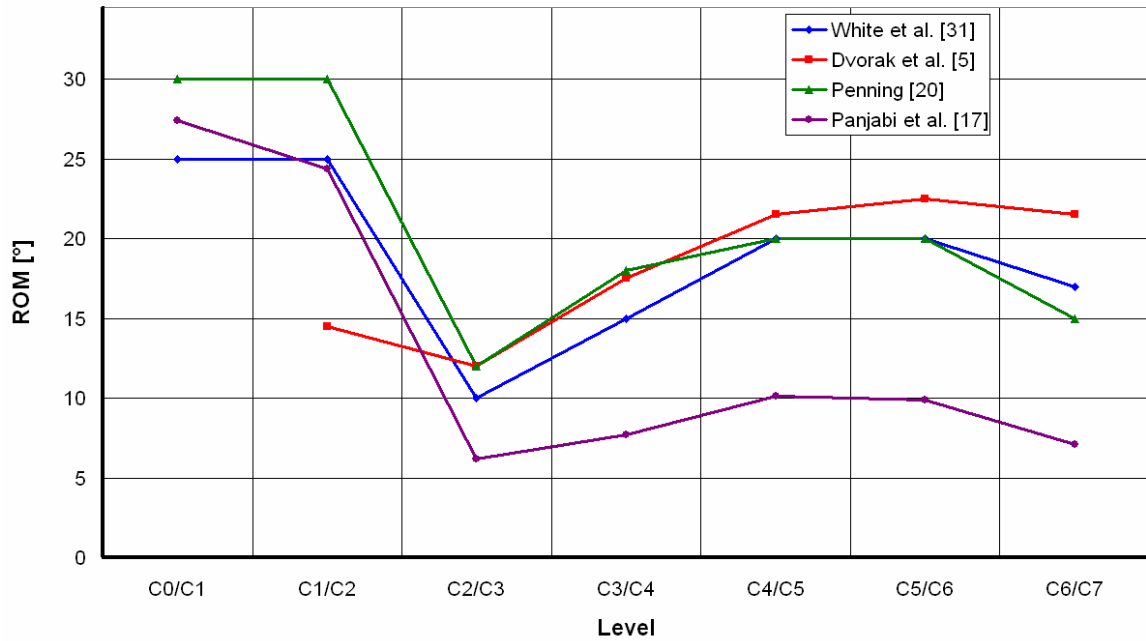


Fig. 2.22: ROM in flexion-extension (extent from maximum flexion to maximum extension)

### Rotation

As mentioned previously, the main part of ROM for axial rotation is in the C1-C2 level, where the atlas, the only vertebrae without vertebral body, rotates about the dens axis. In the other parts of the cervical spine the ROM is very limited; relative rotation for a FSU is highest in the middle region and decreases moving caudally. The occiput-atlant joint offers only a small ROM, because flexion/extension movement is already permitted over a wide range. The data presented in the following graphic are taken from [32] and [20].

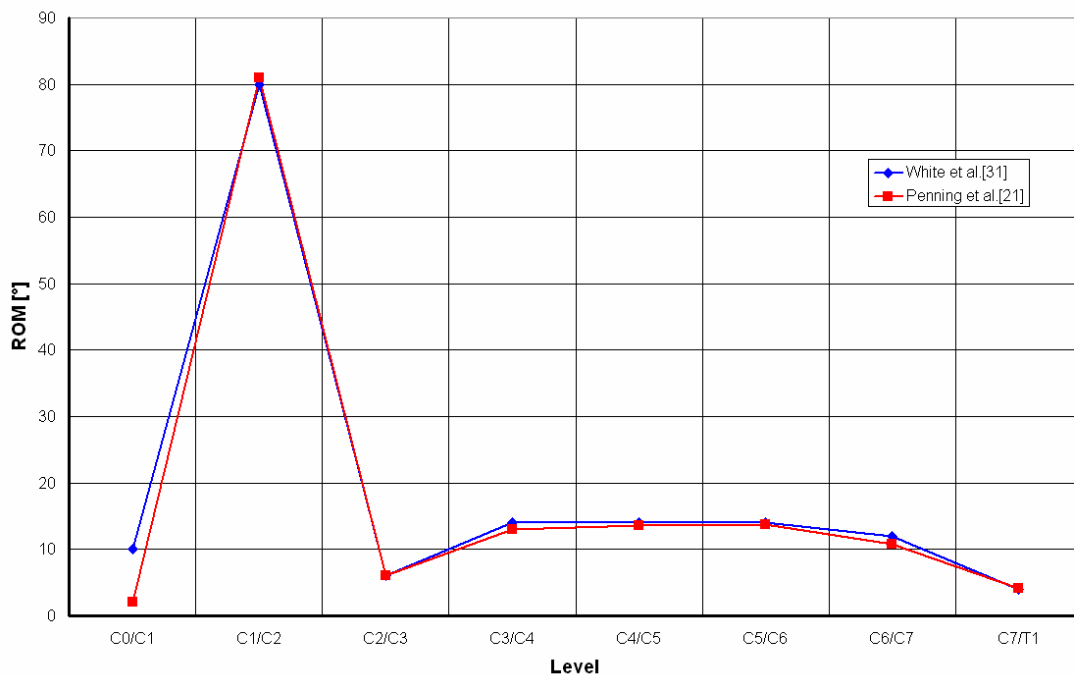


Fig. 2.23: ROM in axial rotation (extent from maximum left to maximum right axial rotation)



### Lateral Bending

Values for ROM in lateral bending are difficult to find; reviewed studies in Watier’s [31] study give a large range of results without indication about methods or subjects state. Values from Watier and Penning are taken from this publication. The third data set is taken from a study done by White et al. [32]. The other values are taken from a book of Szpalski et al. [28]; he indicates minimum and maximum values for each joint.

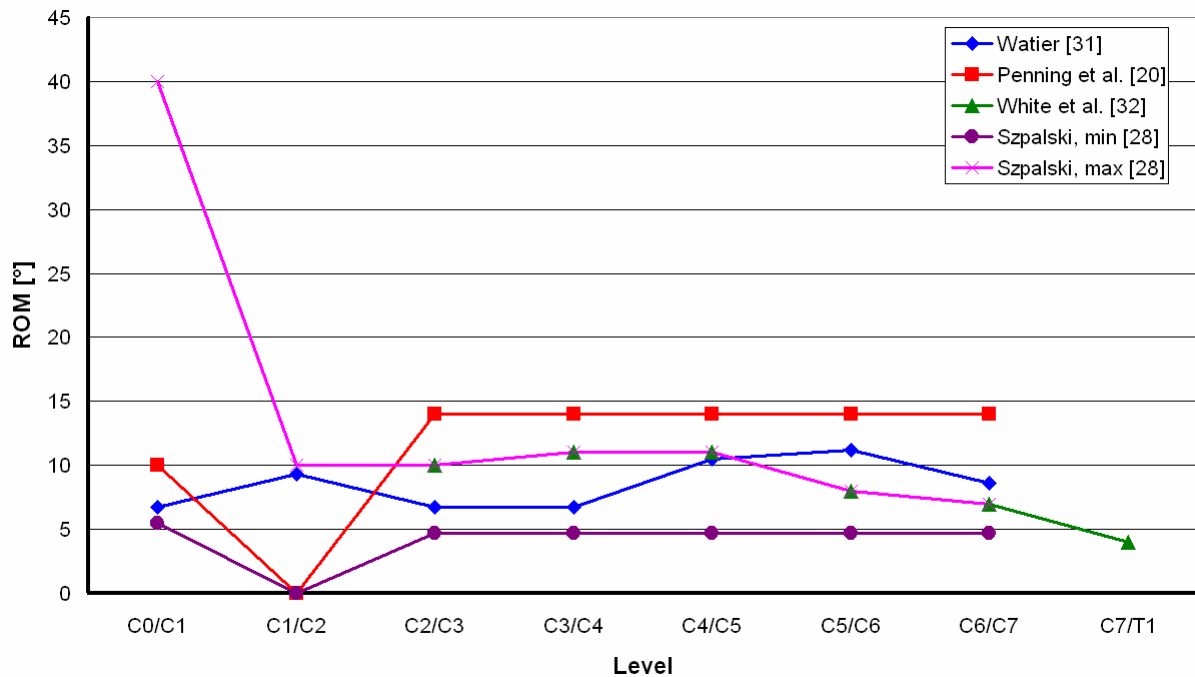


Fig. 2.24: ROM in lateral bending (extent from maximum left to maximum right lateral bending)

The lowest ROM is found at C1/C2 in Penning’s and Szpalski’s (minimum values) studies; this is in accordance with qualitative statements from various anatomy books and coherent with the geometry of these vertebrae. Only Watier indicates a higher ROM on C1/C2 than on the adjacent levels. The joint between the occiput and the atlas has a ROM of 5 to 10°; Szpalski’s maximum value is unrealistic for a healthy spine. Penning’s and Szpalski’s (minimum) values for the middle and lower spine are equally distributed from a global measured ROM. In the same region Watier found an oppositional behaviour in comparison with White’s results: in the former study the maximum is on C5/C6 and the lowest values are at C2/C3 and C3/C4. White found nearly equal values for the three joints from C2 to C5 and decreasing values moving caudally.

### 2.3.4 Load-Displacement Properties of the Spine

#### Flexion/Extension

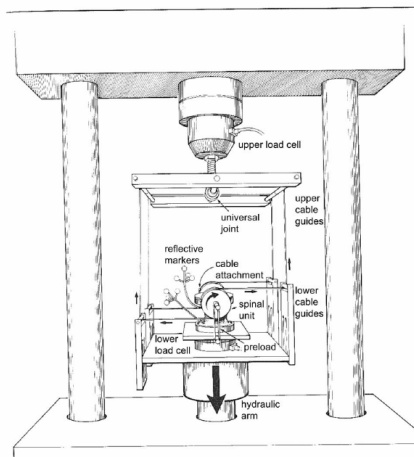


Fig. 2.25 : Test setup for flexion-extension measures, modifiable for lateral bending and axial rotation tests [31]

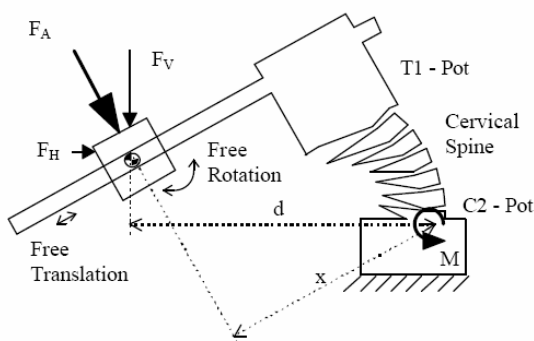


Fig. 3. Force vector diagram showing correct way to calculate the moment at the base of the spine.  $M = F_A \cdot x$

Fig. 2.26: Setup with rod instead of cables, used for flexion-extension tests [7]

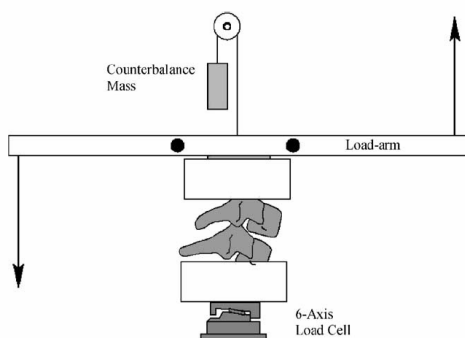


Fig. 2.27: Third test setup; for small rotations the method is equal to the first setup [12]

#### Methods

Many studies have been made to find load-displacement behaviour of motion segments or spinal regions on cadaver. ROM and the NZ were measured, thereby the stiffness can be determined.

There are several different systems for data collection. One of these uses a cable-disc system; the caudal end is fixed on a load cell, on the opposite end discs are attached. A moment is induced by pulling a cable which is wound on the disc. The idea of this construction is to have a pure moment (cf. 2.25).

The second system uses a shaft instead of disc and cable. The caudal end is again fixed on a load cell and the shaft is fixed on the cranial end. A linear actuator, vertically fixed at a certain distance from the load cell moves the shaft. Due to a pivot and a linear bearing only a vertical force is transmitted, thus a pure moment acts on the spine. Because the moment is not constant through the spine, it is fixed upside down to have the maximum torque in the lower regions (cf. 2.6); the moment is:

$$M = F_A \cdot x$$

The distance is actually increasing towards the lower vertebrae (not correctly represented on the drawing).

A further system operates with a shaft horizontally fixed on the cranial end of the spine or motion segment. To balance setup induced loads a counterbalance mass is attached. A moment is applied by pulling in both ends of the shaft in opposite directions. The vertebrae are in general put in a small pot and this pot is filled up with a polymer. In all reviewed papers forces were detected with an attached 6-axis load cell. Spatial displacement is in general collected by optical instruments.

Also publicised studies of in vivo measurements exist, but interpretation of these results is difficult in this context.

**Results**

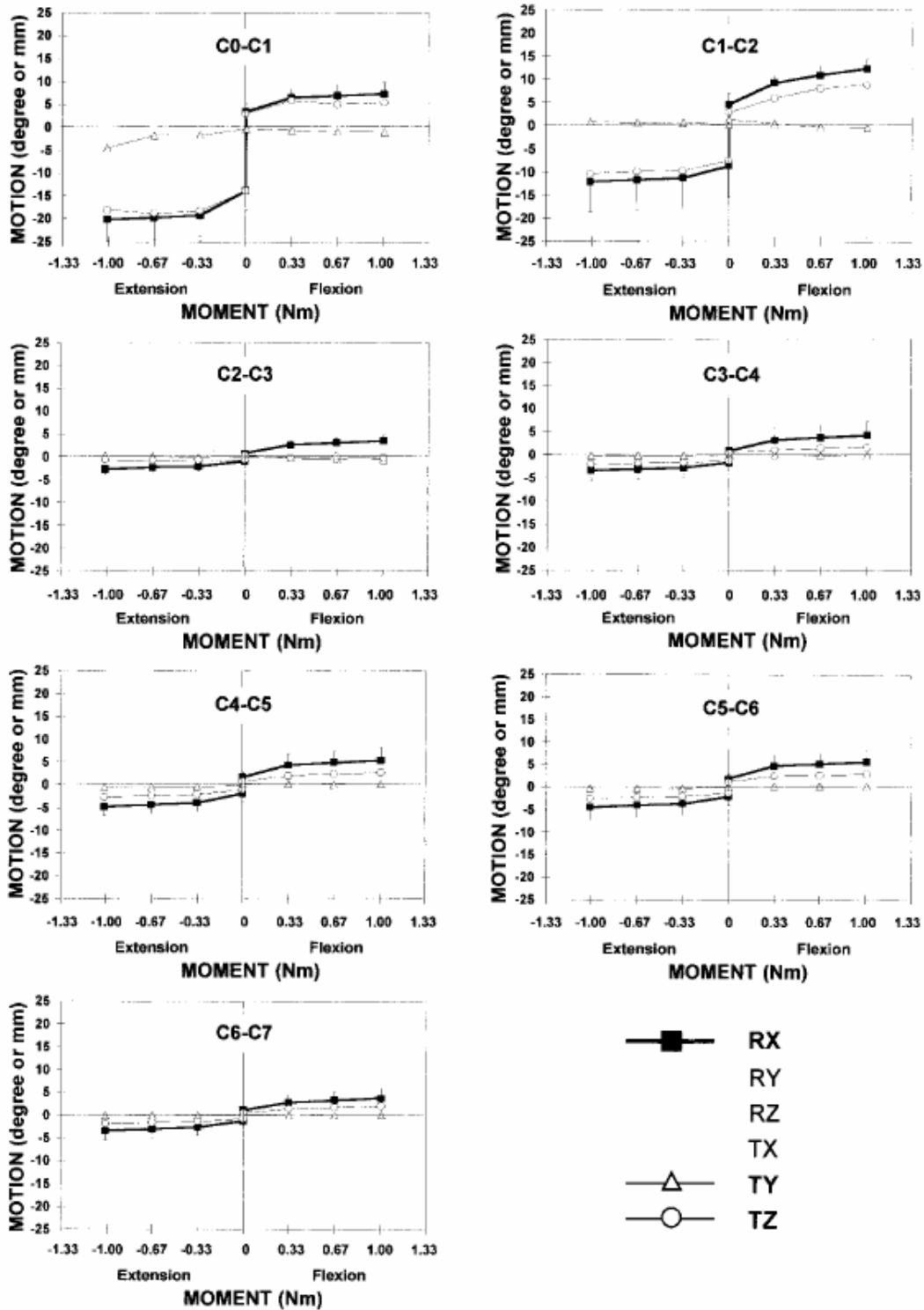


Fig. 2.28: Load displacement curves for flexion-extension. The main motion is represented by a thick line, coupled motions by thin ones [17]

The neutral zone was found to be especially high in C0-C1 and C1-C2 joints; a mean of 17.2° NZ with a total ROM of 27.4° for C0-C1 and 13.3° with 24.4° was measured by Panjabi et al. [17]. In the middle and lower cervical spine the NZ is only 1 to 4°. For all FSU a maximum torque of 1 [Nm] was applied. Results of a study done by Nightingale [12] are showing contradictory results; interestingly flexion seems to be predominant in younger subjects, whereas in older specimens, as in Panjabi's study, the extension part is more important. The maximum of applied moments was 3.5 [Nm] in Nightingale's study.

The following figures show measured force-displacement curves of these two studies. In the first one data for each FSU is represented, in the second one only C3/C4, C5/C6 and C7/T1 (C0-C2 is not of interest in this case) are shown. Furthermore these curves are interpolated from the point measures

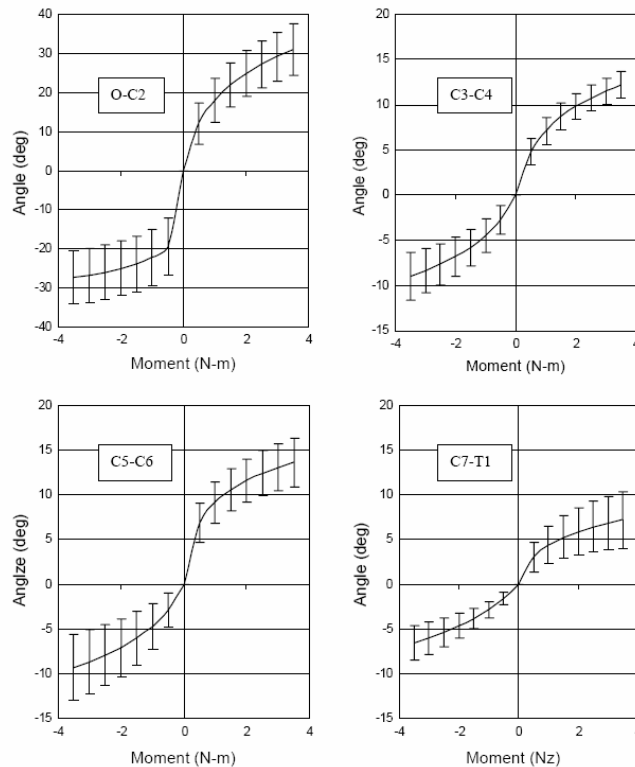


Fig. 2.29: Load-displacement curves for flexion-extension; interpolating model for measured values [12]

Rigidity increases significantly with cumulative flexion and extension, which is a typical property of the ligaments and an efficient protector for excessive movement. Nightingale proposed in his publication a logarithmic model for the load-displacement curve. It has the form:

$$\theta = A \ln ( B M + 1 )$$

Where  $\theta$  is the angle,  $M$  the moment and  $A$  and  $B$  are the parameters of the model. The angular stiffness can be determined by differentiating the inverse function.

$$k = \frac{dM}{d\theta} = \frac{d}{d\theta} \left( \frac{1}{B} \exp\left(\frac{\theta}{A}\right) - 1 \right) = \frac{1}{AB} \exp\left(\frac{\theta}{A}\right)$$

A similar study was done by Wheeldon et al. [33], but in contrast to Nightingale's study, he didn't examined only female subjects, but specimens of both genders. The angle of rotation was lower for a same applied moment in this case.

The calculated parameters are:

	Flexion				Extension			
	[12]		[33]		[12]		[33]	
	A [°]	B [(Nm) <sup>-1</sup> ]	A [°]	B [(Nm) <sup>-1</sup> ]	A [°]	B [(Nm) <sup>-1</sup> ]	A [°]	B [(Nm) <sup>-1</sup> ]
C2 – C3			4.56	3.22			-1.90	-6.35
C3 – C4	4.59	3.72	2.63	11.78	-4.66	-1.64	-2.50	-2.56
C4 - C5			2.94	7.34			-3.54	-1.36
C5 – C6	3.73	10.65	4.02	5.25	-4.76	-1.70	-2.04	-4.44
C6 – C7			4.58	2.83			-1.96	-8.42
C7 – T1	2.48	4.90	1.56	8.72	-4.85	-0.81	-4.76	-0.45

The stiffness graphs for Nightingale’s parameters are shown in the figure below. Because of the method to obtain the graphs, absolute values should be read with care.

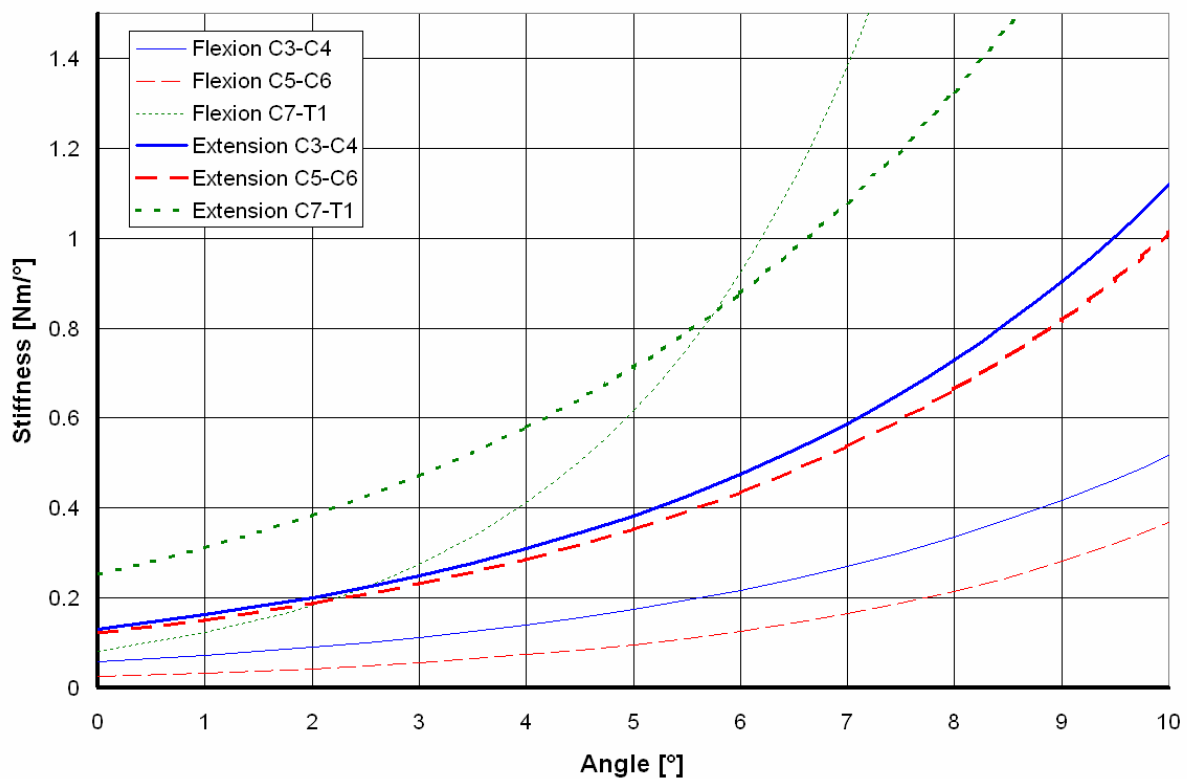


Fig. 2.30: Stiffness in flexion-extension; derivative of the mathematical model proposed by Nightingale [12]

Comparing the values for flexion and extension, the extension stiffness appears to be clearly higher. The lowest level is clearly the stiffest, rigidities of C3/C4 and C5/C6 are similar. From Panjabi’s study determined stiffness (at C5/C6) is the same around 3° of deformation (all values in [Nm/°]):  $k = 0.11$  for flexion,  $k = 0.2$  for extension. For further rotation, the stiffness is increasing more rapidly. At 4° extension  $k = 0.9$  and at 6° flexion  $k = 0.6$ .

**Influence of fusion on stiffness**

In a study mentioned previously [24], stiffness was found not significantly higher for a constant global angle of rotation for any fused level.

**Rotation**

Load-displacement behaviour in axial rotation is quite similar to those on flexion/extension; a neutral zone is followed by an increasing stiffness. The NZ is the highest at C1/C2 with a value of about 40° and makes the major part of the ROM on this level. All other levels have clearly lower NZ and ROM, but in contrast higher stiffness.

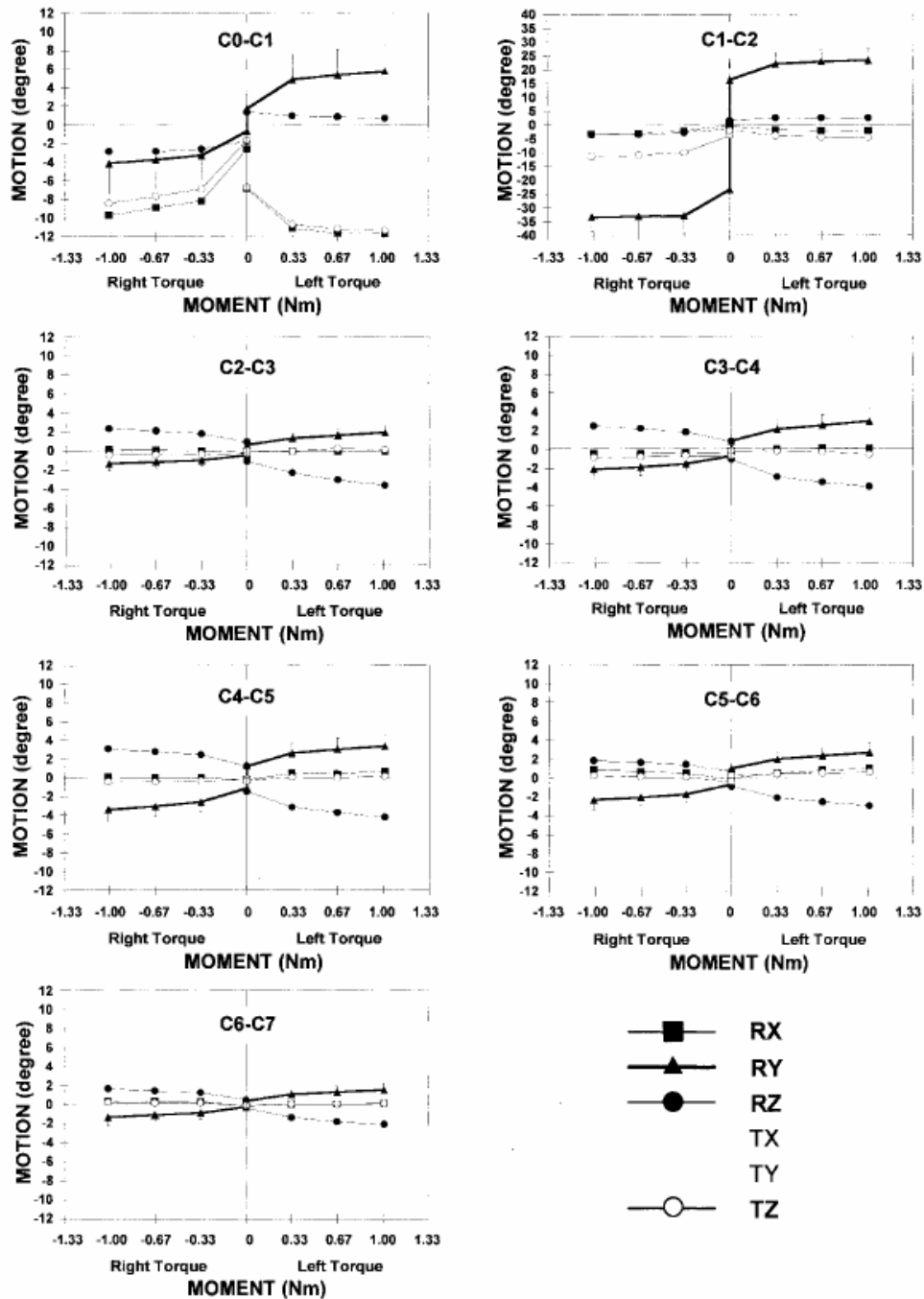


Fig. 2.31: Load-displacement curves for axial rotation. The main motion is represented by a thick line, coupled motions by thin ones.

The load-displacement curves shown in the graphic above are from reference [17].

In the middle and lower cervical spine, the maximum ROM is on C4/C5, lowest are C2/C3 and C6/C7. The stiffness, determined from the graphics above, is about 1.3 [Nm/°] on C2/C3 between 1 and 2° rotation. For the same value of rotation on C4/C5 the stiffness is only 0.22 [Nm/°] and increases to 0.67 [Nm/°] for angles around 3 to 4°.

The thin lines on the graphic above are the coupled movements. Notable is the important translation C0/C1 in the z-direction (laterally). With exception of the first to levels, a coupled flexion/extension rotation in the same order as the induced movement is present.

### Lateral Bending

In lateral bending the NZ and ROM is limited; in contrast to axial rotation and flexion-extension, no joint facilitates particularly the lateroflexion. On C0/C1 and C2 through C5 the measured NZ is around 4°. The value decreases from C5 downwards, also C1/C2 has a smaller value.

From the graphics derived stiffness are: on C2/C3 about 0.2 [Nm/°] in the range from 2 to 5° rotation, 0.6 [Nm/°] for further motion; this level has a rather small stiffness compared to the others. One of the stiffer levels is C6/C7: a mean value in the range from 1 to 2° is about 0.25 [Nm/°] and for further rotation about 1.3 [Nm/°].

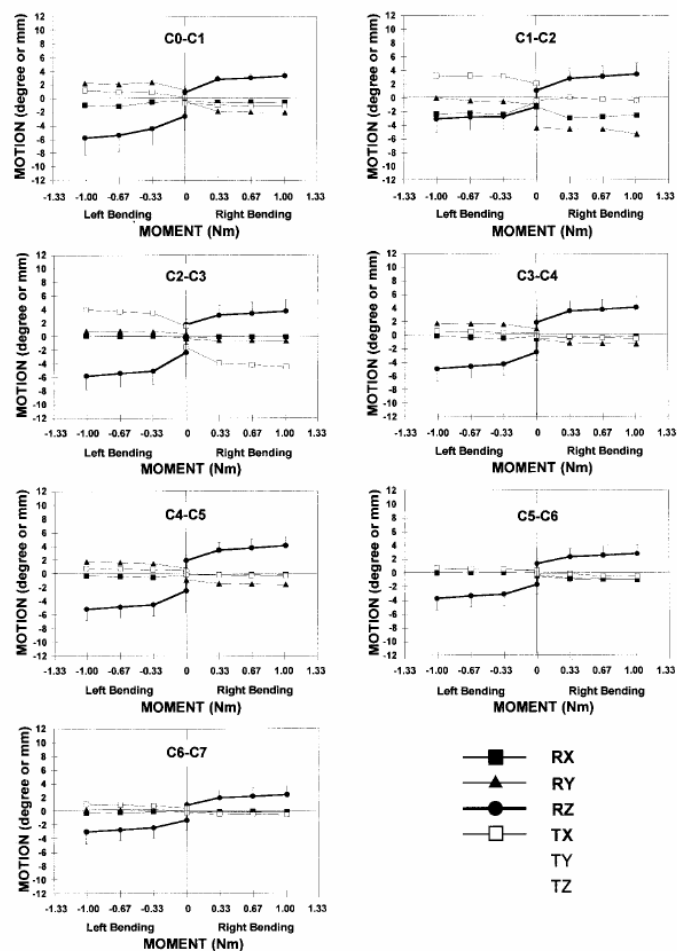


Fig. 2.32 : Load-displacement for lateral bending [17]. The main motion is represented by thick lines, coupled motions by thin ones

## 2.4 Expected Axial Forces in the Cervical Spine in Static Postures

Actual in vivo forces in the spine are almost impossible to determine. Only some rare cases are known where researchers implanted a system to measure the in vivo pressure in the intervertebral disc. In this case, forces can be derived knowing the section of the disc [1]. The application is extremely limited; also the known studies are concerning the lumbar spine. Nevertheless, the loading of the intervertebral disc can be estimated at least in static cases, by analysing geometry of the spine and the most important muscles and calculating the equilibrium.

Such a study is presented in publication lead by Snijders [42]. The cervical spine is divided into several motion segments; the middle and lower spine (C3 – C7) is condensed as one element, but of variable length. The elements of the upper cervical spine are all separate: axis (C2), atlas (C1) and the occiput (C0). There are fixed cinematic relations between the elements for flexion and extension motion (relation of the angles is constant). Four muscles (pairs of muscles respectively) have been chosen to be modelled. The selection criteria were the lever arm and the muscle section found in anatomy text books.

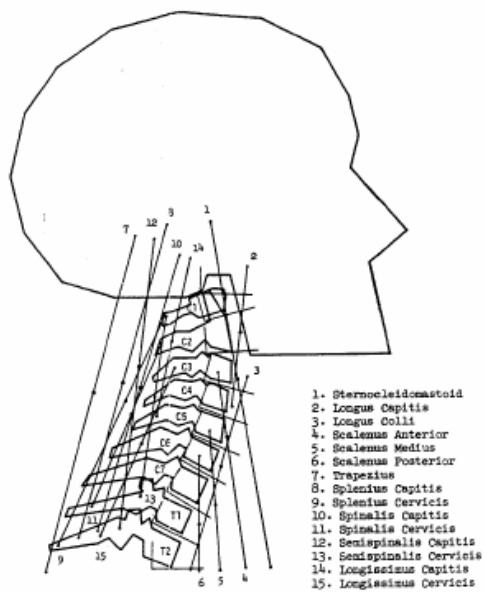


Figure 2.33: Schema of the musculature of the cervical spine and the head [44]

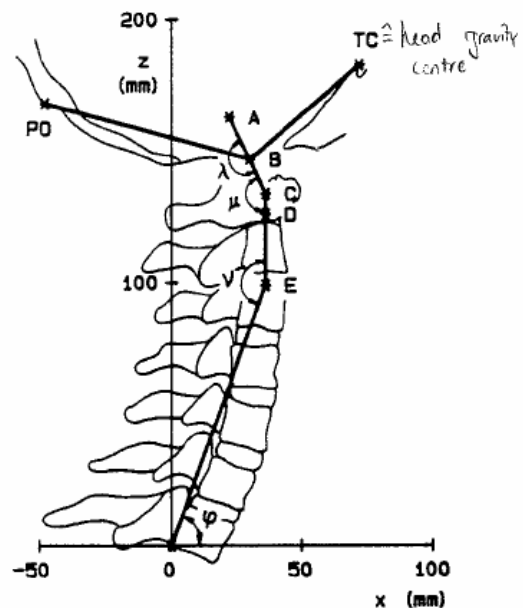


Figure 2.34: Lateral view of a biomechanical model to study static forces [42]

The system of forces to solve (joint reaction forces and muscle forces) is underdetermined. The chosen solution is the one where the joint reaction force in the atlanto-occipital joint is the smallest.



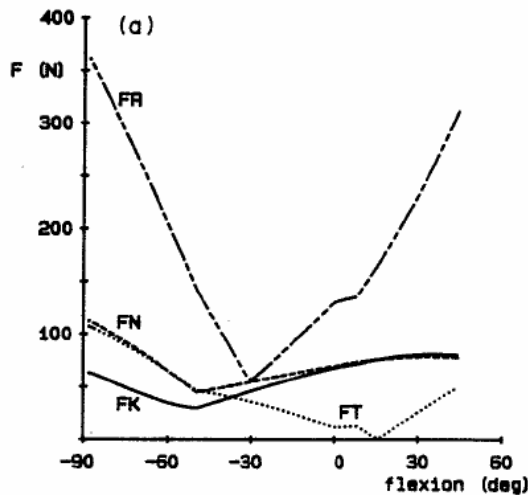


Figure 2.35: Joint reaction forces in function of the flexion/extension angle in the presented biomechanical model [42]. Positive values is flexion motion, negative values is extension.

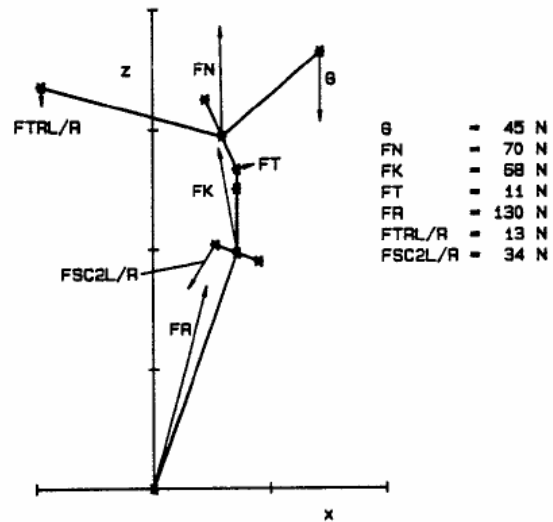


Figure 2.36: Joint reaction and muscle forces in neutral position [42]

The joint reaction force at C7-T1 is the most interesting value in our case. The force is considerable at neutral position. It increases under flexion motion and decreases until the minimum value at an extension angle of 30°. For further extension, the force increases again. The joint reaction forces are - for each joint – always in the same direction, i.e. the forces are compressive. Inverse loading is not observable in daily situations, but can occur in particular cases, as car accidents for example (whiplash).

The compressive load in the C7-T1 joint is 130 [N] at the neutral posture. A similar value is found by Keller [43] in a more simplified biomechanical model; 120 [N] on this level. Furthermore this study shows, that the load from the C2-C3 joint down to C7-T1 is nearly constant. This result seems to be plausible regarding the low curvature in the middle and lower cervical spine.

Joint forces in the cervical spine are distributed on the intervertebral disc and the facet joints. Pal and Routal [13] analysed the contact area of the facet joints and the intervertebral disc and deduced the load distribution, based on the assumption, that the pressure is constant on a level. They found 54% of the load being transmitted through the intervertebral disc and the vertebral body. In fact, the structure of the pedicles is much more robust than the vertebral body, it can thus be suspected, that the actual load distribution is different, with a higher concentration on the posterior elements. Pal and Sherk [14] found 36 % of the load passing through the vertebral body. The value was found by measuring the force in the anterior and posterior column of a loaded cervical spine separately.

It can be concluded, that at neutral position, the intervertebral disc supports a load of about 45 [N].

This distribution is valid for the neutral position; it is supposed that it changes when moving the spine.

## 2.5 Pathology

The following list of cervical spine pathologic cases does not pretend to be complete, but is an overview of diseases, interesting in the point of view of surgical intervention, in particular with anterior instrumentation.

Many of the described pathologic cases are not strictly independent from others and also the classification is not absolute.

### 2.5.1 Degenerative Diseases

#### Degenerative Disc Disease (DDD)

Degeneration of the intervertebral disc, called degenerative disc disease (DDD), is a common, but not exclusive disorder of the lower spine, where the loads are important. Disc degeneration can lead to disorders such as spinal stenosis, spondylolisthesis, and retrolisthesis. Actually, DDD is not a disease but, rather, a degenerative condition. Essentially the disc loses the usual mechanical properties as a spring and damper element; with a decreasing stiffness the disc also sinks down.

Disc degeneration is a normal part of ageing; only secondary effects affect subjects and can cause painful conditions. Typically the degenerated disc exerts stress on the spinal canal.

A part from usual ageing DDD can be accelerated by excessive stresses. Disc repair is in general slow but not impossible.

#### Spinal Disc Herniation

Spinal disc herniation is also known as radiculopathy, prolapsed or ruptured disc. A tear in the outer, fibrous ring allows the inner nucleus pulposus to be extruded. The created bulge exerts a pressure on the nerve root, which causes the pain.

Disc herniation can be effect of ageing (loss of elasticity) or excessive stress (trauma, applied loads).

#### Spondylosis

Spondylosis is a degeneration of the vertebral processes and formation of osteophytes, an ossification of soft tissues. This natural process of aging can be accompanied by a herniation of the nucleus pulposus. Usually this degeneration causes pressure on the nerves which finally generates pain, sensory and motor disturbances. Often axial rotation and lateroflexion is disabled.

#### Spinal Stenosis

Spinal stenosis is a natural age degeneration, where the spinal canal becomes narrower and as a result a pressure on the spinal cord is exercised which generates pain. It can be caused by spondylosis or a calcification of the posterior longitudinal ligament. Spinal stenosis can also be congenital.

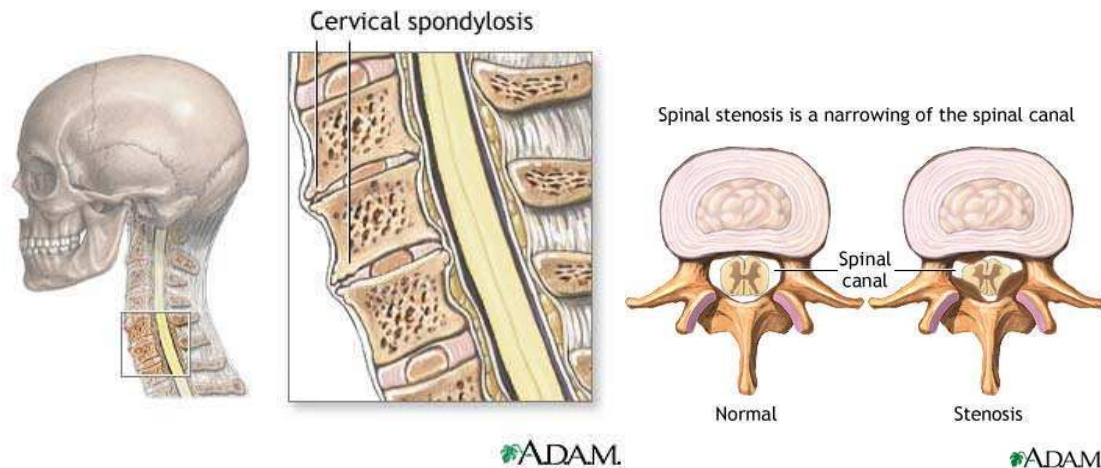


Fig. 2.37: Spondylosis [47]

Fig. 2.38: Spinal stenosis (lumbar spine) [47]

## Myelopathy

Myelopathy is basically a loss of sensation and mobility due to a disorder of the spinal cord and can be of traumatic or disease origin. Depending on the level, different body parts are affected.

## Osteoporosis

Osteoporosis, actually a typical contraindication for many systems is a typical occurrence in older people. In osteoporosis, equilibrium of bone remodelling is no longer intact; bone decomposition works faster than reconstruction. Bone density decreases and thus mechanical properties do too. Changes are not homogeneous; first cancellous bone is affected. In vertebrae osteoporosis starts anteriorly in the vertebral body, actually where bone density and mechanical properties are lowest from the beginning.

Factors for the bone remodelling cycle are mainly mechanical stress (stimulation) and different hormones. Calcium, main element for mineral part of the bone is important, but in general not a determining factor.

Osteoporosis occurs sooner or later in anyone, because it is in fact part of the usual ageing process. Especially women during their menopause are strongly affected when hormonal balance changes significantly.

## 2.5.2 Deformities

### Kyphosis

Kyphosis in the sense of a deformity is the pathologic curving of the spine, where parts of the spinal column lose some or all of their lordotic profile. Symptoms of kyphosis include mild back pain, fatigue, appearance of round back and breathing difficulties. Severe cases can cause much discomfort and even cause death.

### Scoliosis

Scoliosis is an abnormal curvature of the spine away from medial-sagittal plane. There are three causes for this deformation: abnormal development of the vertebrae or ribs, poor

muscular function or control; the idiopathic scoliosis emerges from a originally straight spine and its cause is not known.

### **2.5.3 Tumours**

Spinal tumours can primary or metastatic. Primary tumours may have their origin in any part of the spine (vertebrae, nerve root etc.); metastatic tumours have their origin elsewhere in the body. Symptoms, similar to other spinal diseases, are neck pain and numbness of the limbs. When tumours are removed in a surgical intervention, a stabilisation may be needed. The chosen approach (anterior or posterior) of the instrumentation depends on the location of the tumour.

### **2.5.4 Pathology after Surgical Intervention**

#### **Dysphagia**

Dysphagia is a difficulty in swallowing which occurs currently after anterior surgical interventions. It is caused by the lesion of the tissues, mainly the esophagus. In some cases, the problems may persist. It is theorised that plate thickness can add to dysphagia although this has yet to be clinically verified.

#### **Pseudarthrosis**

Pseudarthrosis is a relative movement of two bone parts fixed originally. This may occur after a bone fracture or after an interbody fusion when the fixation is not sufficient. In stead of a continuous ossification of the joint, only parts are ossificated and a pain is generated.

## **2.6 Surgical Treatments**

### **2.6.1 Discectomy**

Discectomy is a classic surgical procedure when the intervertebral disc is degenerated or herniated. The complete intervertebral disc is cut out and thus pressure exercised by the deformed disc on the spinal cord is released. Usually the freed space is filled with bone graft, artificial bone material or an intervertebral spacer to maintain the height. An anterior plate is sometimes inserted to give additional stability and avoid bone graft or spacer slipping. Without stabilising plate, the patient has to wear external fixation (collar) for a longer period until the joint has a continuous ossification.

### **2.6.2 Corpectomy**

Corpectomy is the removal of a complete vertebral body. It can be applied when performing discectomy over multiple adjacent discectomies, when a spinal stenosis caused by calcification is present.

Liberated space is filled with the same technique as for discectomy. Especially for corpectomy designed spacers do exist and an anterior plating system can give the requested stability.

### **2.6.3 Interbody Fusion**

Interbody fusion is the stiffening of the vertebral joint; the original degrees of freedom are blocked. This fixation may be a bone graft, an intervertebral spacer or a plating system. In any case, the goal of the intervention is to give sufficient stability that complete ossification of the joint can happen. When ossification happens, this is in general in 6 to 24 month after the operation.

### **2.6.4 Arthroplasty**

Arthroplasty applied to the spine is a newer technique. In stead of fusion of parts of the spine, the intervertebral disc is replaced by implant permitting the same degrees of freedom. This method is particularly interesting when large regions should be fused or when young subjects are concerned. Also stress on to fused levels adjacent discs is not increased. A main drawback is the wear and its associated losing of particles.

## **2.7 Anterior Plating Systems**

### **2.7.1 Principle**

Anterior plating systems are widely in use for interbody fusions and various systems are developed to this day.

Two or more vertebrae are fixed with a metal plate, which is fixed by screws entered in the vertebral body. Today used screws are unicortical and the operative risk is thus significantly reduced in comparison to posterior rod systems, where screws pass close to the spinal canal. When treating degenerative disc diseases, the intervertebral disc is in general removed and replaced by bone graft or by an intervertebral spacer. Plating systems can be used over one or more levels, but most applications are for one or two levels. Also stabilisation when performing corpectomies is possible.

The ideal construct generates immediate stability to avoid or at least reduce request for external postoperative fixation, but are not too rigid to provoke an undue stress shielding. Accordant to Wolff's law, a compressive load is needed for adequate bone modelling; and bony fusion should be the goal of any interbody fusion.

### 2.7.2 Access

A skin incision is performed laterally in the area where the discectomy or corpectomy occurs; the underlying sternocleidomastoid muscle and the tracheoesophageal bundle are separated. These tissues are then kept apart by a Caspar distractor. An excessively opened Caspar distractor can damage the esophagus. As a result of the use of the distractor, postoperative dysphagia is quite common for patients undergoing an anterior cervical treatment. Several modified techniques to reduce this problem have been found, but will not be mentioned more precisely here. Afterwards the soft tissues surrounding the vertebrae are palpated and the degenerated disc is removed. The disc is not removed completely in each case; several surgeons prefer cutting the disturbing parts only and leaving the rest of the disc instead of filling the intervertebral space with bone graft or a cage.

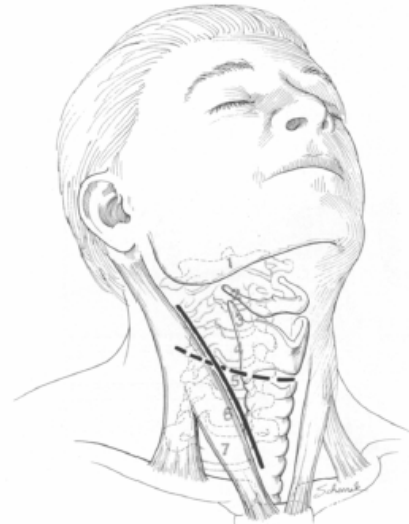


Fig. 2.39 : Incision for anterior cervical operation [3]

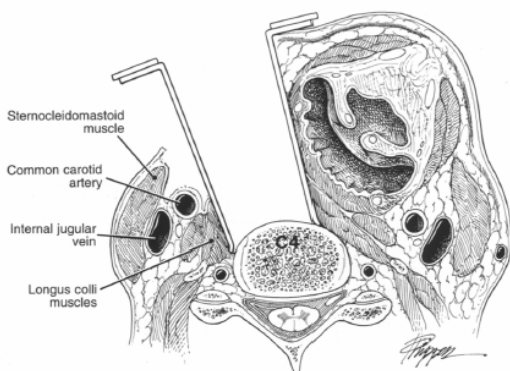


Fig. 2.40: Section view of the prepared cervical access; when a larger access is needed (instrumentation), risk for damaging adjacent soft tissues increases [3]

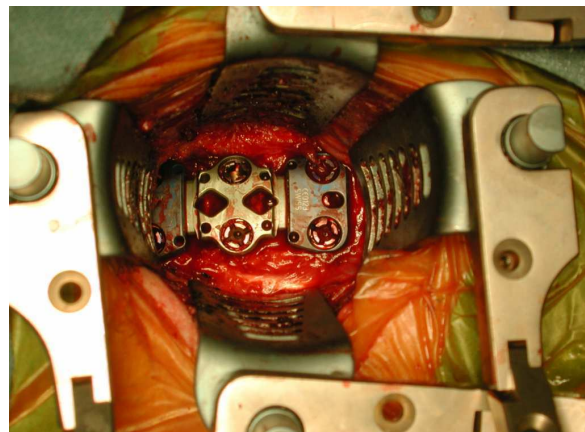


Fig. 2.41 : Distractors used on four sides for an easier access; fixed 2 level anterior plate (Vectra-T, Synthes)

### 2.7.3 Types

In the early eighties first experiences were made with anterior plating systems. Several of the early construct failed mechanically, so plates became more and more rigid. Too stiff plates have the problem, that the endplate and the inlayed bone graft or spacer are completely stress isolated. Fusion is inhibited; strong subsidence, possibly with spine deformation can occur or

a mechanical part (screw or plate) can fail because of fatigue. Today, the following systems are in use:

**Rigid systems:** Rigid fixations are still frequently used; they can be especially useful for treating deformities and trauma.

**Toggling screws:** Toggling screws may be helpful for a continually better stress distribution. They permit a settling of the bone without damaging the vertebra.

**Dynamic Plates:** A recent development leading to a similar effect as the toggling screws is the so called *dynamic plate*. In fact this nomenclature is misleading, because the system is sufficiently rigid that ossification can happen. A certain settlement of the system is permitted by modifiable screw distances, but this is on long term. The system should thus be called adaptive, but not dynamic.

### 2.7.4 Intervertebral Spacer

Intervertebral spacers are destined to fill up the space of the removed disc. They provide further stability and when a correct load sharing between the plate and the spacer is achieved, subsidence is minimal. Furthermore ossification on this level can happen when the spacer is sufficiently stressed. Hence the spacer is in general chosen slightly bigger than the actual intervertebral height. Today construct have hence a quite open design where the free space can be filled with bone graft or artificial bone - its presence seems to enforce ossification.

Some surgeons are even using spacers as stand alone constructs; so no plating systems fixes the vertebrae.

Micromotion can become a problem, as a result fusion is inhibited. Surprisingly fusion rates are similar to fixations with plating systems. The cage can be excessively charged when it is not in a stable position. Cases of implant failure have been reported.



Fig. 2.42: Intervertebral spacer (with holding tool)

### 2.7.5 Indications

The indications for anterior plating systems are various; pathology requesting cervical decompression, deformities, tumours and in some cases also traumatic indications can be treated. A contraindication is in general strong osteoporosis, which makes a correct and secure fixation of the plate impossible.

### 2.7.6 Main Drawbacks

Fixation of plating systems is difficult on the upper levels close to the mandibule and for the lower regions at the passage to the thoracic spine. A contraindication for plating systems is osteoporosis, which affects particularly the cancellous bone. In consequence unicortical screws don't provide sufficient stability.

A current complication is dysphagia; as the esophagus is directly located anteriorly to the spine, it can be affected by plates. Efforts have been made to reduce the plate height, but this is of course adversarial for the mechanical resistance. The thinnest plates on the market have about 1.5 mm thickness.

Adjacent intervertebral discs of multi-level fusions are exposed to an increased stress because of the high stiffness of the plate constructs.

### 2.7.7 Clinical Experience

Anterior plating systems are commercially available since 1980, the first documented treatments are even dating from 1964. Clinical experience is thus considerable; today systems are sophisticated and different types are obtainable, targeted for the various indications.

## 2.8 Posterior Fixation Systems

### Rod systems

Posterior rod fixation systems offer a large variability. Principally, there is no limit in the number of fused levels. Access is easy over the complete spine, not only in the limited range of the cervical spine. With the commonly used flexible rod systems, fusions from the occiput down to the sacrum are possible. The good stability permits that levels can be skipped.

A part from the rod systems, which are fixed by screws, hook systems and cable fixations are common; these systems are not depicted in a more concrete way.

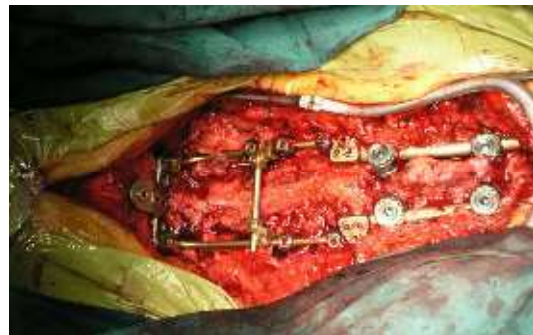


Fig. 2.43 : Posterior fixation with a rod system; the fused levels in this case are C0, C5-C7, T3 and T4



## 2.9 Zero Profile Device

The idea behind this new concept is to combine the advantages of an anterior plate and a cage. Like a plate system, the system is rigidly fixed to the vertebral body with screws, micromotion and thus increased device fatigue and bone destruction is limited. In contrast to a plate this new system is very unobtrusive and in this respect is similar to a standard cage. Persistent effects on surrounding soft tissues, in particular the esophagus, should be avoidable with such a device.

The device is divided in a plate and a cage part; their functions are identical to classic anterior interbody fusions. The plate is made of material with high mechanical properties (titanium); the cage is a softer material, more favourable for bony ingrowth. Another reason for choosing rather a polymer than a metal is the radiolucent behaviour on radiographs. Large metal implants are in general disturbing because they create artefacts. The cage part has an angular degree of freedom to have compressive stress only.

The approach is identical to classic technique only that spatial request at the anterior side of the vertebral bodies is smaller.

In contrast to classic plates the new device is not intended to use for corpectomy. Bone quality has to be sufficient; similar to anterior plates, osteoporosis is a contraindication because unicortical screws can't find enough mechanical resistance.

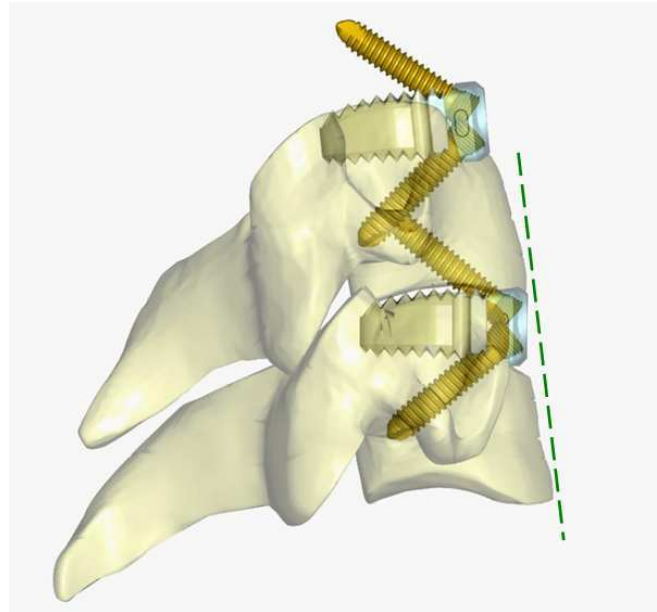


Fig. 2.44: Principle of a zero-profile device; it doesn't preside over the vertebral body, soft tissues should thus not be irritated.

## 2.10 Quantitative Aspect of Anterior Interbody fusions

Shape and geometry of vertebrae vary greatly. From an economic point of view it is not possible to offer absolutely matching implants in each case. It is necessary to optimise the product so that most patients can be treated. Nevertheless, a device should be as general as possible to be used by surgeons.

Interbody fusions of the cervical spine are mostly done on two of the lower levels: the most operations are on C5/C6, slightly more than C6/C7. The reasons will not be debated herein. Some figures taken from different publications shall prove the previous statements. The numbers brought together concern only anterior fusion techniques. The anterior methods are not further distinguished and are sums of one- or multi-level fusions.

	C3/C4	C4/C5	C5/C6	C6/C7	C7/T1	Total
[27] <sup>1)</sup>	0	9	22	16	0	47
[30] <sup>2)</sup>	10	14	47	34	1	106
[26] <sup>3)</sup>	7	11	28	14	0	60
[28] <sup>4)</sup>	3	18	94	74	3	196
[28] <sup>5)</sup>	0	4	13	12	1	35
[28] <sup>6)</sup>	1	9	51	73	2	142
<b>Total</b>	<b>21</b>	<b>65</b>	<b>255</b>	<b>223</b>	<b>7</b>	<b>571</b>
	3.7%	11.4%	44.7%	39.1%	1.2%	

- 1) Anterior plate fixation; including one and two level fusions
- 2) Titanium cage
- 3) Plate systems, one level fusion
- 4) BAK-C Cage
- 5) Plating system
- 6) Carbon fiber cage

## 2.11 Summary and Conclusions

Shape and material properties of the cervical vertebrae underlie a large variation; mean values of the body dimensions of normal spine has been presented previously as well as the range of modulus and mechanical strength of cancellous and cortical bone.

The cervical spine has been recognised as one of the most complex kinematical elements of the musculo-skeletal system. Its main elements are the vertebrae (resist compressive forces, give shape), the intervertebral discs (permit spine mobility), the ligaments (resist tensile forces, limit mobility) and the muscles (active element). Motion can't be limited on a single level, it concerns always a whole region of the spine. Also motion can't be reduced to a simple rotation or translation, but is always coupled.

Studies about range of motion (ROM) of the main motions have been presented and stiffness analysed. In general, lower cervical spine segments are more limited in their ROM for flexion-extension and axial rotation. For both motion types, a joint in the upper cervical spine is particularly enabling this mode. In lateral bending the ROM is more or less distributed equally on all levels.

Most anterior instrumentations concern the levels C5/C6 and C6/C7, over 80 % (including multi-level fusions). The focus for the implant development shall be on these levels, even if the other levels can't be completely disregarded.

### 3 BIOMECHANICAL TESTS

#### 3.1 Introduction

As mentioned previously, the cervical spine is one of the most complex parts of the human musculoskeletal system. Motion is rarely a simple rotation or translation. Also vertebral bone is largely inhomogeneous and anisotropic, so developing a mathematical models is difficult and time intensive.

A physical model is a simplification as well, but can be an effective aid in understanding mechanisms and comparing devices. Test results should never be understood as absolute or directly transferred to clinical application. The goal of the tests describe in this section are to relate the new SynFix-C device to existing plating systems, where clinical studies are already available. In addition several parameters such as screw length and diameter will be evaluated.

The summarized goals of the mechanical tests are:

- relate the new device to clinical known systems
- test the influence of screw length and diameter
- better understand failure mechanisms
- better understand the bone - implant interactions.

The tests were typically performed for:

- compression (eccentric load)
- tension (eccentric load)
- axial rotation
- push-out
- subsidence

#### 3.2 Acceptance Criteria for the Tests

In the following table the test acceptance criteria are presented.

Test	Compared Device	Compared Value	Criteria
Compression	Anterior Plate	Initial Stiffness (k)	$k_{\text{SynFix-C}} \approx k_{\text{compared device}}$
Tension	Anterior Plate	Initial Stiffness (k)	$k_{\text{SynFix-C}} \approx k_{\text{compared device}}$
Axial Rotation	Anterior Plate	Initial Stiffness (k)	$k_{\text{SynFix-C}} \approx k_{\text{compared device}}$
Push-out	Standard Cage	Initial Stiffness (k), Maximum Force (F)	$k_{\text{SynFix-C}} > k_{\text{compared device}}$ $F_{\text{SynFix-C}} > F_{\text{compared device}}$
Subsidence	Standard Cage	Subsidence at 50 [N] (s), Subsidence Rate (t)	$s_{\text{SynFix-C}} \leq s_{\text{compared device}}$ $t_{\text{SynFix-C}} \leq t_{\text{compared device}}$

### 3.3 Testing Standards

In general recommended testing standards have been adopted to aid in comparing with historical testing and to simplify the set-up process. Currently used testing standards are defined by the American Society for Testing and Materials ASTM. These standards define test set-ups, test methods, data analysis and specifications for testing machines. These standard do not however formulate any benchmarks. Acceptance criteria and benchmarks are explicitly left to be defined by the user.

#### **Norm for use of Foam Material as a Bone Model: ASTM F 1839-01 – Standard Specification for Rigid Polyurethane Foam for Use as a Standard Material for Testing Orthopaedic Devices and Instruments**

The proposed foam possesses mechanical properties which are on the order of those reported for human cancellous bone. Different grades (densities) and there corresponding mechanical properties are listed. A grade 15 foam has been chosen for the following tests. This grade has been in use historically for testing of spine products. The largest clinical disparity between the form and human bone is the lack of a cortical shell.

#### **Testing Norm for Subsidence Measuring: ASTM F 2267-04 – Standard Test Method for Measuring Load Induced Subsidence of Intervertebral Body Fusion Device under Static Axial Compression**

This standard is proposed for testing subsidence of non-biological intervertebral body fusion devices under static axial compressive load. Two methods are proposed for the test: Axial compression between metal blocks to measure stiffness of the device and axial compression between foam blocks to determine sensitivity for subsidence. Only the latter method is of interest for our experiments. A grade 15 (ASTM 1839-01) is recommended for this purpose.

#### **Norm for Testing Spinal Implants: ASTM F 1717-04 - Standard Test Methods for Spinal Implant Constructs in a Vertebrectomy Model**

The ASTM F 1717 standard covers a large number of tests for spinal implant components. The set-ups, including dimensions, are for lumbar, thoracic and cervical spine devices. Static and dynamic (fatigue) tests are proposed. The tests are designed to compare existing and future products. The set-up does not represent the complex motion of the cervical spine and also does not set a benchmark. The standard could be used for anterior as well as for posterior fusion devices.

The implants are suggested to be fixed in PE or equivalent material; this means that the test focuses on the implants intrinsic properties.

## 3.4 Test Planning

### 3.4.1 Tested Specimens

One of the goals of these tests is to get information about the importance of screw size, the number of screws and to compare the new product to existing ones. Basically all configurations are examined in each test, except where it makes no sense.

The following screw dimensions are tested (prototype with 3 screws):

- 2.4/16 (diameter in [mm]/ length in [mm])
- 2.7/12
- 2.7/14
- 2.7/16 (“standard screw”)
- 2.7/18
- 3.0/16

Prototype with 4 screws:

- 3.0/16

In the following, the SynFix-C will be abbreviated and the screw dimension coded:

→ SF 015-2.7-16

First, the the prototype number (015) is indicated, then the screw diameter (2.7 [mm]) and then the screw length (16 [mm]).

For comparison, the following reference systems are tested:

- CSLP Small Stature (Synthes)
- Vectra (Synthes)
- Zephir (Medtronic)
- Cervios (Synthes)

Cervios is used as the intervertebral spacer for all plating systems.

All tested prototypes and compared systems are again summarised in the annexe (cf. annexe p 116).

SynFix-C is also tested with a one-side rigid fixation to compare the one-screw to the two-screw interface.

Rotation, compression and tension are performed with all specimens except the Cervios as a stand-alone cage.

The existing set-up did not permit subsidence testing of the plate systems. The influence of screw size was assumed to be of little importance and the SynFix-C was tested with standard screws and a stand alone cage.

SynFix-C was tested with a rapid prototype cage. Therefore material properties for the cage are lower than would be expected with production parts. Because of this the performance of the SynFix-C device will be underestimated particularly in the push-out test results.

In the first phase, only a few of each tested specimen type were tested in favour of screening a larger field of specimens. This screening permitted a first sorting of the specimens. Selected

specimens were then repeated in order to obtain more powerful statistics. Simultaneously new prototypes were included in the analysis.

The test planning for the screening and specimens are summarised in the annex.

### 3.4.2 Statistical Considerations

An balance needed to be found for the sample size. For more powerful statistics it is best to perform a large number of tests. Testing quantities are limited on the other hand by economic considerations such as time and specimen costs.

After the first series of tests, the relative standard deviation was about 1 to 2 % for the maximum force and around 10 % for the deformation at maximum force. This standard deviation was assumed remain similar for further tests. Difference between specimen types was generally more than 15 %. A  $\Delta$  is defined as the maximum acceptable relative error on the measured mean compared to the effective value.

$$\Delta = \frac{x_{mean} - \mu_0}{\mu_0}$$

Where  $x_{mean}$  is the sample mean and  $\mu_0$  the effective mean;  $\Delta$  is fixed at 10 %. Furthermore a confidence interval of 95 % is fixed.

The basic equation is [6]:

$$t_0 = (x_{mean} - \mu_0) \frac{\sqrt{n}}{s}$$

This equation is modified by using the previously defined parameters:

$$t_0 = \frac{\Delta}{s_{rel}} \sqrt{n}$$

To satisfy criteria set by the confidence interval the following equation has to be fulfilled:

$$|t_0| > t_{1-\alpha/2, n-1}$$

Where  $t_{1-\alpha/2, n-1}$  is taken from a table in [2]. Because  $t_{1-\alpha/2, n-1}$  depends on n itself, calculating n is an iterative process.

$$n > t_{1-\alpha/2, n-1}^2 \frac{s_{rel}}{\Delta}$$

The minimum found for n is 7.

### 3.5 Data Analysis

#### 3.5.1 Data Collection and Treatment

##### Mean Curve

A mean curve between 0 displacement and maximum load was calculated. In steps of 0.1 [mm] the corresponding force for each specimen was recorded; the mean value and the standard deviation of all experiments of the same specimen type were calculated.

##### Stiffness (Displacement as Selection Criteria)

Maximum forces for the different systems and configurations have a large spread, so it can be of interest, to compare stiffness in a particular region of displacement.

Stiffness is calculated in the regions 0 to 1 [mm], 1 to 2 [mm] etc until a maximum displacement of 5 [mm]. The force values are mean values of the considered sample type.

$$k_{0...1} = \frac{F_{@1} - F_{@0}}{1} \left[ \frac{N}{mm} \right]$$

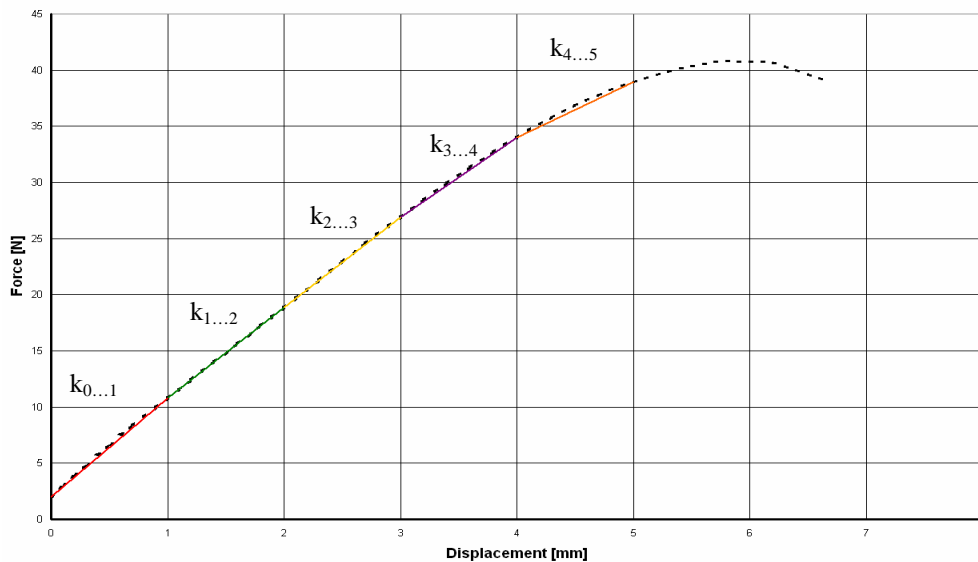


Fig. 3.1: Stiffness (displacement as selection criteria); the stiffness between 0 and 1 mm displacement is denoted  $k_{0...1}$  or initial stiffness

The stiffness between 0 and 1 mm displacement is noted as the *initial stiffness*.

### 3.5.2 Statistical analysis

#### Screened Data

Data obtained from the screening are relatively limited. In general only two repeats of each specimen type are performed, when relative standard deviation of the maximum force exceeded 10 % a third test was performed. For calculating significance of the tests, standard deviation from small sample sizes is not ideal. The assumption was made, that the standard deviation for each test is the same as for the standard specimen (i.e. SynFix-C with 2.7/16 screws).

Thus a z-test is performed to analyse significance of the difference between the different samples. The same procedure is done for maximum force data, its displacement and stiffness values.

The test is formulated:

Hypothesis:

- $H_0: x_{\text{mean}} \neq x_{\text{standard}}$
- $H_1: x_{\text{mean}} = x_{\text{standard}}$

Where  $x_{\text{standard}}$  is the mean of the reference sample (i.e. SynFix-C 2.7/16) and  $x_{\text{mean}}$  the mean of the tested sample.

The test uses a two-sided confidence interval of 95 %. Thus, the test is formulated as:

$$z = \frac{x_{\text{mean}} - x_{\text{standard}}}{\sigma} \sqrt{n}$$

z is then compared to tabulated values found in reference [2].



## 3.6 Compression Tests

### 3.6.1 Set-up for the Compression Test

The compression test set-up is based on the ASTM F 1717 standard. Dimensions proposed for testing of implants destined for the cervical spine were kept unchanged. Mounting blocks made of PE were substituted with block made of a combination of aluminium and polyurethane foam. The goals of these tests indicated the use of PUR foam: The bone-implant interface is of interest, including the comparison between conventional anterior plating systems and the new SynFix-C device. A PUR foam of grade 15 according to ASTM F 1839-01 has been chosen. In order to limit foam deformation, a block of 18 mm length, 18 mm width and 13 mm height was used which was sufficient for mounting all desired samples. To satisfy the dimensions proposed in the ASTM standard, the PUR foam part is fixed on an aluminium block. (cf. 3.2 and drawings in the annex).

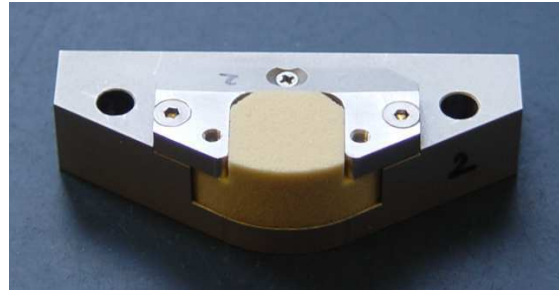


Figure 3.2: PUR foam block fixed on aluminium block. Main dimensions correspond to ASTM 1717-04 for the testing of cervical spine implants.

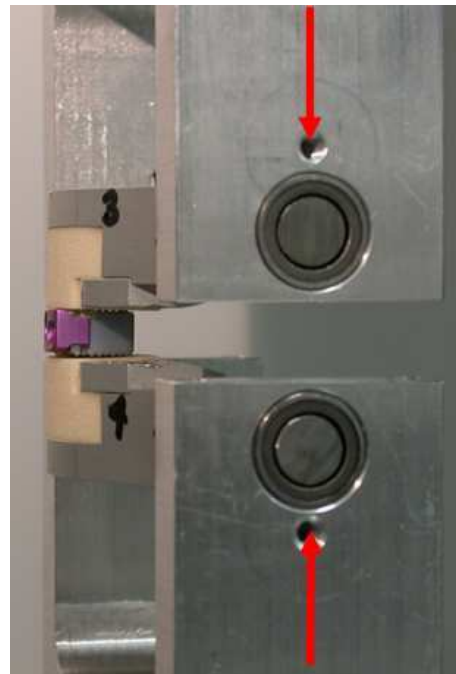


Figure 3.3 and 3.4: Set-up for tension and compression tests: the lower piling is rigidly fixed, the upper is mobile and contains the load cell; the test blocks are mounted in a bearing perpendicular to the sense of the applied force

Assumption to verify:

- Stiffness of the new SynFix-C device is in the same order as known anterior plating systems

The compression tests were performed in two distinct series. In a first session, all sample types have been tested 2 times. When the standard deviation exceeded 10 %, a third test was made. The goal was to get a good overview of different configurations and relate the prototype to existing products. After analysing the data, three configurations were chosen to get statistically more precise information. Of each of the selected sample types further tests have been performed to have a total of seven tests at the end.

### 3.6.2 Forces in the Specimen under Compressive Loads

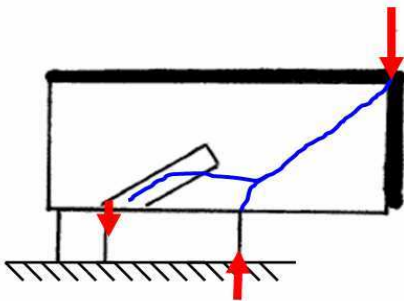


Figure 3.5: The cage sustains a compressive, the plate a tensile load. The forces in the construct are assumed to be symmetric to the horizontal mid-plane. The thick line is the rigid test block.

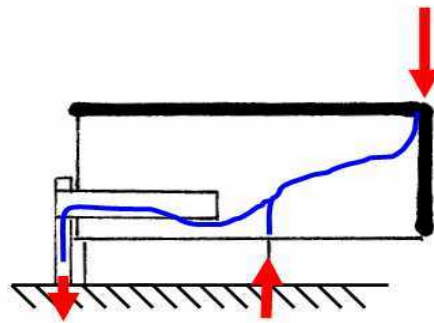


Figure 3.6: The loading in the plate is similar to SynFix-C. The cage is compressed, the plate is under tension

In the figure above, the forces in the construct are shown schematically. The cage transmits a compressive load. The foam rotates about the posterior edge of the cage. The plate resists thus a tensile load.

The loading mechanism in the plate construct is similar. The cage resists a compressive force and in the plate at the anterior side results a tensile load.

### 3.6.3 Test Results Compression Tests

#### Inconsistency in the Foam Quality

The foam blocks for the two series came from two different machining runs. Several significant differences could be detected by a t-test, especially differences on the maximum force were obvious. The reason was assumed to be the foam blocks.

Measuring the mass of ten used foam blocks of each of the series (unused ones from the first series were not available anymore) a significant difference of about 3 % was found ( $\alpha=0.01$ ). For a better comparison in both cases only foam blocks from compression tests used on the one-screw interface were included in the measures; the foam blocks were previously stored in the same location and measured at the same time; difference of water content can thus be excluded. It can be expected, that the mechanical properties are lower with the lower weight.

	1 <sup>st</sup> series	2 <sup>nd</sup> series
N	10	10
Mean	1.4271	1.3877
Standard deviation	0.03582	0.02206

This difference is basically in the tolerances proposed in the ASTM F1839-01, there is a range from 14 to 16 pcf for a grade 15 foam which is considered within the standard.

Possible reasons are:

- Manufacturing problems
- Admissible deviation in foam density (defined by the manufacturer)
- Differences in quality (storage, manufacturing)

No one of these points can be completely excluded. At the least, the amplitude on the material properties has to be analysed. This can be made by the means of representative samples from the basic material.

The reported inconsistency affects only the compression tests.

### Results

The following graphics are showing the mean load-displacement curves of all compression tests. The first one arranges all tested configurations of the three screw prototypes; the means are calculated for each screw size. All tests were performed with the same prototype (015), with exception of the 3.0 mm diameter screw (017).

In the second graphic, the tested four screw prototypes are represented. For all of these tests, the same screw size of 3.0 mm diameter and 16 mm length has been used. As a reference, the mean curve of the three screw prototype with the “standard” screw (2.7/16) is included.

The third graphic embraces the mean load-displacement curves of the plating systems. Again the reference system SynFix-C 015 with 2.7/16 screws is indicated.

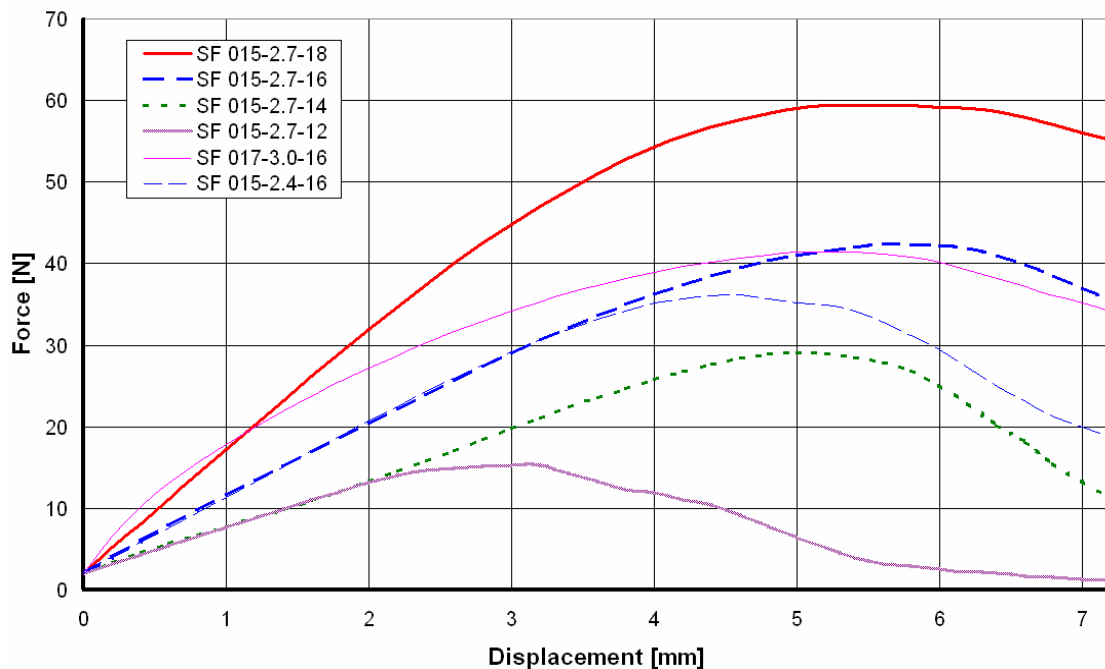


Figure 3.7: Mean load-displacement curves for all screw dimensions of the three screw concept. It is clearly visible, that the longer screws have a higher stiffness and higher maximum forces than shorter screws. The difference for different screw diameters seems to be smaller, with exception of the higher stiffness of the 3.0 mm diameter screw (Abbreviations see on page 107; implant types see in annexe on page 116).

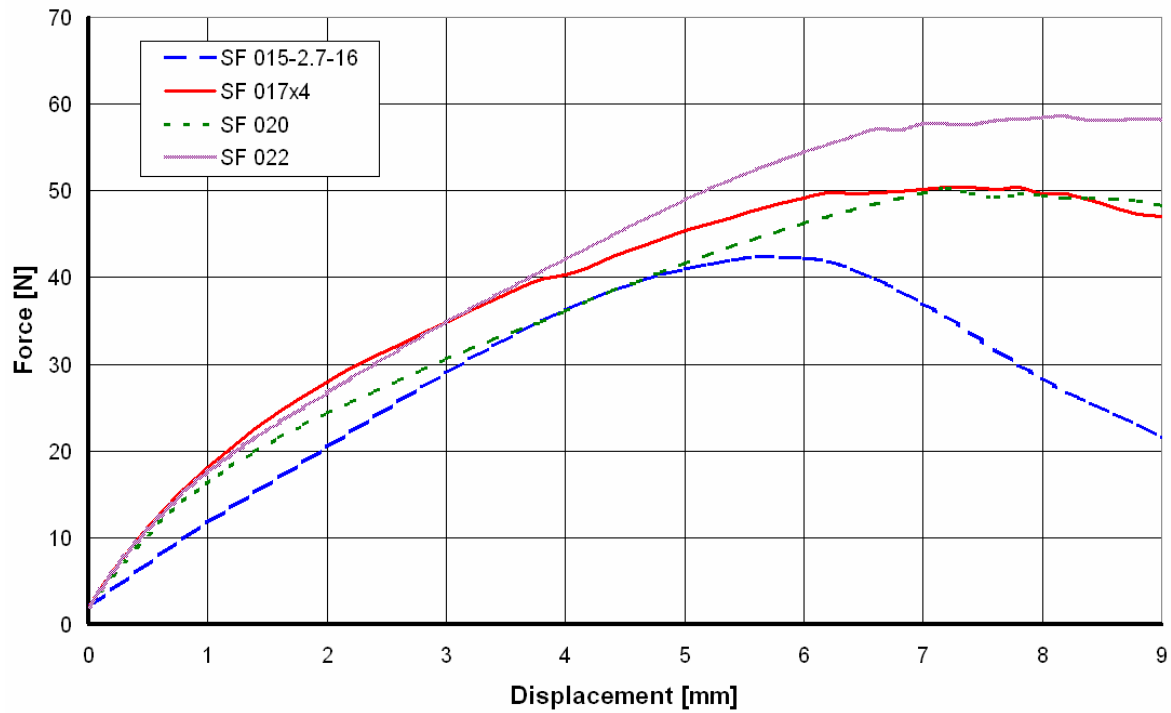


Figure 3.8: Mean load-displacement curves of the four screw concepts; SF 015 is indicated as a reference value. The four screw concept provides a higher initial stiffness (Abbreviations see on page 107; implant types see in annexe on page 116).

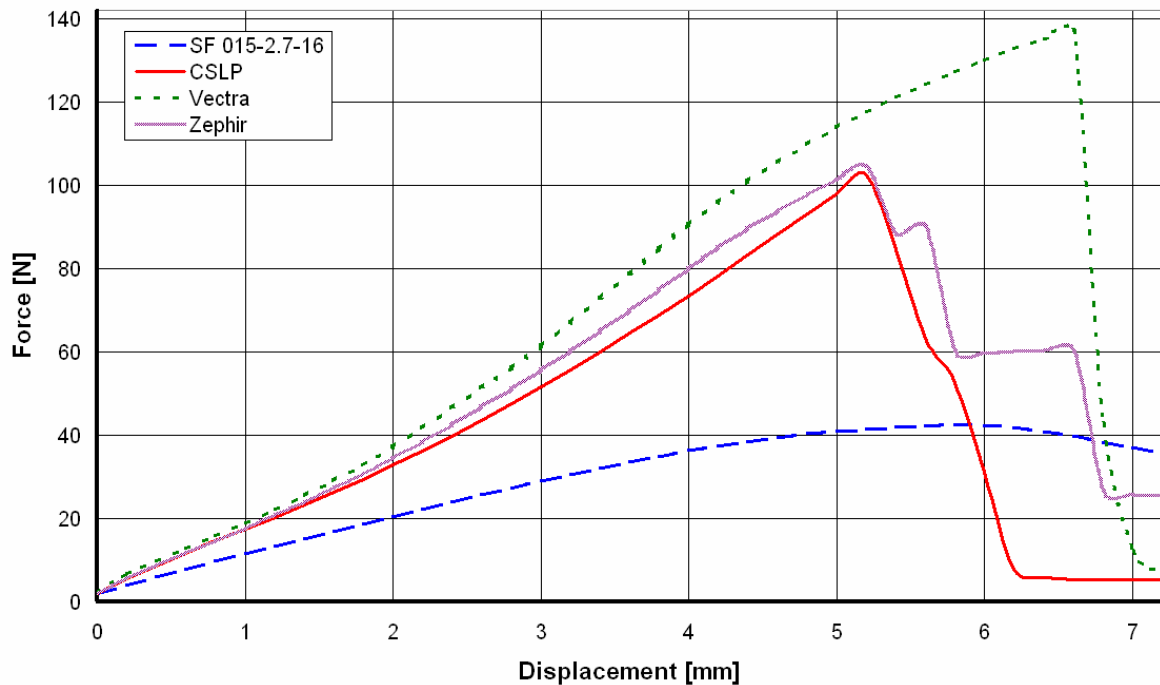


Figure 3.9: Mean load-displacement curves of the plating systems; SF 015-2.7-16 is indicated as a reference value. The characteristic of the plating systems is completely different: the stiffness increases with increasing displacement, while the new device has the initial stiffness as the highest (Abbreviations see on page 107; implant types see in annexe on page 116).

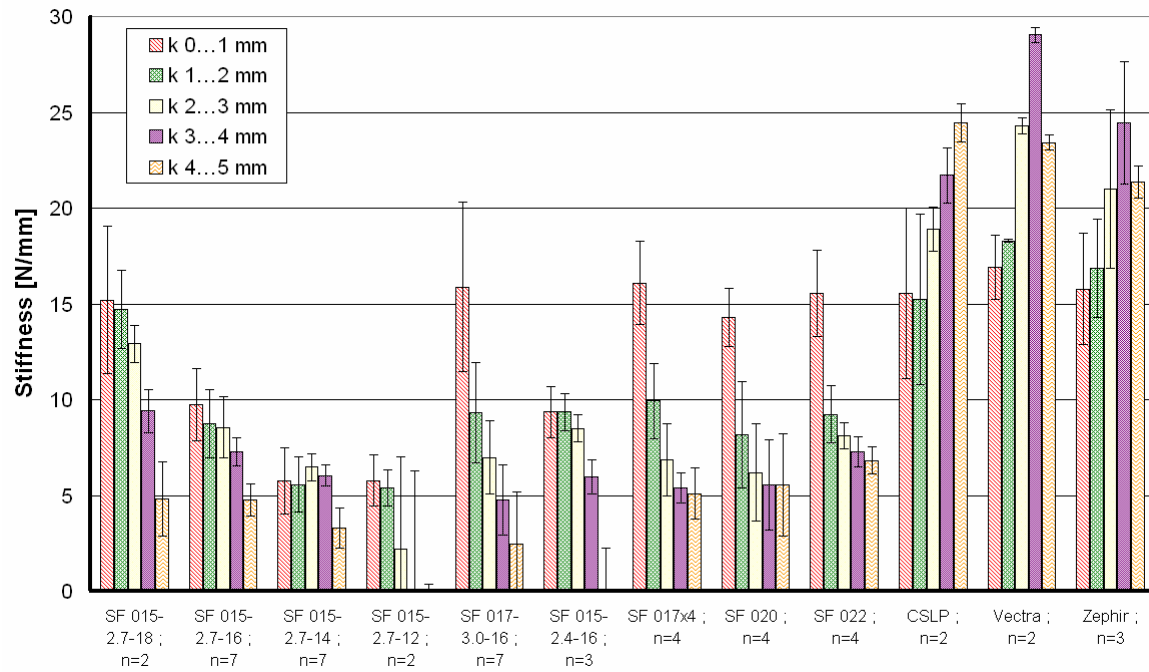


Figure 3.10: Stiffness in compression for different regions of displacement. The number of repeats is indicated for each specimen type. SF 015 are the prototypes with a three screw concept, SF 017x4, 020 and 022 those with a four screw concept (Abbreviations see on page 107; implant types see in annexe on page 116). The initial stiffness of the standard configuration (2.7/18) is inferior to the plating systems. In contrast, the configurations with the longest (18) and the thickest (3.0) screw as well as the four screw concepts reach the level of the plating systems (CSLP).

In figure 3.8, the stiffness calculated is a function of the displacement as shown. The most important measure is the first value, which represents the initial stiffness when starting the deformation. A general characteristic of the SynFix-C device is, that the first stiffness value is the highest (except 2.4/16) and decreases for further deformation. All plates in contrast, have an oppositional behaviour where stiffness increases with deformation. The same could already be stated in the load-displacement graphics before.

The plating systems have an initial stiffness of about 16 [N/mm]; the SynFix-C device configurations are less stiff, with the exception of the configurations with 2.7/18 and 3.0/16 screws as well as the 4 screw devices which are reaching the same level (15 [N/mm]).

The material and the geometry are not linear. It is thus not possible to derive the limit of elasticity directly from the test results. The limit can be estimated by comparing the stresses found in the FE model (cf. chapter 4): it is reached when the stresses exceed the “linear” region of the material.

The limit of elasticity found by this method is 1 [mm] of displacement, based on the assumption that the material is elastic for stresses lower than 3.4 [MPa] (cf. Material test in the annexe).

Under normal conditions the elastic range should not be exceeded. Nevertheless it is advantageous to maintain a certain stability when leaving the elastic domain.

The stiffness of the four screw prototypes (SF 017x4, 020, 022) decreases rapidly. Thus no significant differences for  $k_{1...2}$  and  $k_{2...3}$  is present. The angle between the parallel screws is small ( $5^\circ$ ) and can not provide additional stability.

The inconsistency in the foam quality unfortunately requires separate analyse for the different foam series. The focus will be set on the most relevant values, the stiffness values in function of the absolute displacement.

In a t-test the second series foam appeared to be significantly different from the first series for the test using 3.0/16 and 2.7/14 screws (t-test,  $\alpha = 0.05$ ). The third test performed in both

foam series was with 2.7/16 screws; a difference of the mean can be found, but is not considered significant.

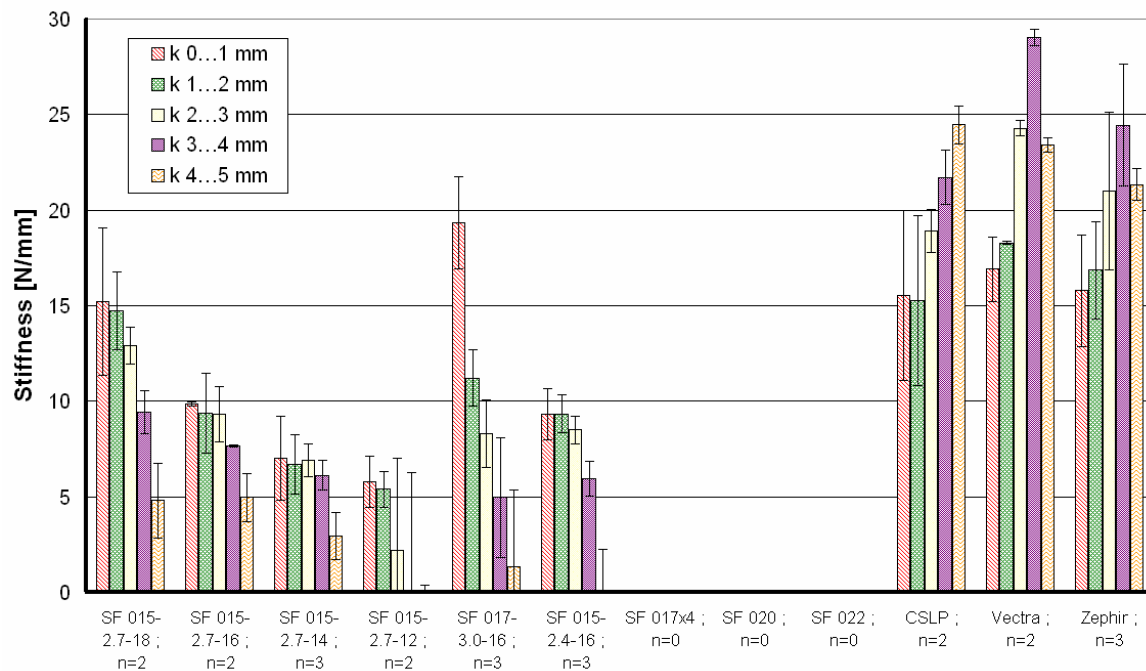


Figure 3.11: Stiffness in compression for different regions of displacement; 1<sup>st</sup> series of tests. The initial stiffness value of the new device with 3.0/16 mm screw is doubtful. The initial stiffness for the plate systems are higher (Abbreviations see on page 107; implant types see in annexe on page 116).

The graphic above shows the stiffness results from the first series. The specimens tested in both foam series are higher in this statistic compared to the overall values. This is the case for 2.7/16, 2.7/14 and 3.0/16, the other tests do not change (tested in foam series 1 only).

The following figure shows the stiffness results of the second series tests. Only the 2.7/16, 2.7/14 and 3.0/16 screws in a three screws concept and all four screws concepts (3.0/16 screws) have been tested. In this graphic a difference between the three and the four screws concept is visible, even if it is not significant. An uncertainty is the different size of the cage used with the 3.0/16 screws.

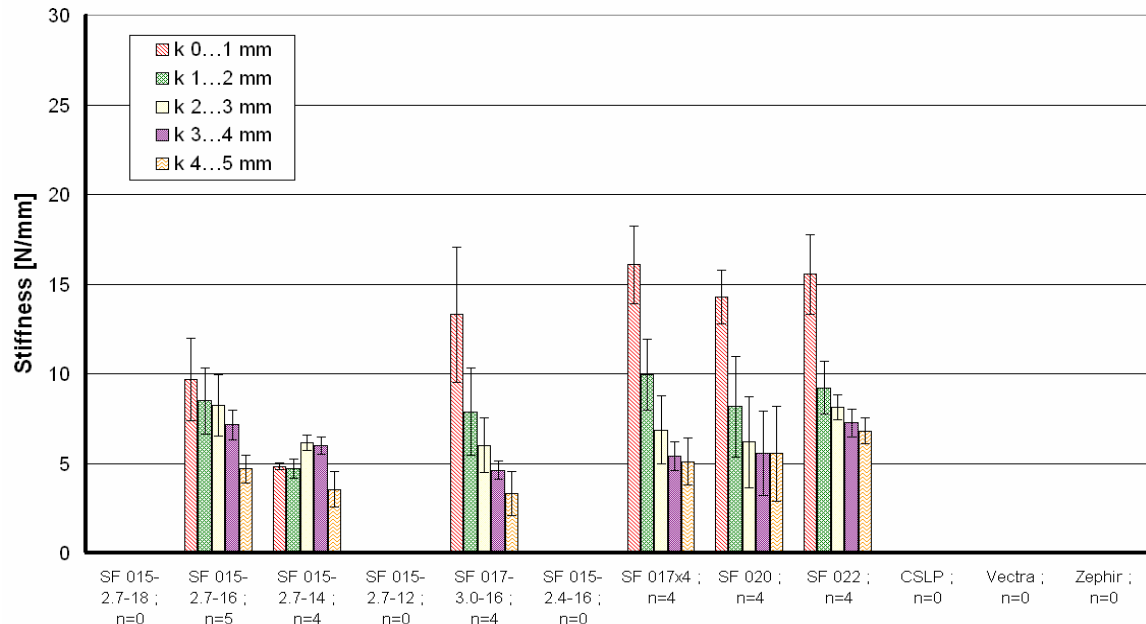


Figure 3.10: Stiffness in compression for different regions of displacement; 2<sup>nd</sup> series of tests. The four screw concept (SF 017x4, 020, 022) has the highest initial stiffness (Abbreviations see on page 107; implant types see in annexe on page 116).

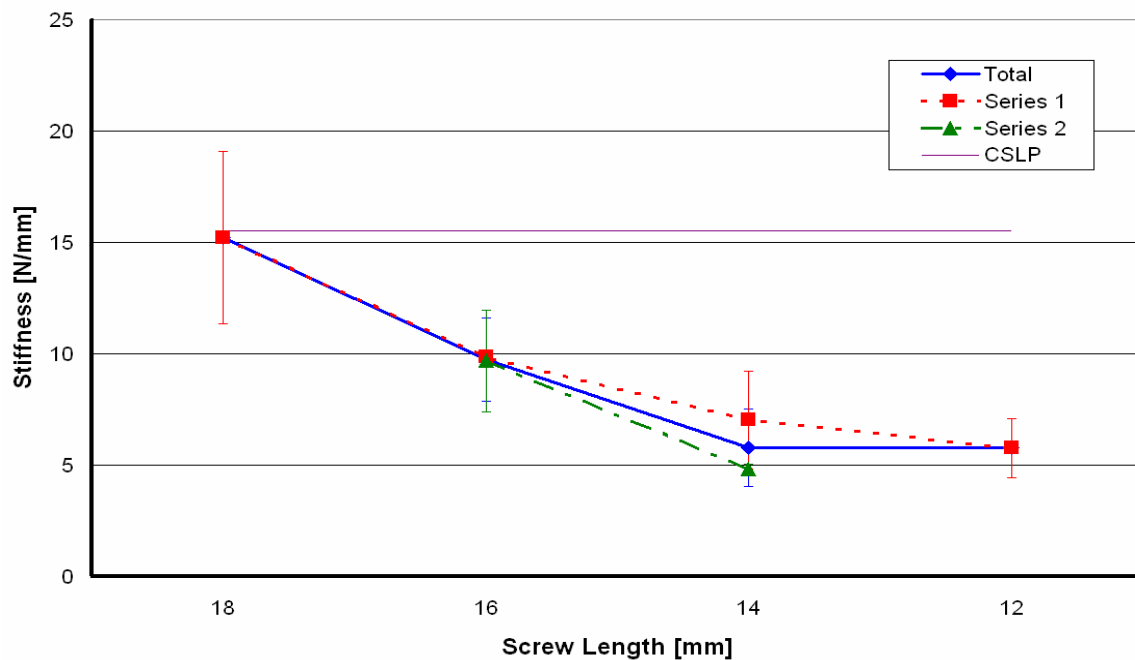


Figure 3.11: Influence of screw length on compression stiffness. The compared value is the stiffness between 0 and 1 mm displacement. All screw diameters are 2.7 mm, all tests with SF 015 with three screws. The values of the two test series are indicated as well as a reference value of an anterior plate (CSLP, 1<sup>st</sup> series of tests)

The figure above shows the most relevant stiffness value in function of the screw length. The values for all measures and separated for the foam series are indicated. As a comparison the corresponding values of a plate system is represented (CSLP). Stiffness seems to increase quadratically; differences between the two shortest screws are not significant. The standard screw has a stiffness of about 10 [N/mm], the longer 18 mm screw, with a stiffness of 15

[N/mm] (significant, t-test,  $\alpha=0.01$ ), reaches the level CSLP and Zephyr. The shortest screws are significantly less stiff than the 16 mm screw (t-test,  $\alpha=0.01$ ).

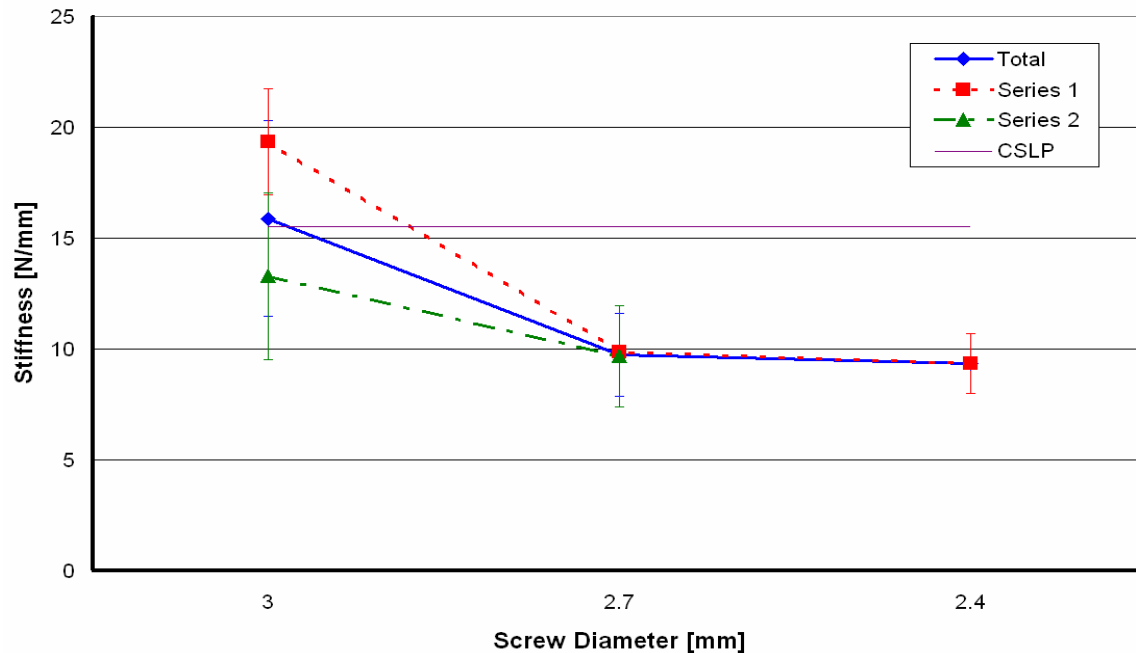


Fig. 3.12: Influence of screw diameter on compression stiffness. The compared value is the stiffness between 0 and 1 mm displacement. All screw lengths are 16 mm; diameter 2.4 and 2.7 with SF 015, diameter 3.0 with SF 017; both prototypes using three screws. The values of the two test series are indicated as well as a reference value of an anterior plate (CSLP, 1<sup>st</sup> series of tests); (Abbreviations see on page 107; implant types see in annexe on page 116).

The graphic above shows the influence of screw diameter on the initial stiffness. No difference exists between the 2.4 mm and the 2.7 mm screws. The mean value of the 3 mm screw is higher but the difference is not significant. The standard deviation for the 3 mm screw is higher than for the other screws. The 017 prototype (used for the 3 mm screws) has a bigger cage (height 8 mm in stead of 7 mm for all other prototypes). This results in an enabled vertical degree of freedom of the plate (cf. figure 3.14). It is probable that this permits a better preconstraint of the construct and thus the initial stiffness is increased.

*Failure mechanisms*

All test with SynFix-C showed the same behaviour: The 2 screw interface was clearly stronger and though no movement could be observed on this side. On the one screw interface side, the foam block rotated about the posterior edge of the cage. For small deformations, the screw was pulled out nearly in its own axis, so resistance was low (cf. figure 3.13). Only a relatively small foam part was broken out of the foam.

Only the configuration with 3.0 mm diameter screws showed a different behaviour: the two screw interface was weaker at the beginning, a movement could be observed first at this side. At an angle of 5 to 10° between the spacer and the foam-block the

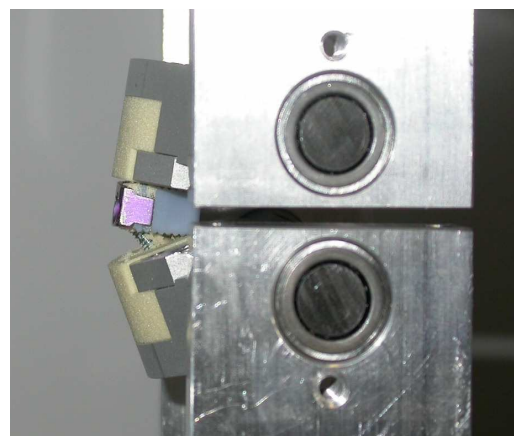


Fig. 3.13 : Test 033, displacement of 6 [mm] : SynFix-C 015 2.7/16



movement stopped and continued on the other interface (cf. figure 3.14). This could be caused by the preconstraint different from the other screw dimensions as previously mentioned.

The same effects could also be observed directly on the foam blocks. On the two screw

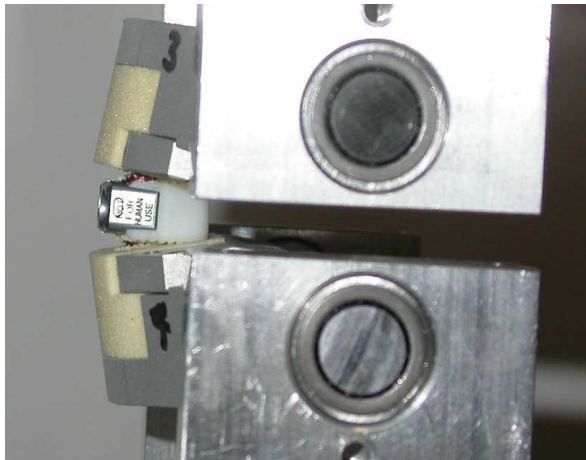


Fig. 3.14 : Test 044, displacement of 7 [mm] : SynFix-C 017 3.0/16

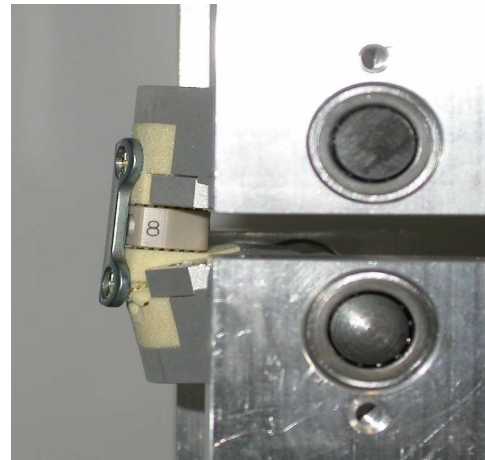


Fig. 3.15 : Test 030, displacement of 7 [mm] : CSLP

interface nearly no damages can be seen, the holes of the screws were intact, impression of the cage was minimal. On the one side screw, an impression of the posterior edge is easily visible. A small part of the foam has been lifted by the screw.

In figure 3.15 the typical failure mode of the plate systems under compression is shown. The plate itself is very stiff, the crack starts anteriorly in the plane of the screws and goes to the posterior end of the spacer.

### Test acceptance criteria reached?

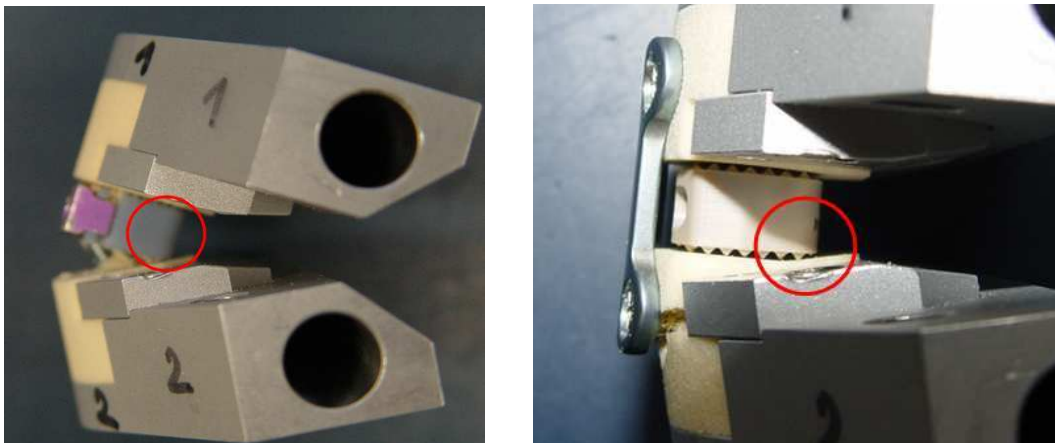
The value for the comparison was defined as the initial stiffness; the stiffness of the new device should reach the level of an anterior plate. The criterion is achieved for the following prototypes and screw dimensions:

- SynFix-C P015, 2.7/18, 3 screws
- SynFix-C P017, 3.0/16, 3 screws
- SynFix-C P017x4, 3.0/16, 4 screws
- SynFix-C P020, 3.0/16, 4 screws
- SynFix-C P022, 3.0/16, 4 screws

### 3.6.4 Discussic

Data from the mechanical compression test are probably the most interesting data. The situation tested comes closest to the anatomical case of extension. In this case a compressive load is applied behind the vertebral body and as a result the vertebrae models experience a relative rotation. The centre of rotation is forced to be on the posterior edge of the implant (cf. figures 3.16, 3.17). It is supposed that the centre of rotation is fix during the complete deformation. Impressions on the foam blocks support this assumption as no cage sliding is apparent. The centre of rotation corresponds to the location of the intervertebral disc; the IAR in a healthy spine is in this area at the lower cervical spine regions (C5 - C7). For the tested

plates we are facing the same situation, because the IAR is again forced to be at the posterior edge of the spacer.



Figures 3.16 and 3.17: Centre of rotation for SynFix-C (left) and plate with cage (CSLP and Cervios, right)

An important question is how the in the mechanical model measured values can be compared to the reality. Would the displacement where failure occurs in the mechanical experiment occurs still be in the natural ROM, or would FSU fail before? Deformation in the mechanical test can be compared to the extension movement quite easily; it is in fact a simple geometric analyse. Comparing forces (moments respectively) is delicate, because the material properties differ.

In the following, the focus is on the lower cervical spine – C5/C6 and C6/C7. The mechanical test is closest to these levels as described previously (cf. fig 3.18) and also the main part of the interbody fusions concerns the same levels (cf. 2.9).

As a simplification, it is assumed that the movement is symmetric about the horizontal plane, i.e. the rotation of the upper and the lower test block is the same. The rotation is about the posterior edge of the spacer, which has a distance to the



Fig. 3.18 : IAR of the lowest levels of the cervical spine [5]. The IAR is close to the intervertebral disc on these levels

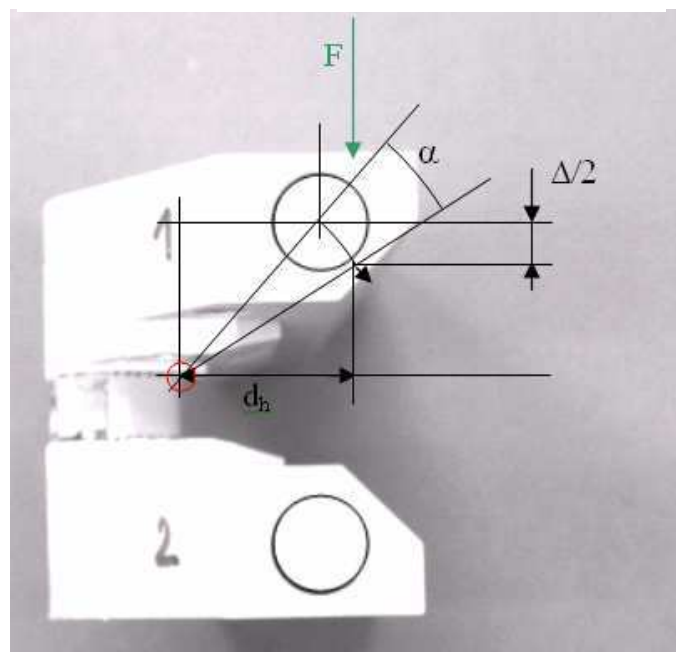


Fig. 3.19: Geometric relation between linear displacement and angular rotation.  $\Delta$  is the measured displacement, the red circle symbolises the centre of rotation,  $d_h$  is its distance to the applied force  $F$  and  $\alpha$  is angular rotation of the testblock to the symmetry plane.

applied force of 15 [mm] horizontally as well as vertically.

The angle of rotation of the test block to the symmetry plane is  $\alpha$ , the displacement of the applied load  $\Delta$ ;  $\alpha$  is expressed as a function of  $\Delta$ :

$$\alpha = -\arcsin\left(\frac{1}{d}\left(15 - \frac{\Delta}{2}\right)\right) + 45^\circ$$

The angle of  $45^\circ$  is an offset to have an initial angle of  $0^\circ$ ; signs are set to obtain positive values for increasing displacement.

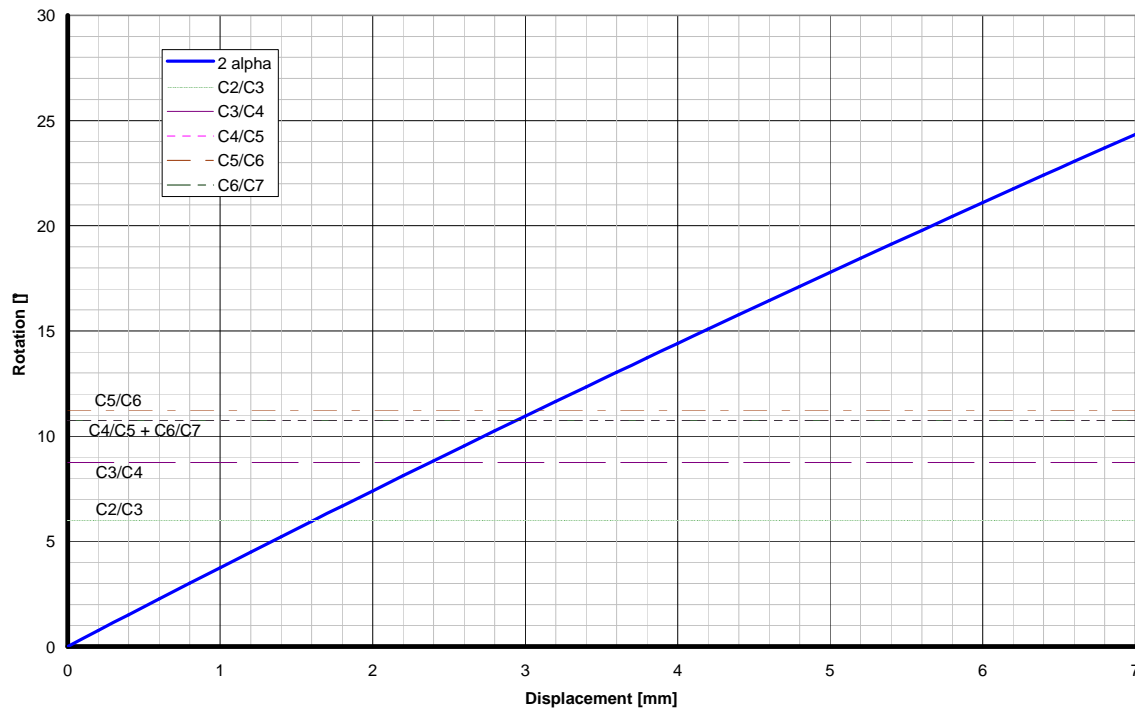


Figure 3.20: Relation of the measured displacement to the angular rotation, measured between the two testblocks ( $2\alpha$ , cf. in figure 5.4); as a reference, estimated extension ROM are indicated. The elastic range of the bone-device model is estimated at 1.1 [mm] which corresponds to an angle of  $4^\circ$ .

The graphic above shows the relation between the displacement and the angle of rotation; the blue line is  $2\alpha$ , the actual appearing angle between the two test blocks.

The ROM values from Dvorak [5] already presented in chapter 2 are recapitulated. As an assumption, the extension part is 50% of the complete measured ROM, so these values are shown as reference lines on the graphic above. From literature it is not unambiguous if flexion or extension makes the major part; it seems as in younger subjects the flexion is more important than extension and in older subjects the adverse is found. Anyway, differences in healthy subjects are not enormous, except from C0/C1 level, which is not of interest herein. Ideally, when deforming the fused level, all components would still be in the elastic zone. The limit of elasticity was estimated to be at about 1 [mm] (foam or bone is the limiting element), which corresponds to a rotation of about  $4^\circ$ .

As a next step, let us compare the stiffness values. For this we have to transform the measured linear stiffness in a angular stiffness, where values from biomechanical tests are known.

$$k_{lin} = \frac{dF}{d\Delta} \quad \rightarrow \quad k_{ang} = \frac{dM}{d\gamma}$$

The load-displacement behaviour is nearly linear until 80 % of the maximum force, so the assumption of a constant linear stiffness value is justifiable. The apparent moment is calculated ( $F$  and  $d_h$ ) and derived numerically; also the angle is derived numerically.

The angular stiffness is about 0.04 [Nm/°] and slightly increasing with the angle of rotation. CSLP has an angular stiffness of about 0.06 [Nm/°]; the graphs are represented in the figure below; the four screw prototypes reached the same level. The FE model showed that stiffness increases considerably when a bone-like material is applied instead of a PUR foam material. Even with a rather weak cancellous bone, the stiffness was multiplied by a factor 5. The simulation was made on the base of a three screw model. It is assumed, that the influence of the vertebral bone material is equivalent for the four screw model. This stiffness value is indicated in purple on the graphic below. As a reference, two measured stiffness values from biomechanical analyses are indicated (Nightingale and Panjabi, cf. chapter 2.3 and [12, 17]).

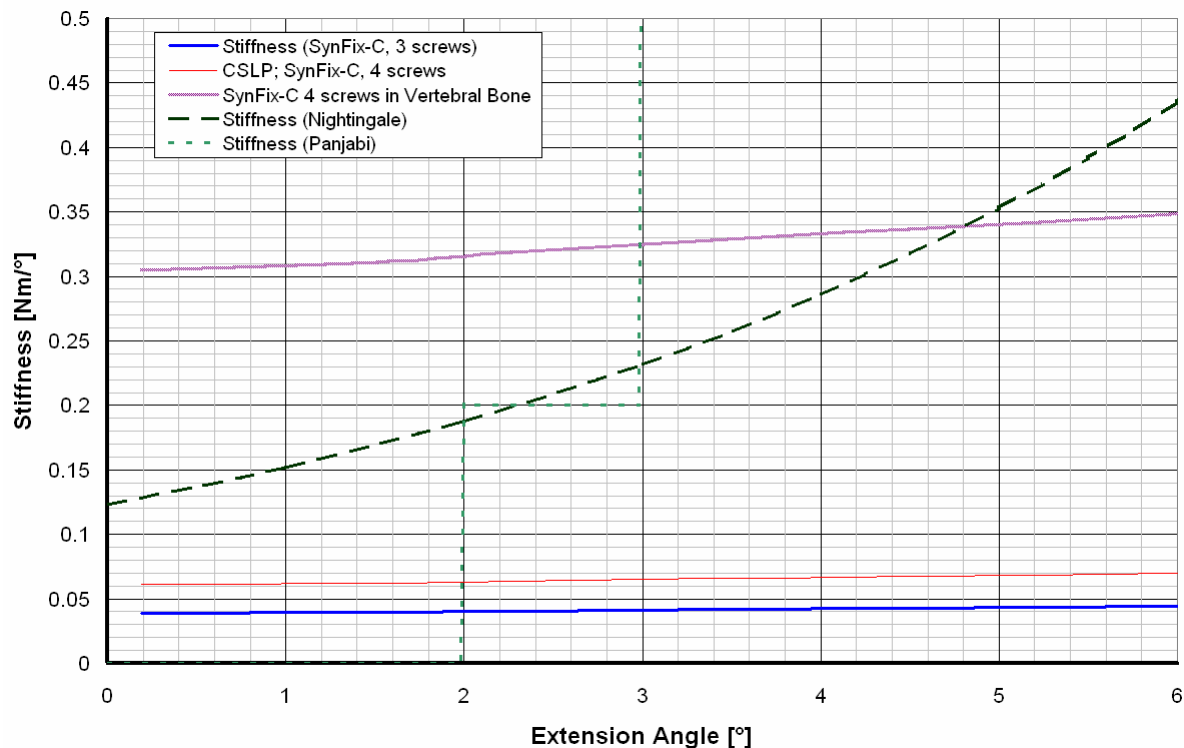


Fig. 3.21: Stiffness in function of the extension angle: the linear stiffness of SynFix-C and CSLP is assumed to be constant; the variation in this graphic is due to the angle-displacement relation. The tested four screw prototypes had a similar stiffness as CSLP. The FE model showed a stiffness 5 times higher for a weak cancellous bone. Two comparative values from biomechanical tests are indicated. From the Panjabi study, only a few data points are given, Nightingale proposed a mathematical model.

The presented stiffness curve is of course in an “intact” cervical spine; in case of an interbody fusion, the intervertebral disc will be removed. The decrease of stiffness in this case would probably not be enormous and the exponential stiffness – displacement will not be influenced, because this is mainly due to the ligaments.

From the graphic before, it is known that the elastic ranges is below 4°. In the real bone model this corresponds to a torque of about 1.2 [Nm] (stiffness ≈ 0.3 [Nm/°], 4°). Comparing this value to the load-displacement data in extension (cf. chapter 2.3.4), it becomes clear, that a

large mobility of the cervical spine is permitted without damaging permanently any structures.

In the mechanical tests the influence of the screw length has been shown. Longer screws induced a higher stiffness. The longest screw (18 mm) reached even the level of CSLP (initial stiffness). In most cases a surgeon will not use such long screws because of the risk damaging the spinal cord. Most surgeons demand screw which do not overlap the footprint of the cage. The longest screw in this case is the 16 mm screw. The clear advantage of a longer screw has to be transmitted to the surgeons to provide maximum stability.

No significant influence could be found for the screw thickness. For this decision material strength has a more important influence. In particular the endurance performance has to be considered.

A fact, which has not been mentioned until now, is that the spine supports compressive loads, independently of extension and flexion (cf. 2.4). In the performed extension simulation no preload was present. The load on the vertebral body in neutral position is about 45 [N]. It increases under flexion and decreases under extension (minima at 30° extension).

The loading situation in the device will change under the preload. The cage will clearly to have more compressive load to sustain. The tension load in the plate will be reduced, depending on the amplitude of the eccentric load (depending on extension angle of the cervical spine) the load could also become of compressive nature (neutral position when the eccentric load is low).

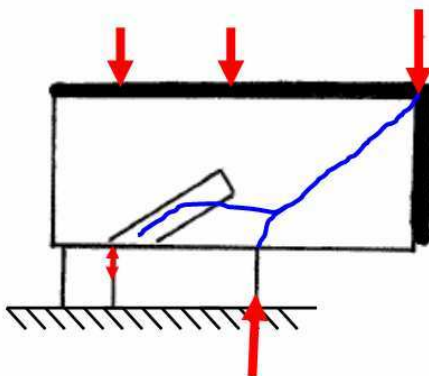


Figure 3.22: Load situation in the device including a preload.

## 3.7 Tension Tests

### 3.7.1 Set-up for the Tension Test

The tension test has the identical set-up to the compression test, except that a tensile force is applied instead of a compressive one.

Assumption to verify:

- Stiffness of the new SynFix-C device is in the same order as known anterior plating systems

### 3.7.2 Forces in the Specimen under Tensile Loads

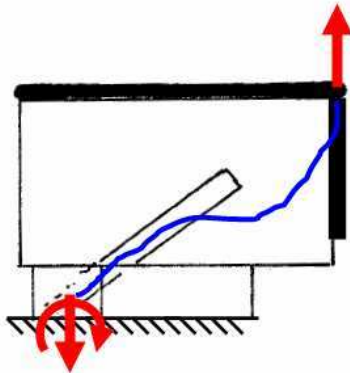


Figure 3.23: A tensile load is applied at a fixed distance posterior to the implant (red arrow top right). The reaction forces in the plate (symmetry plane) are indicated with the red arrows (force and moment). The blue line shows schematically where the force “passes”.

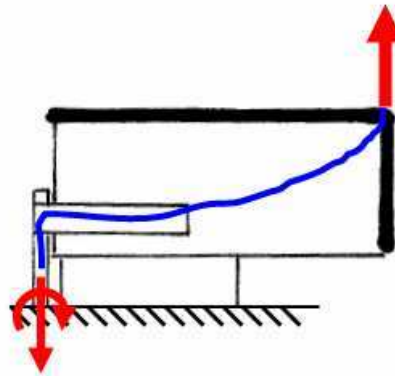


Figure 3.24: The loading in a plate is similar to SynFix-C. The cage is not loaded, all the forces pass through the plate. The resulting moment caused a rotation of the screw in the plate.

The figure above shows the loading situation in the device. The cage can not transmit tensile loads, thus the force passes completely through the plate which results in a moment in the plate also. The force between the foam and the plate is transmitted through the screw. The plate is much more rigid than the screw. The highest deformation is expected in the screw close to the plate (highest bending moment in the screw).

A similar loading scheme is found in the anterior plate. The cage does not sustain tensile loads, the force passes through the plate. The force transmission from the foam to the plate is again through the screw.

### 3.7.3 Test Results Tension Tests

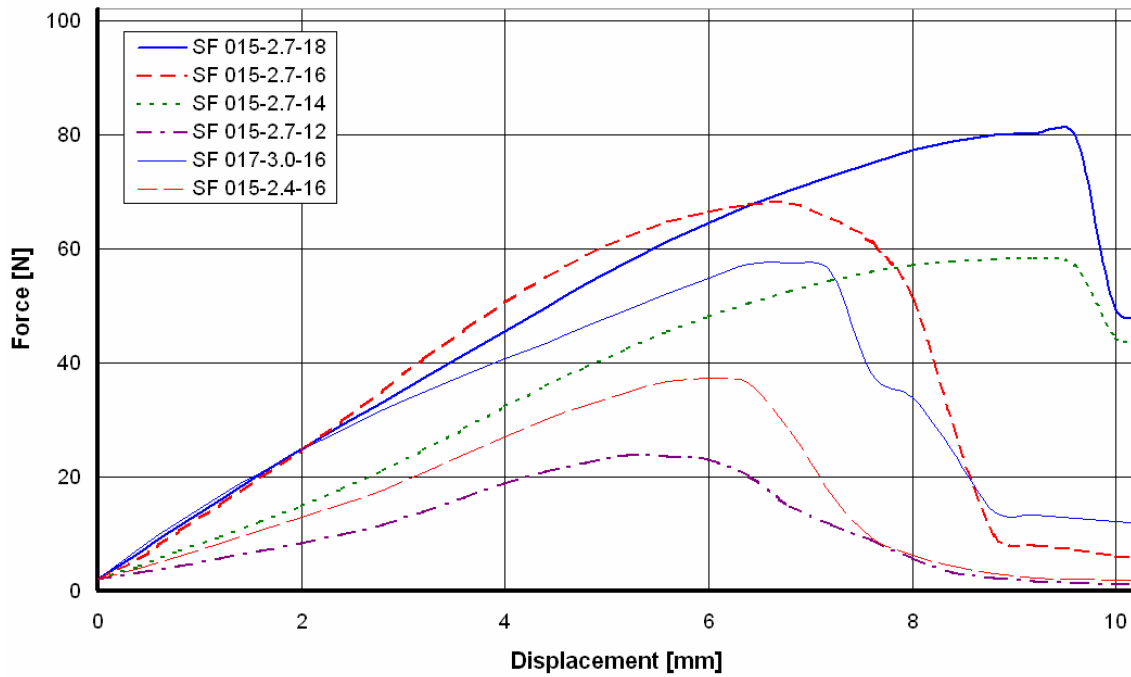


Fig. 3.25: Mean load-displacement curves for the tested SynFix-C devices; (Abbreviations see on page 107; implant types see in annexe on page 116)

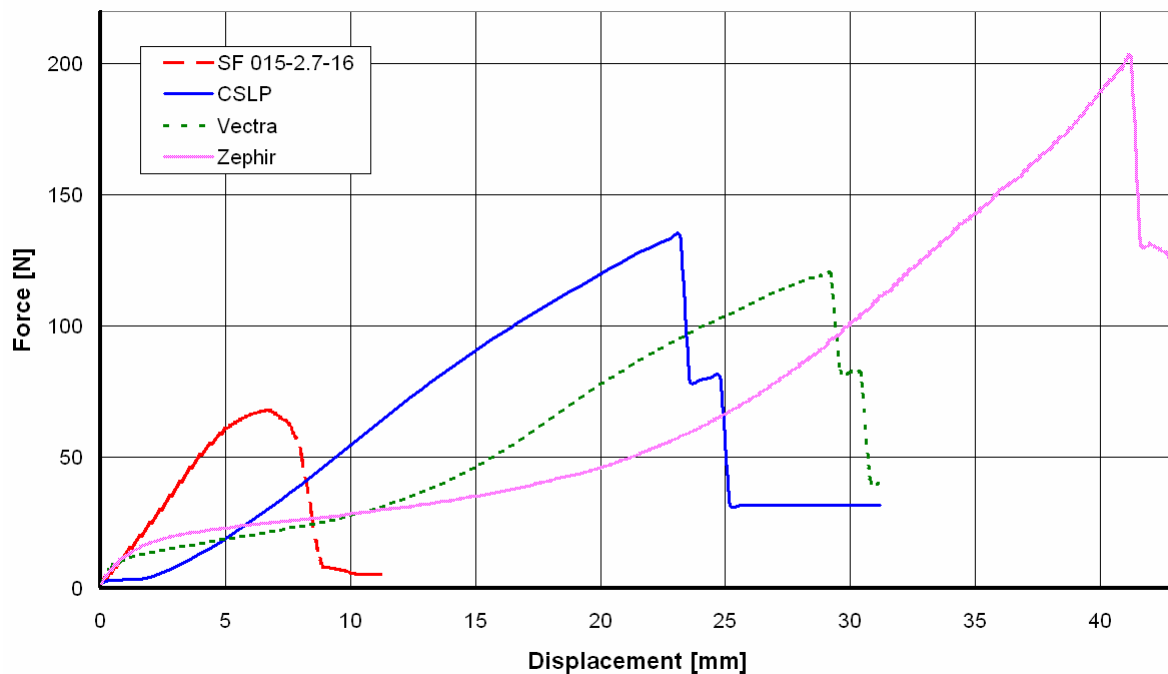


Fig. 3.26: Mean load-displacement curves for the tested plating systems; as a reference the SynFix-C device with the “standard” screw dimension is indicated (SF 015-2.7-16); the load-displacement characteristic of the plating systems is fundamentally different from the new device (Abbreviations see on page 107; implant types see in annexe on page 116).

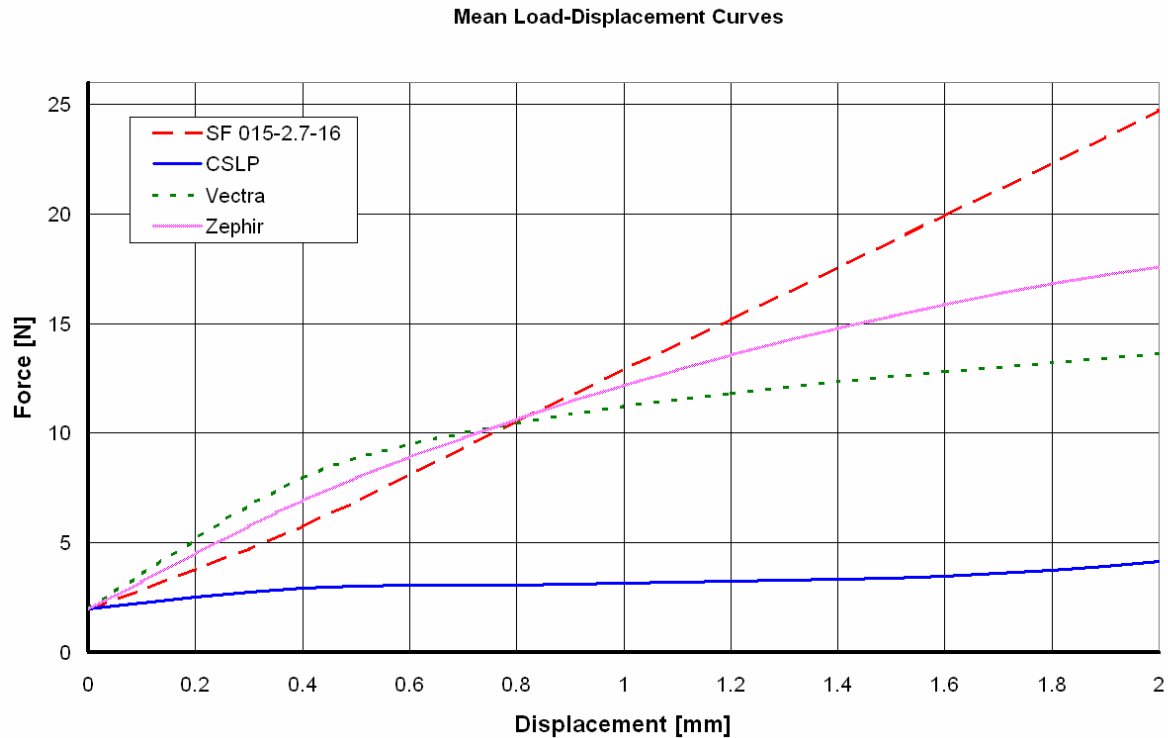


Fig. 3.27: Enlarged detail of the mean load-displacement curves of the plating systems; the initial stiffness is similar for Vectra, Zephir and SynFix-C, CSLP is clearly softer. The stiffness decreases for Vectra and Zephir on the next mm of deformation, while for SynFix-C, the stiffness stay constant (Abbreviations see on page 107; implant types see in annexe on page 116).

In the two figures above the results of all tested sample types are shown; the first one assembles all configurations of SynFix-C, the second one the plate systems; a reference is also included (SynFix-C 2.7/16). All plate systems have considerably higher maximum forces than the SynFix-C device and failure occurs at displacement 2 to 4 times higher. After the maximum load, in plate systems a drop of the force is observed, in contrast to SynFix-C, where the force decreases rather slowly. Load-displacement is more or less linear for SynFix-C, stiffness has tendency to decrease before rupture; the plates are rather weak at the beginning and stiffness increases with displacement. CSLP and Vectra become softer again near the maximum load, for Zephir stiffness increases until failure.



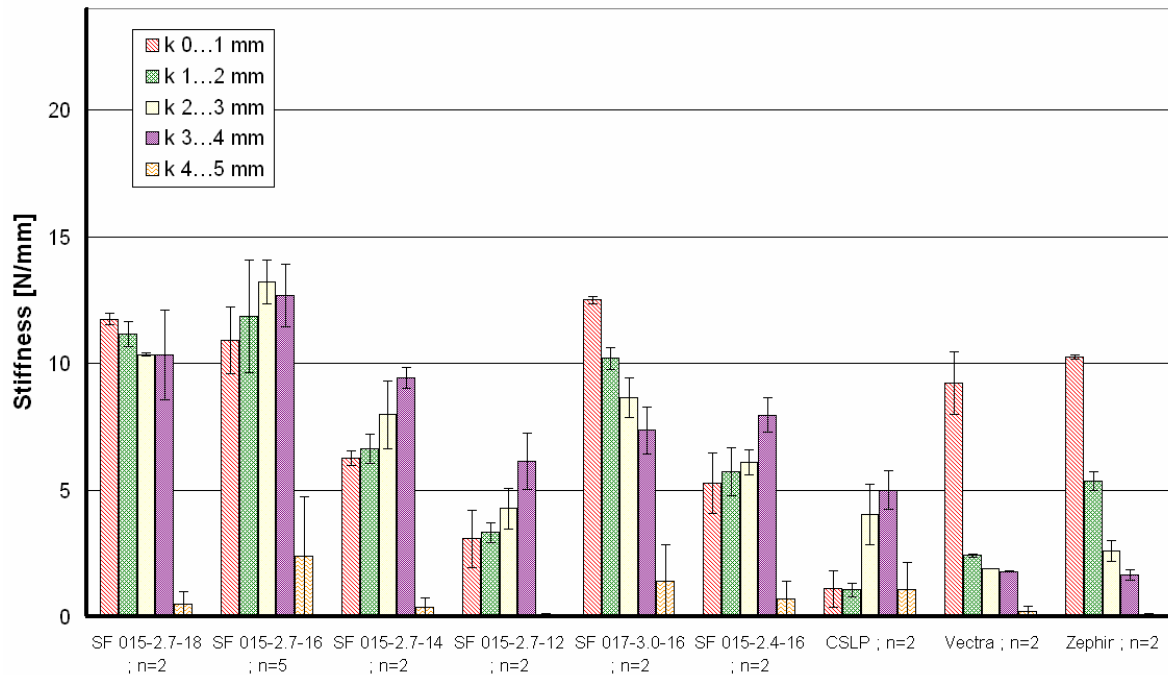


Fig. 3.28: Stiffness in tension for different regions of displacement. The number of repeats is indicated for each specimen type, standard deviation bars are indicated (Abbreviations see on page 107; implant types see in annexe on page 116). The standard configuration of SynFix-C (2.7/16 screws) has a higher initial stiffness than the plating systems. All plating systems are rather weak at small deformations.

The graphic above shows the stiffness for all tested specimen types. The stiffness is calculated for different regions of the absolute displacement. The most interesting value is the initial stiffness value. Its value for the prototype with the “standard” screw (2.7/16) is 11 [N/mm]. The longer (2.7/18) and the thicker (3.0/16) screw have a slightly higher value. Two of the compared plating systems have a slightly lower value. The thinner (2.4/16) and the shorter screws (2.7/14, 2.7/12) have a clearly lower stiffness (30 – 50% of the stiffness). The lowest initial stiffness offers the third plating system, CSLP. Its value is only about 20% of the stiffness of the prototype with the standard screws. For the prototype with the longest and with the thickest screw, the stiffness decreases with increasing displacement. Vectra and Zephyr are showing the same behaviour, but much more pronounced. For the screw sizes and for CSLP has a stiffness which increases with increasing displacement.

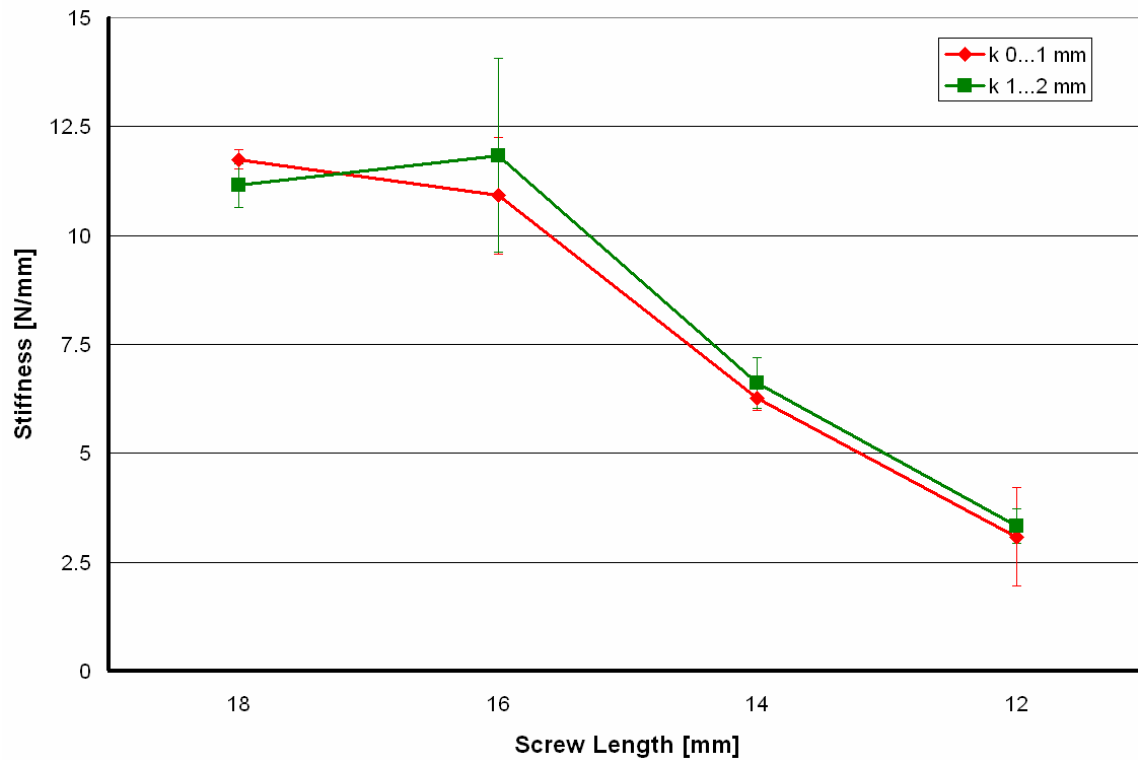


Fig. 3.29: Stiffness in function of the screw length; all tests with SynFix-C prototype 015, screw diameter 2.7 mm (Abbreviations see on page 107; implant types see in annexe on page 116). In general, the stiffness increases with a longer screw

The figure above points out the influence of the screw length; maximum force and the most relevant stiffness value (mean stiffness between 0 and 1 mm displacement) is shown. The maximum force is roughly linear function of the screw length. The stiffness value for the 18 mm screw is lower than could be expected for a linear length-stiffness behaviour. Between the 12 mm and the 16 mm screw a difference of almost factor 4 is present for the stiffness. All differences are significant with used z-test with  $\alpha = 0.05$ .

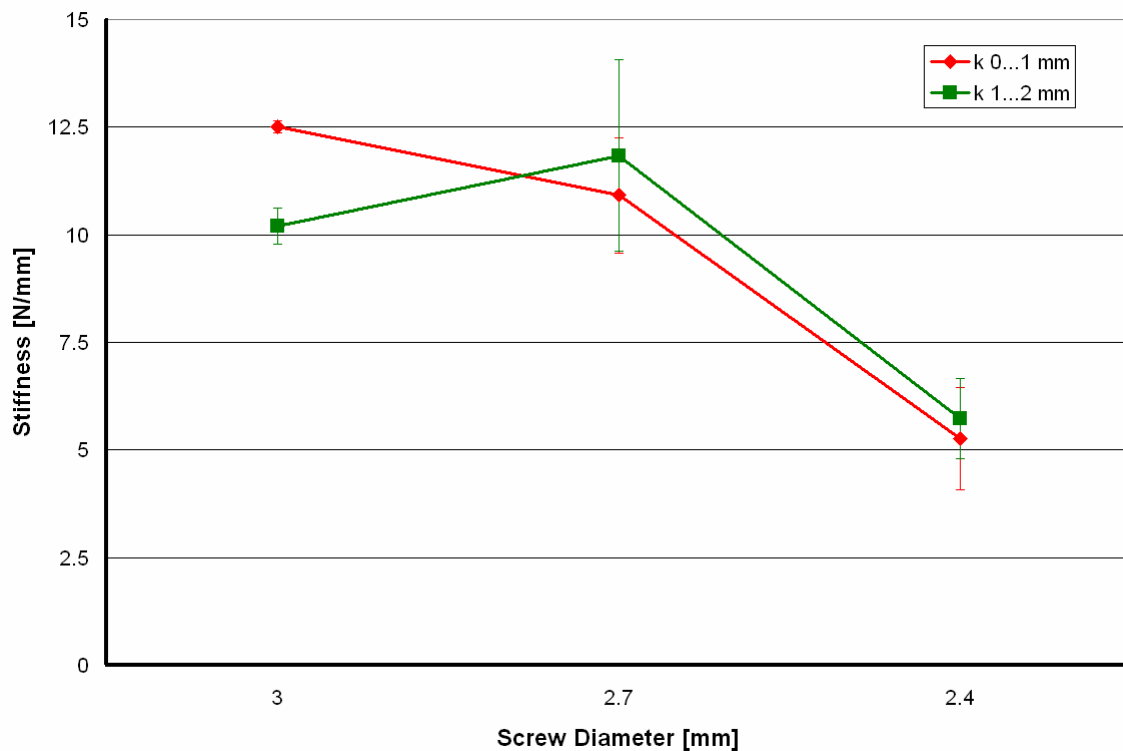


Fig. 3.30: Stiffness in function of the screw diameter; diameter 2.4mm and 2.7mm tests with SynFix-C prototype 015, diameter 3.0 mm with SynFix-C prototype 017, screw length for all tests 16 mm (Abbreviations see on page 107; implant types see in annexe on page 116).

Maximum force and stiffness in function of the screw diameter is represented in the figure above. Surprisingly, the 3.0 mm has a lower maximum force than the thinner standard screw. The differences to the reference sample are all significant (z-test,  $\alpha = 0.05$ ). An explanation for the relative weakness of the 3 mm screw could be caused by the set-up: a priori the prototype used in relation with the thicker screws has the same geometry as the prototype used with the 2.7 and 2.4 mm screws. In contrast, the attached cage had a height of 8 mm in stead of only 7 mm. The sleeve used for predrilling had not an absolute angular stability. The set-up with the 3 mm screws made thus the weaker impression before testing.

#### *Failure mechanisms*

In the 3.31 the typical failure mode for all SynFix-C configurations can be seen. The interface with two screws was again much more rigid and permitted only minimal movement. Most of the movement happened on the one screw interface, where the screw broke out a big part of the foam.

In one test, the single screw broke instead of the foam (figure 3.32). The damaged screw had a diameter of 2.4 mm, the failure was in the lower part of the screw head. The crack position corresponds moreover to the lower edge of the thread from the plate. In general, the 2.4 mm screws had a visually more damaged head after testing, some shafts showed a light curvature, so for both tests, new screws have been used. The crack is at the location of the highest bending moment (cf. loading schema).

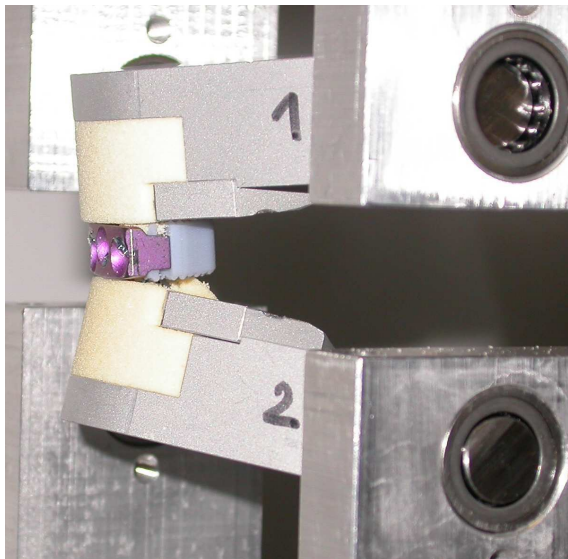


Fig. 3.31: Test 020, 8 mm displacement; SynFix-C 015 2.7/16



Fig. 3.32: Test 017, broken screw; SynFix-C 015 2.4/16

The screws in all plates rotated slightly in their fixation before an important part of the foam broke. The fissure always started at the front side besides the screws and propagated posteriorly to the surface. A characteristic example is shown in the figures 3.33 and 3.34 (example with Vectra).

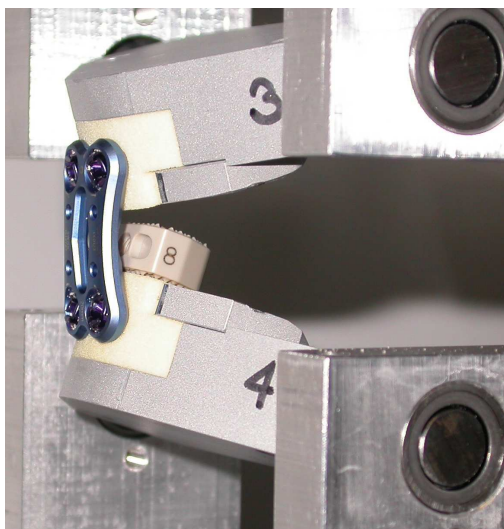


Fig. 3.33: Test 015, 16 mm displacement; Vectra

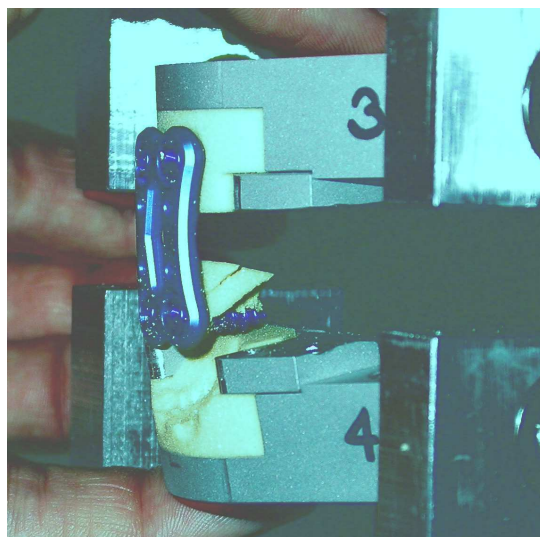


Fig. 3.34: Test 015, after failure; Vectra

**Test acceptance criteria reached?**

The value for the comparison was defined as the initial stiffness; the stiffness of the new device should reach the level of an anterior plate. The criteria is achieved for the following prototypes and screw dimensions:

- SynFix-C P015, 2.7/18, 3 screws
- SynFix-C P015, 2.7/16, 3 screws
- SynFix-C P017, 3.0/16, 3 screws

**3.7.4 Discussion**

Tension loads as they are simulated in the ASTM F 1717 test are not realistic under normal conditions. The artificial vertebrae are rotating about the anterior edge. The movement is quite close to biomechanical studies of the 1970ies [32]. An important observation is that the spacer surface is completely discharged; in the case of the zero profile device, the screw is thus pulled out more or less in its own axis. Behaviour under such tensile loads has been investigated, but it can not be associated to daily situations; a car accident may be a possible origin.

With some modifications, the test could simulate the flexion motion. A preload should be added, or at least the posterior located tensile load should be replaced by a compressive load anterior to the implant. The second point of improvement is the centre of rotation during the experiment. It is at the anterior side so far, induced by the implants. The centre should be forced to be at the normal IAR, near the posterior side of the intervertebral disc.

The simulation of the flexion motion is basically of interest for the device evaluation. The motion is important for the most daily situations and thus the device can be improved through this test type.

### 3.8 Isolated Interface Tests

#### 3.8.1 Set-up for the Isolated Interface Test

The isolated interface test has the identical set-up to the compression test. Behaviour under compressive and tensile loads is tested.

Assumptions to verify (for each test type separately):

- Stiffness of the two screw interface is clearly higher than that of the one screw interface

#### 3.8.2 Test Results Isolated Interface Tests

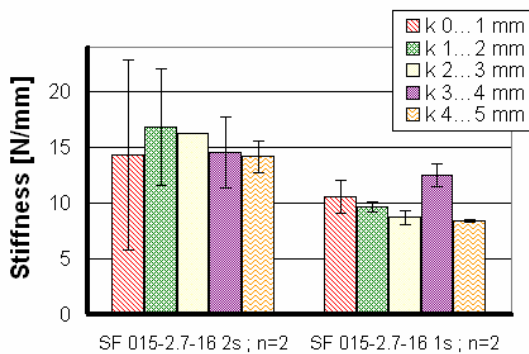


Fig. 3.35: Stiffness in tension for different regions of displacement. Interface tests; 2 screws on the left, 1 screw on the right

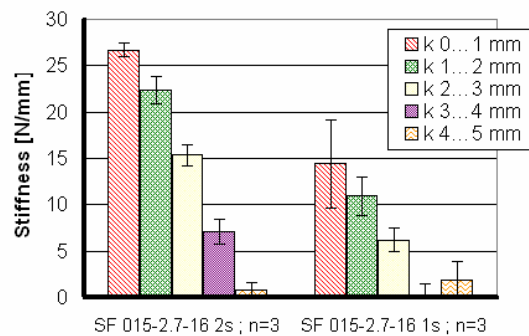


Fig. 3.36: Stiffness in compression for different regions of displacement. Interface tests; 2 screws on the left, 1 screw on the right

In the two graphics above, the results of the isolated interface tests are presented. This means, the tested interface was fixed in a foam block, the opposite interface was rigidly fixed directly in an aluminium block. On the left side, the results from the tension test are shown, on the right side the results from the compression test.

Surprisingly, the initial stiffness of the two screw interface is only slightly higher than the stiffness of the one screw interface. Also the initial stiffness is not the maximum stiffness. Analysing the individual load-displacement curves it appears that this is most probably caused by an error in the set-up or the procedure of the experiment, which explicates the high standard deviation. The valid experiment has an initial stiffness of about 20 [N/mm]; this is almost two times the stiffness of the one screw interface and is in coincidence with the expectation.

The results of the compression test are in accordance with the expectation: The initial stiffness of the one screw interface is about 55% of that of the two screw interface.



Fig. 3.37: Test 045, 8 mm displacement; SynFix-C, one-screw interface

In figure 3.37 an example of a one-side fixed interface is shown. The posterior edge is again centre of rotation for the adjacent foam-block. The rotation of the rigid block (below) is smaller than with a foam-block (see picture of test 033, figure 3.13). Displacement at failure is smaller than the standard configuration with one screw in foam and slightly higher with two screws in foam.

Hence the isolated interfaces tests should be compared to the complete device test with care. However, the measured values are consistent: If we take the two measured rigidities from the isolated interfaces and add them serially, we have:

$$k_{tot} = (k_1 k_2) / (k_1 + k_2)$$

where  $k_1$  and  $k_2$  are the rigidities taken from the isolated interface tests with 1 respectively 2 screws. The mean stiffness between 0 and 1 mm displacement is:

$$k_1 = 14.41 \text{ [N/mm]}$$

$$k_2 = 26.67 \text{ [N/mm]}$$

That would result in a total stiffness of

$$k_{tot} = 9.4 \text{ [N/mm]}$$

which is just slightly higher than the actual measured stiffness  $k_{2.7/16} = 8.8 \text{ [N/mm]}$ . A device with four screws would though have a stiffness of:

$$k_{4s} = k_2^2 / (2 k_2) = 0.5 k_2 = 13.4 \text{ [N/mm]}$$

Another approach is to take the difference of the isolated interface experiments; using the same stiffness value, the single screw has 54 % stiffness of the 2 screws interface. As an assumption, this relation is also true for the complete device (both interface in foam), the stiffness would then be:

$$k_{2.7/16} = k_2 \cdot 0.54k_2 / (k_2 + 0.54k_2) = 0.54/1.54 k_2$$

$$k_2 = 1.54/0.54 k_{2.7/16} = 25.1 \text{ [N/mm]}$$

The complete device with four screws would then have a stiffness of:

$$k_{4s,2} = 12.5 \text{ [N/mm]}$$

	Standard implant	4 screws first approach	4 screws second approach
	$k_{2.7/16}$	$k_{4s}$	$k_{4s.2}$
Stiffness [N/mm]	8.8	13.4	12.5
[%]	100	151	142



## 3.9 Rotation Tests

### 3.9.1 Set-up for Rotation Tests

First, the intention was to keep the set-up from the tension and compression tests also for the rotation tests. The axis of rotation passes in this case 30 [mm] posteriorly to the front side of the implants; the additional axis of rotation perpendicular to the actual axis lead to a wedging of the implant (cf. figures below). After the pretests, this set-up was considered not reasonable and was though improved.

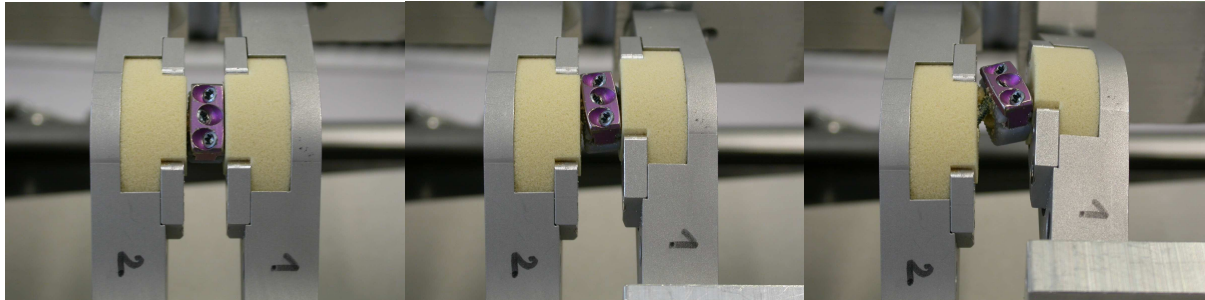


Fig. 3.38: Wedging of the implant in the first set-up (sequence of test 027); this set-up was considered not suitable

The improved set-up has a fixed axis of rotation; its distance from the anterior side of the implant can nevertheless be adjusted ( $r$  is modifiable). This feature permits to simulate different IAR. For the first series the axis was set at the posterior side of the cages (15 mm from the anterior side).

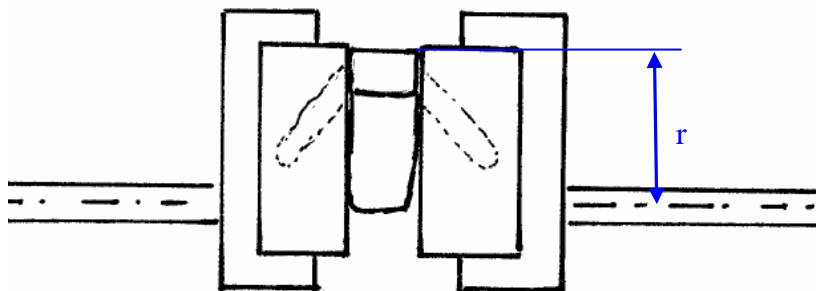


Fig. 3.39: Modified test set-up ; the axis of rotation is rigidly fixed at a distance  $r$  from the anterior side of the implant

Assumptions to verify:

- Maximum torque of the new SynFix-C device is in the same order as known anterior plating systems
- Stiffness of the new SynFix-C device is in the same order as known anterior plating systems

### 3.9.2 Test Results Rotation Tests

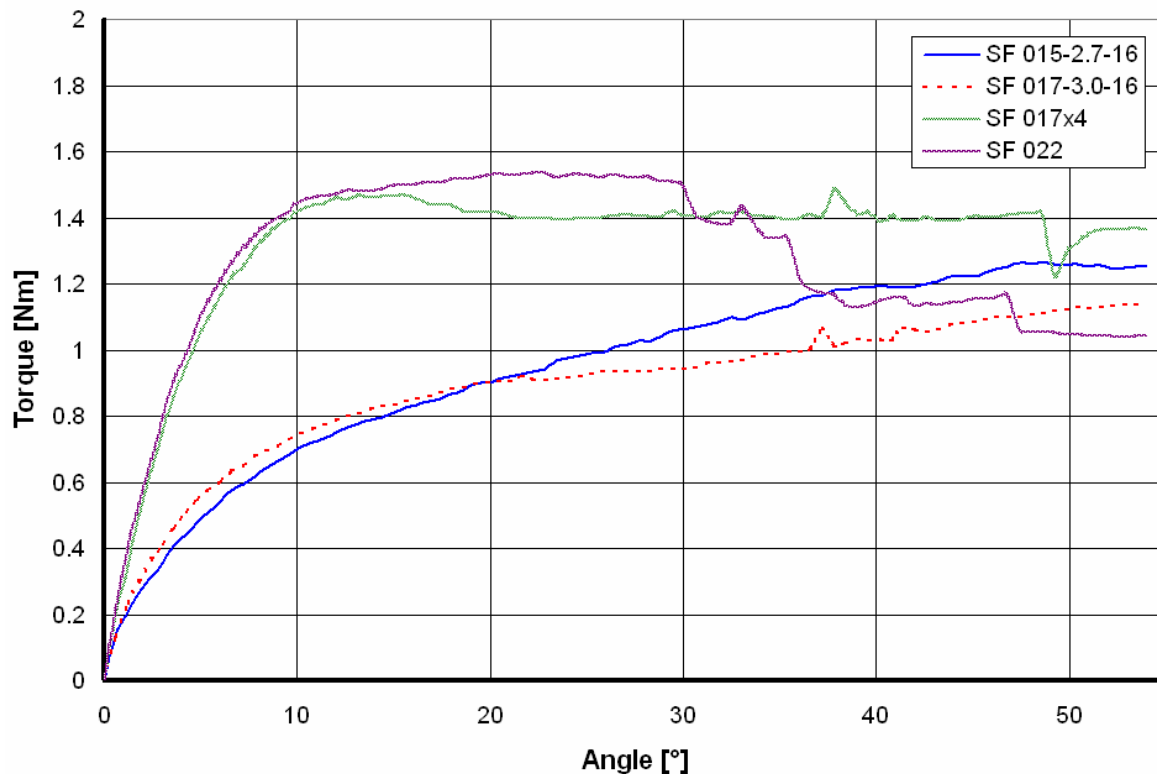


Fig. 3.40: Torque-angle curves for the axial rotation test; three screw concepts with different screw diameters (prototype 015, diameter 2.7 mm, thick blue line; prototype 017, diameter 3.0 mm, dashed red line) and four screw concepts (prototype 017x4 and 022, both using diameter 3.0 mm screws). The experiments with the same concept are close to each other; the stiffness at small deformations is clearly higher for the four screw concept than for the three screw concept.

In the figure above, mean torque-angle data of the tested samples are represented. The most interesting question at this point of the project, was the difference between the three- and the four-screw concept, so two types of each concept were tested; prototype 015 has 3 2.7/16 screws, 017 has 3 3.0/16 screws; 017x4 and 022 have both 4 3.0/16 screws, but the geometry is slightly different. From the graphic above the difference between the concepts appears clearly. 015 and 017 have almost identical curves: the initial stiffness is considerable but decreases rapidly. Between 10 and 40° the curve is more or less linear, the maximum torque is reached at about 50°. 017x4 and 022 with four screws are much stiffer at the beginning. 017x4 has the maximum torque at 12°; 022 continues increasing minimally.

The actual maximum torques are represented in the figure below; the amplitudes for the 3 screw concept are at about 80% of the 4 screw concept. The differences for the angle at the maximum torque are bigger – a factor two can be found between the concepts.

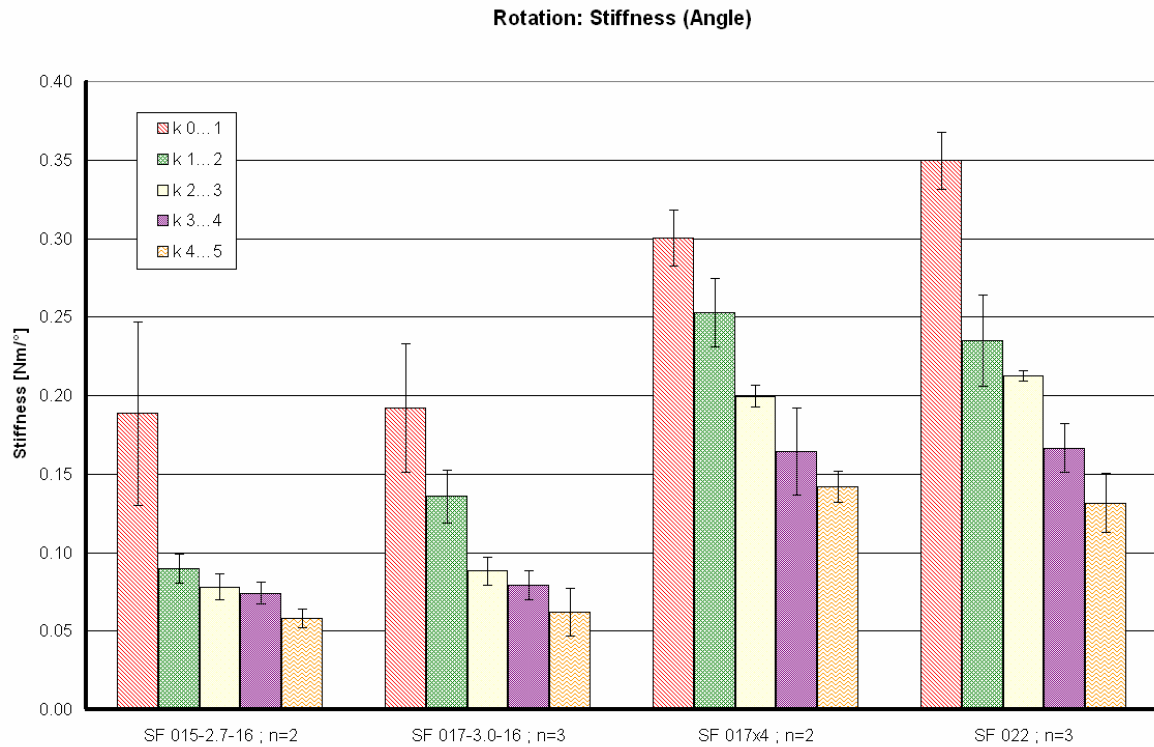


Fig. 3.41: Stiffness in function of the angle (axial rotation); the graphic underlines what already has been seen on the graphic before: the four screw concepts provide a higher initial stiffness than the three screw concept.

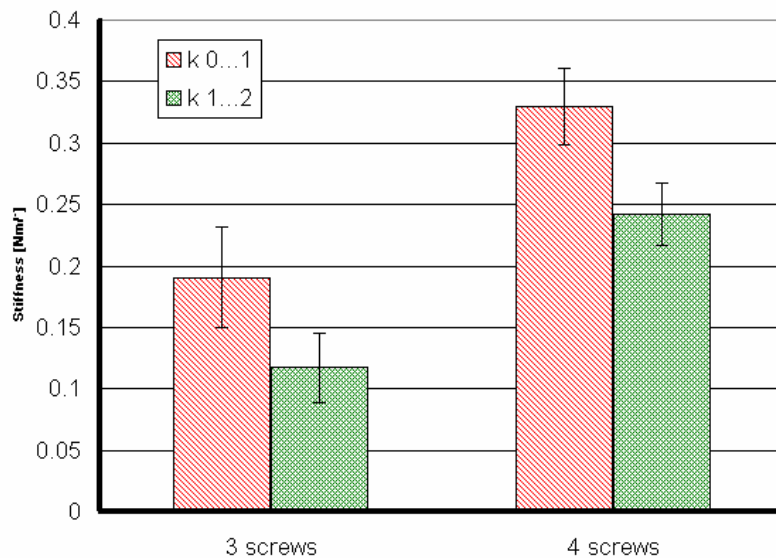


Fig. 3.42: Stiffness; 3 vs 4 screws; graphic to emphasize the difference of the number of screws, independent of screw size

In independently of the screw size; four screws are showing a higher stiffness than 3 screws (cf. figure 3.42).

**Test acceptance criteria reached?**

No statement can be made about the reaching of the test criteria, because no plating systems were tested on the improved test set-up.

**3.9.3 Discussion**

The first setup, an adaptation from ASTM F-1717, proved to be not of use for comparing the biomechanics of the different test specimens. The improved setup showed a much more realistic behaviour because the axis of rotation was in the area of the intervertebral disc, which is similar to a healthy spine. In contrast the new setup doesn't account for the inclination of the instantaneous axis of rotation or IAR (cf. 2.3.2). The preload of 50 [N] is basically the estimated load on the vertebral body in neutral position. Despite the fact that the movement in the test set-up is an isolated rotation without coupled movements the test data is still useful for the implant improvement. A motion complementary to the flexion-extension simulation can give new information about the device's properties.

Due to the lack of time, only a few systems could be tested. Plates were not included, but the 3 and the 4 screw concept were compared. Two screw sizes with the screw concept (2.7/16, 3.0/16) and two 4 screw prototypes (017x4, 022), both with 3.0/16 mm screws were included. The results showed a clear advantage in stiffness for the 4 screw concept. This reinforced the decision to focus on this concept.

The neutral zone (NZ) on C5/C6 is about 1° on each side; the four screw concept showed the highest stiffness in this region. The axis of rotation in the mechanical tests is similar to the real IAR so stiffness values are directly comparable even though dissimilar materials were used. Experiments by Panjabi et al. [18] showed a stiffness of about 0.3 [Nm/°] in the region from 1° to 2° rotation. Results in foam are relatively close at about 0.3 [Nm/°] from 0...1° rotation and 0.25 [Nm/°] from 1 to 2°. The influence of the cortical shell is likely less influential compared to flexion-extension testing. Additional stability is provided in rotation by the vertebral body shape (processus uncinati). Helping as well is the enormous NZ on C1/C2, which supersedes that of the other levels and can be considered sufficient for daily activities under normal conditions.

The rotation tests can give complementary information to the extension tests even if the axis of rotation is not physiologically correct.

## 3.10 Push-out Tests

### 3.10.1 Set-up for Push-out Tests

The device is mounted on foam blocks (according ASTM F 1839-01). The foam blocks are then fixed on the testing machine; an axial preload simulates the head weight. A pusher in control displacement exercises a force on the implant until the implant drops out of the foam. The test set-up does not accord to a particular standard, but has been already applied for previous implants.

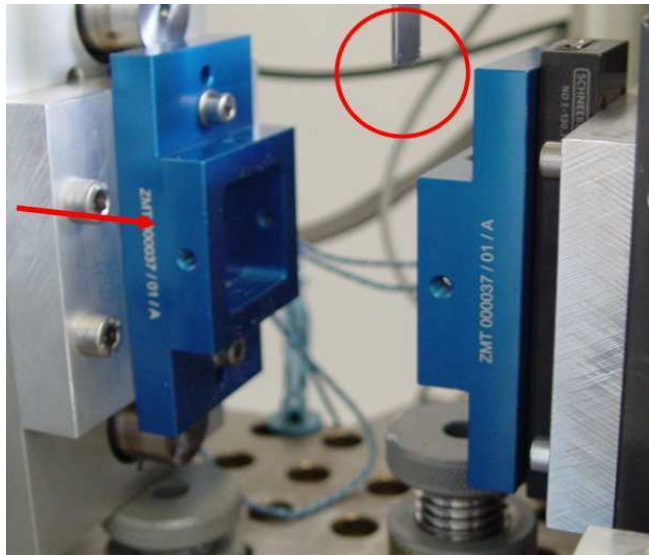


Fig. 3.43: Set-up for the push-out test; the pusher is in the red circle; the left side is preloaded with 50 [N] and rigidly fixed in push-out direction; the right side is completely constrained

Assumption to verify:

- Maximum force of the new SynFix-C device is clearly higher than that of known standard cages

### 3.10.2 Test Results Push-out Tests

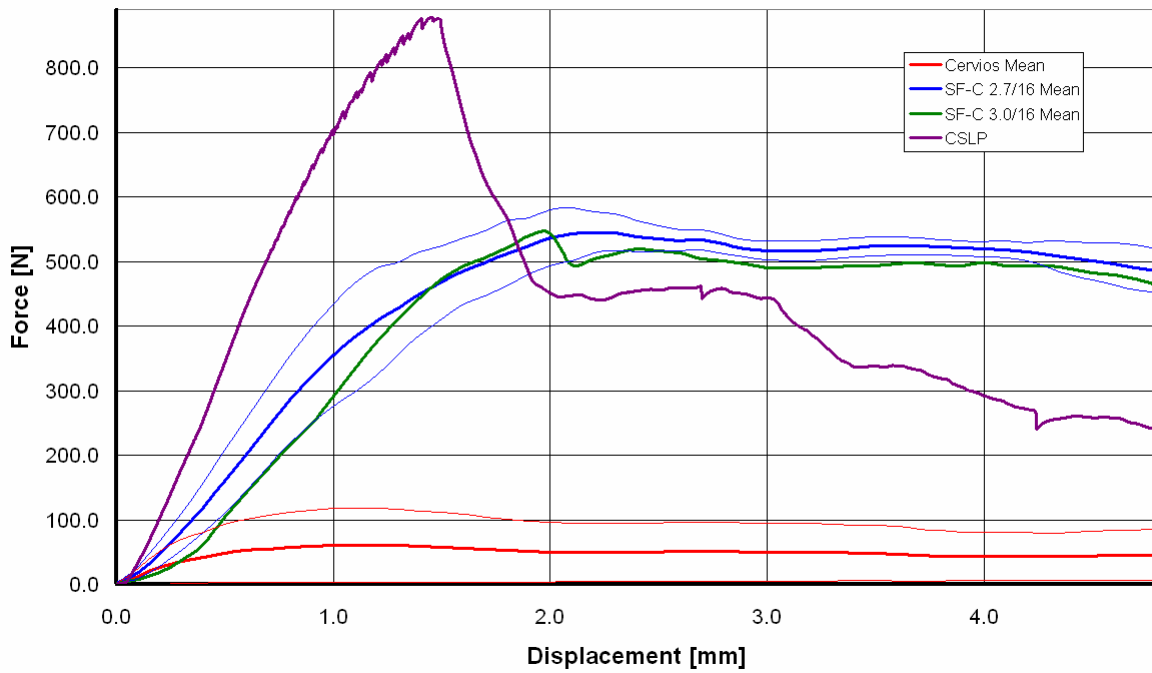


Fig. 3.44: Load-displacement curves from push-out test; mean curves are shown, standard deviation curve is indicated for Cervios and SynFix-C 2.7/16 (thinner lines); SynFix-C has a clearly higher maximum force than the standard cage (Cervios); CSLP has the highest maximum force (CSLP: n=1)

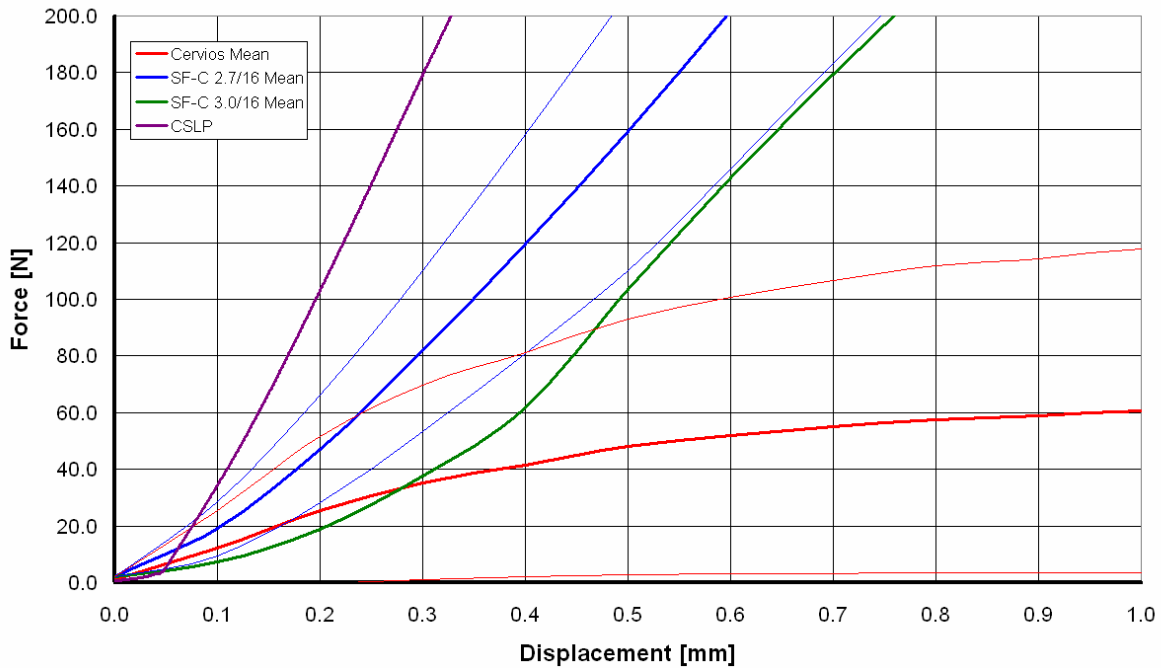


Figure 3.45: Enlarged detail of the previous figure. At the beginning, an extremely low stiffness can be seen for CSLP. The standard cage has the highest stiffness right at the beginning of deformation, SynFix-C has its highest stiffness after several tenth of millimetres of displacement.

Figure 3.44 shows the mean load-displacement curves of all samples types; the standard deviation is indicated for Cervios and SynFix-C 2.7/16 (for both: n=5). The standard cages are the weakest with a maximum force of about 100 N. The SynFix-C with 2.7/16 and 3.0/16 screws are clearly stronger with a maximum of about 550 N. A part from an initially flatter load-displacement curve for the 3.0/16 screws, no difference can be detected for the two screw sizes. CSLP is again clearly better than SynFix-C, its maximum force is 850 N. Once this force reached, it drops rapidly to the half; the screws are completely detached at 5.2 mm displacement. Cervios and SynFix-C are showing both a different behaviour: force decreases slowly after the peak over a large displacement.

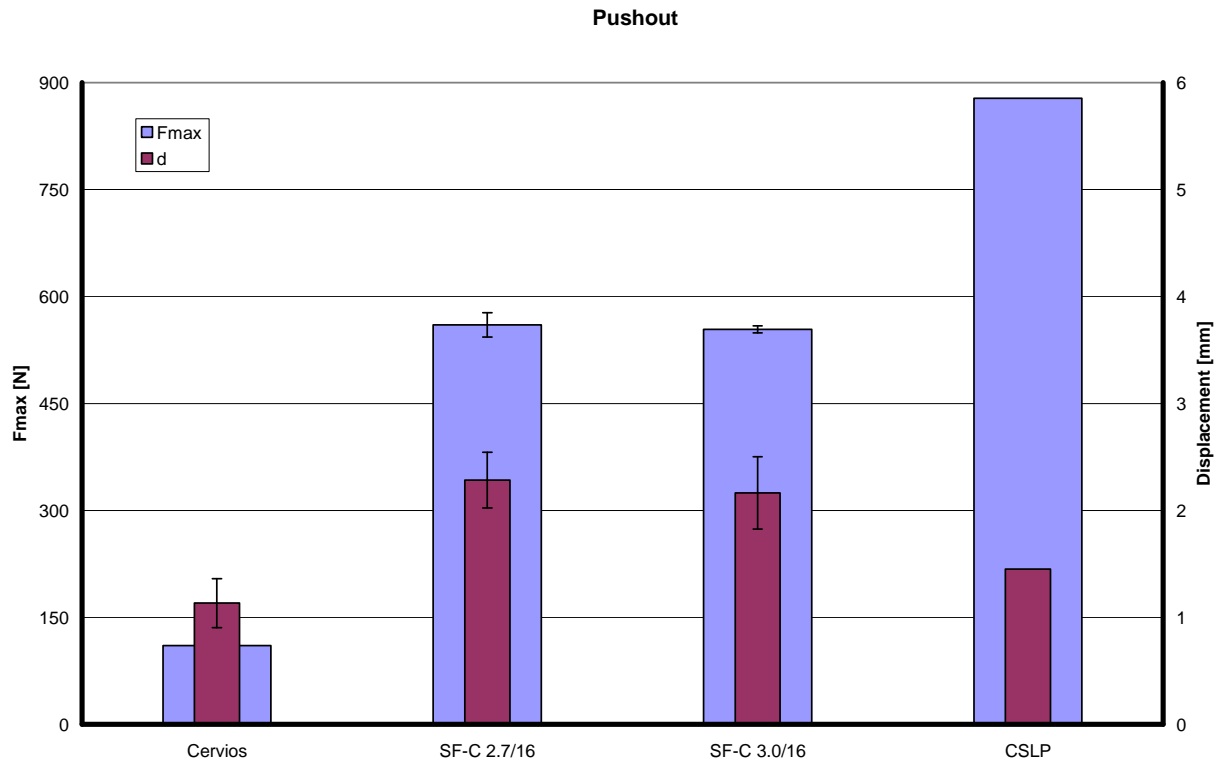


Fig. 3.46: Maximum force and corresponding displacement (push-out); the standard cage has clearly the lowest maximum force, the maximum force in the new device seems not to be dependent on screw diameter; the highest maximum force has clearly CSLP.

In figure 3.46 the mean values of the maximum force and their corresponding displacement are represented. Obviously there is no significant difference for the two screw diameters. Cervios has a mean maximum force of 110 N at 1.1 mm displacement, SynFix-C with 2.7/16 screws 560 N at 2.3 mm, SynFix-C with 3.0/16 screws 550 N at 2.2 mm and CSLP 880 N at 1.5 mm.

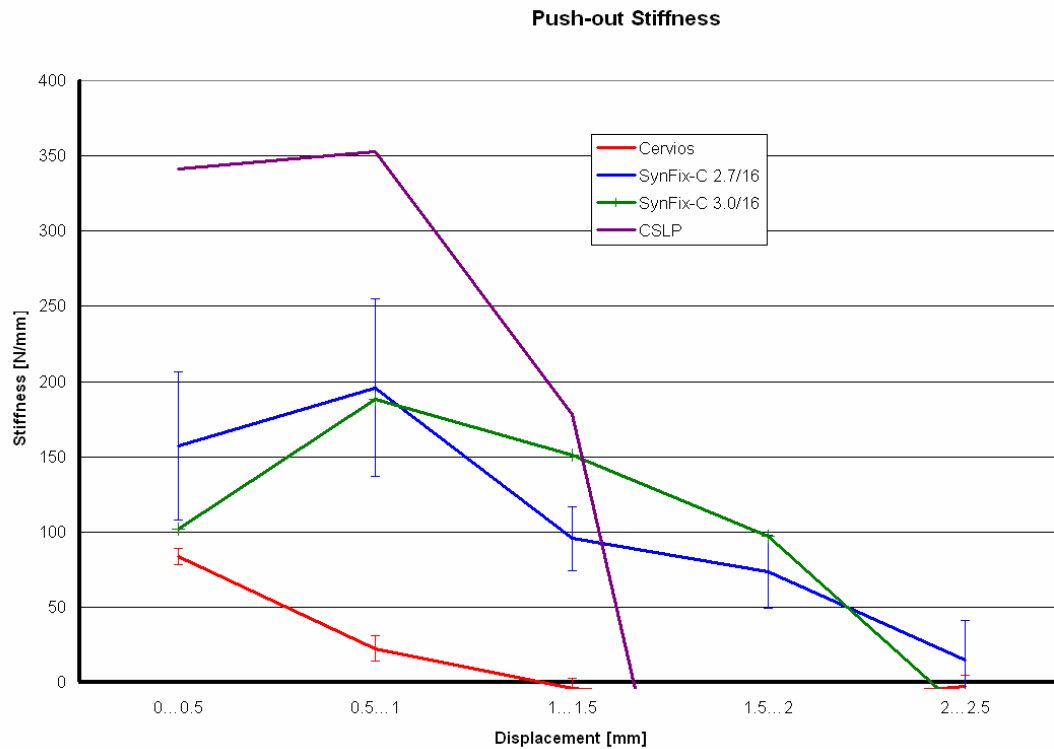


Fig. 3.47: Stiffness (displacement criteria, push-out)

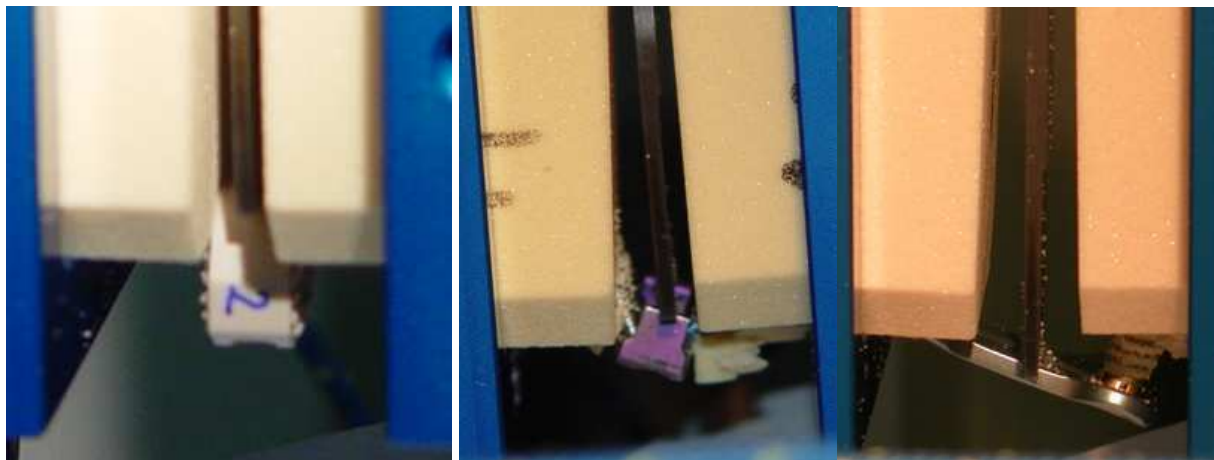


Fig. 3.48-50: Push-out tests: Standard cage (left), SynFix-C (central) and anterior plate (right)

Cervios is showing maximum stiffness from the beginning. This is due to the teeth which are already indented into the foam because of the axial preload of 50 N.

Of course the side with the single screw is weaker and so SynFix-C is pushed out asymmetrically (fig. 3.49). The plate is rotating about an axis located approximately on the front edge of two screw side. Maximum force is high because the single screw has to brake out a big part of the foam.

In the case of CSLP, the pusher couldn't be placed exactly in the middle because of the dimensions of the plate; screws on the side closer to the pusher were pulled out. Resistance dropped after reaching the maximum force, because the screws had pulled out a cylinder which could slide through the holes.



**Test acceptance criteria reached?**

The test criteria have been reached, as the stiffness and the maximum push-out force of the new device is superior to the standard cage.

**3.10.3 Discussion**

The push-out test is a standard test for spine implants. Information from this testing is of secondary importance for the comparisons of the described implants. SynFix-C is a cross between a plate system and a stand alone cage. This test should prove the superiority of the new device as compared to the cage. Push-out respectively back-out of plates is not a problem anymore since locked screws are currently standard of care. The new device is fixed with screws between the vertebrae and thus it is not surprising that the rigidity and the maximum force are 4 to 5 times higher than for a stand alone cage. These results are sufficient and no further test are required for the design evaluation.

There may be some value in retesting push-out using the matching cage out of PEEK material.

The test is run under a preload of 50 [N], which corresponds approximately to the load on the intervertebral disc in neutral position (C5...C7). It is questionable, if this load shouldn't be decreased, because a push-out of the implant occurs most probably under extension, when intervertebral space is opened anteriorly and the load is minimal. A reduced load would mostly reduce the performance of the standard cage, screw fixed device would be less influenced by the preload.

The test is relevant from a physiological point of view, but of limited use for the comparison of the devices under consideration. Performing this test is not particularly interesting during the development; as it is quasi a standard test, it should be performed with the final product.

### 3.11 Subsidence Tests

#### 3.11.1 Set-up for Subsidence Tests

Subsidence tests have been performed on other products in development before. The set-up is slightly different from the standard. In contrast to the ASTM F 2267 standard the axe where the compression force is applied is rigid; also the implant is only tested between foam blocks. The used foam was a PUR foam of grade 15 according to ASTM F 1839-01.



Fig. 3.51: Set-up for the subsidence test; the lower foam block is rigidly fixed; the upper one is on the actuator and connected with the load cell

Assumption to verify:

- Subsidence is not significantly higher in the new SynFix-C device than in a known standard cage

#### 3.11.2 Forces in the Specimen

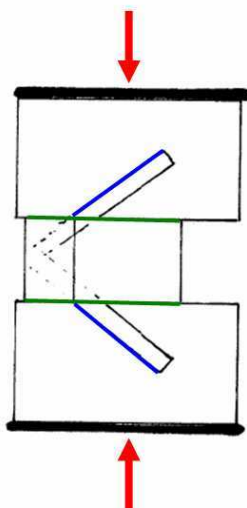


Figure 3.52: Loading of the specimen in the subsidence test. The exterior force (red) is supported by the screws (blue) and the cage surface (green)

The axial force is applied on the upper and lower surfaces of the foam blocks. In the case of the standard cage, the force is transmitted through the cage surface only (green line); in SynFix-C, the screw is loaded as well (blue line). The cage surface is much larger than the screw section. It can thus be expected that the screw influence is limited.

### 3.11.3 Test Results Subsidence Tests

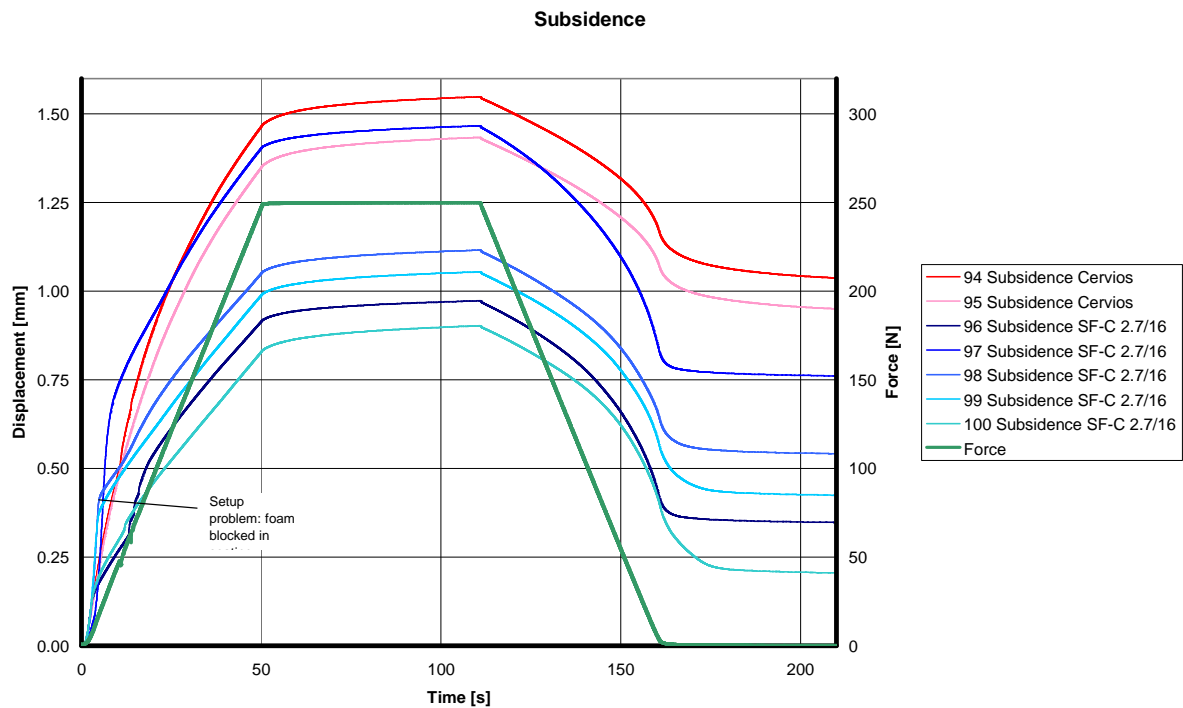


Fig. 3.53: Displacement-time curves in subsidence test; load-time curve (imposed) indicated (green)

In the figure 3.53, displacement-time curves for all samples are represented. Also the imposed force in function of time is shown (green curve). Absolute subsidence for the Cervios is about 1.5 mm. SynFix-C shows an important deviation, 4 of the five maximum values are at 1 mm, one value is on the level of Cervios. The important deviation is partially caused by problems with the set-up: Both foam-blocks were attached to the SynFix-C, and afterwards put in a retainer. The resistant force due to friction was higher than the preload, so part of the subsidence of SynFix-C is caused by this fact.

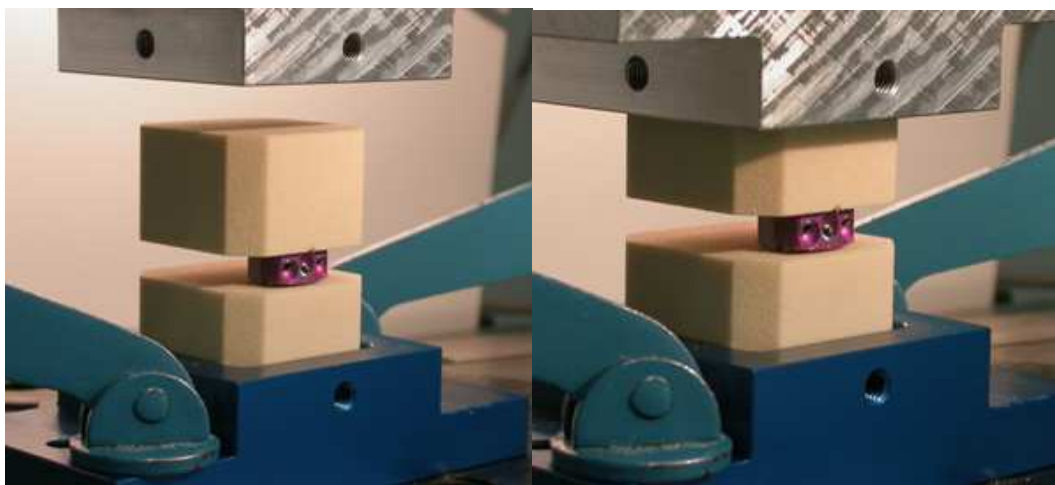


Fig. 3.54: Push-out test: the SynFix-C device has to be mounted previously

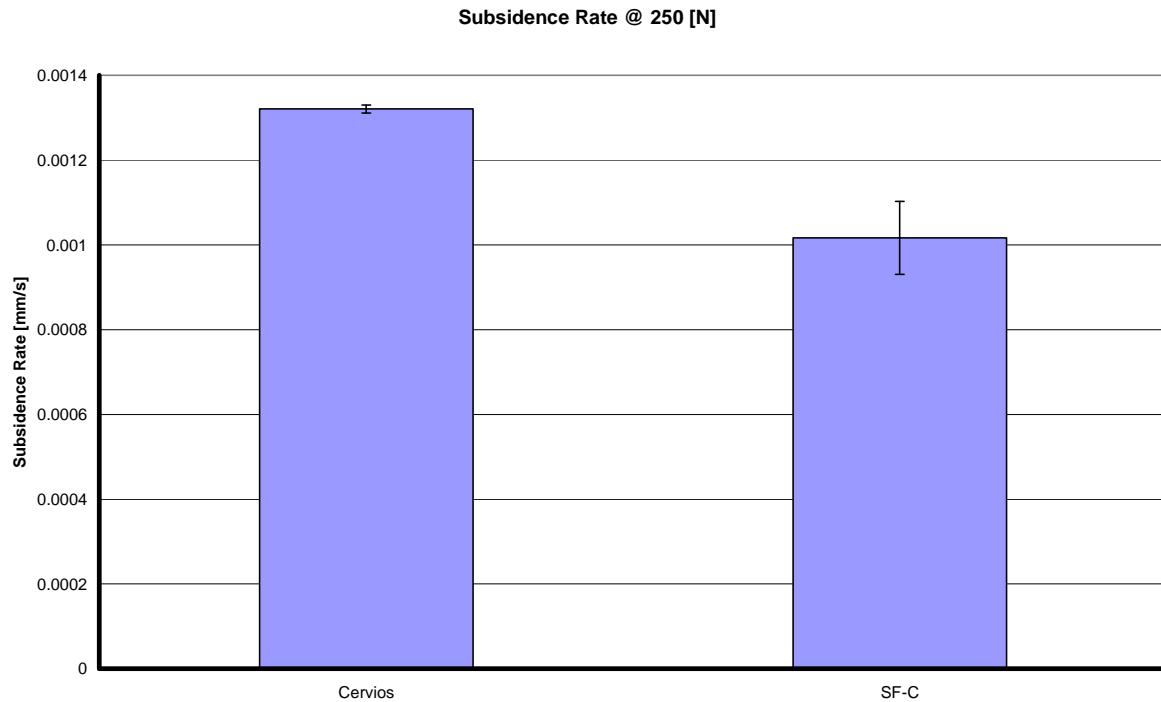


Fig. 3.55: Subsidence rate at 250 [N]; it is clearly lower than for the new device (SynFix-C) than for the standard cage. SynFix-C was tested in the standard configuration (2.7/16 screws).

Figure 3.55 shows the subsidence rates for Cervios and SynFix-C. Subsidence rate  $d_{sr}$  is calculated as:

$$d_{sr} = (d_{@t=110} - d_{@t=50})/60 \text{ [mm/s]}$$

Where

$d_{@t=50}$  : displacement at  $t = 50$  and

$d_{@t=110}$  : displacement at  $t = 110$ .

Subsidence rate is slightly but statistically significantly lower for SynFix-C than for Cervios. There shouldn't be an influence from the set-up problems on these values, but this can't be proved without further experiments.

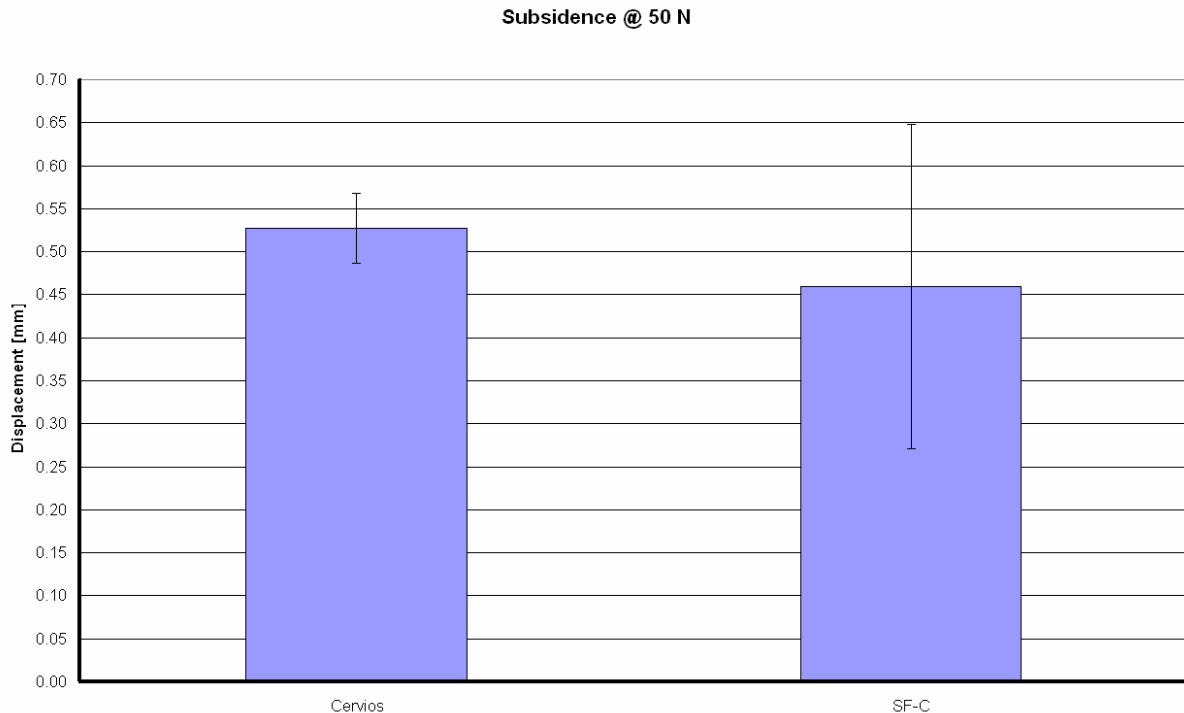


Fig. 3.56: Subsidence at 50 [N]; subsidence of SynFix-C is lower, but the standard deviation is enormous.

Subsidence value at 50 N axial load is shown in the figure above. This value is chosen because it represents approximately the load of the head. The Cervios value is slightly higher; values of SynFix-C would probably be lower without set-up problems. Because of the set-up problems and the resulting large standard deviation, the difference is not statistically significant in a z-test ( $\alpha = 0.05$ ).

### Test acceptance criteria reached?

The subsidence rate of the new device is clearly lower than that of the standard cage. The subsidence at 50 [N] is not significantly higher for the new device than for the standard cage. Thus, the test criteria are achieved.

### 3.11.4 Discussion

Subsidence was in the past a common clinical complication. Experience pushed design modifications and thus subsidence incidences are today quite rare. Nevertheless subsidence behaviour is necessary to prove.

From clinical experience it is known that open cage design is favourable for bone fusion when the space is filled with bone graft, what should be the goal of each interbody fusion implant.

Stress distribution of intervertebral discs is centred on the annulus. The structure of the vertebral body is perfectly adapted for this situation because endplate thickness is less in the centre. Analyses on stress distributions for different cages have also been made. A clear advantage was found for a design forcing contact on the border of the endplate.

Keeping the same shape is sufficient to avoid any subsidence problems. The expressiveness of the purely mechanical subsidence test is very limited. In fact the test gives little more

information than a simple comparison of cage area. Comparing the device with screws to a standard cage is not possible. The cage and the screw are in contact with the same material, while in reality the cage lies on the hard cortical shell and the screw is in cancellous bone. The influence of the screws is thus overestimated.

The subsidence rate is a measurement of the viscoelastic properties of the PUR foam and not an evaluation of the device. Its status as a as a “standard” test should be revised.

The set-up of the test is basically not wrong in a physiological point of view, but the bone model is in this case not sufficient, to evaluate the product.

## 3.12 Summary of the Test Results

### 3.12.1 Acceptance of Test Criteria

The following table recaps the test acceptance criteria presented in chapter 3.2 with the corresponding decision.

Test	Compared Device	Compared Value	Criteria	Decision
Compression	Anterior Plate	Initial Stiffness (k)	$k_{\text{SynFix-C}} \approx k_{\text{compared device}}$	Partially <sup>1)</sup>
Tension	Anterior Plate	Initial Stiffness (k)	$k_{\text{SynFix-C}} \approx k_{\text{compared device}}$	Partially <sup>2)</sup>
Axial Rotation	Anterior Plate	Initial Stiffness (k)	$k_{\text{SynFix-C}} \approx k_{\text{compared device}}$	Open <sup>3)</sup>
Push-out	Standard Cage	Initial Stiffness (k), Maximum Force (F)	$k_{\text{SynFix-C}} > k_{\text{compared device}}$ $F_{\text{SynFix-C}} > F_{\text{compared device}}$	Yes
Subsidence	Standard Cage	Subsidence at 50 [N] (s), Subsidence Rate (t)	$s_{\text{SynFix-C}} \leq s_{\text{compared device}}$ $t_{\text{SynFix-C}} \leq t_{\text{compared device}}$	Yes

- 1) Some of the tested prototypes do have reached the criterion, but not all of them
- 2) Some of the tested prototypes do have reached the criterion, but not all of them
- 3) Anterior plating systems were not included in the experiments with the improved set-up, so no decision can be made

### 3.12.2 Method

The test method for the compression and tension test has proven to be useful in comparing relative construct stiffness. The same can be said about the set-up for the push-out test. The subsidence test set-up is basically correct and doesn't cause problems with a standard cage. For the SynFix-C device, where both foam blocks are previously fixed together, the set-up is over constrained and thus the results are confounded. The set-up for the rotation tests had to be modified and the second set-up proved to be more useful.

Minimal deviations in foam quality seem to add variation to the measures. It is therefore recommended to test the foam blocks prior to testing and to use foam blocks manufactured in the same series out of the same block of material.

### 3.12.3 Results

Maximum force under tension was clearly higher in all tested plating systems than in all configurations of the SynFix-C device. In contrast stiffness was slightly higher for the new device with exception of the shortest screw.

In compression maximum force and the stiffness is higher for the plates. The SynFix-C device with 4 screws and 3 bigger screws (length 16, 18 [mm]) have an initial stiffness at the same level. The stiffness increases with displacement for the plates and decreases for the SynFix-C device.

In rotation only a comparison between the 3 and the 4 screw concept was made. The 4 screw concept appeared clearly stiffer; the maximum torque was at the same level.

The assumptions made for the push-out and the subsidence test have been proved.

## 4 VERTEBRAL BONE MODEL

The reason for developing a finite element model was to have an easily modifiable model which is comparable to the mechanical experiments. Once calibrated, the model parameters, such as the screw size, may be varied. Much more interesting is the variation of material parameters, the main drawback of the foam used as a bone model in the mechanical tests. Compared to mechanical tests on cadaveric bone the FE model is cheaper and results are 100 % repeatable, thus comparison can be made easily when studying effects of model parameters.

### 4.1 Material Model

Material data for the foam used is available on the distributor’s web site [42]. The complete data sheet is in the annex. The model relevant data are:

$E_{comp} = 140$ [MPa]	Compressive Young’s Modulus
$E_{tens} = 150$ [MPa]	Tensile Young’s Modulus
$\nu = 0.3$	Poisson Coefficient

These data are valid at room temperature.

The use of a linear material model including the mentioned data lead to an overly rigid assembly. This results because the modulus is only valid for a limited range of deformation and even the mechanical strength is rapidly exceeded. For this reason material measures have been made and collected data directly introduced in the model. The test protocol is included in the annex. Instead of a linear material model a hyperfoam model is selected. Test data from a uniaxial test setup are inserted, the Poisson coefficient is assumed to be constant. The software interpolates the complete stress-strain relation with a model. Simulating the material test a model of strain energy potential order 6 was revealed to be the best. The same material model was used for the actual simulation (cf. figure below).

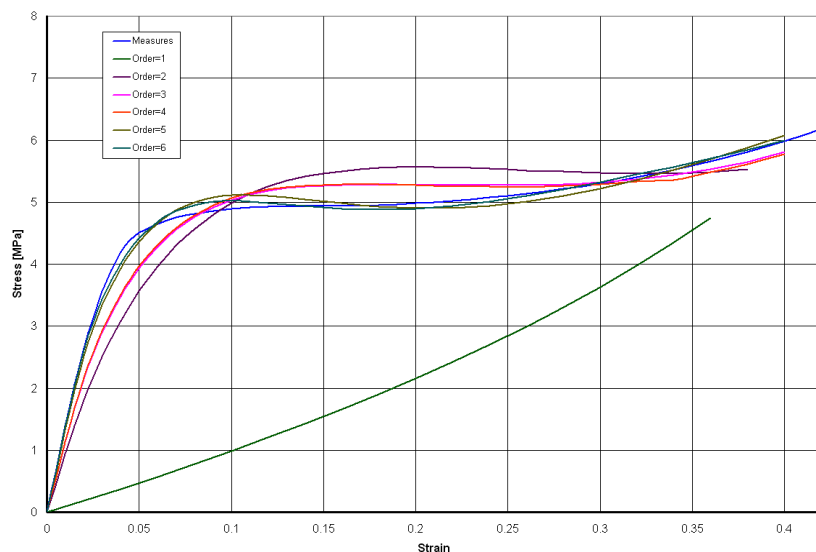


Fig. 4.1: Simulation of the compression test: different material models; the model of order 6 provides the best match



## 4.2 Basic Model

Developing an FEA Model is basically finding a compromise between maintaining accuracy and keeping the model simple enough to avoid resolution problems.

### 4.2.1 Assumptions

Simplifications are based on the following assumptions:

- The model is symmetric about the median-sagittal plane
- The foam – test block assembly is rigidly tied together
- Plate and cage are rigidly fixed
- Rigidity of plate and cage are infinitely high vis-à-vis the foam properties
- The central hole in the cage has no significant influence
- The screws are rigidly fixed in the plate
- Failure and plastic deformation is not predominant at the beginning of the simulation (i.e. the model is valid at small deformations)

### 4.2.2 Geometry

Basically the main symmetry plane (sagittal plane) is used; only one half is modelled which is an important save of computing capacity.

The implant, plate and cage, is represented as one part. The part is simplified to a quadric element; the posterior tapering is included because this is an important reduction of the supporting area (as seen in the mechanical tests, the device rotates about the posterior edge). The surfaces contacting the foam have rounded edges in order to avoid singularity cases in these locations. The screw threads are in the correct position and are staged. This is simply an artifice for constraining the screw on the plate easier.

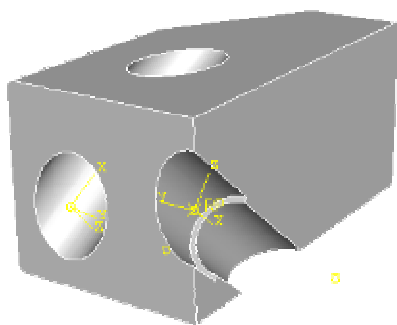


Fig. 4.2: Plate model

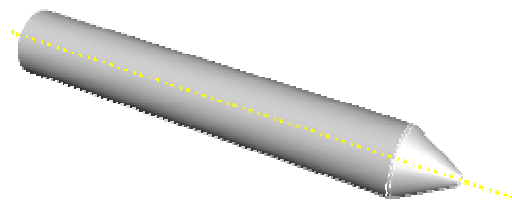


Fig. 4.3: Screw model

The screws are modelled as simple cylinders; at the front a cone is added. This is similar to the real screw and has two raisons d'être: the defined contact surface (foam – screw) needs to surpass the actual contact region in order to avoid nodes flipping “behind” the surface. The second reason is to have comfort of corresponding total length in the simulation and the

physical model when actual contact lengths are equal. The screw diameter has been set to 2.4 [mm], a mean value between core and outer diameter (cf. figure 4.2).

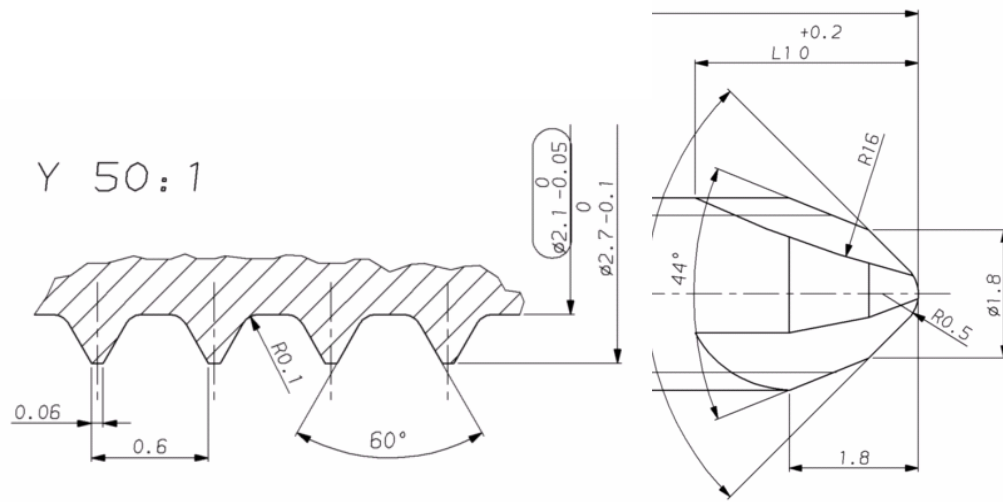


Fig 4.4: Core and outer diameter of the screw; cone at the peak

It is not practical to model the whole thread. In [38] a simulation of a screw pull-out experiment was done. In this case a quarter cylinder of the screw was sufficient (symmetry) and the model needed already a lot of capacity. In the case of the compression test simulation, one complete screw and one half screw would be needed. The requested calculating capacity would be extremely large and would not justify the gain of information.

The foam part is a quadric part as well; a hole is “predrilled” for inserting the screw; it is slightly deeper than necessary (the screw does not touch the bottom). The foam has the same height as the original foam part. Width and depth are equal to the free standing surface. A round on the anterior side is not included.

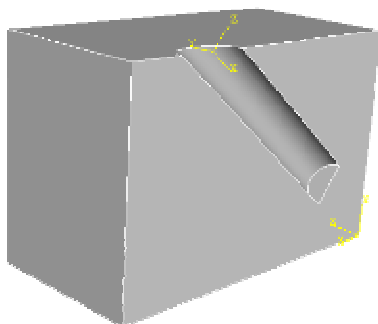


Fig. 4.5: Foam block for one-screw interface

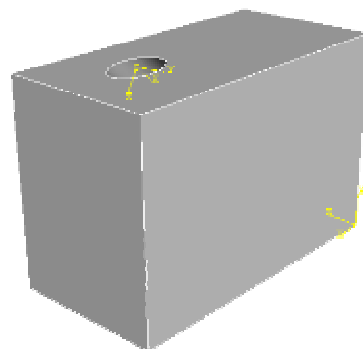


Fig. 4.6: Foam block for two screw interface

The two test blocks have two inner surfaces, designed to cover the corresponding foam block planes completely. A part from these surfaces only the axis has a relevant function; the reference point is chosen on this feature; other dimensions are arbitrary (cf. fig. 4.7).

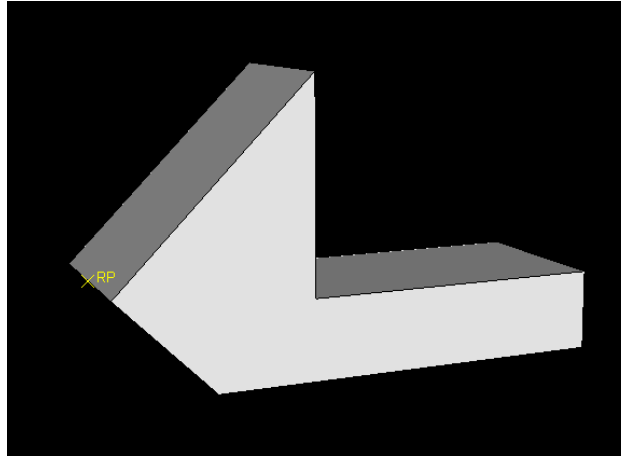


Fig. 4.7: Testblock; reference point on the axis

### 4.2.3 Material Properties

The screws are modelled in a steel equivalent material. Only the modulus of elasticity and the Poisson coefficient has to be defined:

$$E = 210 \text{ [GPa]}$$

$$\nu = 0.27$$

The foam is represented by a hyperfoam material model, as described in paragraph 4.1.

### 4.2.4 Boundary Conditions and Contacts

Constraints have to be set in the sagittal symmetry plane. Translation in z-direction and rotations about x and y are thus blockaded. The constraint is set for the complete surfaces in this plane for both foam blocks, for the rigid plate it is sufficient to set this constraint in the reference point.

The foam block is rigidly fixed on the according test block on both contact surfaces. This is coherent to the situation in the mechanical test blocks where the foam is clamped. Also the screws are rigidly fixed in the plate on the contact surface of the shaft.

The axes of the test blocks have a prescribed displacement in the y-direction, similar to the mechanical tests. The rotation of the reference point on this axis has of course to be unconstrained. All other degrees of freedom are restricted.

In this model two types of contacts are defined: a contact between the plate and the foam without

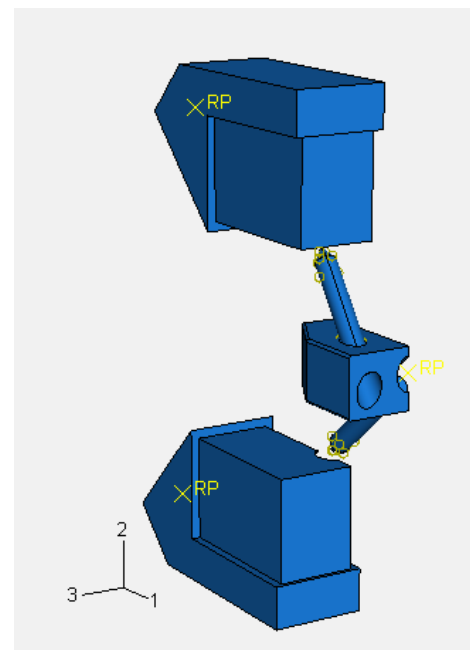


Fig. 4.8: Assembly

friction and a contact pair between the screw and the foam where a friction in order to compensate the lack of thread is present. The surface definition on the plate includes the round on the extreme surfaces. Similar is on the screw, where the front rounds are included. This should help to avoid that points of the foam surface can “fall” behind its opponent.

### 4.2.5 Simulation

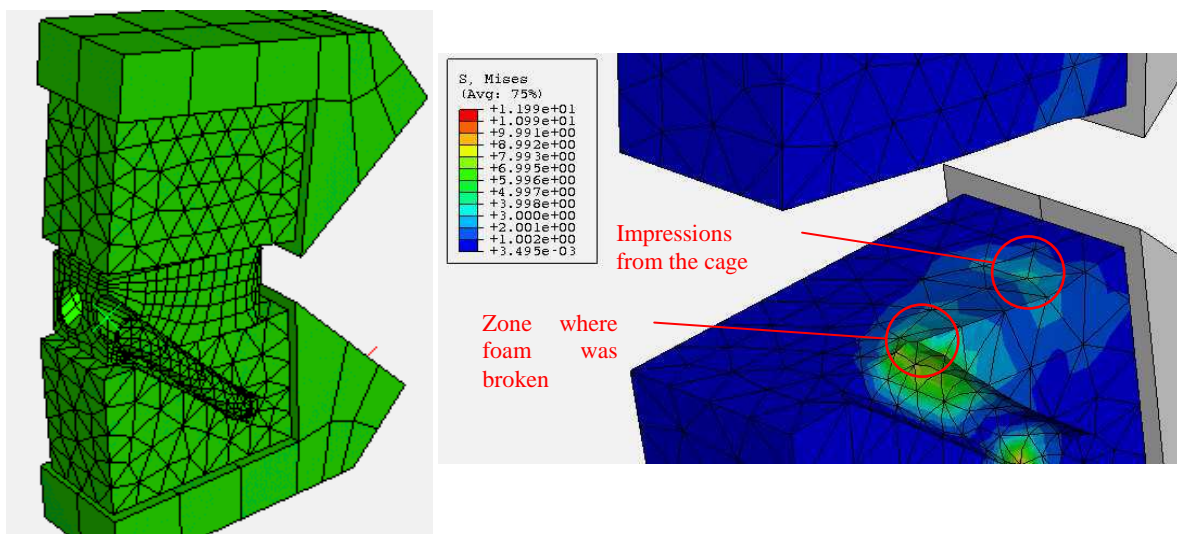
For good functioning of the model, the simulation is divided in several steps. Initially three unconnected parts are placed. The foam blocks are attached to the test blocks and the screws are inserted in the plate.

- Step 1: All elements are fixed in the global coordinate system. This should avoid redundant rigid body motion.
- Step 2: The screws are introduced into the foam blocks. The plate reference is still fixed, the test blocks are approaching the plate; the motion is along the screw axes.
- Step 3: The plate reference is still fixed, but the rotation constraints in the mobile axes are released. This step is introduced, because at the end of step 2, considerable forces on the mobile axis could be found.
- Step 4: In the actual deformation step, the plate constraint for y displacements and rotation about z are released. The mobile axes both effectuate a movement along the y axis. In this step, the maximum increment size is reduced and each one of them is recorded.

All steps are time independent, i.e. the simulation is static.

### 4.2.6 Results

Qualitatively the results are similar to what was observed in the mechanical tests: The deformation on the side with only one screw is dominant (cf. fig. 4.9) and the most important stresses appear in the model at the locations where the material failure occurred; the part



<p>Fig. 4.9: Deformation on the one screw interface is dominant</p>	<p>Fig. 4.10: High stress zone corresponds to observations in the experiments</p>
---	---

between the single screw and the plate and the regions where the plate is pushed into the foam on the posterior edge (cf. fig. 4.10).

The graph below shows the comparison between the FEA and the measure (mean data) for the load-displacement curve; the FEA data have been shifted to have a virtual preload of 2 [N]. The FE model was calibrated on the test data by modifying the friction coefficient. A dry friction model was used, the coefficient was set to 2. The model is not very sensitive on the parameter.

It is difficult to model the non linear behaviour when the material fails, so the data for a displacement more than 2 [mm] can't be stated valid, even if they still match with the experimental values. For a displacement exceeding the 2 [mm], the stresses are locally above the ultimate strength, which physically not possible. A part from the ambiguity of the material definition, numerical problems become more probable because of the large distortion of the elements.

The analyse is problematic because of the contacts; in particular the contacts with friction.

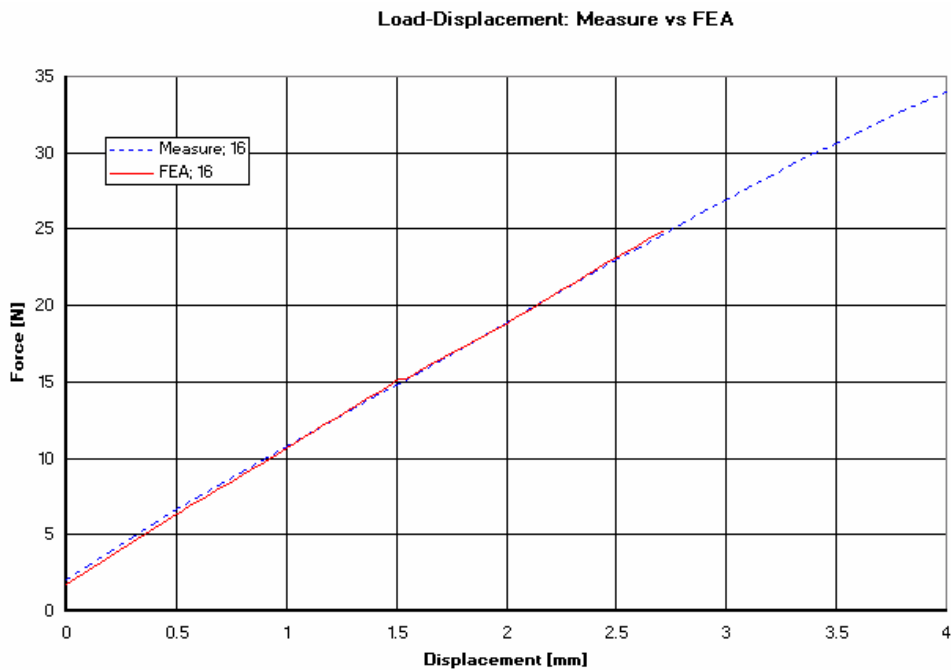


Fig. 4.11: FEA vs. experimental data; 2.7/16 screw, compression; the FE model is calibrated on the experimental data; validity of the model is limited to displacements lower than 2 [mm].

## 4.3 Vertebral Bone Model

An important thing to know is the behaviour in bone material. This permits a better interpretation of the results of the mechanical test using foam as a bone model.

### 4.3.1 Material Properties and Dimensions

Material properties and dimensions are taken from chapter 2. For the cancellous bone two extreme values and a medium value are used for the simulation; the identical material model was used as for the previous simulation. The medium material properties are taken from [25]. The complete data set was simply scaled by a factor 0.5 to obtain a degenerated cancellous bone respectively by a factor 2 to have a young, ideal cancellous bone. Cortical bone is generally less affected by osteoporosis and thus a single value is chosen; for cortical bone a linear material model was used.

The thickness of the cortical shell is fixed at 0.55 [mm]; this corresponds to what Panjabi [15] found on vertebrae on level C5/C6.

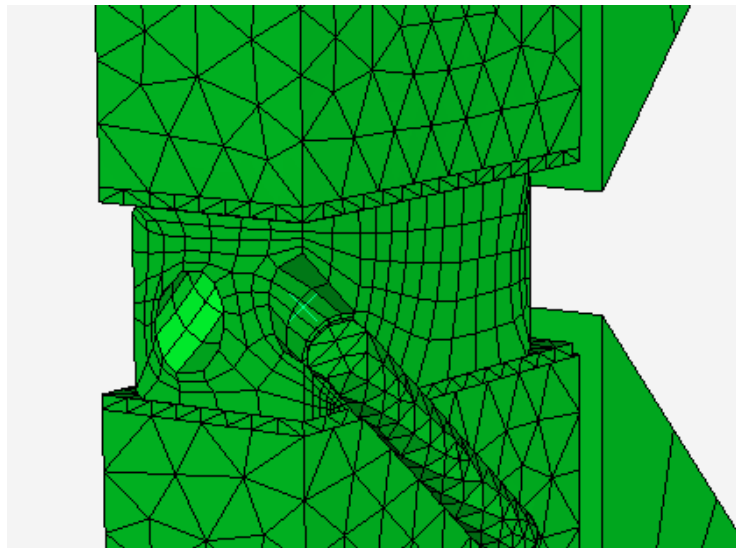


Fig. 4.12: Simulation with bone model: Thin cortical layer and cancellous bone

### 4.3.2 Results

The graphic 4.13 shows the results of the modified model. Four analyses have been performed; the first one was a simulation with the modified geometry, but still using the same material properties (blue). This proves that the geometric modifications did not change the model behaviour. Then the material properties were changed and analyses with three different cancellous bone qualities were performed (pink, purple, orange).

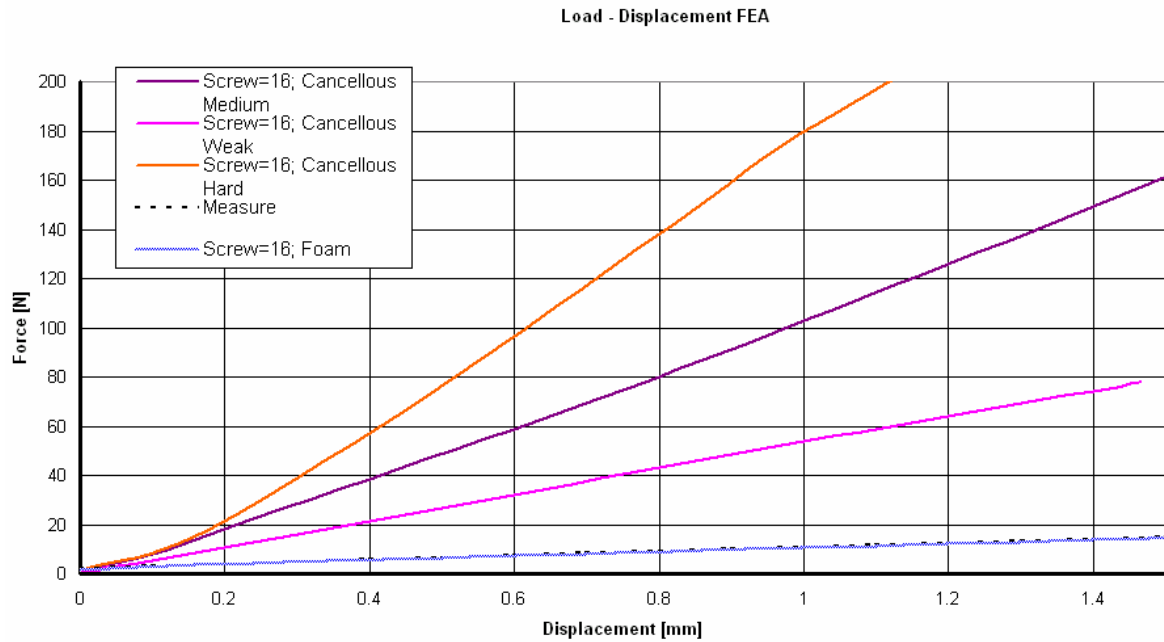


Fig. 4.13: Results of the bone model simulation: the changed geometry with foam properties (cancellous and cortical bone) is still in accordance with the experimental data; three levels for cancellous bone (pink, purple, orange). Even the weakest cancellous bone provides a stiffness five times as high as the basic foam model.

All bone models are clearly stiffer than the foam model; the weakest material has still a stiffness about five times higher than the foam. A break in all curves can be seen between 0.1 and 0.2 mm displacement; at this break the stiffness increases. It is most pronounced on the strongest model. The behaviour is caused by a small initial space between the cage and the bone surface. This feature was used to permit resolution of the preconstraint step. The maximum stiffness are about 200 [N/mm] for the “most dense” bone, 100 [N/mm] for the medium bone and 60 [N/mm] for the weakest.

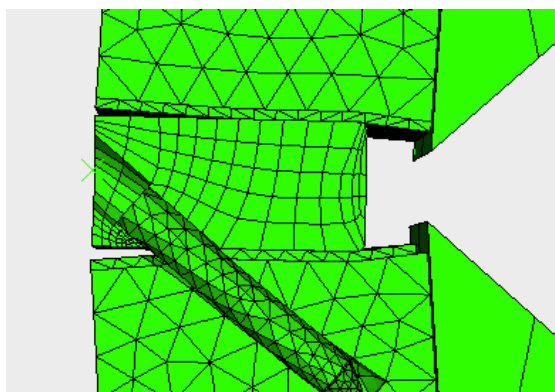


Fig. 4.14 : Bone model (≈2.6 mm displacement)

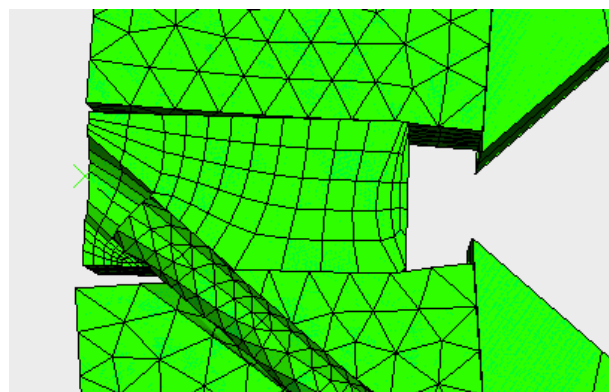


Fig. 4.15 : Foam model (≈2.6 mm displacement)

Comparing the bone model and the foam model simulation (cf. fig. 4.14 and 4.15), we recognise, that the qualitative differences are not enormous. In the lower part, foam respectively the bone is shut between the screw and the cage. Anterior to this screw a

difference can be detected: in foam the material anterior to the screw is almost not deformed. In contrast, because of the rigid layer this part is lifted. The anterior front doesn't sustain any deformations. Regarding model cuts the same effects can be observed with the upper screw.

### **The limitations of the model**

The material has to be in the limits of the ultimate strength; this limit passed, in reality the material (bone) would break. In this model, material failure can't be simulated. Then, the geometric model is strongly simplified; the influence of a stabilising anterior cortical shell and lateral elements is not considered; in contrast, the posterior elements are infinitely rigid (cf. boundary conditions). At last, the thread of the screw is reduced to a friction contact. For the thread, resistive force increases with displacement, for the friction contact, the shear force depends on the contact pressure.

The friction coefficient has been chosen to satisfy the modelling of the foam model. It should be analysed, if the same value is still valid for the real bone model.

## **4.4 Conclusions**

The model has more potential. From the simulations run to date the following conclusions can be made:

- The FE model is valid in the range of 0 to 2 [mm] deformation. For deformation greater than this value the material model is not sufficient anymore because it fails locally.
- Even with rather weak cancellous bone, the stiffness is about five times the stiffness measured in foam.
- For an ideal cancellous bone, the determined stiffness is 20 times the stiffness measured in foam.
- A qualitative analysis of the deformations reveals a high degree of similarity in the mode of deformation of the bone and the foam model.



## 5 DISCUSSION

In this chapter some general points about mechanical testing of implants will be discussed. The function of this chapter is to get together the gain of information of the previous chapters and to trace further steps in the development of the product and the necessary biomechanical tests.

### 5.1 Comparing PUR Foam to Vertebral Bone

One of the key questions for the relevance of all performed mechanical tests, is if PUR foam is an acceptable model for vertebral bone.

The used foam has an E modulus two times lower than average cancellous bone; the mechanical strength is only 20% lower for the foam. In contrast to the bone which has clear structural orientations, foam is almost isotropic: directional differences are in the order of several percents.

Comparing the characteristic of the stress-strain relation under compression a quite good accordance can be stated (cf. foam test in annexe and [25]). For small deformations, stress is very low; with further deformation the stiffness increases and is nearly linear; it decreases again before fracture. Strain at rupture is clearly lower for cancellous bone (same strength, module higher). Failure behaviour under tension is for both materials rather brittle; the fact was obvious when inspecting the used foam blocks.

More important than the actual failure is the behaviour at small deformations. For both materials, foam and cancellous bone, the material properties of the devices are two to three orders of magnitude superior. Thus, similar effects can be expected and the foam can be considered as an acceptable bone model. This statement is underlined by the FEA comparison of the bone and the foam model.

What is missing in the vertebral model, is the cortical shell. The thickness of this surrounding layer has shown to be in the order of 0.5 to 1 mm. The influence of the cortical shell has been shown in the FE model; for small deformation the stiffness, but not the mode of deformation is influenced. This is of course only valid for the new device in a compression test (modified ASTM F-1717).

The used PUR foam is an acceptable match, restricted on small deformations. The mode of deformation is similar to models with a cortical shell, the amplitude is lower than real vertebral bone.

### 5.2 Lateral Bending

No mechanical tests have been performed which are simulating lateral bending. In contrast to flexion-extension and axial rotation there is no joint which facilitates this movement. Stiffness and ROM are typically considered to be equally distributed. This could potentially be a problem because the operated level risks being the weakest element. It is not apparent why most biomechanical analyses don't investigate lateral flexion, but it is generally considered of secondary import when compared with flexion and extension.

A comparison of anterior plating systems and the new device under lateral flexion would of course be interesting. Thereby two facts have to be considered: First, it is not obvious how to define an axis of rotation and how a setup should be designed. Second, even with reasonable setup it is questionable, if the results could provide any results useful for the design improvement.

It is probably more judicious to forgo mechanical lateral flexion tests and to eventually do tests on cadavers later. These tests would only be to indicate mechanical performance.

## 5.3 Preload

In all of the performed test, preload is a point of discussion. In the tension and the flexion a preload was not simulated. In the rotation and the push-out test the preload was set to 50 [N], which is a good estimation of the load in a neutral position of the spine.

On the other hand it has to be considered, that the vertebral bone model is clearly weaker than real bone (cf. chapter 4). Thus it could be argued to reduce the load to respect this simplification and to maintain proportion of the applied loads (flexion and extension).

Furthermore it is not evident if the changing of the axial load should be modified to simulate conditions away from the neutral position.

Another question is the implication of the implants in the spine. It is difficult to know how the force distribution changes with an implant.

However, the preload is one of the parameters which should be added when doing future flexion and extension tests.

## 5.4 Limit of Elasticity

The limit of elasticity had to be estimated by the means of the FE model. It is of interest to know this limit more precisely and for all configurations. The limit could be determined by doing cycles at lower deformations instead of inducing deformation until complete failure.

The limit of elasticity is not of importance for the push-out test. This is in any case a particular situation, because a sliding (push-out) is a failure or misuse of the device.

## 5.5 Further Analyses

### 5.5.1 Planned Tests

The design continues being evolved; the next prototypes are already in the pipeline. The focus will be on compression tests which appeared to be the most relevant. Several fatigue tests have also been performed which have an influence mainly on screw design. They will be pushed the next time because this is an important component of the product evaluation. Parallel to this, the implants are evaluated by surgeons. The tests will be concluded by biomechanical experiments on cadaver.

### 5.5.2 FE Model

The present model, especially for the real bone model should be reviewed again. Time circumstances did not permit to focus more on this case. Further mesh refinement should be incorporated. An improved tensile test of the foam would also be useful.

The possibilities of the FEA are by far not exhausted. Future refinements could proceed in three directions: Modelling a plate system used as a comparison in the mechanical tests, simulation of other experiments with more complex movements and studying more parameters such as screw orientation.

An FE model of a plate system for comparison would be of interest. This could answer the question which one of the implants is more dependent on the cortical shell and which one offers better stability for osteoporotic cancellous bone.

The calibrated model can also be used for other simulating other movements like axial rotation, lateral bending or even coupled motions. Of course it has to be verified how the elements have to be constrained.

Different screw orientations have already been tested on the four screw concept (prototypes 017x4, 020 and 022). Measured differences were statistically insignificant and the design was ultimately decided based on surgeon preference. FE simulation of different conditions could strengthen the choice.

### 5.5.3 Proposition of a New Test Setup for Adequate Flexion and Extension Simulation

The weaknesses of the existing test setup have been previously discussed in comparison with different aspects of in vivo situation. Proposed improvement would include a fixed centre of rotation and an axial load simulation. The sketch below is only a schematic demonstration of the idea. The realisation will not be discussed in detail, but nevertheless some further ideas shall be listed:

- As drawn on the sketch, a linear force is applied at a certain distance and perpendicular to the axis of rotation. The distance has to be large relative to the intended angle of rotation. Another solution would be the application of a torque on the axis.
- The preload is simply a ballast; it is dependent on position. It could be substituted by a spring or a cable system could be built.
- The centre of rotation should be modifiable: different level could be simulated.
- The position of the foam blocks should adjustable after mounting the implants (reduce standard deviation).
- The setup could be modifiable to test lateral bending
- Test proceeding: cycles with small amplitudes to find the limit of elasticity

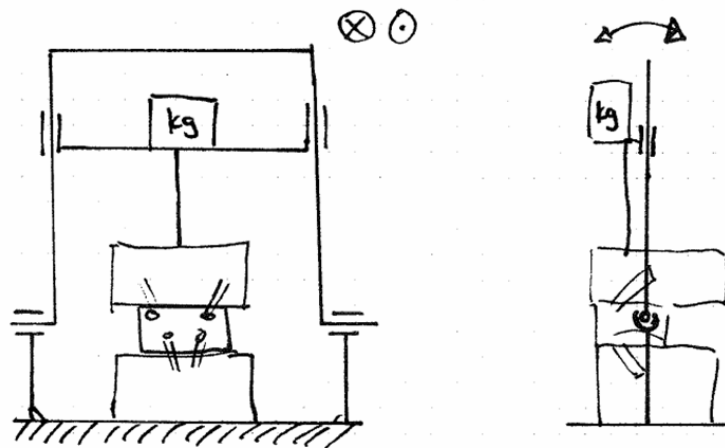


Figure 5.1: Schema of a new test setup

#### 5.5.4 Improved Vertebra Model

An important limitation of the used vertebra model is the homogenous foam which lacks a cortical shell. Its influence on the amplitude of the stiffness has been showed by the FE model.

The new model proposes a vertebra made of to different materials, a foam piece used to model the cancellous bone which would then be covered by a thin layer of a harder material. The difficulty is to find a material with properties similar to cortical bone that can be manufactured in the required thickness. Costs would also be of consideration for such a test device.

One possibility for this simulated cortical bone would be PEEK. This high-performance polymer has a module in the lower range of what would be expected in cortical bone. One appreciable difference would be the dissimilarity in material porosity.

## 6 CONCLUSIONS

At the beginning of the project several questions were set forth for consideration (cf. 1.1). The conclusions to these project objectives are summarized below.

- The most relevant test for determining if a three screw concept offers sufficient stability is the compression test. A three screw concept with the “standard” screws (2.7 mm diameter, 16 mm length) has a clearly lower initial stiffness. A longer (18 mm, 2.7 mm diameter) and a thicker (3.0 mm, 16 mm length) reach almost the level of CSLP. In most cases the 18 mm screw will be too long; the value of the 3.0 mm thick screw is statistically insecure.
- In the compression test the initial stiffness of the two screw interface was clearly superior to the one screw interface.
- Screw length had a significant influence on the device rigidity. A longer screw leads to a more rigid device. The difference between the shortest two screws (12, 14) was not significant.
- Screw diameter appeared to be less important than screw length. No significant differences could be detected for the diameters tested.
- Only the thin screws (2.4 mm diameter) proved to be too weak. One of these screws failed in a tension test. For all other tests and configurations, the PUR foam was the source of failure.
- A compression test according to the modified ASTM F-1717 setup is an acceptable test method. Using an intervertebral cage, the movement is comparable to the flexion-extension movement of C5/C6 and C6/C7 in a healthy spine. These levels are also the most often levels fused.
- A tension test according to the modified ASTM F-1717 setup is of limited use. The simulated complete discharge of the implant can not be related to a daily situation. Instead of a tensile load posterior to the implant, a compressive force anterior to the implant should be applied or a preload should be used.
- The second setup of the rotation test simulates not the exact physiological motion. Nevertheless the test can give complementary information to flexion-extension tests.
- The push-out test showed the expected results. The test could not give any information for a design improvement. The set-up is physiologically reasonable, but the amplitude of the preload remains a point of discussion.
- The measurement of the subsidence rate investigates material properties of the foam. Measuring the subsidence comes close to a measurement of the contact area. The subsidence test is defensible in a physiological point of view. In contrast, no gain of information for a design improvement is given by the test results. Considerations from clinical experience and in vitro studies would bring more useful information.
- The used PUR foam is a reasonable material model for cancellous bone; the modulus of elasticity is in the lower half of the range of cancellous bone. The material model is valid for small deformations.  
The model does not represent the cortical shell. For the new device, the FE model showed that the cortical shell influences the amplitude of the stiffness, but not the mode of deformation at small deformations.

## 6.1 Design Improvement Proposals

- The 2.4 mm screws shouldn't be used because the mechanical strength is not sufficient.
- The four screw concept has an initial stiffness superior to the three screw concept. The four screw concept is on the level of CSLP, the "gold standard". The four screw concept should be used instead of the three screw concept.

## 6.2 Reasonable Tests

- Modified ASTM F-1717 for flexion and extension (cf. 5.5.3)
- Rotation tests (improved setup)

## 7 CLOSE

The amount of literature in anatomy, biomechanics and surgery is enormous. Many biomechanic spine studies have been made. However actual useful documents are rather limited. The complexity of the anatomy and kinematics makes an interpretation of results sometimes difficult. Especially biomechanical tests of anterior plating systems would have been interesting, but to the mechanical tests comparable studies with recent systems couldn't be found.

The FEA suffered a bit from a lack of time. It was first the issue to learn and understand the software before starting to develop the model. A priori static problem are not a difficulty for FEA software, but contacts are causing lots of problems. At the end the project was running out of time; so the model has still potential for improvement, particularly the bone model. Some further proceedings have already been proposed.

It was precious experience to do this project at Synthes. The project was integrated in the development of an important product; results were directly incorporated in the design. The design changes made a modification of the test plan necessary several times.

The most exciting work was of course the interpretation of the results; analysing how simple mechanical experiments can be transferred to the complex cervical spine.

A biomechanical study on cadaver is already planned and will show if the mechanical tests were useful and the interpretation valid.

Je tiens à remercier Prof. Dominique Pioletti et Arne Vogel qui ont suivi ce projet de côté de l'école ; ils ont particulièrement contribué à faire un travail complet dans un point de vue scientifique.

Herzlichen Dank an alle Synthes Mitarbeiter, welche direkt oder indirekt zum Gelingen der Arbeit beigetragen haben. Insbesondere natürlich Thomas Küenzi, Leiter der Cervikalen Gruppe, welcher dieses Master Projekt bei Synthes erst ermöglicht hat, das Entwicklungs-Team von SynFix-C mit Markus Hunziker, David Koch und Rainer Ponzer, Jayr Bass, Simon Kamber, Michael Jeger und Daniel Thommen von der Cervikalen Gruppe, Mario Gago und Andi Gfeller welche mich bei der Literatursuche unterstützt haben, Thomas Dürrenberger, Roger Leist, Franz Kamber, Erich Gysin und Bernhard Zbären von der Abteilung Materialkunde und Testungen, welche mich für die mechanischen Testungen in Vorbereitung und Ausführung unterstützt haben und die Mitarbeiter des Prototype Center unter der Leitung von Martin Hess, welche das Testmaterial hergestellt haben.

Oberdorf, 07.02.2007

Michael Davatz

## 8 LITERATURE INDEX

- [1] Y. H. AN, R. A. DRAUGHN, Mechanical Testing of Bone and the Bone-Implant Interface, CRC Press, 2000
- [2] H.-J. BARTSCH, Taschenbuch Mathematischer Formeln, Fachbuchverlag Leipzig, 19. Auflage, 2001
- [3] J. J. BASKIN, A. G. VISHTEH, C. A. DICKMAN, V. K. H. SONNTAG, Techniques of Anterior Cervical Plating, Operative Techniques in Neurosurgery, Vol. 1, No. 2, 1998, pp 90 – 102
- [4] J. C. CAUTHEN, R. P. THEIS, A. T. ALLEN, Anterior Cervical Fusion: A Comparison of Cage, Dowel and Dowel-Plate Constructs, The Spine Journal, No. 3, 2002, pp 106 – 117
- [5] J. DVORAK, M. M. PANJABI, J. E. NOVOTNY, J. A. ANTINNES, In Vivo Flexion/Extension of the Normal Cervical Spine, *Journal of Orthopaedic Research*, Vol. 9, No. 6, 1991, pp. 828 – 834
- [6] A. GARCIA-DIAZ, D. T. PHILLIPS, Principles of Experimental Design and Analysis, Chapman & Hall, 1995
- [7] T. H. JANSEN, D. DIANGELO, Computer Simulation Studies of Cervical Spine Extension Mechanics, School of Biomedical Engineering, University of Tennessee - Memphis
- [8] Y. E. KIM, V. K. GOEL, J. N. WEINSTEIN, T.-H. LIM, Effect of Disc Degeneration at One Level on the Adjacent Level in Axial Mode, Spine, Vol. 16, No. 3, 1991, pp 331 – 335
- [9] J. LANG, *Klinische Anatomie der Wirbelsäule*, Thieme, 1991
- [10] H. LEONHARDT, B. TILLMANN, G. TÖNDURY, K. ZILLES, Anatomie des Menschen, Lehrbuch und Atlas, Band I Bewegungsapparat, Thieme, 2. Auflage, 1998
- [11] B. M. NIGG, W. HERZOG, Biomechanics of the Musculo-Skeletal System, Wiley, 1995
- [12] R. W. NIGHTINGALE, B. A. WINKELSTEIN, K. E. KNAUB, W. J. RICHARDSON, J. F. LUCK, B. S. MYERS, Comparative Strength and Structural Properties of the Upper Cervical Spine in Flexion and Extension, Journal of Biomechanics, 2002, Vol. 35, pp 725 – 732
- [13] G. P. PAL, R. V. ROTAL, A Study of Weight Transmission through Cervical and Upper Thoracic Region of the Vertebral Column in Man, Journal of Anatomy, No. 148, 1986, pp 245 – 261
- [14] G. P. PAL, H. H. SHERK, The Vertical Stability of the Cervical Spine, Spine, Vol. 13, No. 5, 1988, pp 447 – 449
- [15] M. M. PANJABI, N. C. CHEN, E. K. SHIN, J.-L. WANG, *The Cortical Shell Architecture of Human cervical Vertebral Bodies*, Spine, Vol. 26, No. 32, 2001, pp 2478 – 2484
- [16] M. M. PANJABI, J. CHOLEWICKI, K. NIBU, J. GRAUER, L. B. BABAT, J. DVORAK, Critical Load of the Human Cervical Spine: An in Vitro Experimental Study, Clinical Biomechanics, Vol. 13, No. 1, 1998, pp 11 – 17
- [17] M. M. PANJABI, J. J. CRISCO, A. VASAVADA, T. ODA, J. CHOLEWICKI, K. NIBU, E. SHIN, *Mechanical Properties of the Human Cervical Spine as shown by Three-Dimensional Load-Displacement Curves*, Spine, Vol. 26, No. 24, 2001, pp. 2692 – 2700



- [18] M. M. PANJABI, J. DURANCEAU, V. GOEL, Th. OXLAND, K. TAKATA, Cervical Human Vertebrae – Quantitative Three-Dimensional Anatomy of the Middle and Lower Regions, *Spine*, Vol. 16, No. 8, 1991, pp. 861 – 869
- [19] A. G. PATWARDHAN, R. M. HAVEY, A. J. GHANAYEM, H. DIENER, K. P. MEADE, B. DUNLAP, S. D. HODGES, Load-Carrying Capacity of the Human Cervical Spine in Compression Is Increased Under a Follower Load, *Spine*, Vol. 25, No. 12, 2000, pp 1548 – 1554
- [20] L. PENNING, Functional Anatomy of Joints and Discs, In: *The Cervical Spine*, The Cervical Spine Research Society, 2<sup>nd</sup> edition, Lippincott, 1989, pp 33 - 56
- [21] L. PENNING, J. T. WILMINK, Rotation of the Cervical Spine – A CT Study in Normal Subjects, *Spine*, Vol. 12, No. 8, 1987, pp 732 – 738
- [22] W. PLATZER, *Taschenatlas Anatomie – 1 Bewegungsapparat*, 9. Auflage, Thieme, 2005
- [23] J. Y. RHO, R. B. ASHMAN, C. H. TURNER, Young's Modulus of Trabecular and Cortical Bone Material: Ultrasonic and Microtensile Measurements, *Journal of Biomechanics*, 1993, Vol. 26, No. 2, pp 111 – 119
- [24] J. S. SCHWAB, D. J. DIANGELO, K. T. FOLEY, Motion Compensation Associated With Single-Level Cervical Fusion: Where Does the Lost Motion Go?, *Spine*, Vol. 31, No. 21, 2006, pp 2439 – 2448
- [25] V. P. W. SHIM, L. M. YANG, J. F. LIU, V. S. LEE, Characterisation of the Dynamic Compressive Mechanical Properties of Cancellous Bone from the Human Cervical Spine, *International Journal of Impact Engineering*, No. 32, 2005, pp 525 – 540
- [26] K.-J. SONG, K.-B. LEE, A Preliminary Study of The Use of Cage and Plating for Single-Segment Fusion in Degenerative Cervical Spine Disease, *Journal of Clinical Neuroscience*, No. 13, 2006, pp 181 – 187
- [27] J. R. STIEBER, K. BROWN, G. D. DONALD, J. D. COHEN, Anterior Cervical Decompression and Fusion with Plate Fixation as an Outpatient Procedure, *The Spine Journal*, No. 5, 2005, pp 503 -507
- [28] M. SZPALSKI, R. GUNZBURG, *The Degenerative Cervical Spine*, Lippincott Williams & Wilkins, 2001
- [29] S. H. TAN, E.C. TEO, H. C. CHUA, Quantitative Three-Dimensional Anatomy of Cervical, Thoracic and Lumbar Vertebrae of Chinese Singaporeans, *European Spine Journal*, No. 13, 2004, pp 137 - 146
- [30] H.-P. W. VAN JONBERGEN, M. SPRUIT, P. G. ANDERSON, P. W. PAVLOV, Technical Review, Anterior Cervical Interbody Fusion with a Titanium Box Cage: Early Radiological Assessment of Fusion and Subsidence, *The Spine Journal*, No. 5, 2005, pp 645 – 649
- [31] B. WATIER, Comportement mécanique du rachis cervical: une revue de littérature, *ITBM-RBM*, Vol. 27, 2006, pp. 92 – 106
- [32] A. A. WHITE, M. M. PANJABI, *Clinical Biomechanics of the Spine*, Second Edition, Lippincott-Raven,
- [33] J. A. WHEELDON, F. A. PINTAR, S. KNOWLES, N. YOGANANDAN, Experimental Flexion/Extension Data Corridors for Validation of Finite Element Models of the Young, Normal Cervical Spine, *Journal of Biomechanics*, 2006, Vol. 39, pp 375 – 380
- [34] H.-J WILKE, *Biomechanik der Wirbelsäule*, FH Ulm
- [35] R. H. WITTENBERG, M. SHEA, D. E. SWARTZ, K. S. LEE, A. A. WHITE, W. C. HAYES, Importance of Bone Mineral Density in Instrumented Spine Fusions, *Spine*, Vol. 16, No. 6, 1991, pp 647 – 652

- [36] N. YOGANANDAN, S. KUMARESAN, F. A. PINTAR, Biomechanics of the Cervical Spine Part 2. Cervical Spine Soft Tissue Responses and Biomechanical Modeling, *Clinical Biomechanics*, 2001, Vol. 16, pp 1 – 27
- [37] N. YOGANANDAN, F. A. PINTAR, B. D. STEMPER, J. L. BAISDEN, R. AKTAY, B. S. SHENDER, G. PASKOFF, P. LAUD, Trabecular Bone Density of Male Human Cervical and Lumbar Vertebrae, *Bone*, Vol. 39, 2006, pp 336 – 344
- [38] Q. H. ZHANG, S. H. TAN, S. M. CHOU, Effects of Bone Materials on the Screw Pull-out Strength in Human Spine, *Medical Engineering & Physics*, No. 28, 2006, pp 795 – 801
- [39] Norm for Testing Spinal Implants: ASTM F 1717-04 - Standard Test Methods for Spinal Implant Constructs in a Vertebrectomy Model, ASTM International, 2004
- [40] Norm for use of Foam Material as a Bone Model: ASTM F 1839-01 – Standard Specification for Rigid Polyurethane Foam for Use as a Standard Material for Testing Orthopaedic Devices and Instruments, ASTM International, 2001
- [41] Testing Norm for Subsidence Measuring: ASTM F 2267-04 – Standard Test Method for Measuring Load Induced Subsidence of Intervertebral Body Fusion Device under Static Axial Compression, ASTM International, 2004
- [42] C. J. SNIJDERS, G. A. HOEK VAN DIJKE, E. R. ROOSCH, A Biomechanical Model for the Analysis of the Cervical Spine in Static Postures, *Journal of Biomechanics*, Vol. 24, No. 9, 1991, pp 783 – 792
- [43] T. S. KELLER, C. J. COLLOCA, D. E. HARRISON, D. D. HARRISON, T. J. JANIK, Influence of Spine Morphology on Intervertebral Disc Loads and Stresses in Asymptomatic Adults: Implications for the Ideal Spine, *The Spine Journal*, No. 5, 2005, pp 297 – 309
- [44] Y. C. DENG, W. GOLDSMITH, Response of a Human Head/Neck/Upper Torso Replica to Dynamic Loading – II. Analytic/Numerical Model, *Journal of Biomechanics*, Vol. 20, No. 5 , 1987, pp 487 - 497

## 8.1 Electronic Resources

- [45] General Plastics, [www.generalplastics.com](http://www.generalplastics.com), October 2006
- [46] Medcyclopaedia, [www.medcyclopaedia.com](http://www.medcyclopaedia.com), November 2006
- [47] Medline Plus, [www.nlm.nih.gov/medlineplus/encyclopedia.html](http://www.nlm.nih.gov/medlineplus/encyclopedia.html), November 2006
- [48] Neurosurgerytoday.org, [www.neurosurgerytoday.org](http://www.neurosurgerytoday.org), November 2006
- [49] Paracelsus Heilpraktikerschulen, [www.paracelsus.de](http://www.paracelsus.de), December 2006
- [50] North American Spine Society NASS, [www.spine.org](http://www.spine.org), November 2006
- [51] Wikipedia, [www.wikipedia.org](http://www.wikipedia.org), November 2006

## 9 CURRENT ABBREVIATIONS

### 9.1 General Abbreviations

ACDF	Anterior Cervical Discectomy and Fusion
ACF	Anterior Cervical Fusion
ASTM	American Society for Testing and Material
BMD	Bone Mineral Density
EZ	Elastic Zone
FDA	Food and Drug Administration, Regulatory Authority
FSU	Functional Spinal Unit
IAR, ICR	Instantaneous Axe of Rotation
NZ	Neutral Zone
PE	Polyethylene
PZ	Plastic Zone
PUR	Polyurethane
ROM	Range of Motion

### 9.2 Abbreviations for Mechanical Tests

CSLP	Cervical Spine Locking Plate
SF	SynFix-C

SF 015-2.7-16 → SynFix-C, Prototype Number - Screw Diameter – Screw Length  
SF 015-2.7-16-1s → SynFix-C, Prototype Number- Screw Diameter – Screw Length  
– One Screw Interface tested

## 10 ANNEXE

I.	Foam Test	109
II.	Data Sheet PUR Foam Grade 15	111
III.	Specifications for Mechanical Tests	113
IV.	Test Matrix	115
V.	Tested specimens	116
VI.	Tools for implants	118
VII.	Test Protocols	119
VIII.	Complete Test Results	130
IX.	Drawings test material	143

**Content**

I.	Foam Test	109
II.	Data Sheet PUR Foam Grade 15	111
III.	Specifications for Mechanical Tests	113
IV.	Test Matrix	115
V.	Tested specimens	116
VI.	Tools for implants	118
VII.	Test Protocols	119
VIII.	Complete Test Results	130
IX.	Drawings test material	143

# I. FOAM TEST

The material data of the foam obtained from the producers internet site appeared to be no sufficient. Only the modulus of elasticity and the mechanical strength under compression and tension are indicated. The foam behaviour can not be assumed perfectly brittle or perfectly plastic and these stress regions are reached in the simulation quite quickly. So a material test has been performed.

## I.1 Material and Method

Two cylindric foam specimens have been prepared; a length of 25 [mm] and a diameter of 15 [mm] have been chosen arbitrary.

Then the specimen was placed between two plane surfaces; the fixed and the mobile surfaces were parallel and with a rigid angle fixation. The foam was preloaded with 1 [N] and then the stamp compressed the cylinder at a fixed speed (sufficiently slow) of 5 [mm/min]. The load-displacement data were collected and analysed. The test was stopped at approximately 4 [kN] when reaching the end of range of the load cell. Two identical repeats have been performed; statistically this not of high relevance, but already sufficient in this context.

## I.2 Results

In figure below, the load-displacement curves for the two specimens are shown. First a linear load-displacement relation is measured; at 800 to 900 [N] the force ceases to increase. Between a deformation of 2 to 6 [mm] the force stays constant and starts to increase exponentially for further deformation.

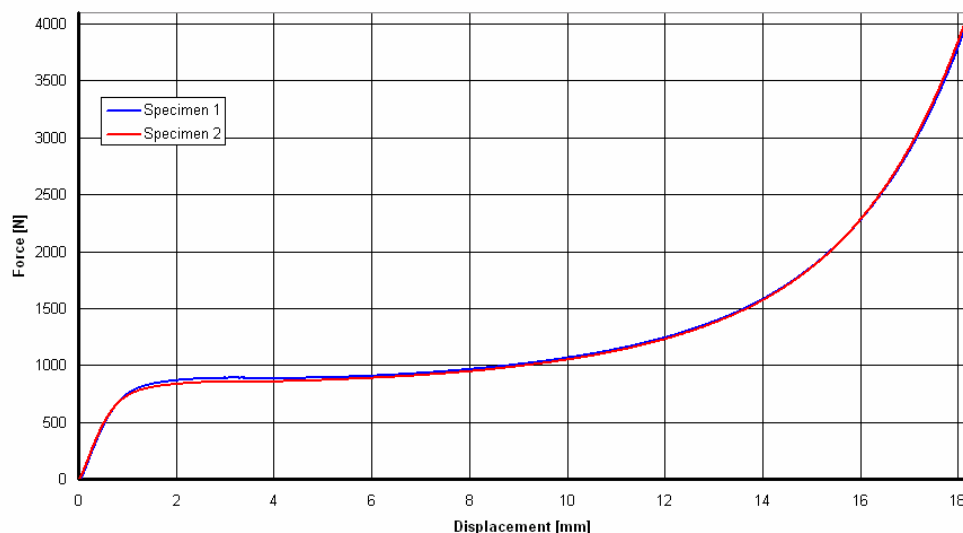


Fig. I.1: Compression test, two repeats of an identic material

Using the section area and the initial length the nominal stress-strain relation can be calculated. These data are represented in the following figure and can be used in a FEA

software. The nominal modulus has been calculated for low strains; only for a limited strain region between 0.005 and 0.015 the modulus reaches the maximum of about 150 [MPa].

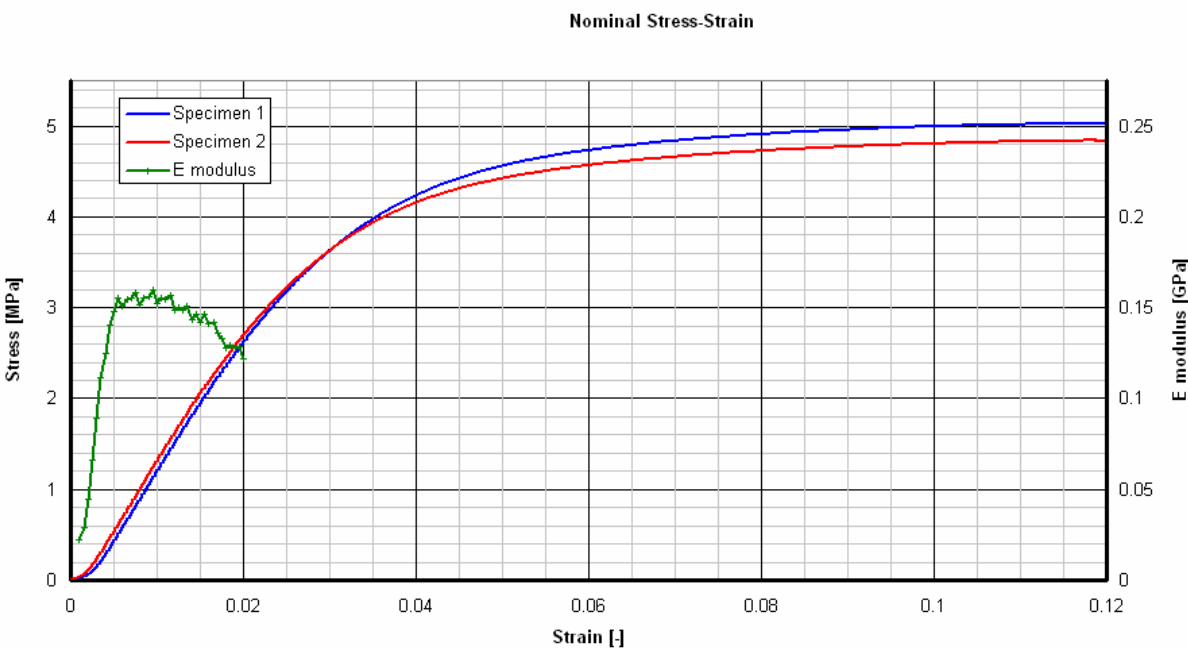


Fig. I.2: Nominal stress-strain curve (axis on the left, [MPa]) and the module of elasticity (axis on the right, [GPa])

## II. DATA SHEET PUR FOAM GRADE 15

<b>Nominal Physical Property Data for LAST-A-FOAM® FR-3700 Rigid Foam at 15 pounds per cubic foot density</b>			
<b><u>Property</u></b>	<b><u>English</u></b>	<b><u>Metric</u></b>	<b><u>Test Method</u></b>
<b>Density (pcf) (kg/m<sup>3</sup>)</b>	15	240	ASTM D-1623
<b>Compressive Strength (psi) (kPa)</b> Parallel to Rise			ASTM-D-1621
@ -65° F	1113	7675	
@ 75° F	728	5017	
@ 200° F	413	2850	
@ 250° F	267	1838	
Perpendicular to Rise			
@ -65° F	1097	7563	
@ 75° F	696	4800	
@ 200° F	415	2860	
@ 250° F	275	1898	
<b>Compressive Modulus (psi) (kPa)</b> Parallel to Rise			ASTM-D-1621
@ -65° F	21923	151159	
@ 75° F	20371	140459	
@ 200° F	14930	102945	
@ 250° F	10959	75564	
Perpendicular to Rise			
@ -65° F	21612	149014	
@ 75° F	18771	129425	
@ 200° F	14067	96994	
@ 250° F	10959	75564	
<b>Tensile Strength (psi) (kPa)</b>			ASTM D-1623 Type A Specimens
Parallel to Rise	601	4143	
Perpendicular to Rise	594	4097	



<b>Tensile Modulus (psi) (kPa)</b>			ASTM D-1623 Type B specimens
Parallel to Rise	21826	150492	
Perpendicular to Rise	22694	156473	
<b>Shear Strength (psi) (kPa)</b>			ASTM C-273 Compression Shear
Rise Parallel to Specimen Width	490	3379	
Rise Parallel to Specimen Thick	479	3306	
<b>Shear Modulus (psi) (kPa)</b>			ASTM C-273 Compression Shear
Rise Parallel to Specimen Width	4941	34071	
Rise Parallel to Specimen Thick	5141	35447	
<b>Flexural Strength (psi) (kPa)</b>			ASTM D-790 Method 1-A
Rise Parallel to Test Span	851	5868	
Rise Parallel to Beam Thick	813	5605	
<b>Flexural Modulus (psi) (kPa)</b>			ASTM D-790 Method 1-A
Rise Parallel to Test Span	25991	179207	
Rise Parallel to Beam Thick	20247	139605	
<b>Poisson's Ratio</b>	~0.3	~0.3	Literature (Gibson and Ashby)
<b>Hardness, Shore-D (cut foam surface)</b>	27	27	ASTM D-2240

### III. SPECIFICATIONS FOR MECHANICAL TESTS

#### III.1 Tension, Compression, Multi-Level

Measured	Displacement	Force
	Dependent (control displacement)	Independent
Range	0... 50 [mm]	0...400 [N]
Resolution	<0.1 [mm]	<0.1 [N]
Speed	2...5 [mm/min] (Definition in protocol)	200 [N/min]
Time resolution/ sample frequency	>10 [sample/s]	>10 [sample/s]

#### III.2 Rotation

Measured	Angular displacement	Torque
	Dependent (control angular displacement)	Independent
Range	0... 90 [°]	0...3 [Nm]
Resolution	<0.05 [°]	<0.01 [Nm]
Speed	5 [°/min] (Definition in protocol)	5 [Nm/min]
Time resolution/ sample frequency	>10 [sample/s]	>10 [sample/s]

#### III.3 Push-out

Measured	Displacement	Force
	Dependent (control displacement)	Independent
Range	0... 20 [mm]	0...1000 [N]
Resolution	<0.1 [mm]	0.1 [N]
Speed	2...5 [mm/min] (Definition in protocol)	200 [N/min]
Time resolution/ sample frequency	>10 [sample/s]	>10 [sample/s]

### III.4 Subsidence

Measured	Displacement Dependent displacement)	Force Independent
	(control	
Range	0... 5 [mm]	0...250 [N]
Resolution	<0.05 [mm]	<0.1 [N]
Speed	1 [mm/min]	5 [N/s]
Time resolution/ sample frequency	>10 [sample/s]	>10 [sample/s]




### IV. TEST MATRIX

	Subject	A	B	C	D	E	F	Total
		Extension (Tension)	Flexion (Compression)	Rotation		Push-out	Subsidence	
				Right	Left			
1	SynFix-C, D2.7, L16	5	2	5	2	5	5	
2	SynFix-C 1-screw, D2.7, L16	2	2	2	-	-	-	
3	SynFix-C 2-screw, D2.7, L16	2	2	2	-	-	-	
4	SynFix-C, D2.4, L16	2	2	2	-	-	-	
5	SynFix-C, D3.0, L16	2	2	(2)	-	2	-	
6	SynFix-C, D2.7, L14	2	2	(2)	-	-	-	
7	SynFix-C, D2.7, L12	2	2	(2)	-	-	-	
8	SynFix-C, D2.7, L18	2	2	2	-	-	-	
9	CSLP	2	2	2	-	-	-	
10	Vectra	2	2	2	-	-	-	
11	Zephir	2	2	2	-	-	-	
12	Cervios only	-	-	-	-	2 - 5 ?	5	
	Total 1-level	21 - 23	11 - 23	17 - 23	2	9 - 12	10	
<i>2-level</i>								
21	SynFix-C	(2)	2	(2)	-	-		
22	CSLP	(2)	2	(2)	-	-		
23	Vectra	(2)	2	(2)	-	-		
24	Zephir	(2)	2	(2)	-	-		
	Total 2-level	(8)	2 - 8	(8)				
<i>3-level</i>								
31	SynFix-C	(2)	2	(2)	-	-		
32	Vectra	(2)	2	(2)	-	-		
	Total 3-level	(4)	4	(4)				
	<b>Total</b>							


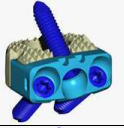
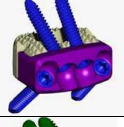
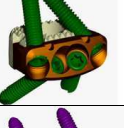
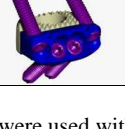
(October 2006)

## V. TESTED SPECIMENS

### Plates

System		Thickness [mm]	Distance hole to hole [mm]	Width [mm]
CSLP		2	20	16.5
Vectra		2.5	20	16
Zephir		1.6	21	15

### Zero Profile Device (Prototypes)

Prototype		Height [mm]	Width [mm]	Nb of screws	Compatible screw diameter [mm]
015		7	15	3	2.4, 2.7
017		7	15	3	3.0
017x4		7		4	3.0
020		7		4	3.0
022		7		4	3.0

All prototypes were used with a matching cage. Only the 017 prototype had a cage which was slightly higher (8 mm instead of 7).

Device	Height	Material	Type	No
SynFix-C (P015)	7 [mm]	Steel	For D2.7 / D2.4 screws	-
SynFix-C (P017)	7 [mm]	Steel	For D3.0 screws	-
SynFix-C Cage	7 [mm]	PA	Parallel	-
Vertebral Spacer	8 [mm]	PEEK	Parallel	889_914
Vectra*	20 [mm]	TAN		04.613.020
Vectra*	38 [mm]	TAN	2-level	04.613.138
Vectra*	57 [mm]	TAN	3-level	04.613.257
CSLP*	20 [mm]	Ti	Small stature	487.222
CSLP*	37 [mm]	Ti	2-level	487.228
CSLP*	57 [mm]	Ti	3-level	487.355
Zephir**	27.5 [mm]			8799027
Zephir	45.0 [mm]		2-level	8799045

\*length: cephalic to caudal hole-pair

\*\* length: over all

Screw	Diameter	Length		
SynFix-C	3.0 [mm]	16 [mm]		-
SynFix-C	2.7 [mm]	16 [mm]		-
SynFix-C	2.4 [mm]	16 [mm]		-
SynFix-C	2.7 [mm]	18 [mm]		-
SynFix-C	2.7 [mm]	14 [mm]		-
SynFix-C	2.7 [mm]	12 [mm]		-
Vectra	4.0 [mm]	14 [mm]	Self-drilling	04.613.514
CSLP	4.0 [mm]	14 [mm]	Self tapping	487.044
CSLP locking screw	1.8 [mm]			497.780
Zephir	3.5 [mm]	13 [mm]	Self tapping	8792113

## VI. TOOLS FOR IMPLANTS

Device	Tool	Number
SynFix-C	Sleeve	313.353
	Drill bit Ø2.0	323.062
	Screwdriver (D2.4, D2.7 screws)	Prototype
	Screwdriver (D3.0 screws)	311.005
CSLP	Holding sleeve	387.286
	Drill bit, for 14 mm screws	387.220
	Screwdriver	387.281
	Screwdriver Locking Screw	387.285
Vectra	Holding sleeve	03.613.001
	Drill bit for 13 mm screws	324.152
	Screwdriver	324.105
	Screwdriver (to remove)	352.311
Zephir	Screwdriver	8796032

## VII. TEST PROTOCOLS

- Compression tests
- Tension tests
- Setup procedure for Tension and Compression
- Push-out tests
- Subsidence tests



## Biomechanical Tests for SynFix-C: Compression

### Study / test objective and acceptance criteria; source for acceptance criteria

The objective of this test is to compare the new device (SynFix-C) to existing plate systems (Vectra and CSLP from Synthes and Medtronic Sofamor Danek Zephir) in a compression test. Load-displacement data and maximum (failure) load are collected.

The set up is based on ASTM 1717-04 norm; the samples are fixed on PUR-foam (representing cancellous bone properties).

#### Samples:

- SynFix-C (P015)
- SynFix-C (P017) for D3.0 screws
- SynFix-C (P015); rigid fixation of one screw interface
- Vectra + Cervios
- CSLP + Cervios
- Zephir + Cervios

For each system, 2 tests are performed. If relative standard deviation of  $F_{\max}$  exceeds 10%, a third test will be performed.

#### Test norm:

ASTM 1717-04; modified

### Identification of study / test material

#### Consumable Materials:

Quantity	Part
20 (24)	Foam-Block

#### Reusable Test Material:

1	SynFix-C, prototype 015 (P015)
1	SynFix-C, prototype 017 (P017)
3	Screws of each size
1 of each	Vectra, CSLP, Zephir plate
4 of each	Screws for Vectra, CSLP, Zephir
2	Testblock 1
1	Testblock 2
1	Testblock 3
2	Screw for rigid fixation

Details of tested samples in chapter “Detailed specifications of test samples”.

**Test equipment**

Zwick: 148670, WN:121253

Load cell: ID: 0, WN 136787 (5 kN)

**Study / test procedure and participants**

**Test parameters**

Force / displacement until Failure (Screw breaks, plate breaks, bone breaks)

Speed 5mm/min

**Test procedure**

See in chapter "Setup"

**Data collection and analysis method / test set up**

The data of interest are the load-displacement curves and maximum (failure) load for each sample.

Data are evaluated with MS Excel. SynFix-C 2.7/16 is used as reference.

## Biomechanical Tests for SynFix-C: Tension

### Study / test objective and acceptance criteria; source for acceptance criteria

The objective of this test is to compare the new device (SynFix-C) to existing plate systems (Vectra and CSLP from Synthes and Medtronic Sofamor Danek Zephir) in a compression test. Load-displacement data and maximum (failure) load are collected.

The set up is based on ASTM 1717-04 norm; the samples are fixed on PUR-foam (representing cancellous bone properties).

#### Samples:

- SynFix-C (P015)
- SynFix-C (P017) for D3.0 screws
- SynFix-C (P015); rigid fixation of one screw interface
- Vectra + Cervios
- CSLP + Cervios
- Zephir + Cervios

For each system, 2 tests are performed. If relative standard deviation of  $F_{max}$  exceeds 10%, a third test will be performed.

#### Test norm:

ASTM 1717-04; modified

### Identification of study / test material

#### Consumable Materials:

Quantity	Part
16 (20)	Foam-Block

#### Reusable Test Material:

1	SynFix-C, prototype 015 (P015)
1	SynFix-C, prototype 017 (P017)
3	Screws of each size
1 of each	Vectra, CSLP, Zephir plate
4 of each	Screws for Vectra, CSLP, Zephir
2	Testblock 1
1	Testblock 2
1	Testblock 3
2	Screw for rigid fixation

Details of tested samples in chapter “Detailed specifications of test samples”.

**Test equipment**

Zwick: 148670, WN:121253

Load cell: ID: 0, WN 136787 (5 kN)

**Study / test procedure and participants**

**Test parameters**

Force / displacement until Failure (Screw breaks, plate breaks, bone breaks)

Speed 5mm/min

**Test procedure:**

See in chapter "Setup".

**Data collection and analysis method / test set up**

The data of interest are the load-displacement curves and maximum (failure) load for each sample.

Data are evaluated with MS Excel. SynFix-C 2.7/16 is used as reference.

## Set-up

### Procedure

- 1) Number the foam-blocks
- 2) Put foam-blocks in the test-blocks (foam-block with odd number up)
- 3) Fix the foam-blocks with the U-plates
- 4) Put the upper test-block on the lower
- 5) Put the align pins into the test-blocks
- 6) SynFix-C: continue with 7; Anterior plate continue with 8
- 7) SynFix-C:
  - 7.1) Place SynFix-C between the foamblocks (one-screw interface up)
  - 7.2) The implant should be in the middle ( $\pm 0.5$  mm, measured from the inner edge of the U-plate)
  - 7.3) The front surface of the implant should be inline with the front surface of the foam block
  - 7.4) Preload the testblock with 0.5 kg (additional to the testblock weight)
  - 7.5) Predrill the holes ( $\varnothing$  2mm); use a sleeve to preserve the correct angle
  - 7.6) Turn in the screws
  - 7.7) The screws have to be fixed with a torque of  $0.8\pm 0.04$  [Nm];  $\varnothing$  3.0 mm screw with  $0.1\pm 0.02$  [Nm]
  - 7.8) Go to point 12)
- 8) Anterior plate:
  - 8.1) Place Cervios between the foamblocks
  - 8.2) The implant should be in the middle ( $\pm 0.5$  mm, measured from the inner edge of the U-plate)
  - 8.3) The front surface of the implant should be inline with the front surface of the foam block
  - 8.4) Preload the testblock with 0.5 kg (additional to the testblock weight)
  - 8.5) Position plate in the middle ( $\pm 0.75$  mm laterally and vertically); CSLP and Vectra only: fix it with adhesive tape
  - 8.6) CSLP: go to 9; Vectra: go to 10; Zephir: go to 11
- 9) CSLP Small stature
  - 9.1) Start with the hole top left: Predrill to make room for the sleeve (not deeper than 2 mm)
  - 9.2) Use the CSLP drill sleeve (387.286) and the drill bit (387.220) for screws of 14 mm length to drill the holes; clean the sleeve and the drill bit of crumbs after drilling; set the screw
  - 9.3) Do the same at the hole bottom right, then top right, then bottom left
  - 9.4) Remove adhesive tape
  - 9.5) Fix the screws with a torque of  $0.5\pm 0.02$  [Nm]; keep same sequence as for setting the screws
  - 9.6) Set the locking screws
  - 9.7) Go to point 12)
- 10) Vectra
  - 10.1) Start with the hole top left: Set sleeve (03.613.001)
  - 10.2) Predrill the hole with a drill bit for a shorter screw (324.152, for 13 mm)
  - 10.3) Set the screw, still using the sleeve
  - 10.4) Do the same at the hole bottom right, then top right, then bottom left
  - 10.5) Fix the screws a quarter revolution after the screw has locked

- 10.6) Remove adhesive tape
- 10.7) Go to point 12)
- 11) Zephir
  - 11.1) Stick two small pins ( $\varnothing$  1 mm) through the designated holes to fix the plate
  - 11.2) Start with the hole top left: Drill a hole with Vectra drill bit (324.152, for 13 mm), set the screw
  - 11.3) Do the same at the hole bottom right, then top right, then bottom left
  - 11.4) Remove the small pins
  - 11.5) Lock the screws with a torque of  $0.5 \pm 0.02$  [Nm]; keep same sequence as for setting the screws
  - 11.6) Set the anti-migration cap
  - 11.7) Go to point 12)
- 12) Remove the pins
- 13) Fix the test-blocks on the testing machine
- 14) Calibrate the testing machine
- 15) Start test
- 16) Test ends when failure criteria reached
- 17) Note test results on protocol and save recorded data

### **Photo documentation**

- Sequence of photos during test (1 photo / 1 mm deformation)
- After test before removing from testing machine
- Lateral, frontal and from above: removed

### **Equipment**

- Ruler (0.5 mm scale)
- Marker
- Standard screwdriver (for M2/M3)
- Hexagon wrench key (for M3)
- Torque limiter
- Tools for implants
- Camera and tripod

## Biomechanical Tests for SynFix-C: Push-out

### Study / test objective and acceptance criteria; source for acceptance criteria

The objective of this test is to compare the new device (SynFix-C) to a standard intervertebral spacer in a Push-out test. Load-displacement data and maximum (or failure) load are collected.

The samples are fixed on PUR-foam (representing cervical vertebral bone properties).

#### Criteria

Push-out at fixed speed; axial compressive preload. Test ends when failure occurs.

#### Samples:

- SynFix-C, without cage (with D2.7, L16 screws)
- Cervios parallel (only in USA)

### Identification of study / test material

#### Consumable Materials:

Quantity	Part
4 (8)	PO Foam-Block

-

#### Reusable Test Material:

1	SynFix-C
3	D2.7, L16 Screws
1	Cervios

Details of tested samples in chapter “Detailed specifications of test samples”.

#### Test equipment

- Zwick: 148670, WN:121253
- Load cell: ID: 0, WN 136787 (5 kN)
- Equipment for push-out test

### Study / test procedure and participants

#### Test parameters

- Preload axial: 50 N compressive
- Preload push-out direction: 0.5 N
- Speed 2mm/min

- Criteria for test end: see above

**Test procedure**

See in chapter “Setup”

<b>Data collection and analysis method / test set up</b>
--

The data of interest are the load-displacement curves and failure (maximum)load for each sample.

Data are evaluated with MS Excel; significance of data is inspected by a statistic z-test,  $\alpha = 0.05$ . SynFix-C 2.7/16 is used as reference; as an assumption, standard deviation of the reference sample is also valid for the other tests.



## Biomechanical Tests for SynFix-C: Subsidence

### Study / test objective and acceptance criteria; source for acceptance criteria

The objective of this test is to compare the new device (SynFix-C) to a standard intervertebral spacer in a subsidence test. Load-displacement data, subsidence at 50 N and maximum displacement (or failure load and displacement) are recorded.

The set up is based on ASTM 2267-04 norm; the samples are pressed into PUR-foam (representing cervical vertebral bone properties).

#### Test sample:

- SynFix-C (D2.7, L16 screws)
- Cervios parallel (only in USA)
- Fixed on PUR-foam (General Plastics FR-3715, 15 pcf)

#### Test norm:

- ASTM 2267-04

### Identification of study / test material

#### Consumable Materials:

Quantity	Part
30	Foam-Block

#### Reusable Test Material:

1	SynFix-C, prototype 015
3	2.7 Screws, 16 mm
1	Cervios parallel

Details of tested samples in chapter “Detailed specifications of test samples”.

#### Test equipment

- Zwick: 148670, WN:121253
- Load cell: ID: 0, WN 136787 (5 kN)

### Study / test procedure and participants

#### Test parameters

- Preload: 1 N
- Speed: 5 N/s
- Force reaches 250 N → hold constant for 60 s
- Dischagement with 5 N/s

**Test procedure:**

See in chapter “Setup”.

<b>Data collection and analysis method / test set up</b>
--

The data of interest are the displacement-time(load) curves, in particular subsidence value at 50 N compressive load and maximum displacement (or failure load and displacement) and subsidence rate (at 250 N) for each sample.

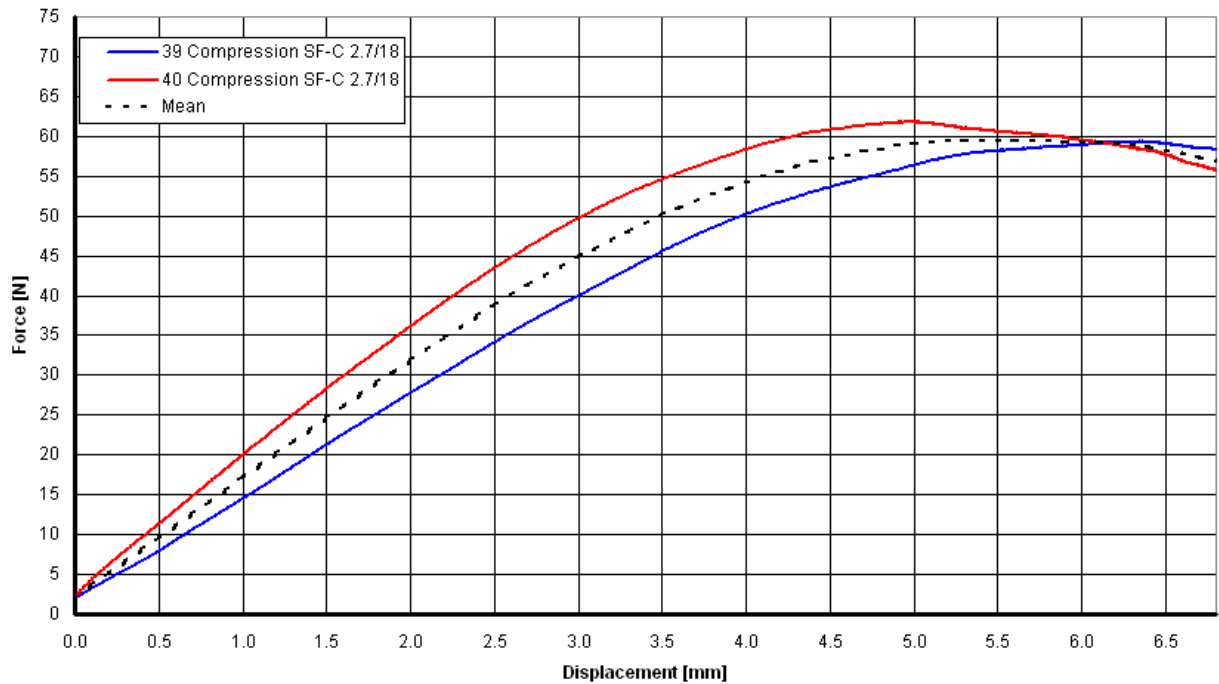
Data are evaluated with MS Excel; significance of data is inspected by a statistic z-test,  $\alpha = 0.05$ . SynFix-C 2.7/16 is used as reference; as an assumption, standard deviation of the reference sample is also valid for the other tests.

# VIII. COMPLETE TEST RESULTS

## VIII.1 Compression

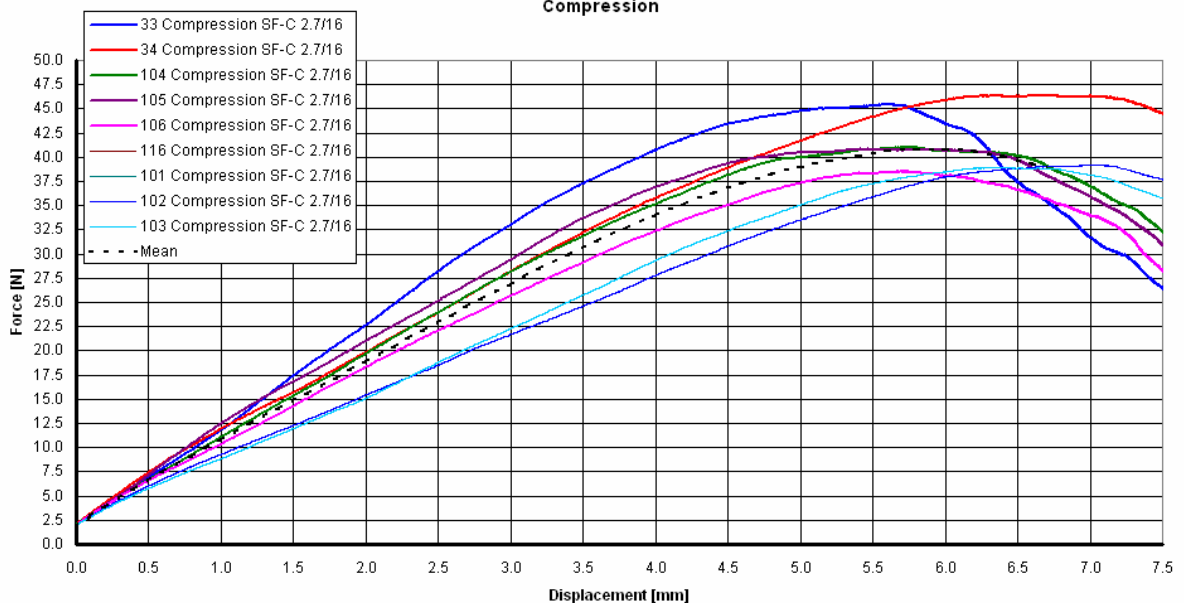
### Compression Test; SynFix-C P015; 2.7/18 screws

Compression

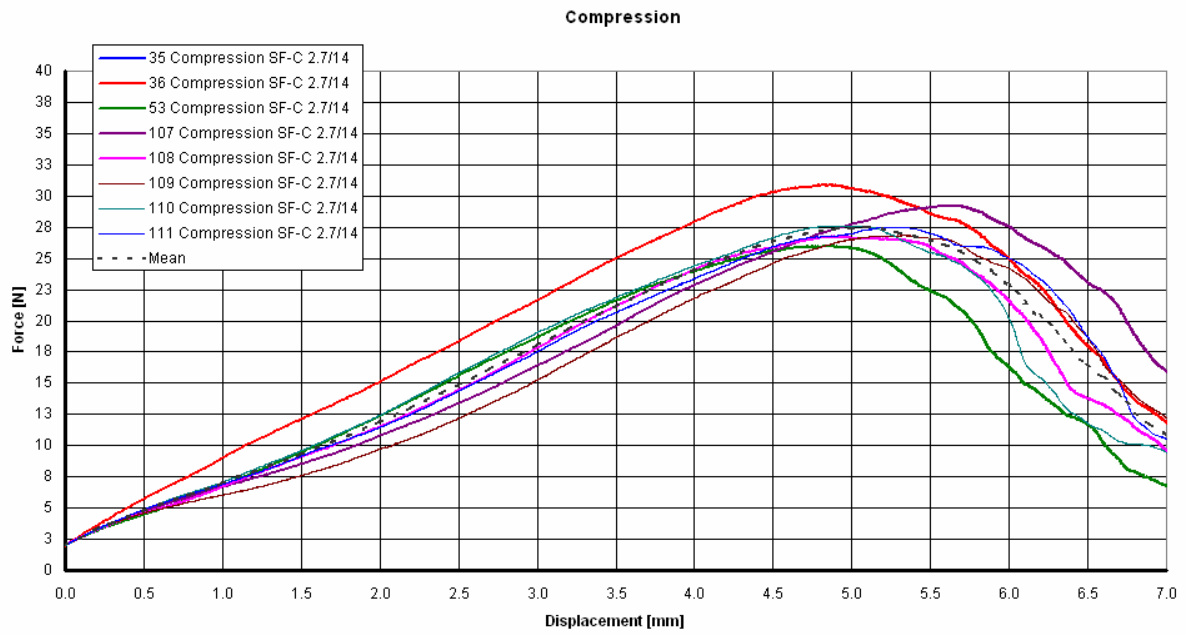


### Compression Test; SynFix-C P015; 2.7/16 screws

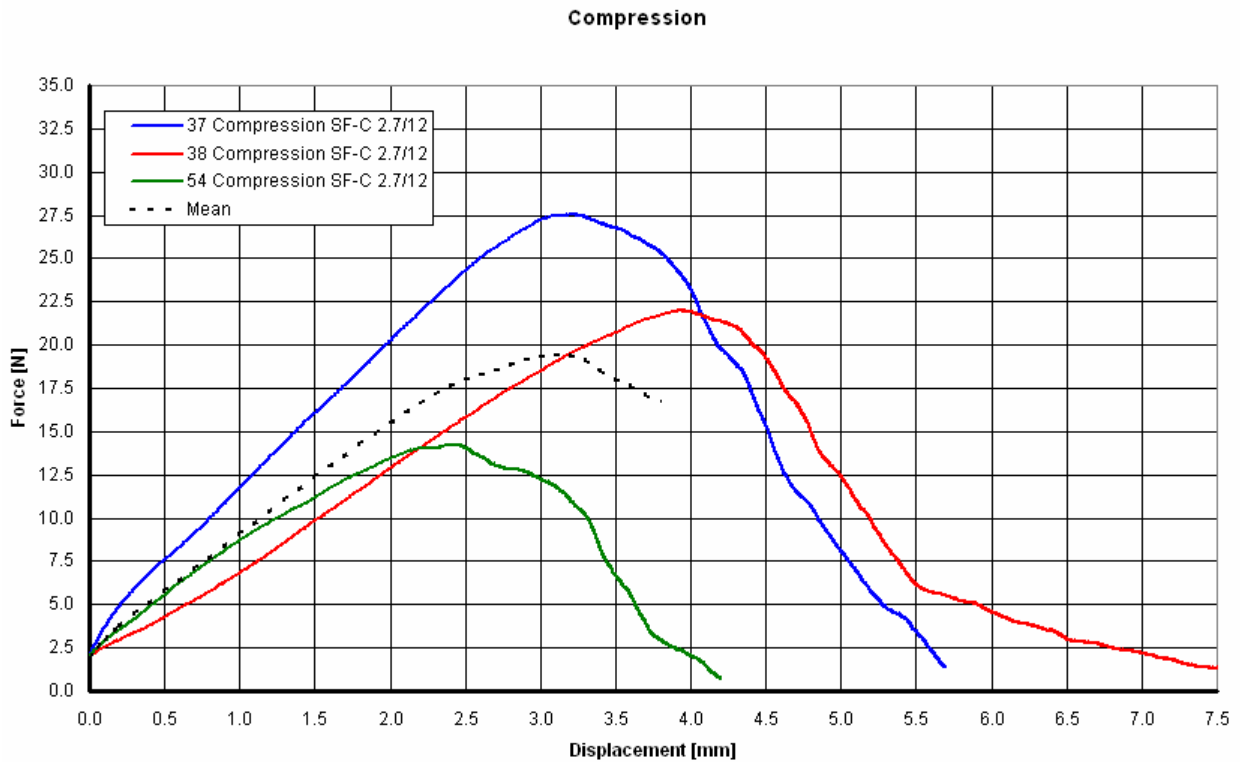
Compression



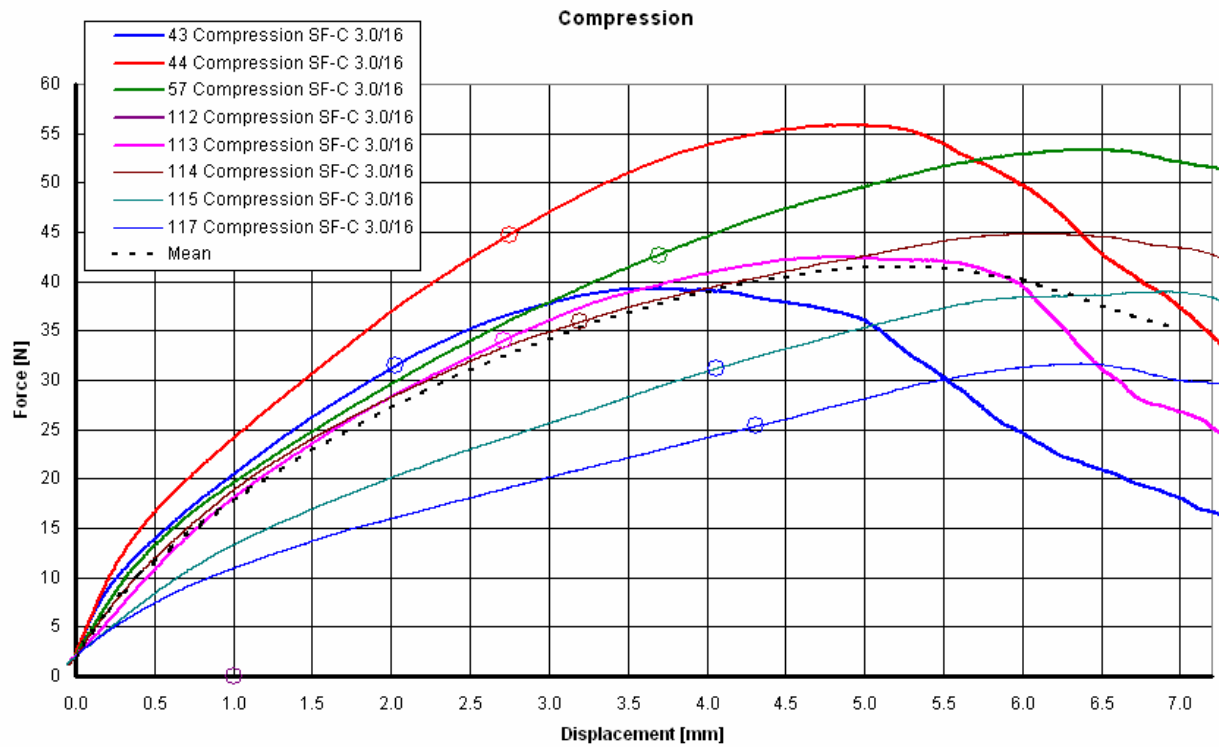
**Compression Test; SynFix-C P015; 2.7/14 screws**



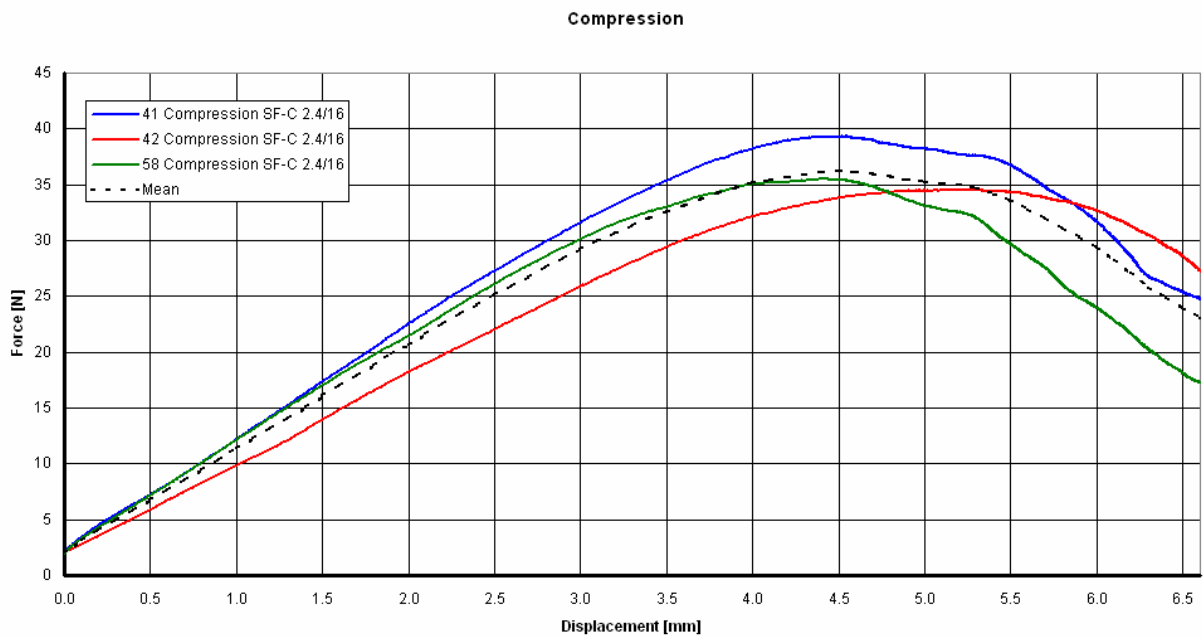
**Compression Test; SynFix-C P015; 2.7/12 screws**



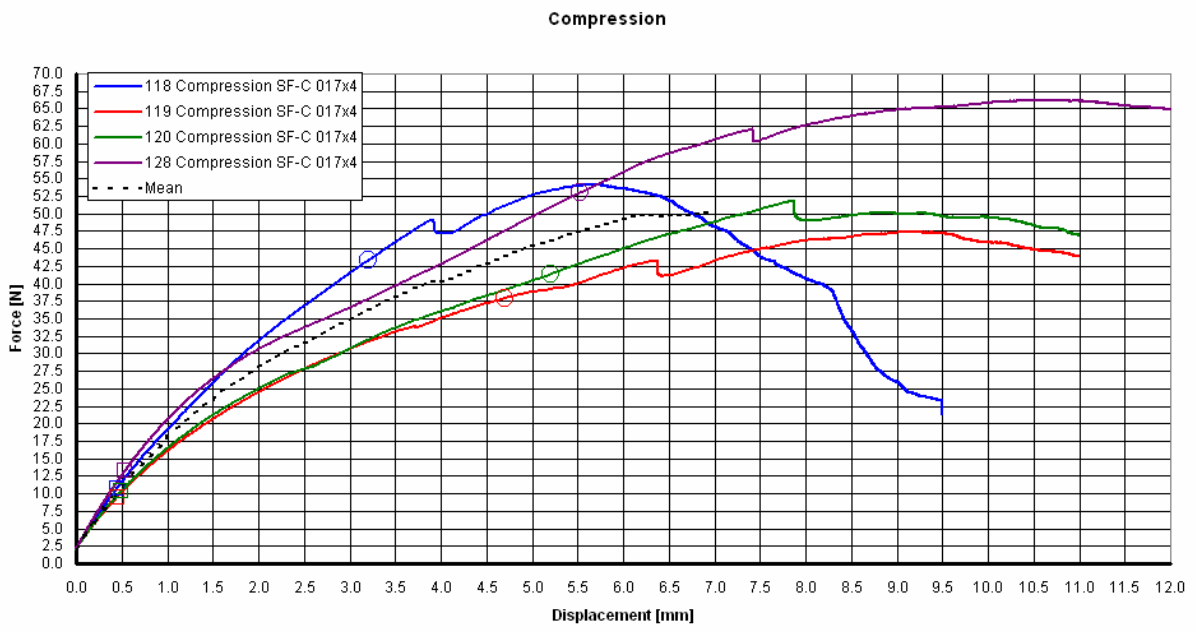
**Compression Test; SynFix-C P017; 3.0/16 screws**



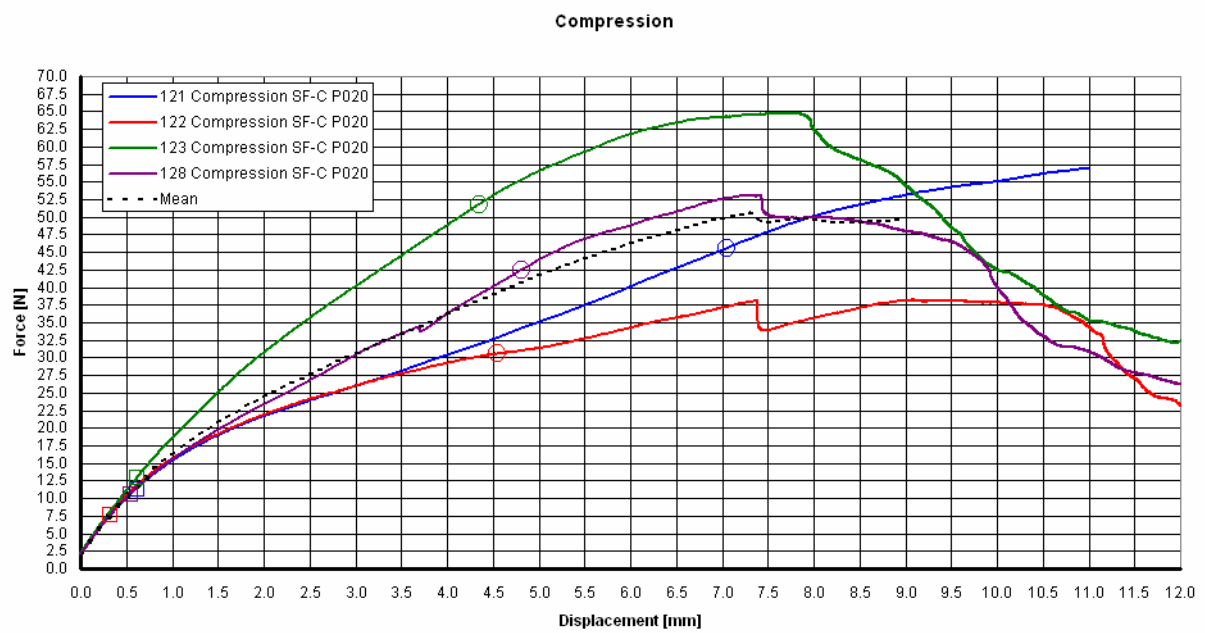
**Compression Test; SynFix-C P015; 2.4/16 screws**



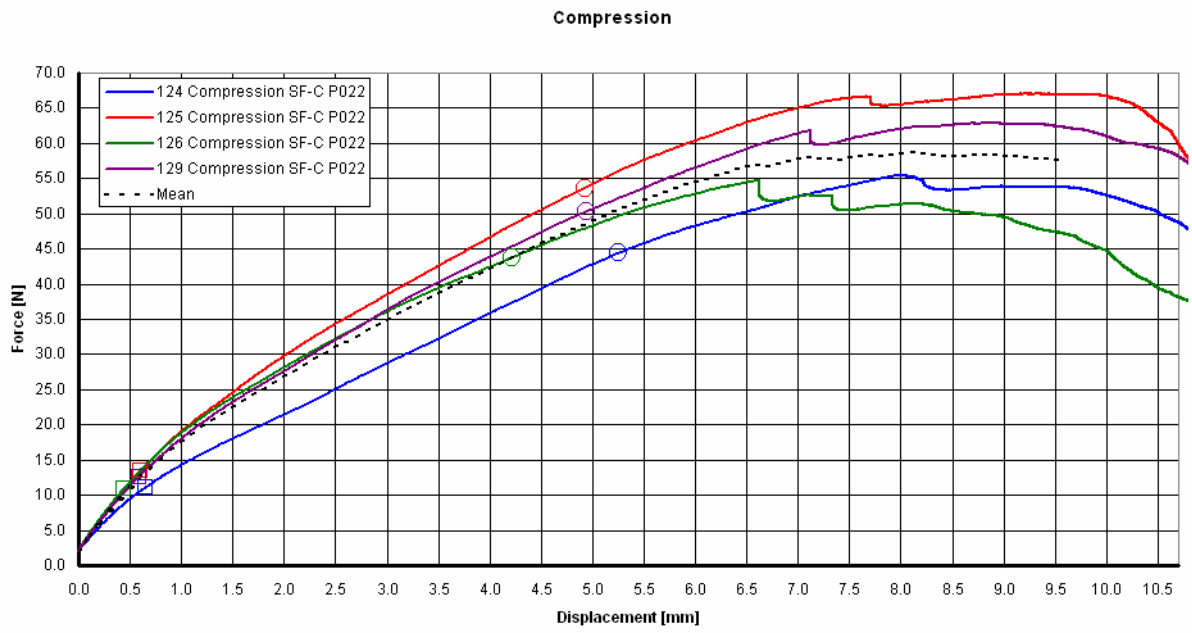
**Compression Test; SynFix-C P017x4; 4x3.0/16 screws**



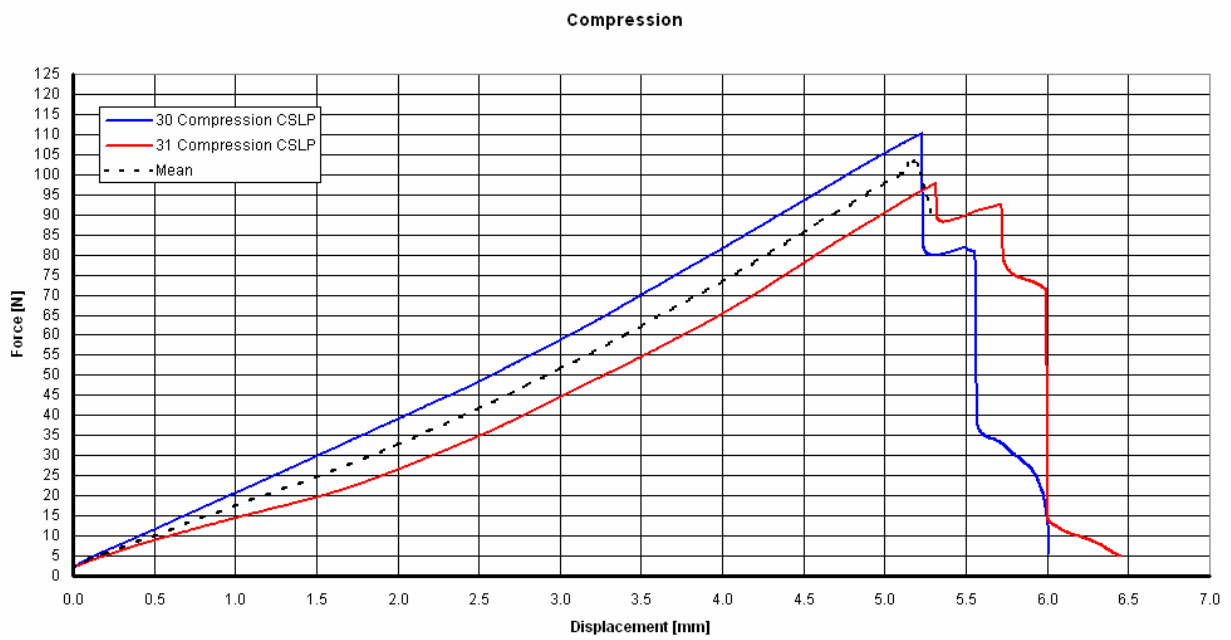
**Compression Test; SynFix-C P020; 4x3.0/16 screws**



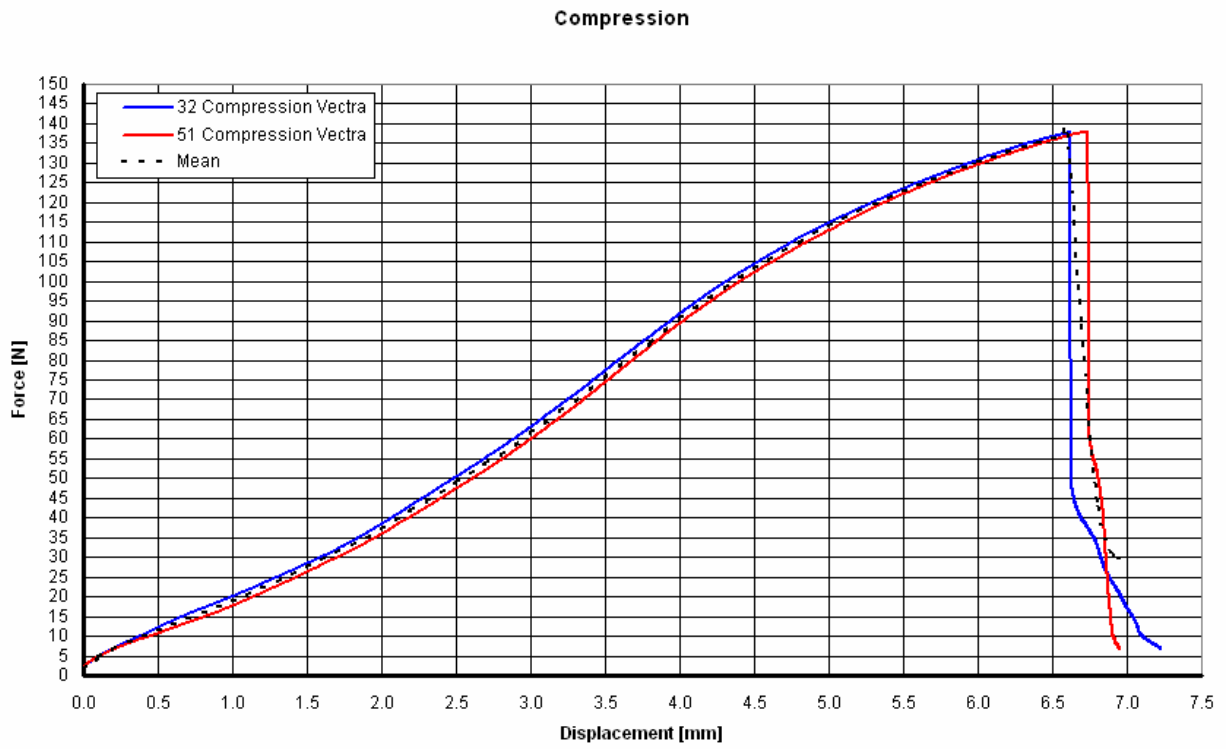
**Compression Test; SynFix-C P022; 4x3.0/16 screws**



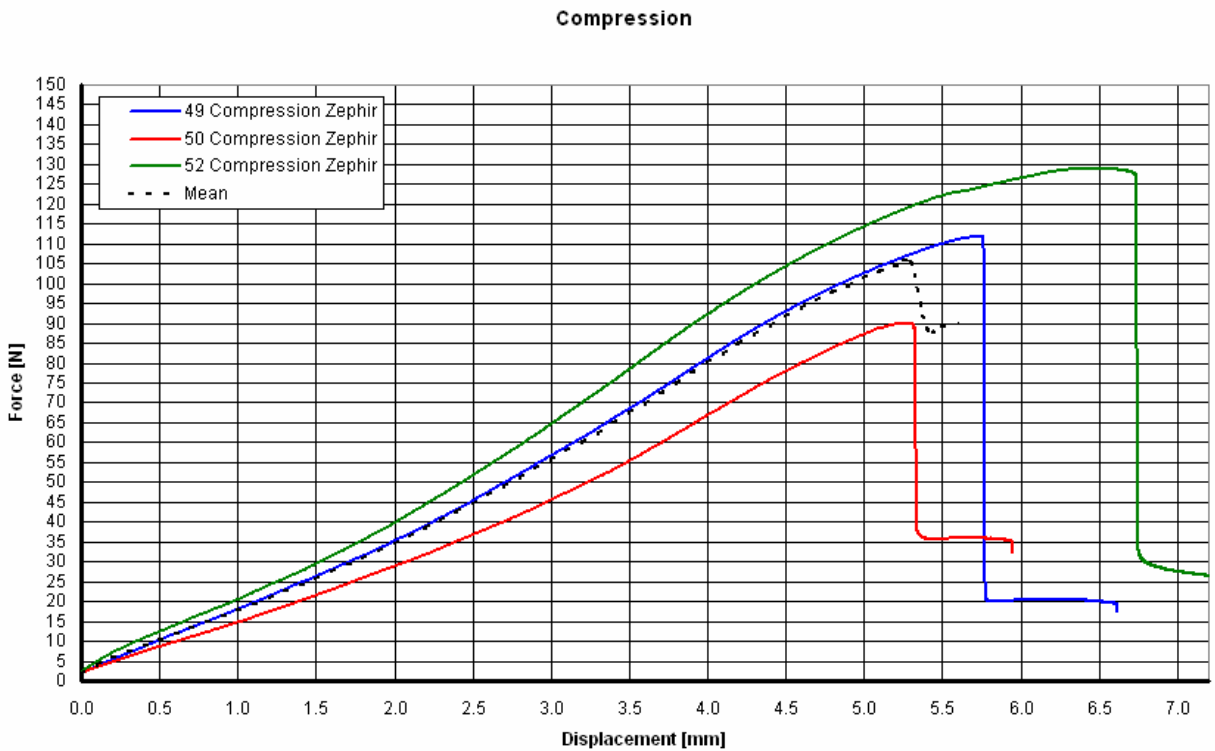
**Compression Test; CSLP**



### Compression Test; Vectra

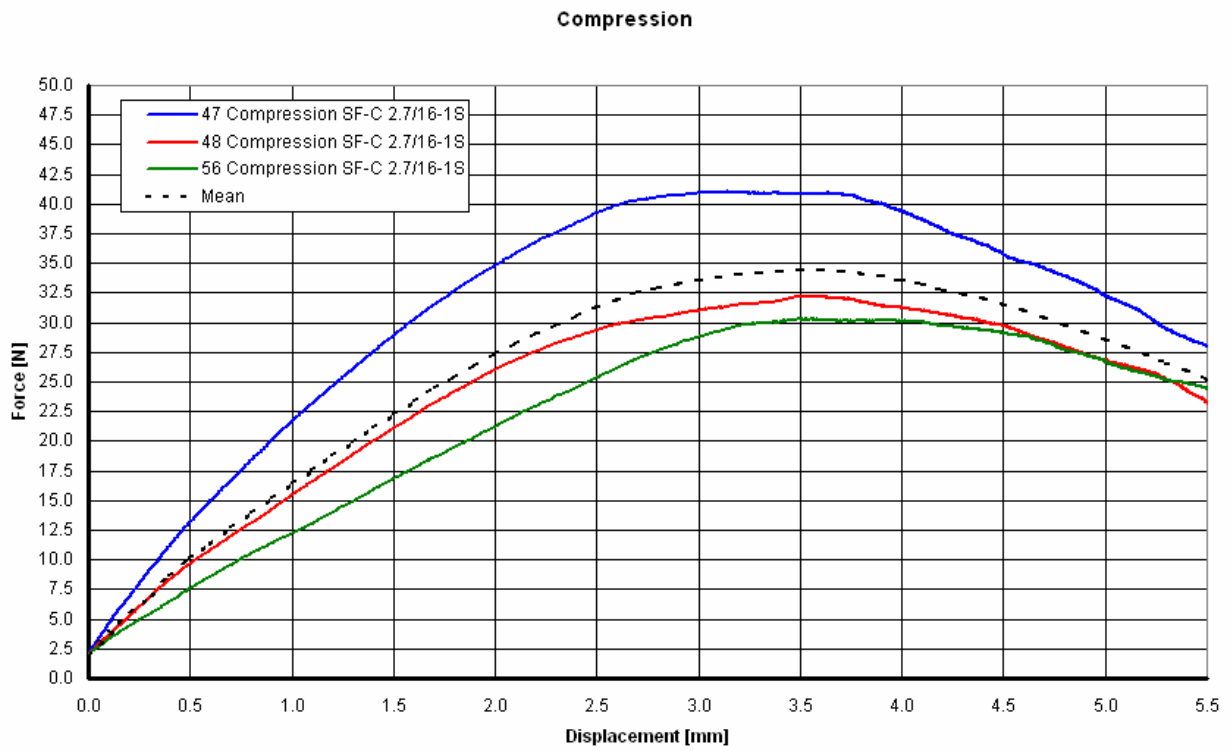


### Compression Test; Zephir

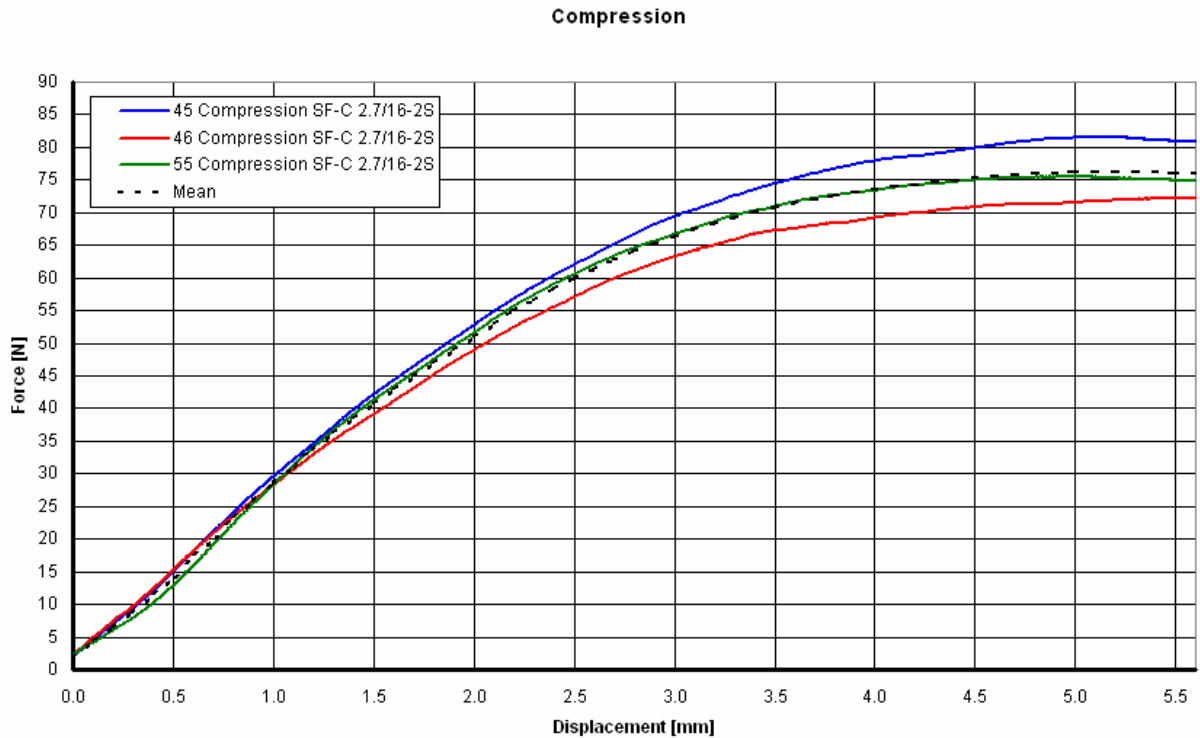




**Compression Test; SynFix-C P015; 2.7/16 screws, 1-screw interface**

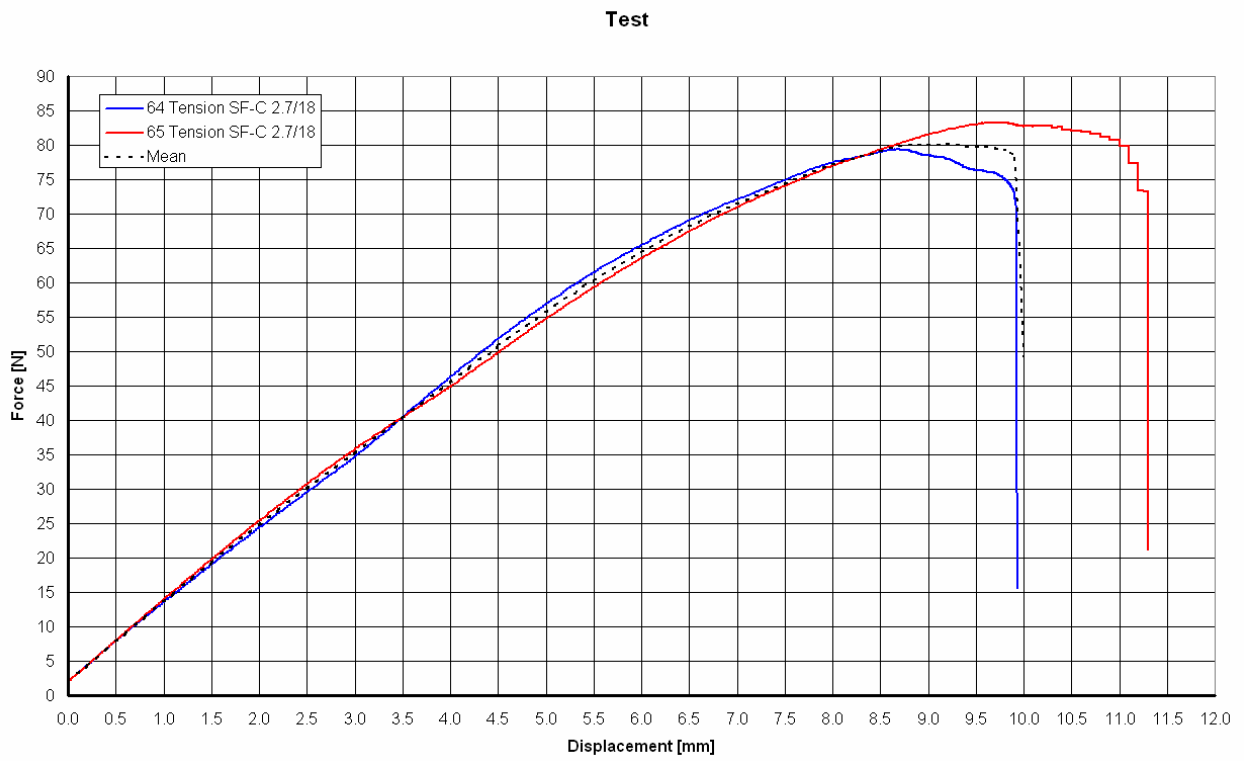


**Compression Test; SynFix-C P015; 2.7/16 screws, 2-screw interface**

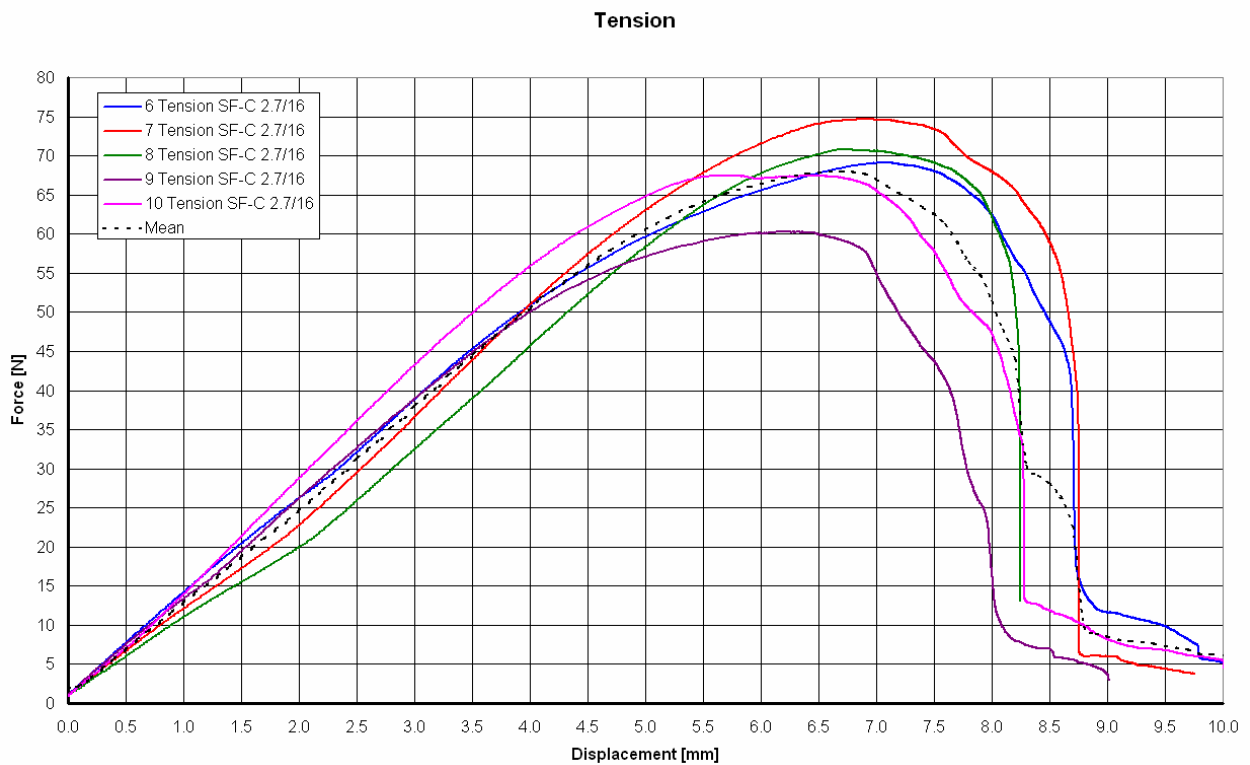


## VIII.2 Tension

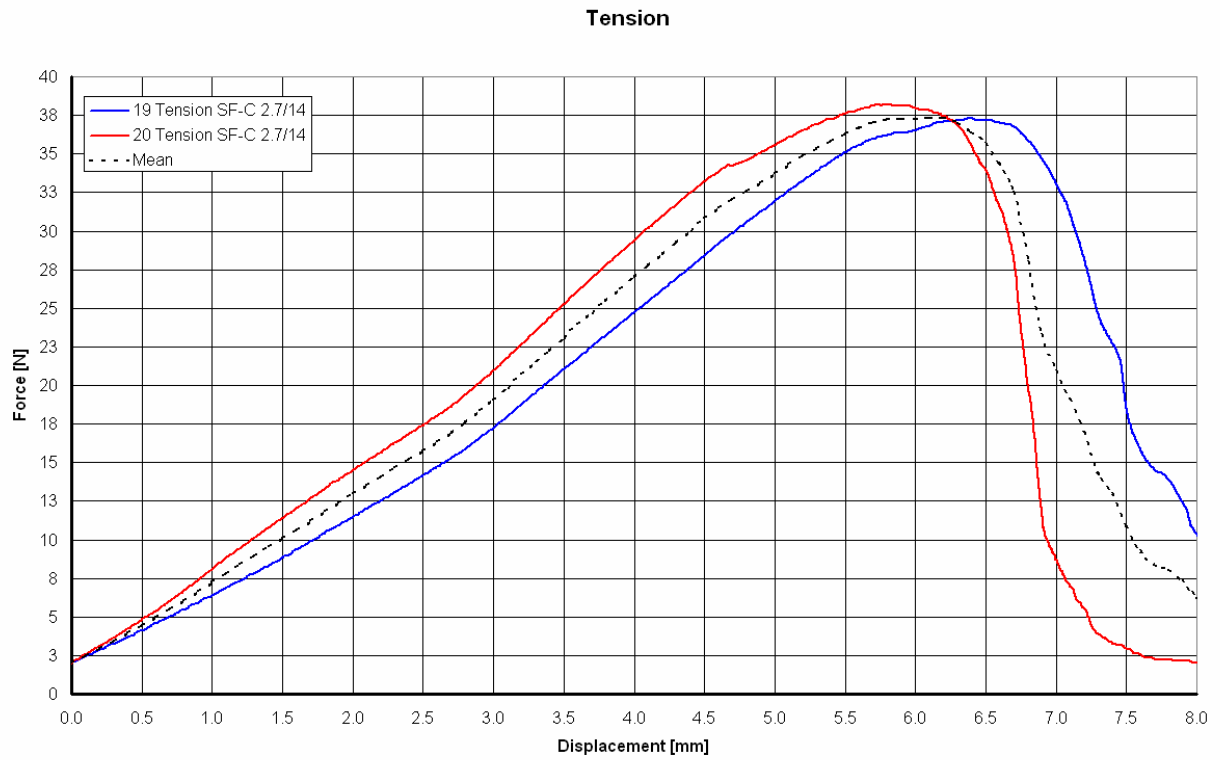
### Tension Test; SynFix-C P015; 3×2.7/18 screws



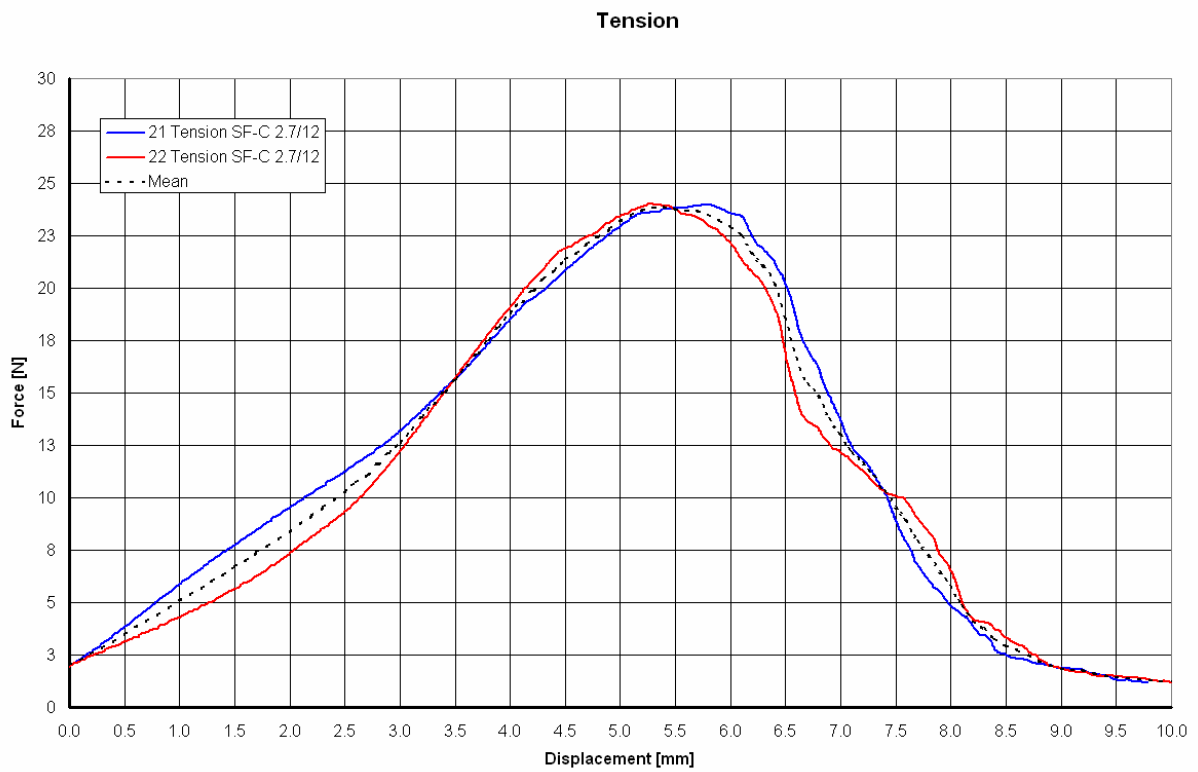
### Tension Test; SynFix-C P015; 3×2.7/16 screws



**Tension Test; SynFix-C P015; 3×2.7/14 screws**

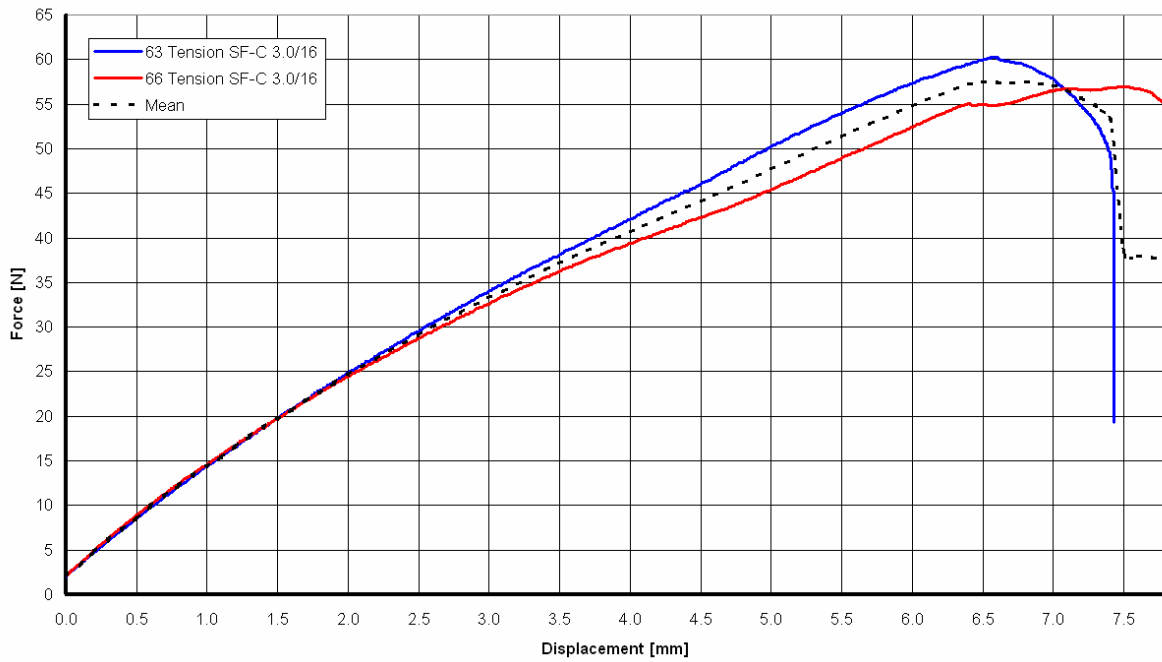


**Tension Test; SynFix-C P015; 3×2.7/12 screws**



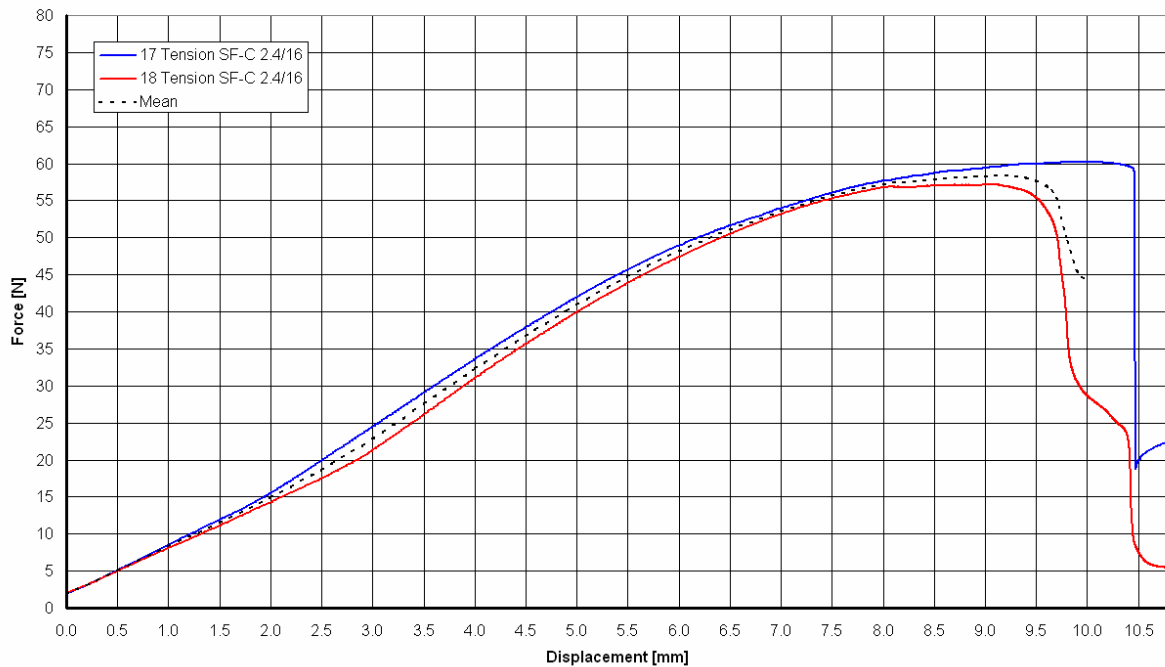
### Tension Test; SynFix-C P017; 3×3.0/16 screws

Test

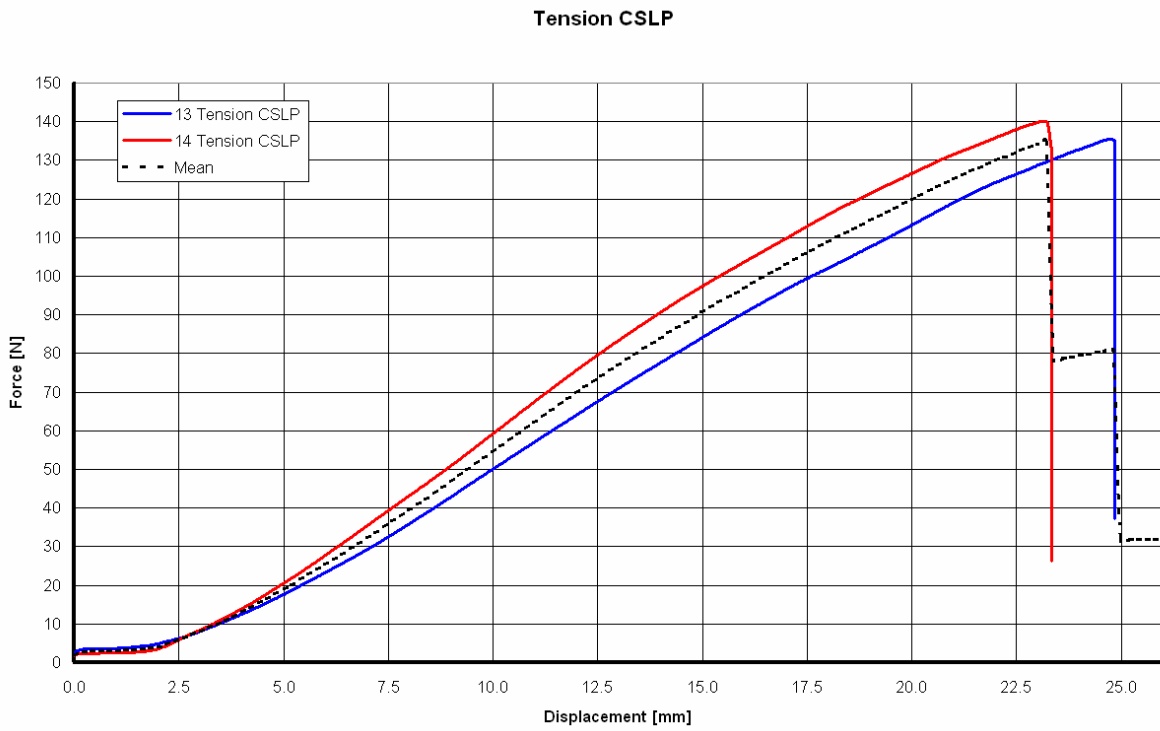


### Tension Test; SynFix-C P015; 3×2.4/16 screws

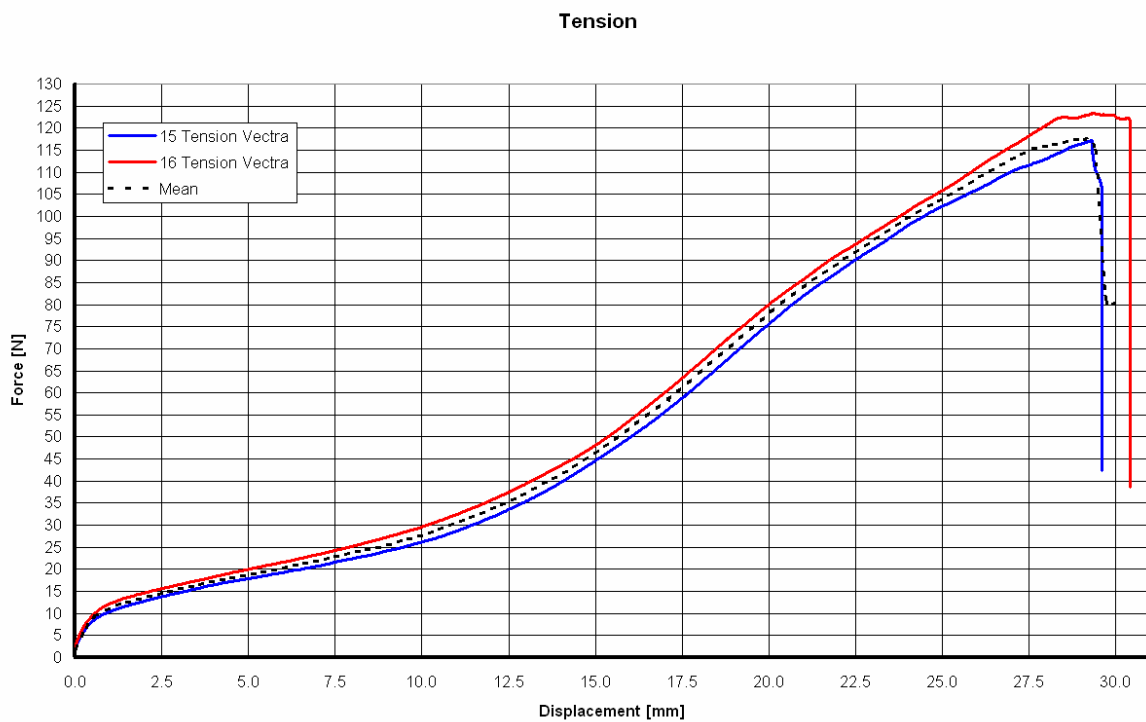
Tension



### Tension Test; CSLP

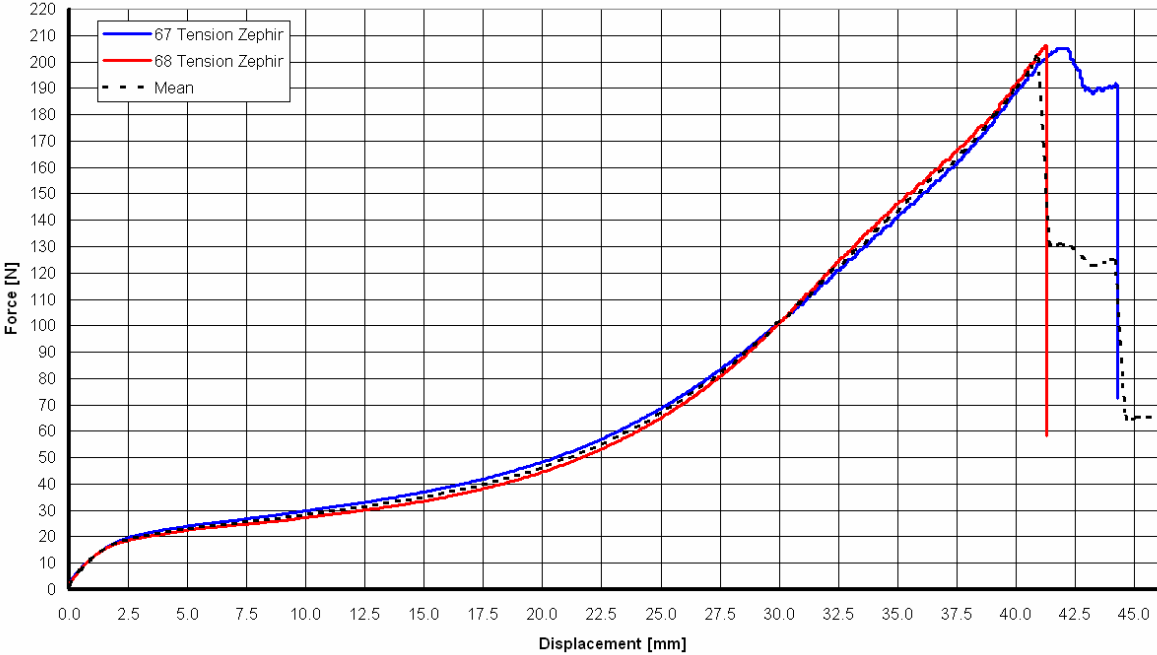


### Tension Test; Vectra

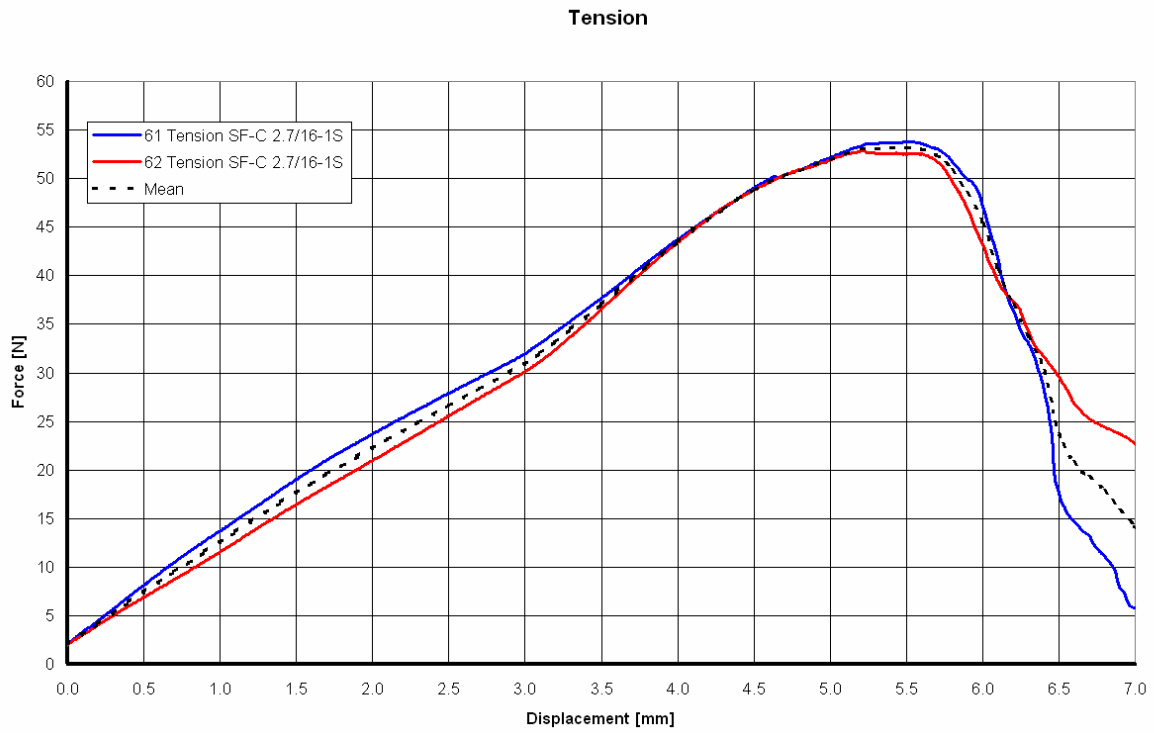


Tension Test; Zephir

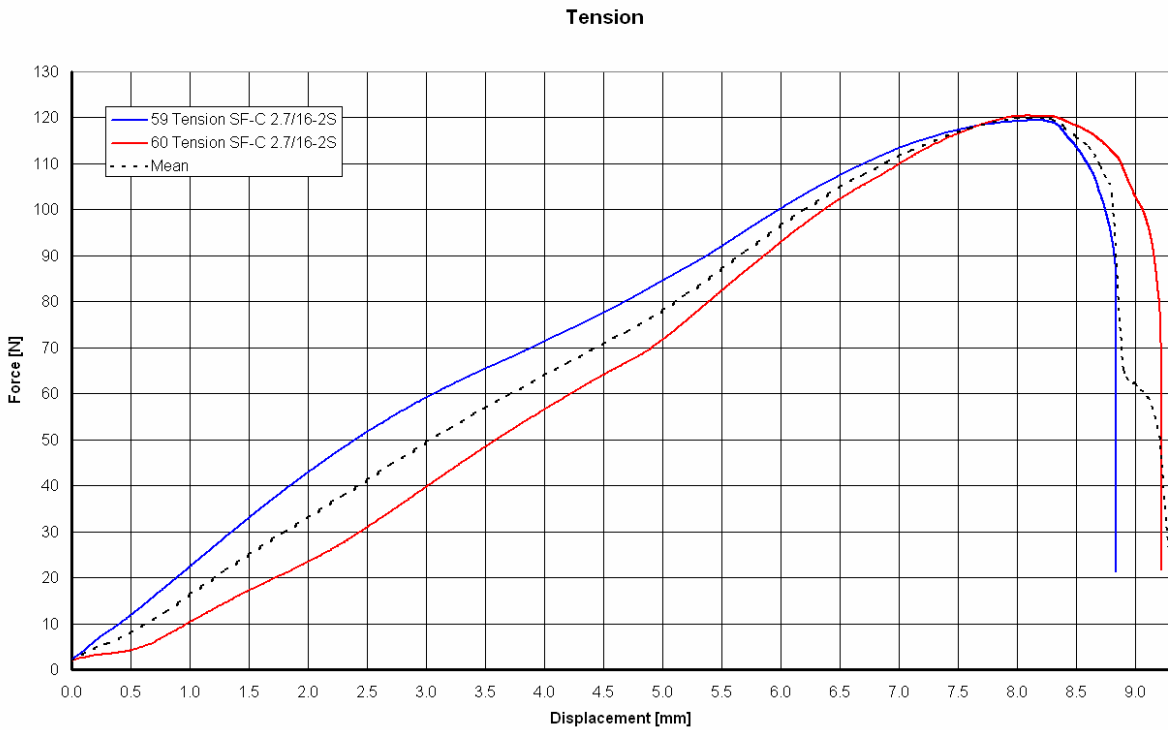
Tension



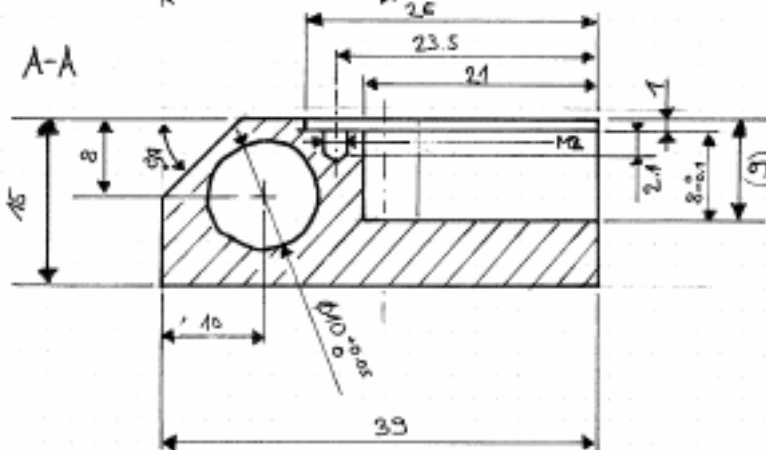
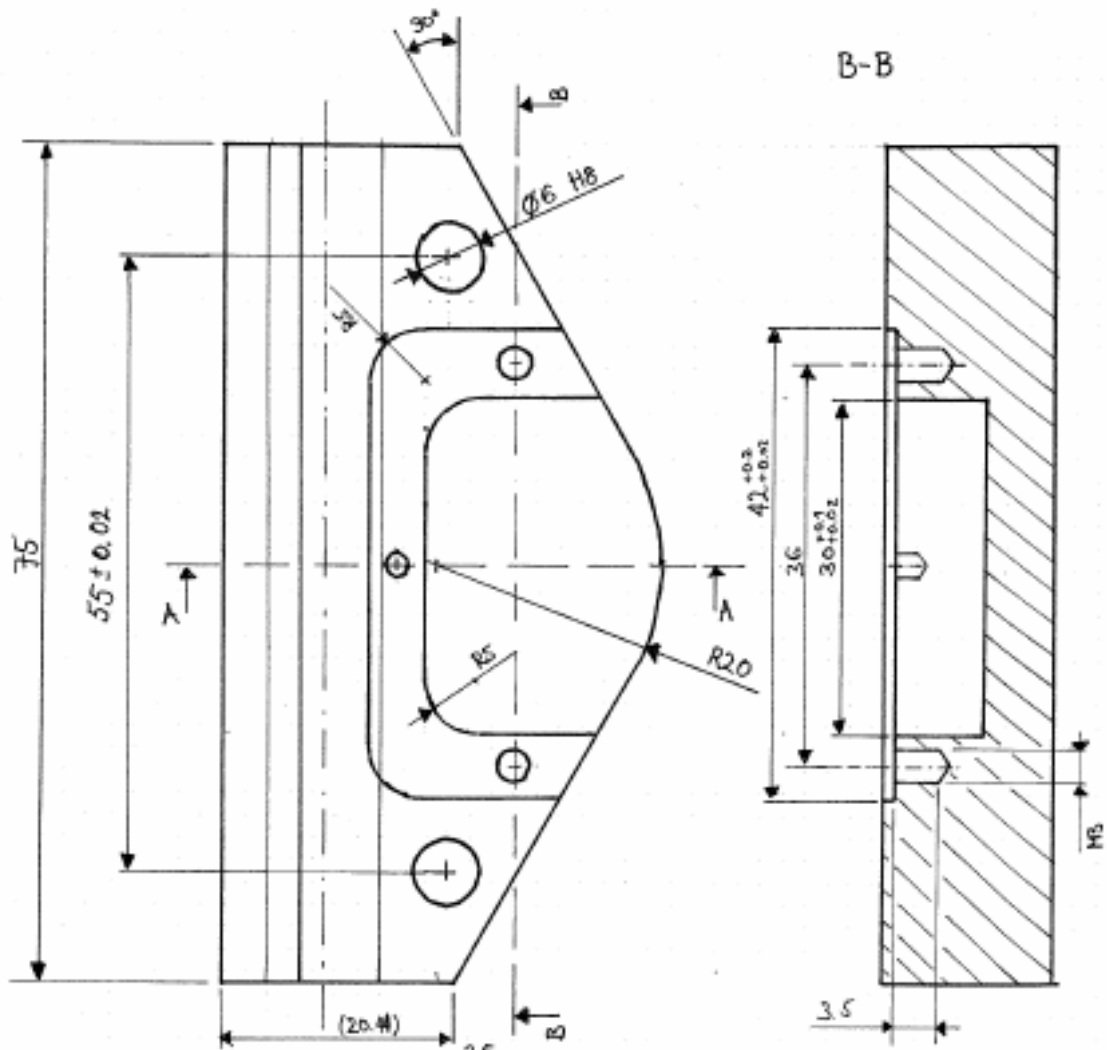
**Tension Test; SynFix-C P015; 2.7/16 screws, 1-screw interface**



**Tension Test; SynFix-C P015; 2.7/16 screws, 1-screw interface**

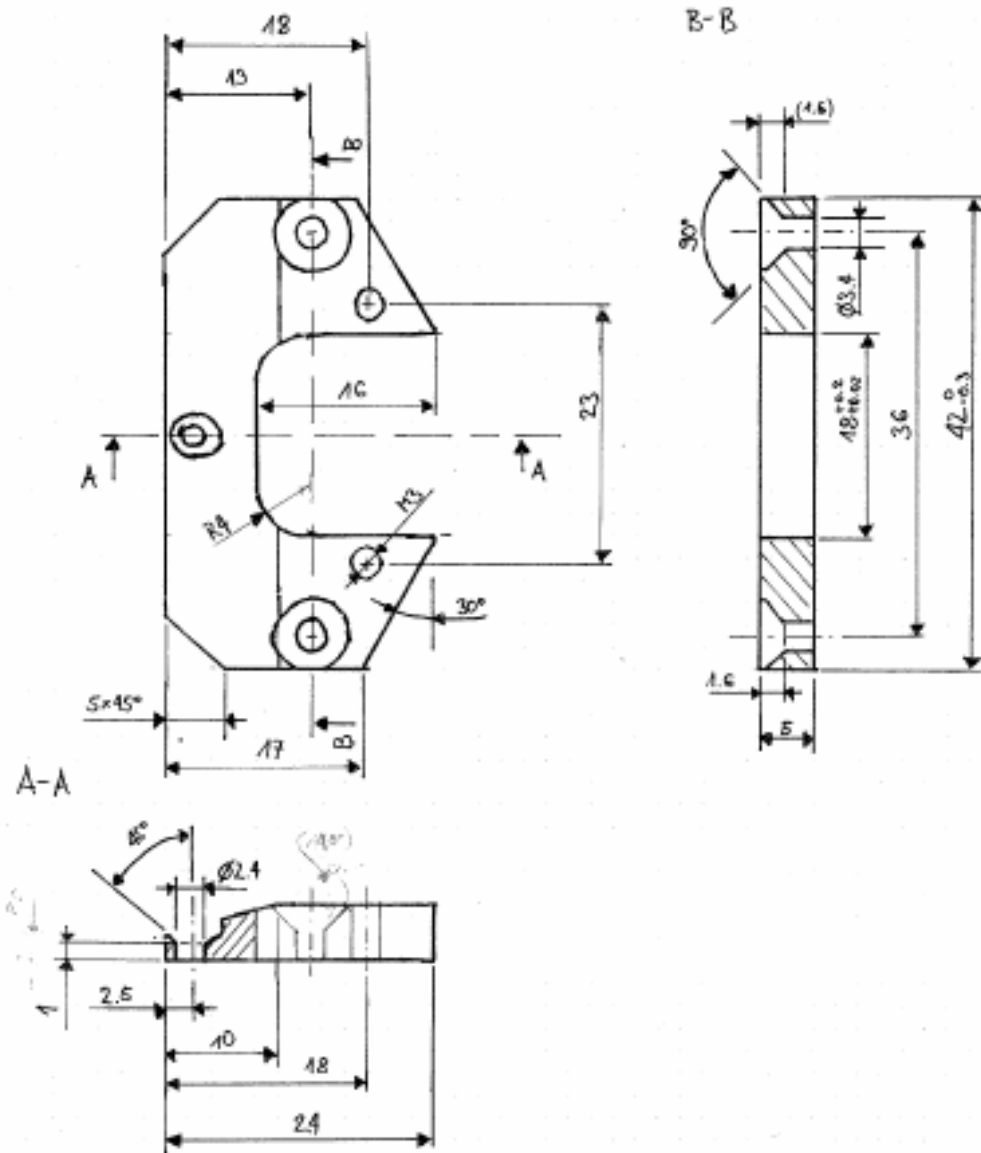


**IX. DRAWINGS TEST MATERIAL**

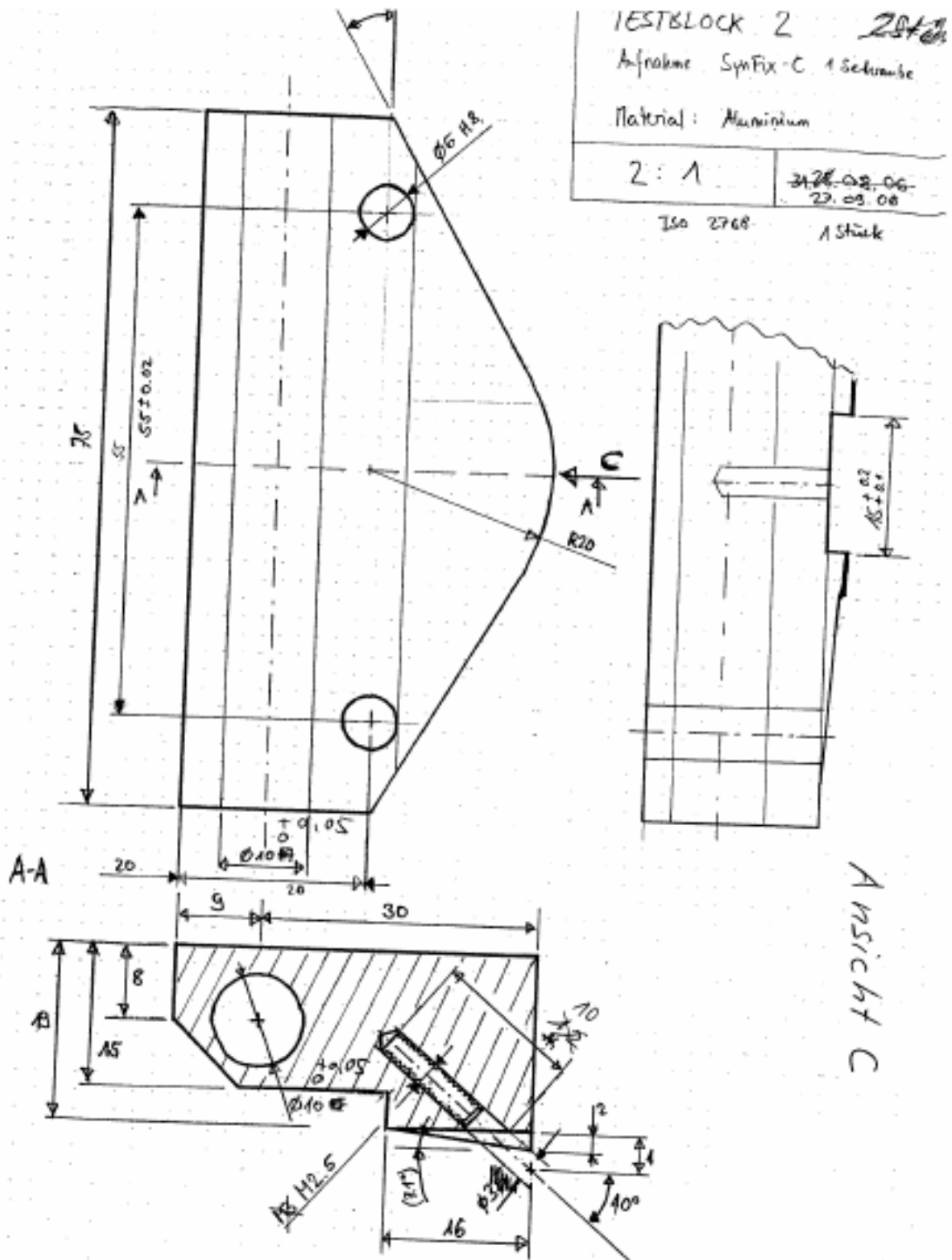


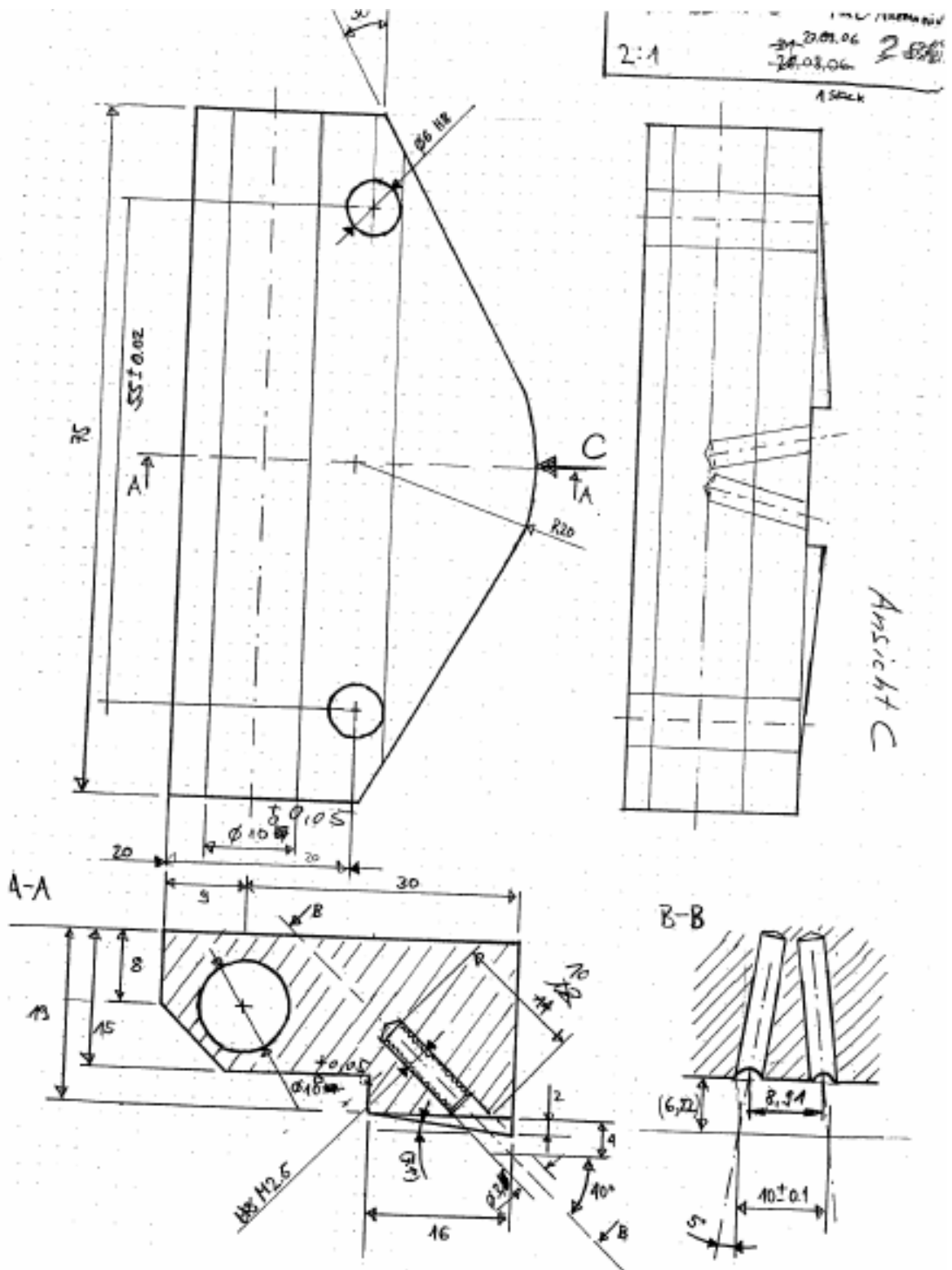
TESTBLOCK 1	
Material: Aluminium	
2:1	31.08.06 H. Devatz

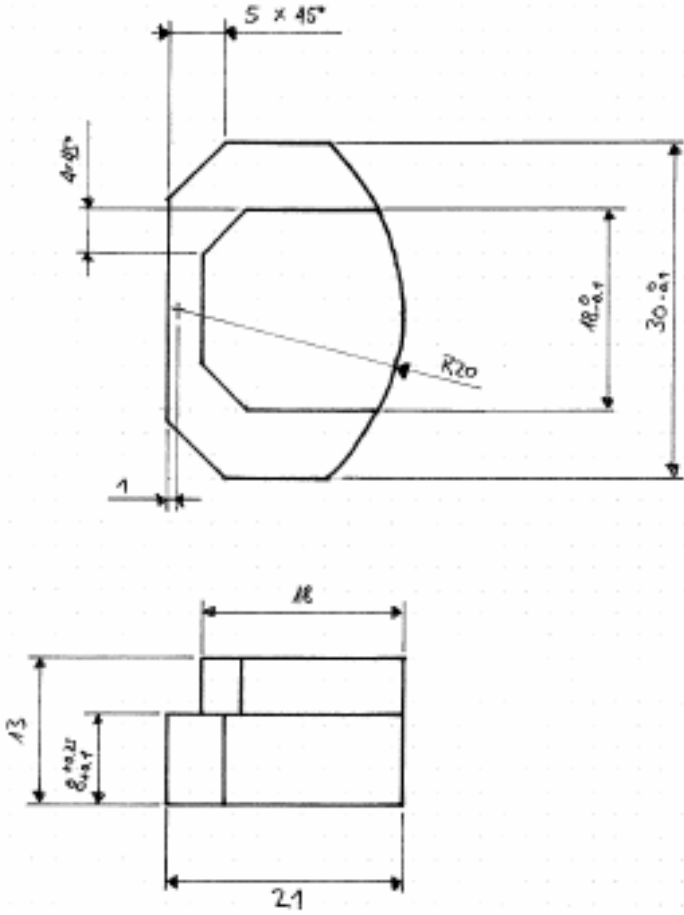




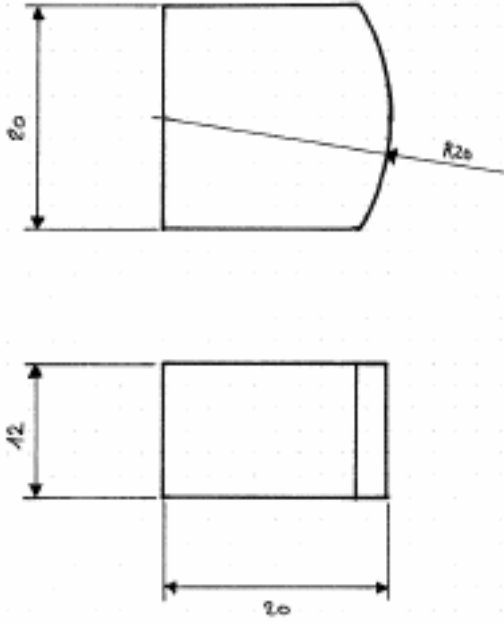
Fixierplatte	
Material:	
2:1	31.08.06
	M. Davate







SCHAUMBLOCK Material: PUR-Schaum (General Plastics FR-3715)	
2:1	01.09.06 M. Dautz



SCHAUMBLOCK MULTI-LEVEL Material: PUR-Schaum (General Plastics FR-3745)		
2:1	01.09.06	M. Guntz